Analysen zur molekularen Charakterisierung von Proteinen des humanen Usher-Syndroms und Evaluation genbasierter Therapiestrategien

Dissertation
zur Erlangung des Grades
„Doktor der Naturwissenschaften"
am Fachbereich Biologie
der Johannes Gutenberg-Universität
in Mainz

von Nora-Lena Overlack
geboren am 06.März 1979
in Dortmund

Mainz, September 2011

Dekan:

1. Berichterstatter:

2. Berichterstatter:

Tag der mündlichen Prüfung: 10. November 2011

<u>Wer nicht selbst denkt, denkt gar nicht.</u>

(Oscar Wilde)

Anmerkungen

Die vorliegende Arbeit ist kumulativ gestaltet und besteht im Kern aus den fünf Publikationen:

Lagziel et al., 2009: "*Expression of cadherin 23 isoforms is not conserved: implications for a mouse model of Usher syndrome type 1D*" (Publikation I), Overlack et al., 2010: "*The role of cadherins in sensory cell function*" (Publikation II), Overlack et al., 2011a: "*Direct interaction of the Usher syndrome 1G protein SANS and myomegalin in the retina*" (Publikation III), Overlack et al., 2011: "*Current therapeutic strategies for human Usher syndrome*" (Publikation IV) und Overlack et al., eingereicht: *Gene Repair of an Usher Syndrome Causing Mutation.* (Publikation V).

Publikation I wurde bereits im September 2009 in der Zeitschrift „*Molecular Vision*" publiziert. Bei den Publikationen II und IV handelt es sich um Kapitel der Bücher „Molecular and Functional Diversities of Cadherin and Protocadherin" (Publikation II), sowie „Usher Syndrome: Pathogenesis, Diagnosis and Therapy" (Publikation IV). Die Bücher sind seit 2010 bzw. 2011 erhältlich. Die dritte aus meiner Doktorarbeit hervorgegangene Publikation liegt seit Juli 2011 als elektronische Versionen bei der Zeitschrift „*BBA-Molecular Cell Research*" vor (Publikation III). Anzumerken ist, dass die Publikation V bei der Zeitschrift „*Proceedings of the National Academy of Sciences USA*" *(PNAS)* eingereicht wurde und somit als Manuskript beigefügt ist. Die Ergebnisse aller fünf Publikationen sind im Abschnitt „Zusammenfassung der Ergebnisse und Diskussion" dargestellt und insgesamt diskutiert. Alle weiteren Publikationen, zu denen im Rahmen dieser Arbeit Beiträge geleistet werden konnten, sind im Text mit einem Stern (*) hervorgehoben. Eine detaillierte Übersicht der geleisteten Beiträge zu der jeweiligen Publikation wird im Anhang gegeben.

Veröffentlichungen und Kongressbeiträge

Teile der vorliegenden Dissertation wurden auf internationalen Kongressen vorgestellt, befinden sich in Vorbereitung einer Publikation, wurden eingereicht oder wurden in folgenden Zeitschriften publiziert:

Publikationen

Overlack N, Goldmann T, Wolfrum U, Nagel-Wolfrum K. Gene Repair of an Usher Syndrome Causing Mutation. - eingereicht

Overlack N, Kilic D, Bauß K, Märker T, Kremer H, van Wijk E, Wolfrum U (2011) Direct interaction of the Usher syndrome 1G protein SANS and myomegalin in the retina. Biochim. Biophys. Acta 1813, 1883-1892.

Overlack N*, Goldmann T*, Wolfrum U, Nagel-Wolfrum K (2011) Current therapeutic strategies for human Usher syndrome. In: Usher Syndrome: Pathogenesis, Diagnosis and Therapy. Ed.: Satpal Ahuja, 377-395 (*both authors contributed equally).

Goldmann T, **Overlack N**, Wolfrum U, Nagel-Wolfrum K (2011) PTC124 mediated translational read-through of a nonsense mutation causing Usher type 1C. Hum. Gene Ther. 22:537-547.

Overlack N, Nagel-Wolfrum K, and Wolfrum U (2010) The role of cadherins in sensory cell function. In: Molecular and Functional Diversities of Cadherin and Protocadherin. Ed.: K.Yoshida, 297-311.

Goldmann T, Rebibo-Sabbah A, **Overlack N**, Nudelman I, Belakhov V, Baasov T, Ben-Yosef T, Wolfrum U, Nagel-Wolfrum K (2010) Designed aminoglycoside NB30 induces beneficial read-through of a USH1C nonsense mutation in the retina. Invest Ophthalmol Visual Sci 51:6671-6680.

Lagziel A, **Overlack N**, Bernstein SL, Morell RJ, Wolfrum U, Friedman TB (2009) Expression of cadherin 23 isoforms is not conserved: implications for a mouse model of Usher syndrome type 1D. Mol Vision. 15:1843-57.

Overlack N*, Märker T*, Latz, M, Nagel-Wolfrum, K and Wolfrum U (2008) SANS (USH1G) expression in developing and mature mammalian retina. Vision Res 48: 400-412 (*first authors contributed equally to the work).

Maerker T, van Wijk E, **Overlack N**, Kersten FFJ, McGee J, Goldmann T, Sehn E, Roepman R, Walsh EJ, Kremer H and Wolfrum U (2008) A novel Usher protein network at the periciliary reloading point between molecular transport machineries in vertebrate photoreceptor cells. Hum Mol Gen 17:71-86.

Reiners J, van Wijk E, Märker T, Zimmermann U, Jürgens K, te Brinke H, **Overlack N**, Roepman R, Knipper M, Kremer H, Wolfrum U (2005) The scaffold protein harmonin (USH1C) provides molecular links between Usher syndrome type 1 and type 2. Hum Mol Gen 14: 3933-3943.

Publikationen in Vorbereitung

Goldmann T, **Overlack N**, van Wyk M, Fabian Möller F, Igor Nudelman I, Timor Baasov T, Wolfrum U, and Kerstin Nagel-Wolfrum K. A comparison of NB30, NB54 and PTC124 as treatment options for the translational read-through of a nonsense mutation. - in Vorbereitung

Chadderton N, Palfi A, Millington-Ward S, O'Reilly M, Carrigan M, Gobbo OL, **Overlack N**, Campbell M, Wolfrum U, Humphries P, Kenna PF, Farrar GJ. Intravitreal AAV mediated delivery of the yeast NDI1 gene protects in a mouse model of LHON. - in Vorbereitung

Kongressbeiträge

Overlack N, Goldmann T, Wolfrum U, Nagel-Wolfrum K (2011) Gene Repair of USH1C Mediated by Zinc Finger Nuclease Induced Homologous Recombination. Gene Targeting. Vienna, Austria (oral presentation)

Overlack N, Goldmann T, Wolfrum U, Nagel-Wolfrum K (2011) Gene Repair by Zinc Finger Nucleases mediated Homologous Recombination of USH1C. Pro Retina Research-Colloquium, Retinal Degeneration: "Vision and Beyond".

Sorusch N, **Overlack N**, Maerker T, van Wijk E, Bauß K, Kersten F, Roepman R, Kremer, Wolfrum U (2011) The USH1G protein SANS is a microtubule-binding protein and part of the cytoplasmic dynein motor in mammalian photoreceptor cells. 9th Göttingen Meeting of the German Neurosience Society, T15-12C

Sorusch N, **Overlack N**, Kunz A, van Wijk E, Bauß K, Maerker T, Kersten F, Roepman R, Kremer, Wolfrum U (2011) The USH1G protein SANS is a novel MAP and a cytoplasmic dynein motor component in mammalian photoreceptor cells. DGZ/FEBS workshop: "The spiders web: How microtubules organize cellular space", Potsdam 2011.

Wolfrum U, Goldmann T, **Overlack N**, Mueller C, Vetter JM, Nagel-Wolfrum K (2011) Expression and subcellular localization of Usher syndrome proteins in the human photoreceptor cells. 9th Göttingen Meeting of the German Neurosience Society,T15-16A.

Goldmann T, **Overlack N**, Möller F, Nudelman I, Baasov T, Wolfrum U, Nagel-Wolfrum K (2011) Read-through of a nonsense mutation as a treatment option for Usher type 1C. 9th Göttingen Meeting of the German Neurosience Society, T11- 22B.

Overlack N, Goldmann T, Wolfrum U, Nagel-Wolfrum K (2011) USH1C gene repair mediated by Zinc Finger Nuclease induced Homologous Recombination. 9th Göttingen Meeting of the German Neurosience Society, T15-14C.

Goldmann T, **Overlack N**, Spitzbart B, Möller F, Nudelman I, Bassov T, Wolfrum U, Nagel-Wolfrum K (2010) PTC124 therapy for a nonsense mutation causing Usher syndrome type 1C. Rhine-Main Neuroscience Network (rmn²), Oberwesel, P60

Goldmann T, **Overlack N**, Spitzbarth B, Möller F, Wolfrum U and Nagel-Wolfrum K (2010) PTC124 therapy for a nonsense mutation causing Usher syndrome type 1C. Pro Retina Research-Colloquium

Nagel-Wolfrum K, Goldmann T, **Overlack N** and Wolfrum U (2010) PTC124-mediated read-through of a nonsense mutation causing Usher type 1C. International Symposium on Usher Syndrome and Related Diseases.

Overlack N, Kilic D, Maerker T, Bauss K, van Wijk E, Stern-Schneider G, Roepman R, Kremer H and Wolfrum U (2010) A new member of the USH protein network: USH1G protein SANS interacts with myomegalin in mammalian photoreceptor cells. International Symposium on Usher Syndrome and Related Diseases

Nagel-Wolfrum K, Goldmann T, **Overlack N** and Wolfrum U (2010) PTC124-mediated read-through of a nonsense mutation causing Usher type 1C. ARVO Annual Meeting 2010 – For Sight, Fort Lauderdale, p3116/A340

Overlack N, Kilic D, Maerker T, Bauss K, van Wijk E, Stern-Schneider G, Roepman R, Kremer H and Wolfrum U (2010) USH1G protein SANS interacts with Myomegalin in mammalian photoreceptor cells. ARVO Annual Meeting 2010 – For Sight, Fort Lauderdale, p2494/A340

Sorusch N, **Overlack N**, Bauß K, Maerker T, van Wijk E, Kersten F, Roepman R, Kremer H and Wolfrum U (2010) The Usher syndrome protein SANS participates in cargo reloading from the post-Golgi transport to the ciliary delivery in photoreceptor cells. FASEB Meeting – Biology of Cilia and Flagella 2010

Sorusch N, **Overlack N**, Bauß K, Maerker T, van Wijk E, Kersten F, Roepman R, Kremer H and Wolfrum U (2010) The USH1G protein SANS interacts with the dynein-dynactin motor component p150^{Glued} and the ciliopathy related CEP290. Pro Retina Research-Colloquium, Retinal Degeneration: 10 years into the new century, where do we go from here?

Wolfrum U, Goldmann T, **Overlack N**, Mueller C, Vetter J M and Nagel-Wolfrum K (2010) Subcellular localization of Usher syndrome proteins in the primate retina. International Symposium on Usher Syndrome and Related Diseases

Jores P, Sorusch N, van Wijk E, Maerker T, Kersten F, Boldt K, **Overlack N**, Bauß K, Glöckner CJ, Roepman R, Ueffing M, Kremer H, Wolfrum U (2009) The periciliary Usher syndrome protein network participates in ciliary cargo delivery in vertebrate photoreceptor cells. ERM-Oldenburg 2009

Wolfrum U, Goldmann T, **Overlack N**, Mueller C, Vetter J M and Nagel-Wolfrum K (2010) Subcellular localization of Usher syndrome proteins in the human retina. ARVO Annual Meeting 2010 – For Sight, Fort Lauderdale, oral presentation

Goldmann T, Rebibo-Sabbah A, **Overlack N**, Nudelman I, Belakhov V, Baasov T, Ben-Yosef T, Wolfrum U and Nagel-Wolfrum K (2009) Pharmacogenetic abatement of a nonsense mutation in Usher syndrome 1C in the retina by aminoglycosides. ARVO Annual Meeting 2009 - Reducing disparities in eye disease and treatment, Fort Lauderdale, 1735/A315

Goldmann T, Rebibo-Sabbah A, **Overlack N**, Nudelman I, Belakhov V, Baasov T, Ben-Yosef T, Wolfrum U and Nagel-Wolfrum K (2009) The potential of aminoglycoside mediated gene based therapy of Usher syndrome 1C in the retina. NWG Meeting, Göttingen, T11-11C

Nagel-Wolfrum K, Goldmann T, Sehn E, Stern-Schneider G, **Overlack N** and Wolfrum U (2009) Subcellular localization of proteins related to the Usher syndrome in human and primate retinas. ARVO Annual Meeting 2009 - Reducing disparities in eye disease and treatment, Fort Lauderdale, 2718/A582

Goldmann T, **Overlack N**, Wolfrum U, Nagel-Wolfrum K (2009) PTC124-mediated translational read through of a nonsense mutation causing Usher type 1C. 9th Annual Meeting of the Interdisciplinary Science Network Molecular & Cellular Neurobiology, Mainz

Nagel-Wolfrum K, Goldmann T, Sehn E, Stern-Schneider G, **Overlack N** and Wolfrum U (2009) Subcellular localization of proteins related to the Usher syndrome in primate retinas. 9th Annual Meeting of the Interdisciplinary Science Network Molecular & Cellular Neurobiology, Mainz

Overlack N, Kilic D, Maerker T, Bauss K, van Wijk E, Kremer H and Wolfrum U (2009) Myomegalin interacts with the USH1G protein SANS and is expressed in mammalian retinas. 8th Annual Meeting of the Interdisciplinary Science Network Molecular & Cellular Neurobiology, Mainz

Nagel-Wolfrum K, Goldmann T, Sehn E, Stern-Schneider G, **Overlack N** and Wolfrum U (2009) Subcellular localization of proteins related to the Usher syndrome in primate retinas. 8th Annual Meeting of the Interdisciplinary Science Network Molecular & Cellular Neurobiology, Mainz

Goldmann T, **Overlack N**, Wolfrum U, Nagel-Wolfrum K (2009) PTC124-mediated translational read through of a nonsense mutation causing Usher type 1C. 8th Annual Meeting of the Interdisciplinary Science Network Molecular & Cellular Neurobiology, Mainz

Sorusch N, **Overlack N**, Bauß K, Maerker T, van Wijk E, Kersten F, Roepman R, Kremer H and Wolfrum U (2009) The mircotubule associated proteins p150^{Glued} and CEP290 are novel binding partners of USH1G protein SANS. 8th Annual Meeting of the Interdisciplinary Science Network Molecular & Cellular Neurobiology, Mainz

Overlack N, Maerker T, van Wijk E, Kersten F FJ, McGee J, Goldmann T, Sehn E, Roepman R, Walsh E J, Kremer H, Wolfrum U (2009) The USH 1 and 2 protein network at the photoreceptor ciliary complex. Pro Retina Research-Colloquium, Retinal Degeneration: Genes-Progression-Therapy, Potsdam

Lagziel A, **Overlack N**, Wolfrum U, Bernstein S L, Morell R J, Friedman T B (2008) Differential expression of cadherin 23 alternate transcripts and protein isoforms in the mouse and primate inner ear and retina. 48th Annual Meeting of the ASCB, San Francisco

Overlack N, Märker T, van Wijk E, Bauß K, Kersten K, Roepman K, Kremer H and Wolfrum U (2008) Novel Components in the Periciliary Usher Syndrome Protein Network of Photoreceptor Cells. ISOCB, San Diego, P20

Wolfrum U, Bauß K, **Overlack N**, van Wijk E, Kersten F, Roepman R, Kremer H and Märker T (2008) Novel SANS interactors in the periciliary Usher syndrome protein network of photoreceptor cells. Arvo Annual Meeting 2008 – Eyes on innovation

Märker T, **Overlack N**, van Wijk E, Bauß K, Frickenhaus M, Kersten F, Goldmann T, Kremer H and Wolfrum U (2008) The periciliary Usher syndrome protein network participates in the molecular transport of vertebrate photoreceptor cells. 31st Annual Meeting of the German Society of Cell Biology (DGZ), Marburg, p14 – S1-23

Lagziel A, **Overlack N**, Wolfrum U, Bernstein S.L, Friedman T.B, Morell R.J (2007) Tissue specific expression of *Cdh23* isoforms during development of the mouse inner ear and retina. 47th Annual Meeting of the ASCB, Washington DC, P233

Bauß K, Märker T, **Overlack N**, van Wijk E, Kersten F, Goldmann T, Kremer H, Wolfrum U (2007) SANS interactors in the periciliary Usher syndrome protein network in photoreceptor cells. 7th Annual Meeting of the Interdisciplinary Science Network Molecular & Cellular Neurobiology, Mainz

Märker T, **Overlack N**, van Wijk E, Roepman R, Kremer H, Reiners J, Gießl A, Wolfrum U (2007) Synaptic localization of a protein network related to the human Usher syndrome in the mammalian retina. European Retina Meeting (ERM), Frankfurt

Märker T, **Overlack N**, van Wijk E, Goldmann T, Kremer H, Uwe Wolfrum (2007) The periciliary Usher syndrome protein network in vertebrate photoreceptor cells. 100th Annual Meeting of the German society of zoology (DZG), Köln, p121 – N41

Märker T, **Overlack N**, van Wijk E, Goldmann T, Roepman R, Kremer H, Wolfrum U (2007) The periciliary Usher syndrome protein network and its role for the molecular targeting to the connecting cilium in mammalian photoreceptor cells. FASEB summer research conferences - "The biology of Cilia and Flagella", Vermont

Wolfrum U, **Overlack N**, van Wijk E, Reidel B, Goldmann T, Roepman R, Kremer H, Märker T (2007) The molecular arrangement of an Usher syndrome protein network at the photoreceptor cilium and its role in the intersegmental transport in photoreceptors. Arvo Annual Meeting 2007 – The aging eye, Fort Lauderdale, p3066/B422

Märker T, **Overlack N**, van Wijk E, Reidel B, Goldmann T, Roepman R, Kremer H, Wolfrum U (2007) The molecular arrangement of an Usher syndrome protein network at the photo-receptor cilium and its role in the intersegmental transport in photoreceptors. 3rd Pro Retina Research-Colloquium Potsdam, Retinal Degeneration: Genes -Progression -Therapy, p46

Overlack N, Märker T, van Wijk E, Reidel B, Goldmann T, Roepman R, Kremer H, Wolfrum U (2007) Retinal expression and integration of the USH1G protein SANS in the USH protein interactom. 7th Meeting of the German Neurosience Society/ 31th Göttingen Neurobiology Conference pTS-15A

Märker T, **Overlack N**, van Wijk E, Reidel B, Goldmann T, Roepman R, Kremer H, Wolfrum U (2006) The molecular organization of an Usher syndrome protein network at the ciliary apparatus and its function in molecular trafficking in photoreceptor cells. IAK 6th Annual Meeting of the Interdisciplinary Science Network Molecular & Cellular Neurobiology, Mainz p15

Märker T, **Overlack N**, van Wijk E, Reidel B, Goldmann T, Roepman R, Kremer H, Wolfrum U (2006) SANS (USH1G) – a scaffold protein in the Usher interactome of photoreceptor cells. Usher syndrome and related disorders symposium, Omaha, p45

Märker T, **Overlack N**, van Wijk E, Reidel B, Roepman R, Kremer H, Wolfrum U (2006) SANS (USH1G) – a scaffold protein in the Usher interactome of photoreceptor cells. ISOCB, Cambridge, P56 (IS6094)

Märker T, **Overlack N**, van Wijk E, Reidel B, Roepman R, Kremer H, Wolfrum U (2006) SANS (USH1G) – a scaffold protein in the Usher interactome of photoreceptor cells. Illuminating Molecular Complexities of the Retina, Potsdam

Märker T, Reiners J, Jürgens K, **Overlack N**, Goldmann T, Wolfrum W (2005) The scaffold protein harmonin (USH1C) also integrates Usher syndrome 2 proteins into synaptic Usher protein complexes in retinal photoreceptor cells. Sixth Meeting of the German Neurosience Society/ 30th Göttingen Neurobiology Conference p160 B

Märker T, Reiners J, van Wijk E, Zimmermann U, Jürgens K, Harf J, te Brinke H, **Overlack N**, Roepman R, Knipper M, Kremer H and Wolfrum U (2005) Usher syndrome type I and II are molecularly linked via the scaffold protein harmonin (USH1C). 5th Annual Meeting of the Interdisciplinary Science Network Molecular & Cellular Neurobiology, Mainz p7

Danke!

Inhaltsverzeichnis

Abbildungsverzeichnis

1. Einleitung

Grundlagenforschung ist notwendig, um weitreichende Erkenntnisse zum Verständnis biologischer Funktionen zu erlangen. Des Weiteren ist Grundlagenforschung unabdingbar, um die Ursachen von Erkrankungen aufzuklären und mit dem gewonnenen Wissen wirksame therapeutische Strategien entwickeln zu können. Die vorliegende Arbeit befasste sich mit der Erforschung der Grundlagen und molekularen Mechanismen der häufigsten Form erblicher Taub-Blindheit beim Menschen, dem Usher-Syndrom (USH). USH-Patienten leiden unter dem Verlust von Hören und Sehen, den zwei wichtigsten Sinnen des Menschen (Saihan et al., 2009; Wolfrum, 2011). Aufbauend auf den Ergebnissen der molekularen und zellulären Grundlagen von USH lag ein weiterer Fokus der vorliegenden Arbeit auf der Entwicklung therapeutischer Strategien zur Behandlung dieses Syndroms. Dabei standen in der vorgelegten Dissertation USH-Typ1-Gene und deren Genprodukte im Mittelpunkt. Insbesondere wurde die Rolle der USH1-Genprodukte Cadherin23 (CDH23/USH1D) und SANS („Scaffold protein containing Ankyrin repeats and SAM domain"/USH1G) im zellulären Kontext der Retina analysiert. Die Erforschung geeigneter Therapiekonzepte konzentrierte sich auf eine Mutation im *USH1C*-Gen, die in einer deutschen Familie vorkommt.

1.1 Das Usher-Syndrom des Menschen

Das Usher-Syndrom (USH) wird autosomal rezessiv vererbt und anhand seiner klinischen Phänotypen in drei Gruppen unterteilt (USH1-3) (Reiners et al., 2006; Saihan et al., 2009; Yan und Liu, 2010; Wolfrum, 2011). Symptome von USH sind Schwerhörigkeit bis hin zur Taubheit, kombiniert mit der Degeneration der Retina (*Retinitis Pigmentosa*), die bis zur vollständigen Erblindung führen kann. Des Weiteren können Gleichgewichtsstörungen auftreten. USH-Typ1 ist die schwerwiegendste Form der Erkrankung. Die betroffenen Kinder werden taub geboren und die retinale Degeneration setzt bereits vor Beginn der Pubertät ein (Reiners et al., 2006; Saihan et al., 2009; Yan und Liu, 2010; Wolfrum, 2011). Bei USH handelt es sich sowohl in Bezug auf die Gene als auch auf die betroffenen Proteine, bzw. Proteinfamilien um eine sehr heterogene Erkrankung (Reiners et al., 2006; Saihan et al., 2009; Yan und Liu, 2010; Wolfrum, 2011).

Die einzelnen klinischen USH-Typen, die betroffenen Gene und die kodierten Proteine mit ihrer Funktion sowie die jeweilige Referenz sind in Tabelle 1 aufgelistet. USH1, die schwerwiegendste Form (Saihan et al., 2009), hat ihren molekularen Ursprung in Defekten der Gene kodierend für MyosinVIIa (USH1B), Harmonin (USH1C), Cadherin23 (USH1D), Protocadherin15 (USH1F), bzw. SANS (USH1G). USH2, die am häufigsten diagnostizierte Form von USH (Bolz, 2009; Saihan et al., 2009), wird durch Defekte von USH2A Isoform b

(USH2A), GPR98/VLGR1b (USH2C) oder Whirlin (USH2D) verursacht. Bei Clarin-1 (USH3A) handelt es sich um den bisher einzig bekannten Vertreter von USH3 (Saihan et al., 2009).

Typ	Lokus	Gen	Protein	Funktion	Referenz
1B	11q13.5	*MYO7A*	MyosinVIIa	molekularer Motor	Weil *et al.*, 1995; Astuto *et al.*, 2000
1C	11p14-15	*USH1C*	Harmonin	Gerüstprotein	Bitner-Glindizcz *et al.*, 2000; Verpy *et al.*, 2000
1D	10q21-q22	*CDH23*	Cadherin23	Zell-Zelladhäsion	Bolz *et al.*, 2001; Bork *et al.*, 2001
1E	21q21	**--**	--	--	Chaib *et al.*, 1997
1F	10q11.2-q21	*PCDH15*	Protocadherin15	Zell-Zelladhäsion	Ahmed *et al.*, 2001; Alagramam *et al.*, 2001
1G	17q24-25	*SANS*	SANS	Gerüstprotein	Kikkawa *et al.*, 2003; Weil *et al.*, 2003
1H	15q22-23	--	--	--	Ahmed et al., 2009
2A	1q41	*USH2A*	USH2A (Usherin)	Zell-Zelladhäsion, extrazelluläres Matrixprotein	Eudy *et al.*, 1998; Bhattacharya *et al.*, 2002; van Wijk *et al.*, 2004
2C	5q13.	*GPR98*	GPR98 (VLGR1b)	Zell-Zelladhäsion, Rezeptor	Burgess *et al.*, 2001; Weston *et al.*, 2004; Yagi *et al.*, 2005
2D	9q32-q34	*DFNB31*	Whirlin	Gerüstprotein	Ebermann *et al.*, 2007
3A	3q25	*CLRN1*	Clarin-1	Zell-Zelladhäsion	Joensuu *et al.*, 2001; Adato *et al.*, 2002

Tabelle 1. Gliederung des Usher-Syndroms (USH) (Stand: September 2011). Den bisher bekannten USH-Subtypen sind Genlokus, identifiziertes Gen, Protein und Funktion zugeordnet. **--** = nicht bekannt.

Obwohl die Mutationen in den bislang neun identifizierten Genen alle zur ähnlichen klinischen Symptomatik von USH führen, erfüllen die betroffenen Proteine ganz unterschiedliche zelluläre Funktionen (Tab. 1). Bei MyosinVIIa beispielsweise handelt es sich um ein Motorprotein, welches den gerichteten Transport entlang von Aktinfilamenten vermittelt (Udovichenko et al., 2002; Inoue und Ikebe, 2003). Die Proteine Harmonin, SANS und Whirlin werden als Gerüstproteine („scaffold proteins") bezeichnet, da sie Interaktionspartner zu zellulären Netzwerken organisieren (Reiners et al., 2005b*; Reiners et al., 2005a; van Wijk et al., 2006; Märker et al., 2008*; Wolfrum, 2011). Die USH-Cadherine Cadherin23 (CDH23) und Protocadherin15 (PCDH15) sind Transmembranproteine, deren extrazelluläre Domänen maßgeblichen Anteil an der Ausbildung von Membran-Membran-Adhäsionen haben (Wolfrum, 2011) (Publikation I und II). Die Gene *USH2A* und *USH2C* kodieren für die größten USH-Proteine (Saihan et al., 2009). *USH2A* kodiert für drei Isoformen, Usherin und zwei Transmembranproteine USH2A Isoform a und b (Eudy et al., 1998; van Wijk et al., 2004). GPR98/VLGR1b (USH2C) (G protein-coupled receptor 98 / very large G protein-coupled receptor 1b) ist der größte bekannte G-Protein gekoppelte sieben-Transmembranrezeptor (Weston et al., 2004). Bei Clarin-1 (USH3A) handelt es sich

um ein vier-Transmembran-Domänen-Protein (Saihan et al., 2009; Wolfrum, 2011). Weitere USH-Genloci konnten bereits eingegrenzt werden. Allerdings konnten die entsprechenden Genprodukte bzw. Proteine bislang noch nicht identifiziert werden (Tab. 1).

1.2 USH-Proteinnetzwerke

Die USH-Proteine gehören unterschiedlichen Proteinfamilien an, und trotzdem kann ein einzelner Defekt zu der Ausprägung von USH führen (Saihan et al., 2009; Wolfrum, 2011). Die Arbeiten der letzten Jahre zur molekularen Charakterisierung von USH machten deutlich, dass die einzelnen Proteine des USH-Komplexes in ihrer zellulären Funktion nicht für sich alleine stehen, sondern über Interaktionen untereinander in USH-Proteinnetzwerken integriert sind (El Amraoui und Petit, 2005; Reiners et al., 2006; Märker et al., 2008*; Wolfrum, 2011). Die einzelnen Netzwerke, die sich in ihrer Proteinkomposition und Funktion unterscheiden, können in ihrer Gesamtheit zu einem USH-Interaktom zusammengefasst werden (Abb. 1) (Roepman und Wolfrum, 2007; Wolfrum, 2011).
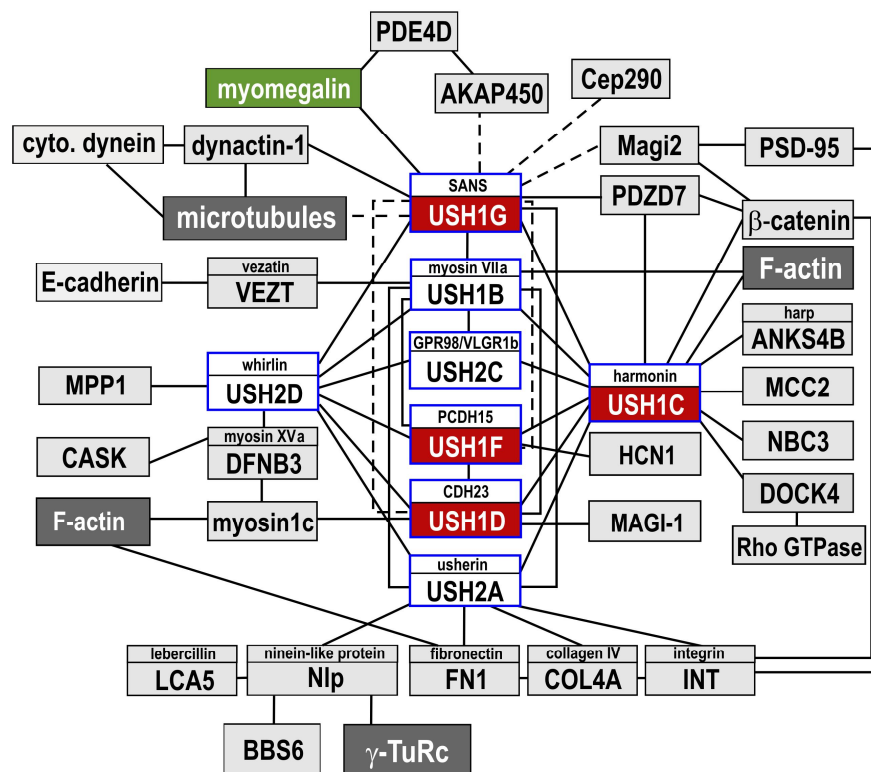
Abbildung 1: Das USH-Interaktom. Eine Auswahl der im USH-Interaktom identifizierten Proteine. Die USH-Proteine sind blau umrandet, hauptsächlich in der Arbeit behandelte Proteine rot unterlegt. Die hier neu charakterisierte Interaktion von SANS mit Myomegalin ist grün hervorgehoben, mit dem Cytoskelett assoziierte Proteine in dunkelgrau. Validierte Interaktionen sind durchgezogene Linien, potentielle Interaktionen gestrichelt dargestellt (modifiziert nach Wolfrum, 2011).

Die Interaktionen der Gerüstproteine Harmonin und Whirlin mit anderen zellulären Partnern werden vornehmlich über ihre PDZ-Domänen (benannt nach den Proteinen PSD-95, DLG,

ZO-1) vermittelt (Boëda et al., 2002; Reiners et al., 2005b*; Reiners et al., 2005a; van Wijk et al., 2006; Märker et al., 2008*). Hier findet die Interaktion meist über sogenannte PBMs (PDZ-Bindemotiv) anderer Proteine, wie zum Beispiel im cytoplasmatischen Bereich von USH2A oder GPR98 statt (van Wijk et al., 2006; Märker et al., 2008*). Auch die USH-Cadherine CDH23 und PCDH15 binden über eine C-terminale PBM an Harmonin (Siemens et al., 2002; Reiners et al., 2005a). Für CDH23 wird diese Interaktion allerdings kontrovers diskutiert (Reiners et al., 2005a; Bahloul et al., 2010; Zheng et al., 2010). Eine aktuelle Arbeit gibt eine interne Sequenz anstelle einer PBM als Bindedomäne an (Zheng et al., 2010). Darüber hinaus konnten Interaktionen von CDH23 mit MyosinVIIa, PCDH15 und MAGI-1 gezeigt werden (Abb. 1) (Reiners et al., 2005a; Xu et al., 2008; Bahloul et al., 2010). Auch SANS, das dritte USH-Gerüstprotein, bindet über seine PBM an Harmonin und Whirlin (Adato et al., 2005; Märker et al., 2008*). Die Bindung an Harmonin wird aber noch über eine zusätzliche Interaktion der C-terminalen SAM-Domäne von SANS an die N-Domäne von Harmonin verstärkt (Yan et al., 2010).

Vorangegangene Arbeiten machten deutlich, dass die USH-Proteine in den von USH betroffenen Sinneszellen in subzellulären Kompartimenten an „hotspots" kolokalisiert sind (Abb. 2) (Saihan et al., 2009; Wolfrum, 2011). Durch eine Vielzahl von Analysen der Expression und der subzellulären Lokalisation der USH-Proteine, sowie deren Interaktions-partnern konnten verschiedene USH-Netzwerke in diversen zellulären Kompartimenten nachgewiesen werden (El Amraoui und Petit, 2005; Reiners et al., 2006; Märker et al., 2008*; Yang et al., 2010; Wolfrum, 2011). So sind alle USH1- und USH2-Proteine an den spezialisierten „Ribbon"-Synapsen der Haarzellen und Photorezeptorzellen lokalisiert. Diese Netzwerke, die vor allem durch Harmonin integriert werden, dürften an der synaptischen Funktion partizipieren (Reiners et al., 2006; Gregory et al., 2011; Wolfrum, 2011).

In den Haarzellen des Innenohrs sind die USH-Proteine an weiteren Netzwerken beteiligt (Abb. 2) (El Amraoui und Petit, 2005; Reiners et al., 2006; Caberlotto et al., 2011; Grati und Kachar, 2011; Wolfrum, 2011). Diese Netzwerke sind für die korrekte Entwicklung der Haarzellen und die mechano-elektrische Signaltransduktion essentiell (El Amraoui und Petit, 2005; Kazmierczak et al., 2007) (Publikation II). Im molekularen Zusammenspiel der Proteine werden transiente Verbindungen durch beispielsweise CDH23, PCDH15, USH2A oder GPR89, gebildet, die für die Heranreifung der Stereocilien notwendig sind (Saihan et al., 2009; Wolfrum, 2011). CDH23 und PCDH15 bilden die für die Signaltransduktion elementaren Untereinheiten der Tip Links an den Spitzen der Haarzellen (Kazmierczak et al.,

2007). Details über die Komposition und Funktion der einzelnen Links in der Organisation, Entwicklung und Stabilisierung der Haarzellen werden in Publikation II dargestellt.
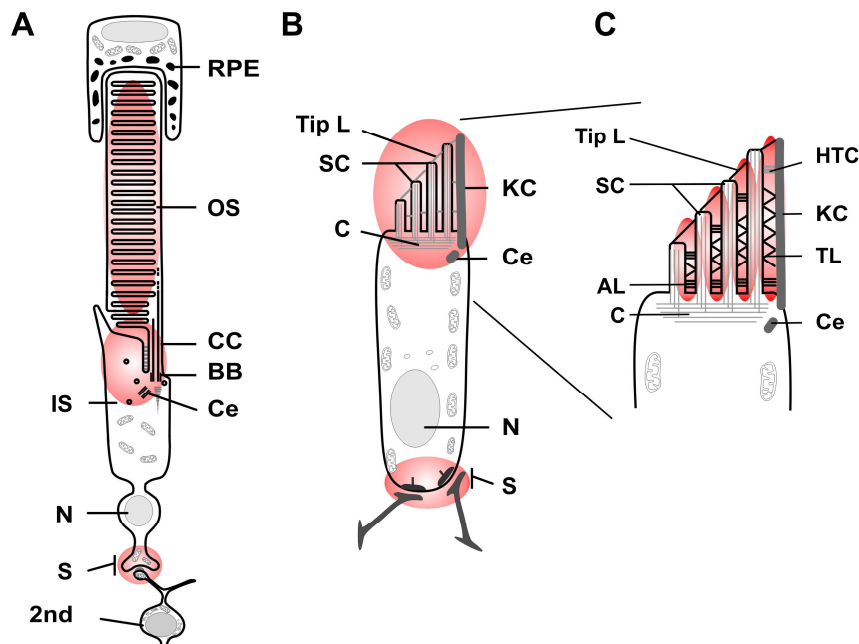
Abbildung 2: Schematische Darstellung der von USH betroffenen sensorischen Zelltypen in Retina und Cochlea. (A) Die Stäbchen-Photorezeptorzelle ist aus morphologischen und funktionalen Kompartimenten aufgebaut. Das lichtsensitive Außensegment (OS) ist über das Verbindungscilium (CC) mit dem biosynthetisch aktiven Innensegment (IS) verbunden. Die „Ribbon"-Synapse (S) verbindet die Photorezeptorzelle mit nachgeschalteten Bipolar- und Horizontalzellen (2nd). N: Nukleus; RPE: retinales Pigmentepithel. **(B, C)** Schema einer Haarsinneszelle. Die Stereocilien (SC) sind in der Kutikularplatte (C) verankert und orgelpfeifenartig angeordnet. Lateral zum längsten SC ist das Kinocilium (KC) lokalisiert. Die benachbarten SC sind an ihren Spitzen über „Tip links" (Tip L) miteinander verbunden. **(C)** Während der Entwicklung existieren noch weitere Verbindungen zwischen den SC, „horizontal top connectors" (HTC), „transient links" (TL) und „ankle links" (AL). Die Lokalisationsschwerpunkte der USH-Proteinnetzwerke in den Photorezeptoren und Haarzellen sind angedeutet (modifiziert nach Overlack et al., 2010/Publikation II).

In den Photorezeptorzellen der Retina sind über die Ribbon-Synapsen hinaus USH-Proteinnetzwerke im Außensegment der Photorezeptorzelle sowie im periciliären Komplex lokalisiert (Abb. 2). Im periciliären Komplex befindet sich eine Art Zielkompartiment, in dem die vesikuläre Fracht von der Transportmaschinerie des Innensegments auf die ciliäre Route in Richtung des Außensegments umgeladen wird (Papermaster, 2002; Märker et al., 2008*). Eine Beteiligung von USH-Proteinen an der Ausbildung dieses Komplexes konnte bereits gezeigt werden (Märker et al., 2008*; Yang et al., 2010; Zou et al., 2011). Interessanterweise wurde das Gerüstprotein Harmonin in diesem zellulären Kompartiment nicht nachgewiesen (Reiners et al., 2003). Vorangegangene Arbeiten zeigten allerdings, dass hier die Funktion des Gerüsts von zwei anderen Proteinen übernommen wird, SANS und Whirlin (Märker et al., 2008*). Für das USH1G-Protein SANS wird eine Beteiligung an gerichteten Transportprozessen im Innensegment zum periciliären Proteinnetzwerk diskutiert (Märker et

al., 2008*). Whirlin dagegen scheint eine Funktion in der Verankerung von USH-Transmembranproteinen, wie USH2A oder GPR98, im Netzwerk zu übernehmen (Märker et al., 2008*). Die beiden „scaffold"-Proteine dienen im molekularen Zusammenspiel mit anderen Proteinen wahrscheinlich der Stabilisierung der Zielmembran und dem Transport von Fracht in Richtung des Außensegmentes von Photorezeptorzellen (Märker et al., 2008*).

Die verschiedenen USH-Netzwerke weisen unterschiedliche Proteinzusammensetzungen auf, wobei die Heterogenität von USH sowie der Proteinnetzwerke durch häufig auftretende Isoformen noch gesteigert wird (Saihan et al., 2009; Wolfrum, 2011). Es existiert eine Vielzahl Isoformen, die mit diversen zellulären Funktionen in den unterschiedlichen Netzwerken einhergehen könnten (Publikation I). Eine Aufklärung der molekularen Komposition der Proteinnetzwerke, aufgebaut durch die USH-Proteine und ihre Isoformen, sollte wichtige Hinweise auf die zelluläre Funktion der USH-Proteine und ihre Netzwerke geben und zudem wertvolle Erkenntnisse zur molekularen Pathogenese von USH aufzeigen. Bei Interaktionspartnern von USH-Proteinen handelt es sich allerdings auch um potentielle Kandidaten für weitere, bisher unbekannte USH-Gene oder um mögliche Modifier von USH-Genen (Bolz et al., 2005; Schneider et al., 2009; Ebermann et al., 2010). Die Suche nach Interaktionspartnern der USH-Proteine ist also nicht nur für die Aufklärung der Netzwerke und deren Funktion notwendig, sondern auch zur weiteren Aufklärung der genetischen Grundlagen von USH.

Die drei ersten Publikationen der vorliegenden Arbeit zielen auf die Analyse der Punkte Expression, Lokalisation und Netzwerkkomposition von USH-Proteinen. Die Expressionsanalyse und subzelluläre Lokalisation von CDH23 und dessen Isoformen stand in Publikation I (und II) im Vordergrund. Publikation III war auf die Analyse von molekularen Interaktionen von SANS in Proteinkomplexen ausgerichtet.

1.3 Therapiestrategien für USH

Bei USH-Patienten sind die zwei Hauptsinne des Menschen, Hören und Sehen, betroffen. Sowohl die USH-Phänotypen, als auch die Analysen von USH-Tiermodellen lassen darauf schließen, dass USH im Innenohr durch Entwicklungsdefekte verursacht wird (Reiners et al., 2006; Saihan et al., 2009; Wolfrum, 2011). Durch Defekte von Proteinen, wie beispielsweise CDH23, können die Stereocilien oder Strukturen wie die Tip Links nicht ordnungsgemäß ausgebildet werden (Di Palma et al., 2001a; Lagziel et al., 2005). Eine Behandlung des Phänotyps in der Cochlea müsste also noch vor der Geburt „*in utero*" durchgeführt werden, damit die Entwicklung der Cochlea korrekt erfolgen kann (Publikation IV). Solche Behandlungen sind z.B. in Mäusen möglich (Dejneka et al., 2004; Bedrosian et al., 2006),

bergen aber große Risiken (Publikation IV). Dagegen werden Cochleaimplantate bereits erfolgreich zur Behandlung des auditorischen Defektes von USH eingesetzt (Pennings et al., 2006). In der Retina ist der Einsatz von Implantaten allerdings noch weit von einer klinischen Routineapplikation entfernt (Stone, 2009). Die Verschaltung und Reizweiterleitung der Impulse im Auge sind sehr viel komplexer als im Ohr (Stone, 2009). Dies macht die Notwendigkeit deutlich, alternative Behandlungsmöglichkeiten für den retinalen Phänotyp von USH zu entwickeln (Publikation IV). Da es sich um eine progressive Degeneration der Retina handelt und nicht um einen Entwicklungsdefekt, besteht ein größeres Zeitfenster für eine therapeutische Intervention zur Behandlung von USH im Auge (Publikation IV).

In den letzten Jahren haben sich eine Reihe von Möglichkeiten zur Behandlung der ophthalmologischen Komponente von USH (*Retinitis Pigmentosa*) potentiell angeboten (Publikation IV). Ein Fokus der vorliegenden Arbeit richtete sich auf die Entwicklung von genbasierten Therapien für USH. Allgemeine Formen der Therapie sind in Publikation IV der vorliegenden Arbeit zusammengefasst.

Seit der Identifizierung des ersten USH-Gens *MYO7A* (Weil et al., 1995) konnten zehn weitere von USH betroffene Genloci bestimmt werden (Tab.1). Die rezessive Vererbung von USH und die Möglichkeit des gezielten Screenings von Patienten nach der jeweiligen Mutation erlauben den Einsatz gentherapeutischer Behandlungsstrategien. Die Kenntnis der spezifischen Mutation ist eine Voraussetzung für den Einsatz von gentherapeutischen Maßnahmen. Da bei ca. 80% der USH-Patienten eine Mutation in einem der bereits bekannten Gene für die Erkrankung verantwortlich ist, kann Gentherapie als eine personalisierte Therapieform für USH eingesetzt werden (Bolz, 2009). Das Wissen um die meisten Gene und die Weiterentwicklungen der Sequenzierungen im „Next Generation Sequencing" erleichtern das Screening nach der spezifischen Mutation (Su et al., 2011).

Die bekannteste Form der Gentherapie ist die Genaddition. Diese kann beispielsweise durch viralen Gentransfer, bei der die exogene wildtypische cDNA unter der Kontrolle eines exogenen Promotors zum Genom „addiert" wird, erreicht werden (den Hollander et al., 2010). Eine weitere Möglichkeit der Gentherapie bietet der Einsatz von Molekülen, die ein Überlesen von Nonsense (Stopp) Mutationen bei der Proteintranslation bewirken (Goldmann et al., 2010*; Goldmann et al., 2011*; Keeling und Bedwell, 2011) (Publikation IV).

Die wahrscheinlich eleganteste Methode zur Therapie von genetischen Erkrankungen stellt allerdings das gezielte therapeutische Gentargeting, also die Reparatur des Gens durch „genomische Chirurgie" dar (Urnov et al., 2010). Hierbei wird die mutierte DNA-Sequenz mittels des zelleigenen Reparaturmechanismus der Homologen Rekombination durch eine

exogene Wildtypsequenz ersetzt und dadurch „repariert" (Porteus und Baltimore, 2003; Urnov et al., 2010). Ein großer Vorteil ist, dass das reparierte Gen unter der Kontrolle des endogenen Promotors verbleibt. Die Expression des Gens erfolgt somit in den natürlichen Mengen und Spleißvarianten. Allerdings ist die spontane Frequenz der Homologen Rekombination in Säugerzellen mit 10^{-6} zu gering, um für therapeutische Maßnahmen geeignet zu sein (Orr-Weaver et al., 1981; Porteus und Baltimore, 2003). Die Frequenz der Homologen Rekombination kann jedoch durch die gezielte Induktion von Doppelstrangbrüchen in der DNA um mehrere tausendfach erhöht werden (Rouet et al., 1994; Choulika et al., 1995). Eine Möglichkeit der gerichteten Induktion von Doppelstrangbrüchen bieten künstlich generierte Zinkfinger-Nukleasen (ZFN) (Kim et al., 1996; Bibikova et al., 2001). Hierbei handelt es sich um chimäre Moleküle, die aus zwei funktionellen Domänen bestehen. Eine dient der DNA-Erkennung und die andere, um die DNA zu schneiden (Abb. 3). Die DNA-Erkennung wird über drei bis sechs aneinander gereihte Zinkfinger (ZF) vermittelt, wobei jeder ZF drei Basen in der DNA erkennt (Pavletich und Pabo, 1991). Die sequenzspezifische ZF-DNA-Bindungsdomäne ist über eine Linker-Sequenz mit der nicht-sequenzspezifischen katalytischen Domäne der Endonuklease FokI fusioniert (Porteus und Baltimore, 2003; Urnov et al., 2005). Durch Kombination der einzelnen ZF kann die DNA-Bindungsdomäne speziell für die jeweilige Zielsequenz designt werden und somit kann, theoretisch, jede DNA-Sequenz geschnitten werden (Abb. 3). Die Funktionalität der ZFN setzt eine Dimerisierung zweier ZFN-Halbseiten oder Module voraus (Kim et al., 1996). Für die Induktion eines Doppelstrangbruchs binden zwei ZFN-Module an gegenüberliegenden Seiten der DNA und bringen die FokI-Untereinheiten in räumliche Nähe zueinander (Porteus und Baltimore, 2003; Urnov et al., 2010). Dabei erkennt jedes ZFN-Modul über seine ZF eine Hälfte der DNA-Zielsequenz. Die Dimerisierung wird über die FokI-Endonuklease induziert und die DNA im Bereich eines 5 - 6 Nukleotide umfassenden „Spacers" zwischen den beiden ZFN-Modulen geschnitten (Abb. 3) (Smith et al., 2000; Porteus und Baltimore, 2003; Mani et al., 2005; Urnov et al., 2010).
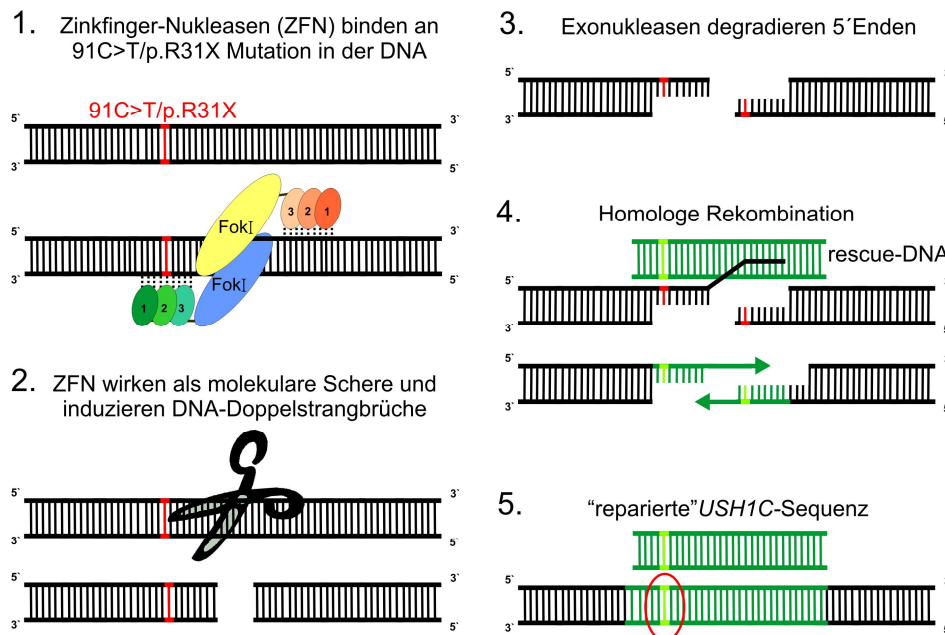
Abbildung 3: Schematische Darstellung der Genreparatur durch Homologe Rekombination vermittelt über Zinkfinger-Nukleasen am Beispiel der *USH1C*-Mutation 91C>T/p.R31X. Zinkfinger-Nukleasen (ZFN) sind als Dimere aktiv. Ein ZFN-Modul besteht aus drei DNA-bindenden Domänen (grüne und rote Kreise) und einer katalytischen Domäne der FokI-Endonuklease (gelbes und blaues Oval). Die ZFN-Module binden spezifisch an die Mutation (rot) flankierenden Basen im „oberen"-Strang (gelb) bzw. „unteren"-Strang (blau) (1.). Die Dimerisierung der FokI-Domänen induziert deren Endonukleaseaktivität und der DNA-Doppelstrang wird geschnitten, die ZFN wirken als molekulare Schere (2.). Der Doppelstrangbruch löst die zelleigenen Reparaturmechanismen der Homologen Rekombination aus, Exonukleasen degradieren die 5´Enden (3. und 4.). Eine exogene rescue-DNA dient während der Homologen Rekombination als Matrize für die Genreparatur von *USH1C* (4.). Dies führt zur Wiederherstellung der nicht-mutierten Gensequenz im endogenen Lokus und somit zur Transkription von funktionalem Harmonin (5.) (modifiziert nach Overlack et al., 2011/Publikation IV).

Im Therapieteil der vorliegenden Arbeit richtete sich der Fokus auf die Entwicklung und Evaluation genbasierter Behandlungsstrategien für USH (Publikation IV und V). Im Mittelpunkt stand dabei die Genreparatur vermittelt über ZFN, die an einer Mutation im *USH1C*-Gen, 91C>T/p.R31X, analysiert werden sollte (Zwaenepoel et al., 2001). Bei dieser Mutation handelt es sich um eine sogenannte Nonsense-Mutation. Durch den Austausch von einem Cytosin zu einem Thymin entsteht an Stelle 91 ein Stopp-Kodon in der cDNA (Abb. 4). Bei der Translation der von diesem defekten Gen gebildeten mRNA wird die Verlängerung des Polypeptids verfrüht gestoppt und ein verkürztes Protein gebildet. Im mutierten USH1C-Protein Harmonin fehlen alle Domänen, die zur Interaktion mit anderen Proteinen notwendig sind (Abb. 4) (Zwaenepoel et al., 2001). Daher kann Harmonin seine Funktion als Gerüstprotein nicht erfüllen, und es kommt zur Ausprägung des schwerwiegendsten klinischen Typs, USH1 (Kremer et al., 2006; Reiners et al., 2006; Saihan et al., 2009; Wolfrum, 2011). Harmonin wird in mindestens 12 verschiedenen Isoformen exprimiert, die in die drei Gruppen a, b und c unterteilt werden können (Abb. 4) (Verpy et al.,

2000; Reiners et al., 2003). Alle Gruppen besitzen eine N-Domäne, die nicht weiter charakterisiert ist, für die aber gezeigt werden konnte, dass sie an der Interaktion von Harmonin mit SANS und CDH23 beteiligt ist (Pan et al., 2009; Yan et al., 2010; Zheng et al., 2010). Die Isoform-Gruppen unterscheiden sich in der Anzahl der vorhandenen PDZ-Domänen sowie coiled-coil-Domänen (Abb. 4). Gruppe b besitzt zusätzlich eine PST-Domäne (Prolin-Serin-Threoin), die mit Aktinfilamenten interagiert (Boëda et al., 2002; Reiners et al., 2003). Insgesamt wurde durch Analysen der *in vitro* Interaktionen gezeigt, dass das USH1C-Protein Harmonin mit allen anderen USH1- und USH2-Proteinen interagiert (Reiners et al., 2006; Wolfrum, 2011; Nagel-Wolfrum persönliche Kommunikation).
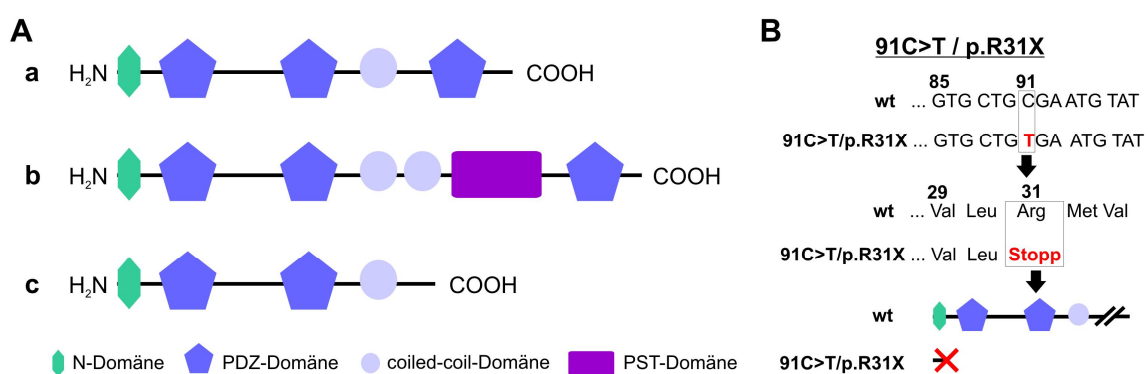
Abbildung 4: Schematische Darstellung der Harmonin-Isoformen und 91C>T/p.R31X-Mutation.
(A) Die Isoformen des USH1C-Proteins Harmonin können in drei Gruppen unterteilt werden a, b und c. Alle Gruppen besitzen N-terminal eine N-Domäne, sowie je nach Gruppe zwei oder mehr PDZ-Domänen und ein bis zwei coiled-coil-Domänen. Isoformen der Gruppe b enthalten zusätzlich eine PST-Domäne.
(B) Eine Nonsense-Mutation an Stelle 91 im *USH1C*-Gen bewirkt einen verfrühten Stopp der Proteintranslation. Das entstehende Peptid enthält keine funktionalen Proteindomänen.

1.4 Zielsetzung der Arbeit

Ziel der vorliegenden Dissertation war es, weitere Erkenntnisse über die molekularen Grundlagen des humanen Usher-Syndroms (USH) zu erarbeiten und damit die Basis für fundierte molekulargenetische Therapiemöglichkeiten in der Retina zu legen. Dabei wurden aktuelle Fragestellungen der USH-Forschung auf unterschiedlichen Ebenen verfolgt. Zum einen wurde das Expressionsprofil eines USH1-Proteins und seiner Isoformen in der Retina und dem Innenohr analysiert. Zum anderen stand die Analyse der Funktion eines USH1-Proteins und dessen Integration in Proteinnetzwerke im Vordergrund. Die Erkenntnisse aus diesen Bereichen der Grundlagenforschung stellten eine notwendige Voraussetzung für die Entwicklung fundierter Therapieverfahren für USH dar, die Ziel des letzten Teils der vorliegenden Arbeit war. Insgesamt wurden in der vorliegenden Arbeit folgende Ziele verfolgt: Die Aufklärung der Expression und Lokalisation von USH-Proteinen, speziell von Cadherin23 (CDH23) **(A)** sowie der molekularen Interaktionen von USH-Proteinen in Proteinnetzwerken und deren Funktion **(B)** in der Retina. Darauf aufbauend war die Evaluation von Therapiestrategien für USH ein Ziel der vorliegenden Arbeit **(C)**.

Zu Teil A: Analyse der Expression und Lokalisation von USH-Molekülen in der Retina.
Vorangegangene Arbeiten zeigten, dass das USH1D-Protein CDH23 differentiell gespleißt wird und an der Entwicklung der Stereocilien der Haarzellen im Innenohr beteiligt ist (Di Palma et al., 2001a; Di Palma et al., 2001b; Lagziel et al., 2005). CDH23 führt durch die Interaktion mit Protocadherin15 zur Ausbildung der Tip Links, die essentiell für die Mechanotransduktion in der Cochlea sind (Siemens et al., 2004; Kazmierczak et al., 2007; Alagramam et al., 2011). Allerdings war bislang über die Expression und Lokalisation der einzelnen Isoformen von CDH23 in der Retina und den Photorezeptorzellen weit weniger bekannt (Reiners et al., 2003). CDH23 und die verschiedenen Isoformen sollten im Hinblick auf die zeitliche und räumliche Expression und Lokalisation - speziell in den Photorezeptorzellen - analysiert werden. Des Weiteren sollten vergleichende Analysen der Isoformexpression zwischen der Cochlea und Retina der Maus sowie der Retina von Primaten durchgeführt werden. Hier sollte analysiert werden, ob sich Unterschiede in der (sub-) zellulären Lokalisation zwischen den Spezies zeigen.

Zu Teil B: Analyse der molekularen Interaktion von USH-Proteinen in retinalen Netzwerken und deren Funktion.

Die Interaktion von Proteinen lässt wichtige Rückschlüsse auf deren zelluläre Funktion zu. In vorangegangenen Arbeiten der AG Wolfrum konnten bereits einige Interaktionspartner des USH1G-Proteins SANS identifiziert werden (Märker, 2007; Märker et al., 2008*). Insgesamt wiesen die Ergebnisse auf eine Beteiligung des Gerüstproteins SANS an Transportprozessen hin (Märker et al., 2008*; Overlack et al., 2008*). Im Vorfeld der vorliegenden Arbeit wurde Myomegalin, mittels Hefe-2-Hybrid Screen, als möglicher Interaktionspartner von SANS identifiziert. Zur Validierung der Interaktion sollten unabhängige Interaktionsassays und Expressionsanalysen von Myomegalin durchgeführt werden. Des Weiteren sollte erstmals die (sub-) zelluläre Lokalisation der Interaktionspartner in der Retina von Mäusen, nicht-humanen Primaten und des Menschen analysiert werden, was Rückschlüsse auf die Funktion des Komplexes ermöglichen sollte.

Zu Teil C: Evaluation von Therapiestrategien für USH, mit dem Fokus auf ZFN-vermittelter Genreparatur.

Für den retinalen Phänotyp von USH und auch viele andere genetisch vererbte Erkrankungen existiert bisher keine effektive Behandlungsmethode. Ein besonderer Fokus der vorliegenden Arbeit lag auf der Evaluation der „Reparatur" eines defekten Genes mittels „genomischer Chirurgie" als Therapie für USH1C. Diese Genkorrektur sollte über die gezielte Induktion von Doppelstrangbrüchen - mittels Zinkfinger-Nukleasen - in der DNA erreicht werden (Bibikova et al., 2001). Die Strangbrüche werden über einen zelleigenen Reparaturmechanismus, die Homologe Rekombination, repariert (Bibikova et al., 2001; Porteus und Baltimore, 2003). Eine exogene „rescue"-DNA dient als Matrize, um die nicht-mutierte Sequenz in das Gen einzubauen (Urnov et al., 2005). Die Therapiestrategie sollte anhand der 91C>T/p.R31X-Mutation auf Zellkulturebene mit Hilfe verschiedener Analyseverfahren evaluiert werden.

2. Publikationen

2.1 Lagziel A, **Overlack N**, Bernstein SL, Morell RJ, Wolfrum U, Friedman TB (2009) Expression of cadherin 23 isoforms is not conserved: implications for a mouse model of Usher syndrome type 1D. Mol Vision. 15:1843-57.

2.2 **Overlack N,** Nagel-Wolfrum K, and Wolfrum U (2010) The role of cadherins in sensory cell function. In: Molecular and Functional Diversities of Cadherin and Protocadherin. Ed.: K.Yoshida, 297-311.

2.3 **Overlack N**, Kilic D, Bauß K, Märker T, Kremer H, van Wijk E, Wolfrum U (2011) Direct interaction of the Usher syndrome 1G protein SANS and myomegalin in the retina. Biochim. Biophys. Acta 1813, 1883-1892.

2.4 **Overlack N***, Goldmann T*****, Wolfrum U, Nagel-Wolfrum K (2011) Current therapeutic strategies for human Usher syndrome. In: Usher Syndrome: Pathogenesis, Diagnosis and Therapy. Ed.: Satpal Ahuja, 377-395 (*both authors contributed equally).

2.5 **Overlack N**, Goldmann T, Wolfrum U, Nagel-Wolfrum K. Gene Repair of an Usher Syndrome Causing Mutation. - eingreicht

Publikation I

2.1 Lagziel A, Overlack N, Bernstein SL, Morell RJ, Wolfrum U, Friedman TB (2009)
Expression of cadherin 23 isoforms is not conserved: implications for a mouse model of
Usher syndrome type 1D. Mol Vision. 15:1843-57.

Expression of cadherin 23 isoforms is not conserved: implications for a mouse model of Usher syndrome type 1D

Ayala Lagziel,[1] Nora Overlack,[2] Steven L. Bernstein,[3] Robert J. Morell,[1] Uwe Wolfrum,[2] Thomas B. Friedman[1]

[1]Section on Human Genetics, Laboratory of Molecular Genetics, National Institute on Deafness and Other Communication Disorders, National Institutes of Health, Rockville, MD; [2]Johannes Gutenberg-University, Institute of Zoology, Department of Cell and Matrix Biology, Mainz, Germany; [3]Department of Ophthalmology, University of Maryland School of Medicine, Baltimore, MD

Purpose: We compared cadherin 23 (*Cdh23*) mRNA and protein variants in the inner ear and retina of wild-type and mutant mice and primates to better understand the pleiotropic effects of *Cdh23* mutations, and specifically to understand the absence of retinal degeneration in *Cdh23* mutant mice.

Methods: Semiquantitative real-time PCR was used to compare the level of expression of *Cdh23* alternative transcripts in the inner ear and retina of wild-type and homozygous *Cdh23^{v-6J}* (*waltzer*) mice. Antibodies generated against CDH23 isoforms were used in immunohistochemistry, immunohistology, electron microscopy, and western blot analyses of mouse and primate inner ear and retina to study the distribution of these isoforms in various cellular compartments.

Results: *Cdh23* mRNA alternative splice variants were temporally and spatially regulated in the inner ear and retina. In the mature mouse retina, CDH23 isoforms were broadly expressed in various cellular compartments of the photoreceptor layer. The wild-type CDH23_V3 protein isoform, which has PDZ binding motifs but neither extracellular domains nor a transmembrane domain, localized exclusively to the outer plexiform layer of the retina containing photoreceptor cell synapses and to the synaptic region of auditory and vestibular hair cells. The longest CDH23 protein isoform, CDH23_V1, appeared by western blotting to be the only one affected by the *Cdh23^{v-6J}* mutation; it was expressed in the wild-type mouse inner ear, but not in the mouse retina. However, CDH23_V1 was detected in western blot analyses of monkey and human retinas.

Conclusions: The time- and tissue-dependent expression patterns that we have shown for *Cdh23* alternative transcripts suggest developmental roles and tissue-specific functions for the various transcripts. Many of these isoforms continue to be expressed in *waltzer* mice. The longest CDH23 isoform (CDH23_V1), however, is not expressed in mutant mice and is necessary for normal inner ear function. The longest isoform is expressed in the retinas of primates, but not detected in the mouse retina. This species difference suggests that the mouse may not be a suitable model for studying the retinitis pigmentosa phenotype of human Usher syndrome type 1D.

Usher syndrome (USH) is the most common genetic disorder that affects both hearing and vision. It is categorized into three clinical subtypes based on age of onset and severity of sensorineural hearing loss, vestibular areflexia, and retinitis pigmentosa (RP). Usher syndrome type I (USH1) is the most severe clinical subtype [1] and is a genetically heterogeneous autosomal recessive disorder. There are seven USH1 loci (*USH1B*, *USH1C*, *USH1D*, *USH1E*, *USH1F*, *USH1G*, and *USH1H*), and the causative genes for five of the loci have been identified [2-4]. The USH1 proteins myosin VIIa (*USH1B*), harmonin (*USH1C*), cadherin 23 (*USH1D*), protocadherin 15 (*USH1F*), and sans (*USH1G*) interact with each other in the inner ear and retina [5-7].

In humans, some cadherin 23 (*CDH23*) missense mutations cause nonsyndromic deafness (DFNB12), whereas

Correspondence to: Thomas B. Friedman, Laboratory of Molecular Genetics, National Institute on Deafness and Other Communication Disorders, National Institutes of Health, 5 Research Court, 2A-19, Rockville, MD, 20850; Phone: (301) 496-7882; FAX: (301) 402-7580; email: friedman@nidcd.nih.gov

truncating nonsense, frameshift, and splice site mutations have been reported to cause USH1D [8-13]. Most of the reported mutations of mouse *Cdh23* cause the *waltzer* phenotype, which is deafness and vestibular dysfunction but no retinal degeneration. *Waltzer* mice are therefore models of DFNB12 nonsyndromic deafness and not USH1D even though at least 11 of the 12 mutant alleles of *Cdh23* are hypothesized to be functional null alleles and are caused by nonsense (*Cdh23^{v-3J}*, *Cdh23^{v-5J}*, *Cdh23^{v-6J}*), frameshift (*Cdh23^v*, *Cdh23^{v-J}*, *Cdh23^{v-4J}*, *Cdh23^{v-7J}*, *Cdh23^{v-Alb}*), or splice site (*Cdh23^{v-2J}*, *Cdh23^{v-ngt}*, *Cdh23^{v-bus}*) mutations [14-16]. One missense mutation, *Cdh23^{sals}*, appears to be a hypomorph [17]. Although there are mouse models for retinal degeneration [18], thus far all waltzer mice do not develop RP and are therefore not models for USH1D [19]. The same is true for mouse mutants of the other USH1 genes including *Myo7a*, *Pcdh15*, *Sans*, and *harmonin*. Even those mutant alleles, reported to be nulls, have lacked significant retinal phenotypes [20-24]. An exception is the *Ush2a* null mouse, which develops progressive photoreceptor degeneration and
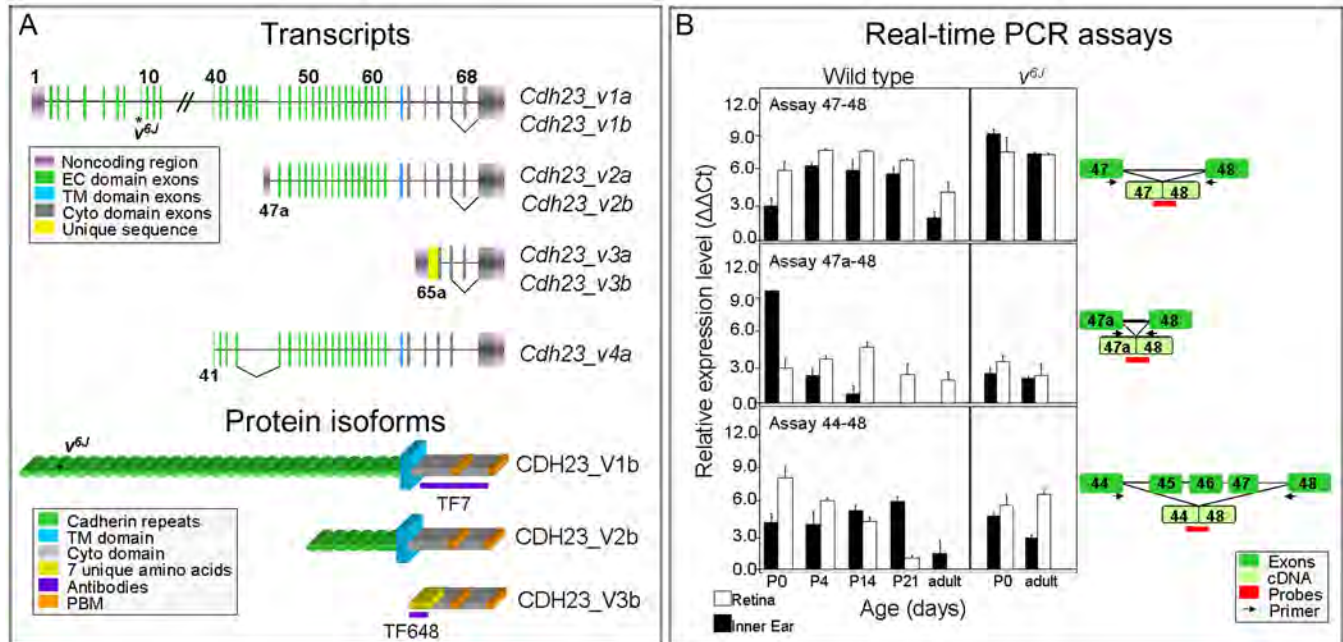
Figure 1. Isoforms, antisera, and expression of cadherin 23 isoforms. **A**: This panel illustrates schematically (not drawn to scale) four classes of *Cdh23* transcripts (GeneID 22295), CDH23 protein isoforms, and the locations of TaqMan probes. Gene and protein variants were designated according to Jax. Transcripts that include exon 68 are designated with an "a," and transcripts lacking exon 68 are designated "b." Protein variants V1, V2, and V3 are encoded by transcripts *v1*, *v2*, *v3*, respectively with (a) or without (b) exon 68. **B**: Bar graphs show data from real-time PCR assays of *Cdh23* transcripts in wild-type and *waltzer Cdh23^{v-6J}* mouse inner ear (black bars) and retina (white bars) during development. The relative expression levels of *Cdh23* transcripts detected with assays 47–48, 47a-48 and 44–48 (**A**) are shown in $\Delta\Delta C_t$ values. Expression levels of *Cdh23* transcripts are reported as $\Delta\Delta C_t$ values, in which the RNA level is: 1) expressed in terms of the cycle at which exponentially accumulating cDNA product can be detected above background in an RT_PCR reaction (the threshold cycle or "C_t"); 2) normalized to the C_t of *Gapdh* as an endogenous control (the "ΔC_t"); and then 3) reported relative to an arbitrarily chosen calibrator, in this case E16.5 inner ear expression level using probe 44–48 ("$\Delta\Delta C_t$"). Abbreviations: extracellular (EC), transmembrane (TM), cytoplasmic (Cyto), PDZ binding motif (PBM).

moderate nonprogressive hearing loss akin to human *USH2A* patients [25].

The longest *Cdh23* transcript (*Cdh23_v1a*) comprises 69 exons encoding 3,354 amino acid residues of a single pass transmembrane protein with 27 extracellular cadherin repeats (ECs). Originally, two *Cdh23* splice isoforms were reported that differed with respect to the presence or absence of exon 68, which encodes a portion of the cytoplasmic domain [8,9,11]. The CDH23 isoform, lacking the 35 residues encoded by exon 68 (*Cdh23_v1b*), is predominantly expressed in the retina [26]. The CDH23 cytoplasmic domain has two putative PDZ binding motifs (PBM; Figure 1A). These PBMs of CDH23 appear to interact with the PDZ domain-containing USH1C protein, harmonin [26], and with the scaffold protein MAGI-1, a member of the membrane-associated guanylate kinase protein family, that was shown to bind to the C-terminal PBM of CDH23 [27].

Additional shorter *Cdh23* transcripts were identified and designated isoform b (*Cdh23_v2*) and isoform c (*Cdh23_v3*). *Cdh23_v2* encodes a protein with only seven EC domains, and *Cdh23_v3* encodes a protein that lacks the EC and transmembrane domains [28,29]. Unlike *Cdh23_v1a*, which

includes exon 68 and is not expressed in the retina [26], transcripts *Cdh23_v2a* and *Cdh23_v3a* are expressed in the retina [28].

In the mouse retina, CDH23 was shown to localize to the inner segment and to the synaptic terminal of photoreceptor cells in the outer plexiform layer [7,30]. In the inner ear, CDH23 was observed to localize to the transient stereocilia lateral links as well as the kinocilial links of the developing sensory hair bundle [28,29,31]. In the mature mouse inner ear, CDH23 expression was detected and was reported by us to be associated with centrosomes, kinocilial links, and Reissner's membrane [28,32]. CDH23 is also a component of the tip link complex [33-37] together with the tip link antigen [38] identified by us as protocadherin 15 [39]. The tip link connects the tips of the shorter stereocilia to the side of its taller neighbor and gates the mechanotransduction channels located on the tops of stereocilia in all but the tallest row [40]. Recently, Rzadzinska and Steel [41] have shown that in the *Cdh23^{v-2J} waltzer* mice, tip links are present in stereocilia bundles of young hair cells, calling into question the role of cadherin 23 as a component of the tip link and suggesting that the molecular composition of the tip link is not yet fully

TABLE 1. PRIMERS AND PROBES DESIGN FOR REAL-TIME TAQMAN ASSAYS OF *CDH23* TRANSCRIPTS.

Assay 47–48	Sequence (5′-3′)
Forward primer	CCAGGAAGACGCCTTTGCT
Reverse primer	CCAGCTCGCGGTTCAGA
Taqman probe	CAGACCCTGTATTGATATTC
Assay 47a-48	
Forward primer	GAGGAGGCGGCCACTC
Reverse primer	CCAGCTCGCGGTTCAGA
Taqman probe	TTCACCATCACAGACCCCT
Assay 44–48	
Forward primer	GCCGAGGTGATGGAGGACT
Reverse primer	CCAGCTCGCGGTTCAGA
Taqman probe	CTCCTGCTGGGTCTGTG

Probes were designed to flank the junctions of *Cdh23* exons 47–48, 47a–48, and 44–48.

resolved. However, the small amounts of normally processed *Cdh23* transcript (approximately 4%) reported in the *Cdh23^(v-2J)* mice [14] may be sufficient wild-type expression to explain the formation of tip links in homozygous *Cdh23^(v-2J)* mice.

There is a range of *Cdh23* transcripts that results from alternate promoter usage (GenBank AY563163, AY563164, AY563159, AY563160) or alternate splicing of cassette exons (GenBank AK039126). The spatiotemporal studies of CDH23 expression thus far can only partially distinguish among the various protein isoforms. In this study we investigate the expression of cadherin 23 mRNA transcripts and protein isoforms to better understand their function in the retina and inner ear, the two tissues affected in USH1D [1]. We also compare the expression of CDH23 protein isoforms in the mouse retina and inner ear as well as human and monkey retinas, in an attempt to gain better insight as to why *Cdh23* mutant mice do not develop RP, unlike humans homozygous for some mutations of *CDH23*.

METHODS

RNA isolation and cDNA synthesis: Total RNA was isolated from 14 to 20 inner ears and retinas of wild-type (B10.A-H2^(h4)/(4R)SgDvEg×C57BL/6)F1 of embryonic day 16.5 (E16.5) and post natal day 0 (P0), P4, P7, P14, P21 as well as RNA from pooled P30 to P90 inner ears and retinas. Total RNA was also isolated from P0 and adult homozygous *v^(6J)* (B10.A-H2^(h4)/(4R)SgDvEg×C57BL/6)F1 mice. Mice were housed in the NIDCD 5 Research Court, animal facility, and were fed NIH 07 ad libitum, and triple filtered chlorinated water was provided. Light cycles are set to be 12 h of light followed by 12 h of darkness. Animals were euthanized by a combination of CO_2 inhalation, cervical dislocation and decapitation. All animal procedures were approved and conducted according to the NIH Animal Care and Use Committee guidelines and Animal Protocol 1263–06 to T.B.F.

RNA was extracted using TRIzol® (Invitrogen, Carlsbad, CA) followed by poly(A)⁺ RNA isolation using Oligotex® mRNA spin-columns (Qiagen, Valencia, CA). First strand cDNA was synthesized from 1 µg of poly(A)⁺ RNA using SuperScript II Reverse Transcriptase and oligo dT priming (Clontech, Palo Alto, CA).

Semiquantitative real-time PCR: TaqMan assays were designed using Assay by Design (Applied Biosystems, Foster City, CA). Probes hybridized to the junctions of *Cdh23* exons 47–48 (NM_023370), the junction of exons 47a-48 (GenBank AY563163, AY563164), and the junction of exons 44–48 (GenBank AK039126; Table 1) are illustrated in Figure 1A. Semiquantitative real-time PCR was performed in triplicates on an ABI 7500 real-time PCR system (Applied Biosystems). PCR reactions were performed in a 50 µl volume containing 1.5 µl cDNA, 25 µl TaqMan Universal PCR Master Mix (Applied Biosystems), 2 µl target primers and probe mix (Applied Biosystems), 1 µl control primers and probe mix (Applied Biosystems) and 20.5 µl of distilled water. Cycling conditions were 50 °C for 2 min, 95 °C for 10 min, followed by 40 cycles of 95 °C for 15 s, and 60 °C for 1 min. A probe to *Gapdh* (Applied Biosystems) was used as the endogenous control. All ΔC_t values are expressed relative to that of E16.5 inner ear cDNA sample using probe 44–48.

Statistical analysis: The data were analyzed by a two-way ANOVA test using GraphPad Prism software version 5 for Windows (GraphPad Software, La Jolla, CA). P values <0.05 were considered statistically significant.

Expression construct: A cDNA encoding the complete sequence of *Cdh23* variant *Cdh23_v3a* (Figure 1A; GenBank AY563159) was PCR amplified from mouse P5 inner ear cDNA [39] using LA Taq DNA Polymerase (Takara Mirus, Madison, WI), cloned into the XhoI and EcoRI sites of GFP-N2 vector (Clontech) and sequence verified. Primers used for cloning: forward (XhoI): 5'-CCG GAT CTC GAG CCT ATG

CAG CCC TGC TGA AGG TTC T-3'; reverse (EcoRI): 5'-CCG GAT GAA TTC CAG CTC CGT GAT TTC CAG AGG GC-3'.

Antibodies: Antisera TF7 was generated against the cadherin 23 cytoplasmic domain (residues 2973–3215 RefSeq NM_023370) [28]. The peptide sequence CMLLPNYRAN derived from the seven unique N-terminus amino acids in CDH23_V3 (residues 1–7; MLLPNYR GenBank AY563159;Figure 1A) with the exception of the N-terminus cysteine (Princeton BioMolecules, Langhorne, PA) was used by Covance (Denver, PA) to immunize three New Zealand white rabbits producing antibodies TF647, TF648, and TF649. We purified antisera using an AminoLink Plus Immobilization Kit (Pierce, Rockford, IL). Antiserum 1D1 was generated against an epitope in the cytoplasmic domain of human CDH23 as previously described [42]. A mouse monoclonal antibody to centrin isoforms Cen1p-Cen4p was used as a molecular marker for the connecting cilium and the adjacent centriole of photoreceptor cells [43]. SNAP25 antibody was used as a marker for hair cell synaptic region (Sternberger Monoclonals Inc., Lutherville, MD). PCDH15 antiserum PB303 was raised in rabbit against a synthetic peptide (CGAEPHRHPKGILRHVKNLAELEK; corresponding to residues 1860–1882 of the mouse PCDH15 sequence, GenBank AAG53891) as previously described by Ahmed et al. [44]. Since PCDH15 was shown to be expressed in the retina, antiserum PB303 was used as a positive control in our retinal western blot analyses.

Transfection of GFP-Cdh23_v3a into HeLa cells: We evaluated the specificity of our antibodies raised against CDH23_V3 (Figure 1A) by performing colocalization assays. Lipofectamine 2000 (Invitrogen) was used to transfect a *GFP-Cdh23_v3a* expression vector into HeLa cells (American Type Culture Collection, Manassas, VA), which do not endogenously express CDH23. After growth for 24 h at 37 °C in 5% CO_2 in Dulbecco's Modified eagle medium (DMEM; Invitrogen) supplemented with 10% fetal calf serum (FCS; Invitrogen), transfected cells were fixed with 4% paraformaldehyde and processed for immunostaining [45] using a 1:200 dilution (roughly 0.5 mg/ml stock) of antibodies TF648 and TF649. Anti-GFP antibody (Sigma-Aldrich, St. Louis MO) was used in western blots of protein extracts of transfected and untransfected HeLa cells.

Western blot analyses: Western blot analyses were performed as previously described [28,44]. Fresh P0 to P90 inner ears and retinas of wild-type C57BL/6J and homozygous *Cdh23*[v-6J] mice were dissected. Proteins were extracted and denatured by boiling for 5 min in SDS–PAGE sample buffer (0.125 M Tris–HCl, 20% glycerol, 4% SDS, 0.005% bromo-phenol blue). A 20 µg protein sample was separated on 4%–20% Tris-glycine gels (Invitrogen) for blots incubated with antibody TF648. We used 3%–8% Tris-acetate gels (Invitrogen) for blots incubated with antibody TF7. SeeBlue Plus2 pre-stained

standard (Invitrogen) was used as size markers. Gels were transferred to polyvinyldifluoride (PVDF) membranes (Millipore, Billerica, MA), and blocked overnight with 5% dry milk in TBST (10mM Tris-HCl pH 7.5, 150 mM NaCl, 0.05% Tween-20). Primary antibodies were diluted 1:1,000 from a roughly 0.5 mg/ml stock. Alkaline phosphatase-conjugated anti-rabbit secondary antibody was used at a 1:10,000 dilution (Promega, Madison, WI). ECL Plex Cy5 and Cy3 secondary antibodies were used in a 1:2,500 dilution. Fluorescent signals were detected and images captured on a Typhoon Trio Plus imaging system (GE Healthcare Bio-Science Corp., Piscataway, NJ). As a control to be sure that large retinal proteins were transferred to the membrane used in this western blot, we used validated antisera PB303 generated against PCDH15 [44] that, as expected, recognized a band of approximately 220 kDa (data not shown).

Immunohistology of mouse retina: Some eyes of adult wild-type mice were cryofixed in melting isopentane without chemical prefixation and cryosectioned as described elsewhere [46]. Cryosections were placed on poly-L-lysine-precoated coverslips and subsequently incubated with 0.01% Tween-20 in phosphate buffered saline (PBS, Quality Biologic, Inc., Gaithersburg, MD; 90 g/l NaCl, 1.44 g/l KH_2PO_4, 7.95 g/l Na_2HPO_4 anhydrous pH 7.4 [10×]) for 20 min. After PBS washing steps (2×5 min at room temperature-RT), sections were, sections were covered with blocking solution that contained 0.5% cold-water fish gelatin plus 0.1% ovalbumin in PBS. Next, sections were incubated for a minimum of 30 min followed by overnight incubation with primary antibodies, diluted in blocking solution at 4 °C. Washed cryosections were incubated for a minimum of 1.5 h at room temperature in the dark with secondary antibodies conjugated to Alexa 488 or Alexa 568 (Invitrogen, Karlsruhe, Germany) in PBS with 4',6-Diamidin-2'-phenylindoldihydrochlorid (DAPI; Sigma-Aldrich, Deisenhofen, Germany) to stain the DNA of the cell nuclei. After 3x10 min washings with PBS at RT, sections were mounted in Mowiol 4.88 (Hoechst, Frankfurt, Germany). Mounted retina cryosections were analyzed by microscopy (DMRB; Leica microsystems, Bensheim, Germany). Images were obtained with an ORCA-ER camera (Hamamatsu, Herrsching, Germany) and processed with Adobe Photoshop CS (Adobe Systems, San Jose, CA).

Immunofluorescence of mouse inner ear: Mouse inner ears were removed by dissection and cochleae were perfused through the round window with 4% paraformaldehyde (PFA) and incubated in PFA for 2 h at RT. The organ of Corti and vestibular tissues were dissected from the cochlear spiral in PBS. Samples were permeabilized in 0.5% Triton X-100 (Acros Organics, Morris Plains, NJ) for 30 min and then washed in PBS. Non-specific binding sites were blocked using 5% normal goat serum (Gibco-Invitrogen) and 2% BSA (BSA, Gibco-Invitrogen) in PBS for 1 h. Samples were
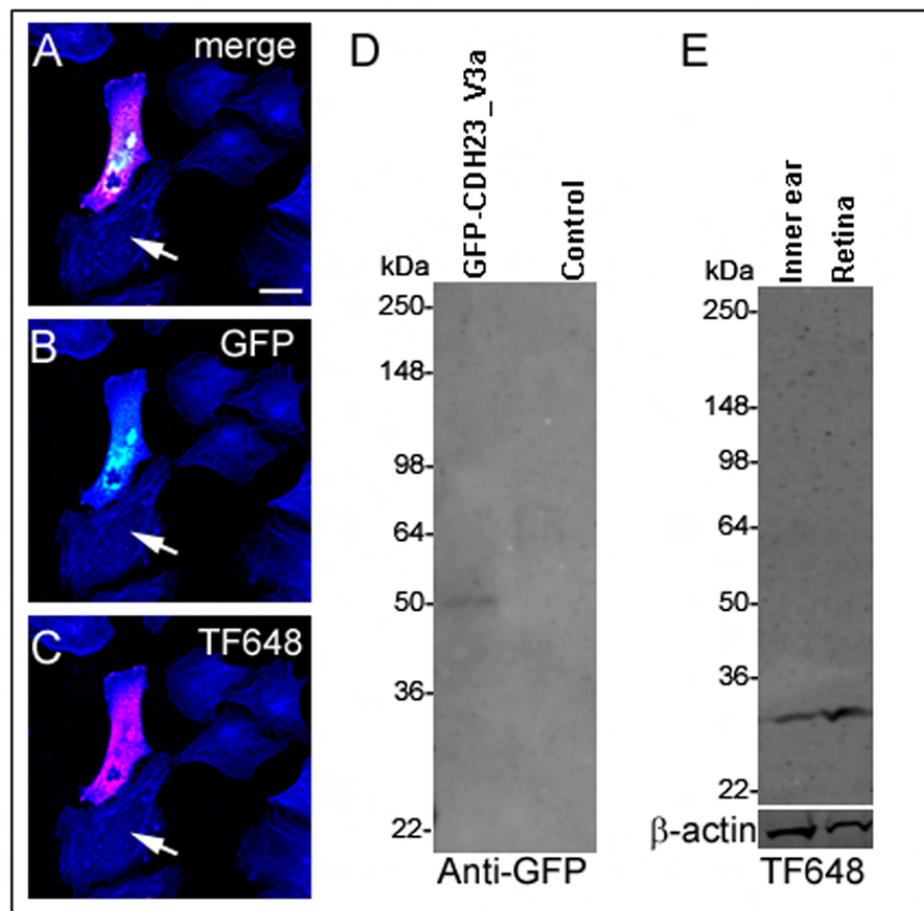
Figure 2. Validation of CDH23_V3 antisera. In **A-C**, arrows indicate untransfected cells; F-actin is stained in blue. **A**: A merged image showing HeLa cells 24 h after transfection with the expression vector *GFP-Cdh23_v3a* (see isoform designation Figure 1A). Cells were stained for CDH23_V3 with antibody TF648 (red) and F-actin antibody (blue). GFP fluorescence of transfected cells (green; **B**) overlapped with TF648 antibody staining (red; **C**) as revealed in the merged image (**A**). Scale bar equals 20 µm. **D**: A western blot was used to analyze protein extracts from HeLa cells transfected with *GFP-Cdh23_v3a* and untransfected controls. In the lysate of transfected cells a band of the expected size of roughly 50 kDa of the GFP-CDH23_V3a fusion protein (GFP approximately 27 kDa; CDH23_V3a approximately 26 kDa) was detected. **E**: Western blot of protein extracts from P60 mouse inner ear and retina revealed a band of roughly 26 kDa corresponding in size to CDH23_V3. β-actin was used as a loading control. Size standards are given in kDa.

incubated for 2 h in primary antibodies at a concentration of ~0.5 µg/µl in blocking solution and rinsed in PBS. Samples were then incubated for 30 min in a 1:200 dilution of anti-rabbit IgG fluorescein 488 (Amersham Biosciences, Piscataway, NJ) and Alexa Fluor 594 goat anti-rabbit (Molecular Probes-Invitrogen Eugene, OR) secondary antibodies. Rhodamine-phalloidin and Alexa fluor 633 (Molecular Probes-Invotrogen) were diluted 1:100 and used to visualize F-actin. Samples were mounted using ProLong Antifade Kit (Molecular Probes-Invitrogen). Images were captured on a Carl Zeiss LSM-510 laser scanning confocal microscope.

Immunoelectron microscopy: For immunoelectron microscopy a recently introduced protocol was applied [47]. Eyes were perforated and lenses were removed during fixation of isolated mouse eyes in 4% PFA in Soerensen buffer that contained 0.1 M disodiumhydrogenphophate and 0.1 M potassiumdihydrogenphosphate, pH 7.3. After washing (4×15 min at RT) retinas were dissected from eye cups and infiltrated with 10% and 20% sucrose in Soerensen buffer, followed by incubation in buffered 30% sucrose overnight. After four cycles of freezing in liquid nitrogen and thawing at 37 °C retinas were washed in PBS and embedded in buffered 2%

agar (Sigma-Aldrich). Agar blocks were sectioned with a vibratome (Leica, Wetzlar, Germany) in 50 µm slices. Vibratome sections were blocked in 10% normal goat serum, 1% BSA in PBS and subsequently incubated with primary antibodies against CDH23 (TF7) for four days at 4 °C. After washing with PBS (4×15 min at RT) the appropriate biotinylated secondary antibodies (Vector Laboratories, Burlingame, CA) were applied to the sections. After washing with PBS (4×15 min at RT) the appropriate were visualized by a Vectastain ABC-Kit (Vector Laboratories) according to manufactor's protocol. Subsequently, stained retinas fixed in 2.5% glutaraldehyde in 0.1 M cacodylate buffer (pH 7.3) and diaminobenzidine precipitates were silver enhanced [48,49], followed by postfixation in 0.5% OsO$_4$ in 0.1 M cacodylate buffer (pH 7.3) on ice. Dehydrated specimens were embedded in araldite. Ultrathin sections (< 60 nm) were analyzed in a Tecnai 12 BioTwin transmission electron microscope (FEI, Eindhoven, The Netherlands).

Immunohistology of human and monkey retinas: Eyes from three-year-old monkeys were obtained by S.L.B. from John Cogan (Bureau of Biologics, FDA, Bethesda, MD). Tissue was fixed in 4% PFA-PBS and frozen in OCT. Frozen sections of 10 µm were blocked for 1 h with 5% normal goat serum
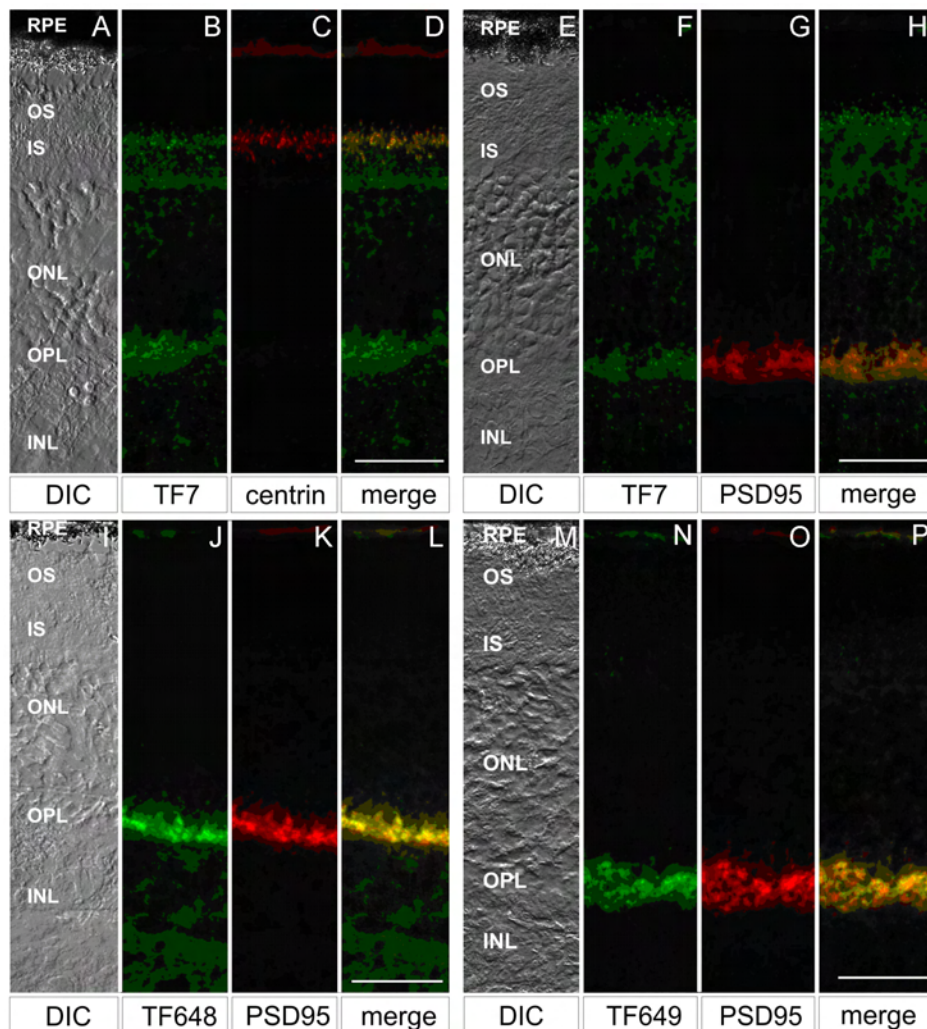
Figure 3. Different CDH23 protein isoforms localize to distinct cell layers of the retina. **A, E, I**, and **M** are differential interference contrast (DIC) images of longitudinal cryosections (**B-D, F-H, J-L** and **N-P**, respectively) through adult mouse retina showing photoreceptors cell layers. Indirect immunofluorescence labeling of CDH23 with the cytoplasmic domain antibody TF7 (**B**) revealed CDH23 in the ciliary region of photoreceptor cells, the ONL, and in the OPL. Double labeling with antibodies TF7 and centrin, a ciliary marker (**C**), revealed colocalization of CDH23 and centrin in the ciliary apparatus of the photoreceptor cells (**D**). **F-H**: Double labeling with antisera TF7 (**F**) and the synaptic protein PSD-95 with antisera PSD95 (**G**) revealed CDH23 colocalization with PSD-95 in the synaptic terminals in the OPL of photoreceptors cells (**H**). Double labeling with CDH23_V3 specific antibodies TF648 and TF649 (**J, N**) and PSD95 (**K, O**) revealed that CDH23_V3 was detected only in the OPL where it colocalized with PSD-95 (**L, P**). Scale bars represent 10 µm. Abbreviations: retinal pigment epithelium (RPE), outer segment (OS), inner segment (IS), outer nuclear layer (ONL), outer plexiform layer (OPL), and inner nuclear layer (INL).

containing 2% bovine serum albumen. Tissue sections were reacted overnight at 4 °C with primary antibody (TF7) at a concentration of 5 µg/ml containing 2% BSA. Treated sections were incubated with alkaline phosphatase secondary antibody (Vector Laboratories, Burlingame, CA). The slides were not counterstained. Human donor eyes were obtained from a Caucasian male (74 years old) who died of congestive heart failure. Human eyes were obtained 6 h post-mortem by S.L.B. from the Maryland State Anatomy Board under IRB exemption SB-019701. The anterior segment eye tissues (cornea, iris) and posterior non-retina tissues (lens, vitreous, ciliary body) were removed. Proteins from human retina were extracted and processed for western analyses.

RESULTS

Cdh23 expression in wild-type and waltzer inner ear and retina: Three semiquantitative real-time PCR assays that could distinguish among some but not all of the *Cdh23* isoforms were used to examine the expression of *Cdh23* transcripts. Real-time PCR assay 47–48 was designed to detect a class of *Cdh23* transcripts, which includes, but is not limited to, full-length *Cdh23_v1* (Figure 1A). Expression of this class of transcripts varied significantly both by age and tissue source (Figure 1B, top panel). Two way ANOVA reveals that the expression of this class of transcripts varies significantly both by age and between tissue types, with a p-value <0.0001 for interaction of age and tissue type. Transcripts with the junction of exons 47–48 were present at all ages in both tissues, but were most abundant around age P14. The sustained expression detected in the adult inner ear was consistent with previous published reports describing expression of the longest CDH23 isoform in wild-type mouse inner ear, which appeared to be a component of the tip link [32,37]. The sustained expression may also be due to the expression of still unknown *Cdh23* splice variants.

In the homozygous mutant *Cdh23^v-6J* inner ear and retina, the transcripts detected by assays 47–48 maintained a stable level of expression throughout development. Age and tissue have no significant effect on transcript expression levels in
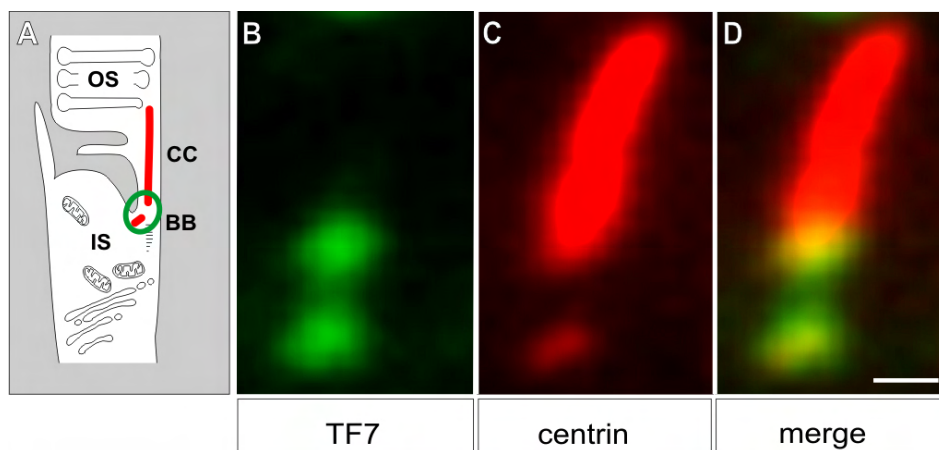
Figure 4. CDH23 is localized in the basal body and ciliary apparatus of photoreceptor cells. **A:** A schematic representation of a part of rod photoreceptor cell: the outer segment (OS) is linked by the ciliary apparatus composed of the connecting cilium (CC) and the basal body complex (BB) to the inner segment (IS). **B-D**: Immunofluorescence microscopy analyses of double labeling for CDH23 with TF7 (**B**) and anti-centrin (**C**) antibodies (marker for the ciliary apparatus: CC and BB) is shown in longitudinal cryosections through the ciliary part of mouse photoreceptor cells. **D**: Merged image of (**B**) and (**C**) indicates partial colocalization of CDH23 with centrin in the BB. Scale bar represents 0.25 µm.

Cdh23^{v-6J} mice (two-way ANOVA, p=0.05 and p=0.08 respectively). However, compared to the corresponding wild-type transcripts expression levels, the *Cdh23^{v-6J}* mutation contributed to a higher level of expression in the adult inner ear and retina (two-way ANOVA; p<0.0001). The *waltzer Cdh23^{v-6J}* allele is a G to T transversion occurring in exon 9 and was predicted to truncate the protein in EC3 of the longest *Cdh23* transcript *Cdh23_v1* [14,15]. Because this nonsense mutation is close to the 5' end of *Cdh23*, transcripts that include exons 47 and 48, but are initiated from promoters downstream of exon 9, would be unaffected and detected in real-time PCR assay 47–48.

Real-time TaqMan assay 47a-48 detects transcripts *Cdh23_v2a* and *Cdh23_v2b* that contain exons 47a and 48 (Figure 1A). These transcripts use an alternate promoter upstream of exon 47a and they lack 20 ECs encoded by exons 2–46 (RefSeq NM_023370) [28]. In wild-type mice these transcripts were expressed in the retina at all time points and only transiently in the inner ear (two-way ANOVA for tissue and age; p<0.0001; Figure 1B). Expression level in the retina was unchanged in the homozygous *Cdh23^{v-6J}* mutant, and was upregulated in the adult inner ear of *Cdh23^{v-6J}* mutants (Figure 1B).

Assay 44–48 recognizes the class of transcripts with exon 44 spliced directly to exon 48, which we designated as isoform *Cdh23_v4 (*Figure 1A). The existence of *Cdh23_v4* was based on a partial cDNA (GenBank AK039126), whose promoter and protein products are unknown. There may be many different cDNAs that omit exons 45–47, so the transcript in Figure 1A was meant to represent a class of potential alternatively spliced transcripts of *Cdh23* that can be identified by our real-time PCR assay.

The expression pattern of *Cdh23_v4* is almost the converse of *Cdh23_v2* in that the expression was maximal at earlier stages in the wild-type retina and was downregulated in adult retina, while moderate expression was observed at all time points in the wild-type inner ear (Figure 1B, lower panel). As with the other assays, transcripts with this structure were detected in both the inner ear and retina of *Cdh23^{v-6J}* mutant mice and were upregulated in the retina relative to the wild-type adult retina (two-way ANOVA; p<0.0001).

Western blot analyses using CDH23_V3 antibodies: *Cdh23_v3a* and *Cdh23_v3b* are short transcripts (708 and 600 nucleotides, respectively) initiated from a promoter in intron 65 and encode 235 and 199 amino acid proteins lacking ECs and transmembrane domains. CDH23_V3a/b expression was evaluated with antibodies TF648 and TF649, directed to the seven unique amino acids encoded at the N-terminus that differentiate this isoform from other CDH23 isoforms (Figure 1A). The antibodies were validated by transfecting a *GFP-Cdh23_v3a* (Figure 1A) expression vector into HeLa cells. Twenty-four hours after transfection the staining pattern obtained with the GFP-CDH23_V3a overlapped with the staining pattern obtained with antibody TF648. Nontransfected cells did not show antibody staining (Figure 2A-C).

Western blot analyses of transfected and untransfected cells revealed a band of approximately 50 kDa corresponding in size to the predicted size of the GFP-CDH23_V3a fusion protein (approximately 53 kDa; GFP approximately 27 kDa and CDH23_V3a approximately 26 kDa; Figure 2D). Western blot analyses of mouse inner ear and retina protein extracts revealed that antibody TF648 recognizes a band corresponding to the predicted size of CDH23_V3 (roughly 26 kDa) both in the inner ear and the retina (Figure 2E). Similar results were obtained with antibody TF649 (data not shown).
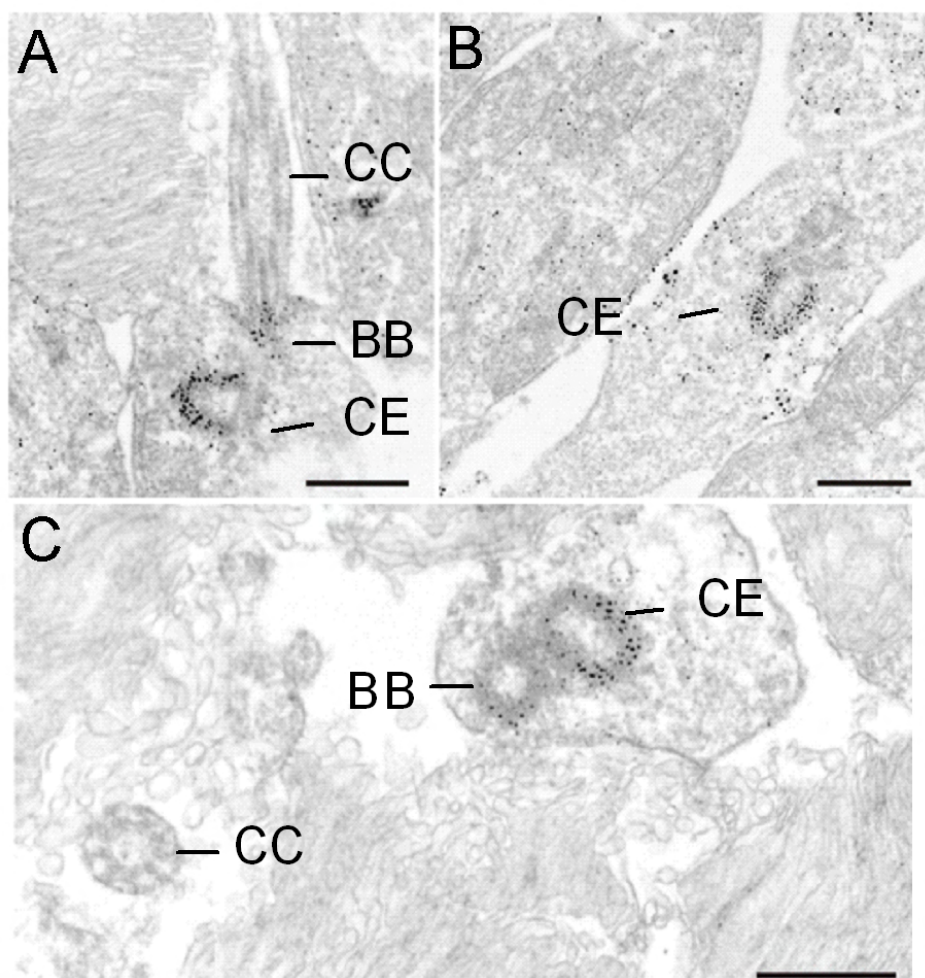
Figure 5. Immunoelectron microscopic localization of CDH23 in mouse rod photoreceptor cells. Electron micrographs show CDH23 labeling with TF7 antibody in ultrathin sections through parts of mouse photoreceptor cells. **A-C**: CDH23 labeling is detected in the basal body (BB) and centriole (CE) of the apical inner segment of photoreceptor cells. **A, C**: The connecting cilium (CC) is not labeled. Scale bar represents 0.2 μm.

Photoreceptor subcellular distribution of cadherin 23 isoforms: The subcellular distribution of CDH23 in the retina was determined by analyzing cryosections through adult mice eyes by immunofluorescence with antibody TF7, which recognizes the CDH23 cytoplasmic domain, and therefore multiple Cdh23 isoforms (Figure 1A, lower panel). Cryosections of mouse retinas were double-labeled either with anti-centrin as a marker for the ciliary apparatus of photoreceptor cells [43], or anti- PSD95 as a marker for the pre- and post-synaptic terminals of photoreceptor cells located in the outer plexiform layer [50]. Double labeling with TF7 and anti-centrin (Figure 3A-D) revealed CDH23 in the ciliary region, the outer nuclear layer, and in the outer plexiform layer. Double-labeling with TF7 and anti-PSD95 (Figure 3E-H) confirmed localization of CDH23 in the outer plexiform layer. Higher resolution imaging of double-labeling immunofluorescence with TF7 and anti-centrin revealed partial colocalization of CDH23 protein isoforms and centrins in the basal bodies of the ciliary apparatus of photoreceptor cells (Figure 4). Pre-embedding high resolution immunoelectron microscopy, using antibody TF7, localized

CDH23 in the basal body of the cilium and its adjacent centriole and confirmed CDH23 as a component of the ciliary apparatus (Figure 5) [42].

CDH23_V3 localizes to the synaptic region of photoreceptor cells: Cryosections through adult mice eyes were double-labeled with the CDH23_V3 isoform specific antibodies TF648 and TF649, and an anti-PSD95, respectively. Immunofluorescence double-labeling showed colocalization of CDH23_V3 and PSD95 at the synaptic terminals of photoreceptor cells (Figure 3I-P). CDH23 immunoreactivity was also observed in this region using antibody TF7 directed against CDH23 cytoplasmic domain (Figure 3E-H). This overlap was expected since antibody TF7 should recognize CDH23 protein isoforms, which include the cytoplasmic domain or portions of it, such as CDH23_V3. No signal was detected in the photoreceptor inner segment and outer nuclear layer with CDH23_V3 specific antibodies TF648 and TF649 (Figure 3I-P).

CDH23_3 is expressed in the synaptic region of auditory and vestibular hair cells: Mouse inner ears hair cells were double-labeled with anti-SNAP25 and CDH23_V3 antibody TF648.
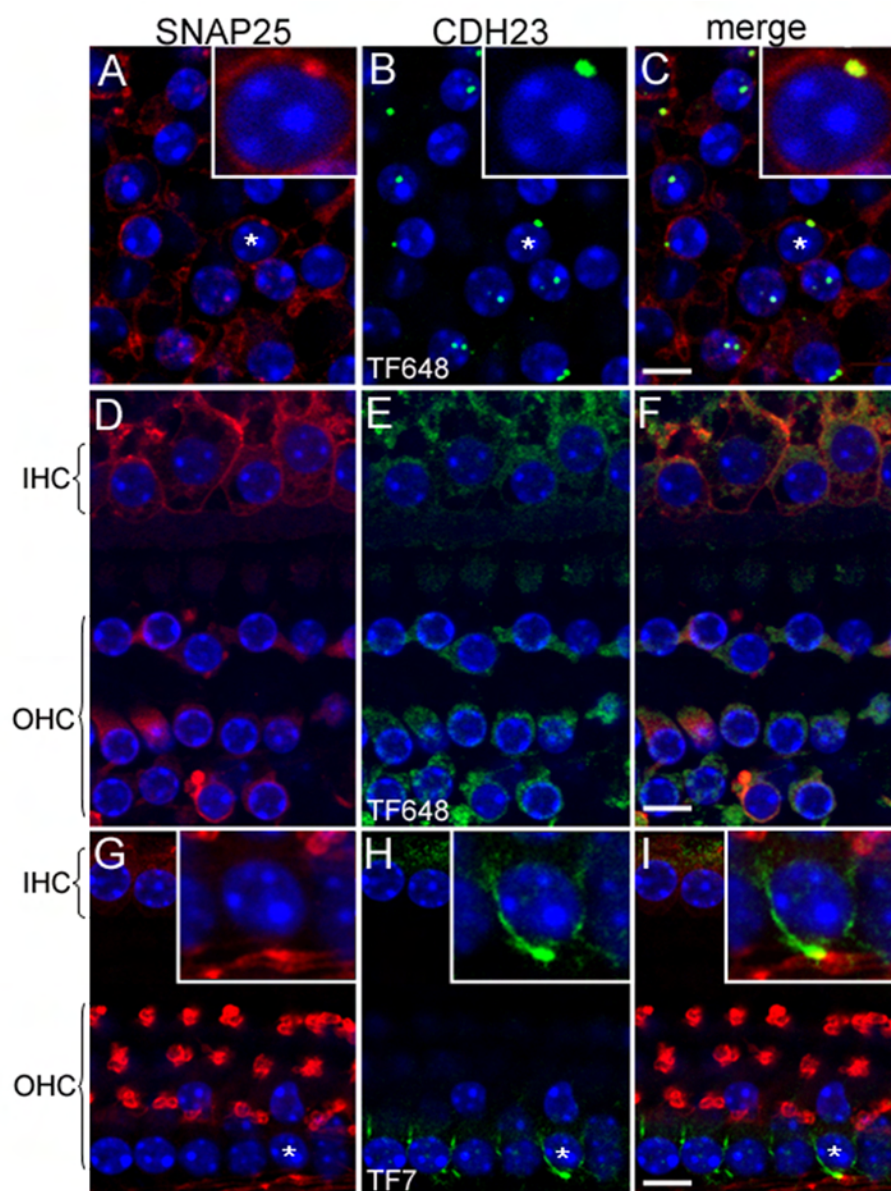
Figure 6. CDH23 localizes with SNAP25 to the synaptic region of mouse auditory and vestibular hair cells. In **A-I** nuclei were stained with DAPI (blue). SNAP25 is shown in red, and CDH23 in green. **A**: The synaptic region of utricular hair cells stained with SNAP25. **B**: CDH23_V3 detected with antisera TF648. **C:** In the merge image (**C**) of panels **A** and **B**, CDH23_V3 shows partial colocalization with SNAP25 in the synaptic region of utricular hair cells. The insets in **A-C** show a twofold magnification of a hair cell (asterisk) synaptic area. In the merge image (**F**) of panels **D** and **E**, CDH23_3 and SNAP25 show partial colocalization in the synaptic region of inner (IHC) and outer (OHC) hair cells. **G**: SNAP25 staining of IHC and OHC synaptic fibers. **H**: CDH23 is detected with antiserum TF7 in the synaptic fibers of IHC and OHC. **I**: In the merge image (**I**) of panels **G** and **H**, CDH23 shows partial colocalization with SNAP25 in the region of the synaptic fibers of IHC and OHC. In **G-I**, the insets are a twofold magnification of the region (asterisk), where CDH23 localizes in the synaptic fibers. Scale bars equal 5 μm.

SNAP25 localizes to the synaptic region of hair cells [51]. CDH23_V3 immunoreactivity was detected as large punctae in the basal end of vestibular hair cells, partially colocalizing with SNAP-25 in the synaptic region of vestibular (Figure 6A-C) and auditory (Figure 6D-F) hair cells. Similar results were seen with for the CDH23 cytoplasmic domain antibody TF7 and anti-SNAP25 in vestibular hair cells (data not shown) and in the synaptic fibers in the region below auditory hair cell nuclei (Figure 6G-I).

Expression of CDH23 in the monkey retina: Using CDH23 cytoplasmic domain antibody TF7, we detected CDH23 immunoreactivity in the region between the inner and outer segments of photoreceptor cells of monkey retina (where the connecting cilium and basal bodies are present), in the outer plexiform, and in the inner and outer nuclear layers, similar to the pattern observed in the mouse retina (Figure 3). Prominent CDH23 immunoreactivity was observed in the base of the cone inner segments (Figure 7A, C), a pattern of staining not observed in the mouse retina (Figure 3). Some CDH23 immunoreactivity was also detected in rod photoreceptors although less prominent than in the cone photoreceptors, possibly due to their structure and because cone photoreceptor staining is more obvious in frozen sections of monkey retina.

CDH23_V1 is expressed in primate retina but not in mouse retina: We performed western blot analyses of mouse protein extracts from P0, P4, and adult wild-type, and P0 and adult mutant inner ear and retinas using TF7 antibody. Results were
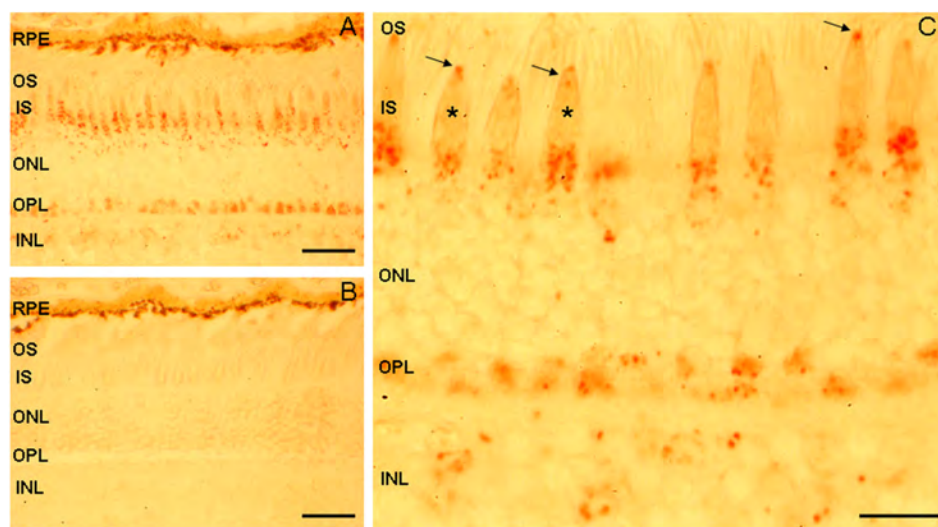
Figure 7. Immunolocalization of CDH23 in photoreceptor cells of monkey retina. **A**: CDH23 immunoreactivity was detected with antisera TF7 in the IS and in the synaptic terminals of the OPL of photoreceptor cells. Some staining is evident in the photoreceptor cell bodies of the ONL and INL. **B**: No immunoreactivity was observed in the controls stained only with secondary antibody. **C**: In a higher magnification, CDH23 staining is visible in the evenly spaced IS of cone-shaped photoreceptors (asterisks) and in the regions between the IS and OS where the ciliary apparatus is present (arrows). Rod photoreceptors are also positively stained (seen as thin long strings). The dark brown pigment in the upper portion of **A** and **B** is melanin of the RPE. **C:** Scale bars represent 5 µM. Magnification: **A, B** 400× and **C** 1000×. Abbreviations: retinal pigment epithelium (RPE), outer segment (OS), inner segment (IS), outer nuclear layer (ONL), outer plexiform layer (OPL), inner nuclear layer (INL).

obtained from 3 to 4 independent protein extractions replicated 2 to 9 times. Representative western blots (Figure 8) revealed a large band of ~350 kDa corresponding in size to CDH23 longest protein isoform (CDH23_V1) only in P0 and P4 wild-type inner ear (Figure 8A-C). This large band was not detected in wild-type P0, P4, P60, or P90 retinas and was not detected in the *waltzer Cdh23^{v-6J}* inner ear or retinal samples (Figure 8A-C). A trace of this high molecular cadherin 23 isoform was detected with antibody TF7 in the P60 inner ear sample (Figure 8B, lane 2), which was consistent with the reported reduction in cadherin 23 in the mature mouse inner ear [28,29,31,32]. Various small bands were also detected both in inner ear and retina that corresponded to the predicted sizes of CDH23_V2, roughly 120 kDa or CDH23_V3, approximately 26 kDa. Some variability in the appearance of the small bands was detected between inner ear or retina, the age of the mouse and the strain, either wild-type or mutant *Cdh23^{v-6J}*. A high molecular weight band of roughly 350 kDa was detected in human and monkey retinas (Figure 8C) corresponding in size to the high molecular weight band detected in P0 and P4 inner ear (Figure 8A-C).

High molecular weight CDH23 detected by western analysis was previously reported in the rat, mouse, and human retina [42]. In the effort to reconcile our data with this report we performed western blot analysis of mouse inner ear and retinas using antibodies TF7 and 1D1 [42] directed against mouse and human CDH23 (respectively, Figure 9). We found that antiserum 1D1 recognized protein bands of roughly 210 kDa and roughly 70 kDa in the mouse inner ear and retina. Antibody TF7 also recognized bands of approximately 210 kDa and approximately 70 kDa, corresponding to the bands detected by antibody 1D1. But TF7 recognizes a larger band (roughly 350 kDa), not recognized by 1D1. This band may represent the longest CDH23 protein isoform with a deduced kDa of 370 that is present in the mouse inner ear at early developmental stages.

DISCUSSION

Most of the available localization data for CDH23 do not differentiate between the substantially different CDH23 protein isoforms [7,30,42]. We undertook this study to better characterize cadherin 23 mRNA and protein isoform expression to gain insight into their roles in the retina and inner ear. We demonstrate that *Cdh23* transcripts are developmentally regulated and have tissue-specific expression profiles. The temporal expression patterns suggest specific roles for some *Cdh23* transcripts. For example, in the inner ear, *Cdh23_v2* expression between P0 to P14 is consistent with the critical period of inner ear development. By P14, when *Cdh23_v2* is expressed at very low levels, all turns of the cochlea have reached their adult size, most vestibular sensory cells have matured, and vestibular sensory epithelia have reached their adult shape and size [52,53]. Furthermore, electrical events that lead to the onset of hearing, occurring at approximately P21, are already detectable during this period including the endocochlear potential (roughly
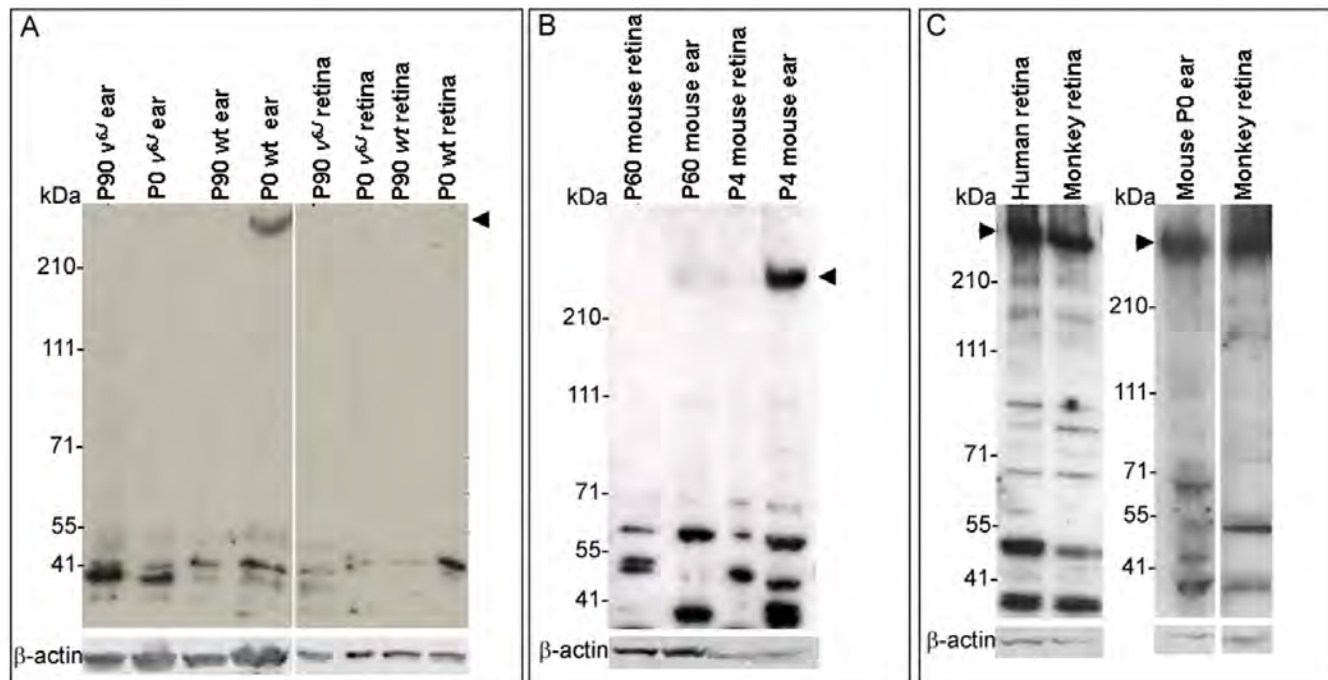
Figure 8. Primate and mouse CDH23 protein in inner ear and retina. **A-C**: western blot analyses of proteins separated on 3%–8% tris-acetate gels using the cytoplasmic domain antibody, TF7. **A**: Western analysis, using protein extracts from P0, and P90 wild-type and mutant mouse inner ear and retina. An approximately 350 kDa band corresponding to the largest CDH23 protein isoform was only detected in P0 mouse inner ear (arrow head). Faster migrating protein bands were present in wild-type and *Cdh23^v-6J* and may represent lower molecular weight CDH23 protein isoforms (such as CDH23_V3). Tissue specific variation of these isoforms is better visualized in the western blot shown in panel **B**. **B**: Western analysis, using protein extracts from P4, and P60 wild-type mouse inner ear and retina. The high molecular weight band at roughly 350 kDa (arrowhead) was detected in the P4 inner ear protein sample. Traces of this band were also detected in the P60 inner ear protein sample. The faster migrating bands detected show variability in their appearance between young and adult tissue as well as variability between the inner ear and retina. **C**: Western analysis, using protein extracts from P0 mouse retina, human retina, and monkey retina. The high molecular weight band (arrow head **A-C**) detected in P0 wild-type mouse inner ear corresponds in size to the largest band detected in human and monkey retinas (arrowhead). β-actin was used as a loading control; size standards are given in kDa.

around P12) and Preyer reflex (around P12) [54]. In the retina, *Cdh23_v4* expression between P0 to P21 is consistent with the time period in which major visual developmental events occur such as the peak of rod neurogenesis (around P0), the onset of retinal waves (approximately P1), and eye opening at approximately P13 [55,56].

In this study, we show that CDH23_V3 is expressed in the synaptic region of photoreceptor cells, and in the synaptic region of auditory and vestibular hair cells. We do not speculate on CDH23_V3 function at this location, but note that this isoform does not have extracellular or transmembrane domains. However the PDZ binding motifs remain intact, indicating it may play a part in the scaffolding network of USH proteins at the synapse [7,42].

The overall expression profile we show here for CDH23 in the outer nuclear layer, the synapse in the outer plexiform layer, and in the ciliary apparatus at the inner segment of photoreceptor cells is in agreement with previous CDH23 localization data in the retina [7,30,42]. It also overlaps with the localization of the USH proteins sans (USH1G), whirlin (USH2D), and VLGR1b, supporting CDH23 as a component

of the USH retinal protein network [47,50]. In this study we show more specifically that in the ciliary apparatus, CDH23 localizes to the basal body and not to the connecting cilium. The presence of CDH23 in the basal bodies and centrioles of photoreceptors cells is in agreement with its localization in the centrosomes of auditory and vestibular hair cells. Basal bodies are analogous to centrioles that are considered to be microtubule organizers as well as the structures from which cilia extend [57,58]. Therefore, it is plausible that CDH23 plays a role in cilia development or maintenance, and in the organization of microtubules.

Our western blot analyses indicated that CDH23 protein isoform expression varies between the mouse inner ear and retina. CDH23_V1 (the longest CDH23 protein isoform) was only detected at P0-P10 in the wild-type inner ear. It was not detected in the adult wild-type inner ear or in the young and adult homozygous *Cdh23^v-6J* mutant inner ear. The lack of CDH23_V1 expression in homozygous *Cdh23^v-6J* mutant mice inner ear is likely to be the cause for deafness and circling behavior of mutant mice, presumably due to the disruption of hair cell bundle architecture and perhaps the tip link.

CDH23_V1 was also not detected in wild-type or *Cdh23^v-6J^* mouse retina at any time point. This observation is inconsistent with a previous report of western analysis demonstrating CDH23_V1 in mouse, rat, and human retinas [42]. We were successful in detecting CDH23_V1 in mature human and primate retinas perhaps due to a higher expression level of CDH23_V1 in these tissues. It is possible that the low
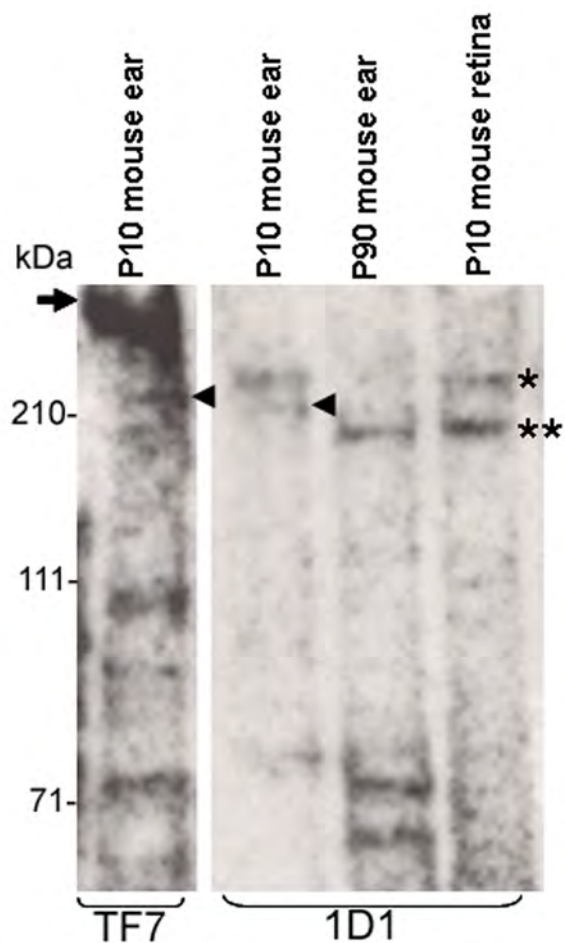

Figure 9. Different CDH23 antisera recognize different protein isoforms. Western blot analyses of protein extracts from P10 and P90 mouse inner ears and retinas were incubated with antisera TF7 and 1D1 generated against mouse and human CDH23 cytoplasmic domain respectively. The highest molecular weight band detected by antisera TF7 (arrow) possibly represents the longest CDH23 isoform (CDH23_V1) expressed in mouse inner ear. The same band was not detected using antisera 1D1 in the inner ear or retina. Antisera 1D1 recognized bands just above (asterisk) and below (two asterisks) the 210 kDa size marker. The band under 210 kDa was also detected by antibody TF7. An additional band (arrowhead) was detected by antisera 1D1, which seems to be detected by antisera TF7 or a band very close in size to it in the inner ear. Antisera TF7 detected a band of roughly 100 kDa that may correspond to CDH23_V2. Additional bands of lesser molecular weights were detected by both antisera, possibly representing smaller still uncharacterized CDH23 protein isoforms.

abundance of CDH23_V1 in mature hair cells and in the mouse retina together with reduced sensitivity of our antibodies made it difficult for us to detect CDH23_V1. Nevertheless, human and mouse retinas appeared to express different CDH23 protein isoforms. Consistent with our data, it is plausible that CDH23_V1 is not expressed or is expressed at low levels in the mouse retina. Williams et al. [59] reported that the largest harmonin isoforms were not expressed in the mouse retina. The absence of CDH23_V1 raises the question of whether a mouse model for USH1D is possible.

Localization studies of CDH23 in the monkey retina indicate expression of CDH23 in the ciliary region, the outer plexiform layer, and in the outer and inner nuclear layer of photoreceptor cells as observed in the mouse retina. Unlike in the mouse photoreceptor cells, CDH23 is localized in the base of the inner segments of monkey cone photoreceptor cells. Considering that cytoskeletal-dependent mechanisms occur in the inner segment of the photoreceptor cells [60], it is possible that CDH23_V1 expression in the inner segment of the primate photoreceptor cells is a representation of the fundamental differences that exist between the human and mouse vision processes [61,62].

In conclusion, we show here that CDH23 protein isoforms are localized in discrete compartments of the photoreceptor layer of the retina and the inner ear. We also show that CDH23 has several wild-type isoforms shorter than CDH23_V1, and demonstrate that there are differences in CDH23 isoform expression between mice and primates. If one of the short isoforms of CDH23 in the mouse retina performs the function of the long isoform of CDH23 in primates, then studying the expression and function of these shorter wild-type isoforms in the mouse retina may lead to a creation of a mouse model for USH1D. A knockout model of CDH23 cytoplasmic domain shared by the majority of CDH23 isoforms would test this hypothesis.

ACKNOWLEDGMENTS

REFERENCES

1. Smith RJ, Berlin CI, Hejtmancik JF, Keats BJ, Kimberling WJ, Lewis RA, Möller CG, Pelias MZ, Tranebjærg L. Clinical diagnosis of the Usher syndromes. Usher Syndrome Consortium. Am J Med Genet 1994; 50:32-8. [PMID: 8160750]
2. Ahmed ZM, Riazuddin S, Khan SN, Friedman PL, Riazuddin S, Friedman TB. USH1H, a novel locus for type I Usher

syndrome, maps to chromosome 15q22–23. Clin Genet 2009; 75:86-91. [PMID: 18505454]

3.   Petit C. Usher Syndrome: from genetics to pathogenesis. Annu Rev Genomics Hum Genet 2001; 2:271-97. [PMID: 11701652]

4.   Weil D, El-Amraoui A, Masmoudi S, Mustapha M, Kikkawa Y, Lainé S, Delmaghani S, Adato A, Nadifi S, Zina ZB, Hamel C, Gal A, Ayadi H, Yonekawa H, Petit C. Usher syndrome type I G (USH1G) is caused by mutations in the gene encoding SANS, a protein that associates with the USH1C protein, harmonin. Hum Mol Genet 2003; 12:463-71. [PMID: 12588794]

5.   El-Amraoui A, Petit C. Usher I syndrome: unravelling the mechanisms that underlie the cohesion of the growing hair bundle in inner ear sensory cells. J Cell Sci 2005; 118:4593-603. [PMID: 16219682]

6.   Kremer H, van Wijk E, Märker T, Wolfrum U, Roepman R. Usher syndrome: molecular links of pathogenesis, proteins and pathways. Hum Mol Genet 2006; 15:R262-70. [PMID: 16987892]

7.   Reiners J, Nagel-Wolfrum K, Jürgens K, Märker T, Wolfrum U. Molecular basis of human Usher syndrome: deciphering the meshes of the Usher protein network provides insights into the pathomechanisms of the Usher disease. Exp Eye Res 2006; 83:97-119. [PMID: 16545802]

8.   Bork JM, Peters LM, Riazuddin S, Bernstein SL, Ahmed ZM, Ness SL, Polomeno R, Ramesh A, Schloss M, Srisailpathy CR, Wayne S, Bellman S, Desmukh D, Ahmed Z, Khan SN, Kaloustian VM, Li XC, Lalwani A, Riazuddin S, Bitner-Glindzicz M, Nance WE, Liu XZ, Wistow G, Smith RJ, Griffith AJ, Wilcox ER, Friedman TB, Morell RJ. Usher syndrome 1D and nonsyndromic autosomal recessive deafness DFNB12 are caused by allelic mutations of the novel cadherin-like gene CDH23. Am J Hum Genet 2001; 68:26-37. [PMID: 11090341]

9.   Bolz H, von Brederlow B, Ramírez A, Bryda EC, Kutsche K, Nothwang HG, Seeliger M. del C-Salcedó Cabrera M, Vila MC, Molina OP, Gal A, Kubisch C. Mutation of CDH23, encoding a new member of the cadherin gene family, causes Usher syndrome type 1D. Nat Genet 2001; 27:108-12. [PMID: 11138009]

10. Friedman TB, Griffith AJ. Human nonsyndromic sensorineural deafness. Annu Rev Genomics Hum Genet 2003; 4:341-402. [PMID: 14527306]

11. Astuto LM, Bork JM, Weston MD, Askew JW, Fields RR, Orten DJ, Ohliger SJ, Riazuddin S, Morell RJ, Khan S, Riazuddin S, Kremer H, van Hauwe P, Moller CG, Cremers CW, Ayuso C, Heckenlively JR, Rohrschneider K, Spandau U, Greenberg J, Ramesar R, Reardon W, Bitoun P, Millan J, Legge R, Friedman TB, Kimberling WJ. CDH23 mutation and phenotype heterogeneity: a profile of 107 diverse families with Usher syndrome and nonsyndromic deafness. Am J Hum Genet 2002; 71:262-75. [PMID: 12075507]

12. Oshima A, Jaijo T, Aller E, Millan JM, Carney C, Usami S, Moller C, Kimberling WJ. Mutation profile of the CDH23 gene in 56 probands with Usher syndrome type I. Hum Mutat 2008; 29:E37-41. [PMID: 18429043]

13. Becirovic E, Ebermann I, Nagy D, Zrenner E, Seeliger MW, Bolz HJ. Usher syndrome type 1 due to missense mutations on both CDH23 alleles: investigation of mRNA splicing. Hum Mutat 2008; 29:452. [PMID: 18273900]

14. Di Palma F, Holme RH, Bryda EC, Belyantseva IA, Pellegrino R, Kechara B, Steel KP, Noben-Trauth K. Mutations in Cdh23, encoding a new type of cadherin, cause stereocilia disorganization in waltzer, the mouse model for Usher syndrome type 1D. Nat Genet 2001; 27:103-7. [PMID: 11138008]

15. Di Palma F, Pellegrino R, Noben-Trauth K. Genomic structure, alternative splice forms and normal and mutant alleles of cadherin 23 (Cdh23). Gene 2001; 281:31-41. [PMID: 11750125]

16. Yonezawa S, Yoshizaki N, Kageyama T, Takahashi T, Sano M, Tokita Y, Masaki S, Inaguma Y, Hanai A, Sakurai N, Yoshiki A, Kusakabe M, Moriyama A, Nakayama A. Fates of Cdh23/CDH23 with mutations affecting the cytoplasmic region. Hum Mutat 2006; 27:88-97. [PMID: 16281288]

17. Schwander M, Xiong W, Tokita J, Lelli A, Elledge HM, Kazmierczak P, Sczaniecka A, Kolatkar A, Wiltshire T, Kuhn P, Holt JR, Kachar B, Tarantino L, Müller U. A mouse model for nonsyndromic deafness (DFNB12) links hearing loss to defects in tip links of mechanosensory hair cells. Proc Natl Acad Sci USA 2009; 106:5252-7. [PMID: 19270079]

18. Punzo C, Cepko C. Cellular responses to photoreceptor death in the rd1 mouse model of retinal degeneration. Invest Ophthalmol Vis Sci 2007; 48:849-57. [PMID: 17251487]

19. Libby RT, Kitamoto J, Holme RH, Williams DS, Steel KP. Cdh23 mutations in the mouse are associated with retinal dysfunction but not retinal degeneration. Exp Eye Res 2003; 77:731-9. [PMID: 14609561]

20. Williams DS. Usher syndrome: animal models, retinal function of Usher proteins, and prospects for gene therapy. Vision Res 2008; 48:433-41. [PMID: 17936325]

21. Gibbs D, Kitamoto J, Williams DS. Abnormal phagocytosis by retinal pigmented epithelium that lacks myosin VIIa, the Usher syndrome 1B protein. Proc Natl Acad Sci USA 2003; 100:6481-6. [PMID: 12743369]

22. Ball SL, Bardenstein D, Alagramam KN. Assessment of retinal structure and function in Ames waltzer mice. Invest Ophthalmol Vis Sci 2003; 44:3986-92. [PMID: 12939319]

23. Haywood-Watson RJ 2nd, Ahmed ZM, Kjellstrom S, Bush RA, Takada Y, Hampton LL, Battey JF, Sieving PA, Friedman TB. Ames Waltzer deaf mice have reduced electroretinogram amplitudes and complex alternative splicing of Pcdh15 transcripts. Invest Ophthalmol Vis Sci 2006; 47:3074-84. [PMID: 16799054]

24. Kikkawa Y, Shitara H, Wakana S, Kohara Y, Takada T, Okamoto M, Taya C, Kamiya K, Yoshikawa Y, Tokano H, Kitamura K, Shimizu K, Wakabayashi Y, Shiroishi T, Kominami R, Yonekawa H. Mutations in a new scaffold protein Sans cause deafness in Jackson shaker mice. Hum Mol Genet 2003; 12:453-61. [PMID: 12588793]

25. Liu X, Bulgakov OV, Darrow KN, Pawlyk B, Adamian M, Liberman MC, Li T. Usherin is required for maintenance of retinal photoreceptors and normal development of cochlear hair cells. Proc Natl Acad Sci USA 2007; 104:4413-8. [PMID: 17360538]

26. Siemens J, Kazmierczak P, Reynolds A, Sticker M, Littlewood-Evans A, Müller U. The Usher syndrome proteins cadherin 23 and harmonin form a complex by means of PDZ-domain

interactions. Proc Natl Acad Sci USA 2002; 99:14946-51. [PMID: 12407180]

27. Xu Z, Peng AW, Oshima K, Heller S. MAGI-1, a candidate stereociliary scaffolding protein, associates with the tip-link component cadherin 23. J Neurosci 2008; 28:11269-76. [PMID: 18971469]

28. Lagziel A, Ahmed ZM, Schultz JM, Morell RJ, Belyantseva IA, Friedman TB. Spatiotemporal pattern and isoforms of cadherin 23 in wild type and waltzer mice during inner ear hair cell development. Dev Biol 2005; 280:295-306. [PMID: 15882574]

29. Michel V, Goodyear RJ, Weil D, Marcotti W, Perfettini I, Wolfrum U, Kros CJ, Richardson GP, Petit C. Cadherin 23 is a component of the transient lateral links in the developing hair bundles of cochlear sensory cells. Dev Biol 2005; 280:281-94. [PMID: 15882573]

30. Bolz H, Reiners J, Wolfrum U, Gal A. Role of cadherins in Ca^{2+}-mediated cell adhesion and inherited photoreceptor degeneration. Adv Exp Med Biol 2002; 514:399-410. [PMID: 12596935]

31. Boëda B, El-Amraoui A, Bahloul A, Goodyear R, Daviet L, Blanchard S, Perfettini I, Fath KR, Shorte S, Reiners J, Houdusse A, Legrain P, Wolfrum U, Richardson G, Petit C. Myosin VIIa, harmonin and cadherin 23, three Usher I gene products that cooperate to shape the sensory hair cell bundle. EMBO J 2002; 21:6689-99. [PMID: 12485990]

32. Rzadzinska AK, Derr A, Kachar B, Noben-Trauth K. Sustained cadherin 23 expression in young and adult cochlea of normal and hearing-impaired mice. Hear Res 2005; 208:114-21. [PMID: 16005171]

33. Siemens J, Lillo C, Dumont RA, Reynolds A, Williams DS, Gillespie PG. Müller U. Cadherin 23 is a component of the tip link in hair-cell stereocilia. Nature 2004; 428:950-5. [PMID: 15057245]

34. Söllner C, Rauch GJ, Siemens J, Geisler R, Schuster SC. Müller U, Nicolson T; Tübingen 2000 Screen Consortium. Mutations in cadherin 23 affect tip links in zebrafish sensory hair cells. Nature 2004; 428:955-9. [PMID: 15057246]

35. Corey DP, Sotomayor M. Hearing: tightrope act. Nature 2004; 428:901-3. [PMID: 15118709]

36. Gillespie PG, Dumont RA, Kachar B. Have we found the tip link, transduction channel, and gating spring of the hair cell? Curr Opin Neurobiol 2005; 15:389-96. [PMID: 16009547]

37. Kazmierczak P, Sakaguchi H, Tokita J, Wilson-Kubalek EM, Milligan RA. Müller U, Kachar B. Cadherin 23 and protocadherin 15 interact to form tip-link filaments in sensory hair cells. Nature 2007; 449:87-91. [PMID: 17805295]

38. Goodyear RJ, Richardson GP. A novel antigen sensitive to calcium chelation that is associated with the tip links and kinocilial links of sensory hair bundles. J Neurosci 2003; 23:4878-87. [PMID: 12832510]

39. Ahmed ZM, Goodyear R, Riazuddin S, Lagziel A, Legan PK, Behra M, Burgess SM, Lilley KS, Wilcox ER, Riazuddin S, Griffith AJ, Frolenkov GI, Belyantseva IA, Richardson GP, Friedman TB. The tip-link antigen, a protein associated with the transduction complex of sensory hair cells, is protocadherin-15. J Neurosci 2006; 26:7022-34. [PMID: 16807332]

40. Beurg M, Fettiplace R, Nam JH, Ricci AJ. Localization of inner hair cell mechanotransducer channels using high-speed calcium imaging. Nat Neurosci 2009; 12:553-8. [PMID: 19330002]

41. Rzadzinska AK, Steel KP. Presence of interstereocilial links in waltzer mutants suggests Cdh23 is not essential for tip link formation. Neuroscience 2009; 158:365-8. [PMID: 18996172]

42. Reiners J, Reidel B, El-Amraoui A, Boëda B, Huber I, Petit C, Wolfrum U. Differential distribution of harmonin isoforms and their possible role in Usher-1 protein complexes in mammalian photoreceptor cells. Invest Ophthalmol Vis Sci 2003; 44:5006-15. [PMID: 14578428]

43. Trojan P, Krauss N, Choe HW, Giessl A. Pulvermüller A, Wolfrum U. Centrins in retinal photoreceptor cells: regulators in the connecting cilium. Prog Retin Eye Res 2008; 27:237-59. [PMID: 18329314]

44. Ahmed ZM, Riazuddin S, Ahmad J, Bernstein SL, Guo Y, Sabar MF, Sieving P, Riazuddin S, Griffith AJ, Friedman TB, Belyantseva IA, Wilcox ER. PCDH15 is expressed in the neurosensory epithelium of the eye and ear and mutant alleles are responsible for both USH1F and DFNB23. Hum Mol Genet 2003; 12:3215-23. [PMID: 14570705]

45. Belyantseva IA, Boger ET, Friedman TB. Myosin XVa localizes to the tips of inner ear sensory cell stereocilia and is essential for staircase formation of the hair bundle. Proc Natl Acad Sci USA 2003; 100:13958-63. [PMID: 14610277]

46. Wolfrum U. Tropomyosin is co-localized with the actin filaments of the scolopale in insect sensilla. Cell Tissue Res 1991; 265:11-7.

47. Maerker T, van Wijk E, Overlack N, Kersten FF, McGee J, Goldmann T, Sehn E, Roepman R, Walsh EJ, Kremer H, Wolfrum U. A novel Usher protein network at the periciliary reloading point between molecular transport machineries in vertebrate photoreceptor cells. Hum Mol Genet 2008; 17:71-86. [PMID: 17906286]

48. Danscher G. Histochemical demonstration of heavy metals. A revised version of the sulphide silver method suitable for both light and electronmicroscopy. Histochemistry 1981; 71:1-16. [PMID: 6785259]

49. Leranth C, Pickel VM, eds. Electron microscopic preembedding double immunostaining methods. In: Heimer L, Zaborszky L, editors Neuroanatomical Tract-Tracing Methods. New York: Plenum Press; 1989. p. 129–172.

50. Overlack N, Maerker T, Latz M, Nagel-Wolfrum K, Wolfrum U. SANS (USH1G) expression in developing and mature mammalian retina. Vision Res 2008; 48:400-12. [PMID: 17923142]

51. Safieddine S, Wenthold RJ. SNARE complex at the ribbon synapses of cochlear hair cells: analysis of synaptic vesicle- and synaptic membrane-associated proteins. Eur J Neurosci 1999; 11:803-12. [PMID: 10103074]

52. Lim DJ, Anniko M. Developmental morphology of the mouse inner ear. A scanning electron microscopic observation. Acta Otolaryngol Suppl 1985; 422:1-69. [PMID: 3877398]

53. Morsli H, Choo D, Ryan A, Johnson R, Wu DK. Development of the mouse inner ear and origin of its sensory organs. J Neurosci 1998; 18:3327-35. [PMID: 9547240]

54. Alford BR, Ruben RJ. Physiological, behavioral and anatomical correlates of the development of hearing in the mouse. Ann Otol Rhinol Laryngol 1963; 72:237-47. [PMID: 14012000]

55. Finlay BL. The developing and evolving retina: Using time to organize form. Brain Res 2008; 1192:5-16. [PMID: 17692298]

56. Wu Y, Lorke DE, Lai H, Wai SM, Kung LS, Chan WY, Yew DTW. Critical periods of eye development in vertebrates with special reference to humans. Neuroembryology and Aging 2003; 2:1-8.

57. Alieva IB, Vorobjev IA. Vertebrate primary cilia: a sensory part of centrosomal complex in tissue cells, but a "sleeping beauty" in cultured cells? Cell Biol Int 2004; 28:139-50. [PMID: 14984760]

58. Dawe HR, Farr H, Gull K. Centriole/basal body morphogenesis and migration during ciliogenesis in animal cells. J Cell Sci 2007; 120:7-15. [PMID: 17182899]

59. Williams DS, Aleman TS, Lillo C, Lopes VS, Hughes LC, Stone EM, Jacobson SG. Harmonin in the murine retina and the retinal phenotypes of Ush1c-mutant mice and human USH1C. Invest Ophthalmol Vis Sci 2009; 50:3881-9. [PMID: 19324851]

60. Eckmiller MS. Defective cone photoreceptor cytoskeleton, alignment, feedback, and energetics can lead to energy depletion in macular degeneration. Prog Retin Eye Res 2004; 23:495-522. [PMID: 15302348]

61. Fu Y, Yao KW. Phototransduction in mouse rods and cones. Pflugers Arch - Eur J Physiol 2007; 454:805-19.

62. Martin RD, Ross CF. The evolutionary and ecological context of primate vision. In: Jan Kremers, editor. The primate visual system: A comparative approach. Wiley 2006; Chapter 1. p. 1–36.
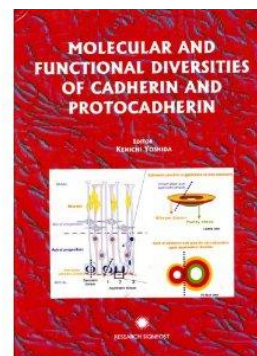
Publikation II

2.2 Overlack N, Nagel‑Wolfrum K, and Wolfrum U (2010) The role of cadherins in sensory cell function. In: Molecular and Functional Diversities of Cadherin and Protocadherin. Ed.: K.Yoshida, 297‑311.

17. The role of cadherins in sensory cell function

Nora Overlack, Kerstin Nagel-Wolfrum and Uwe Wolfrum
Institute of Zoology, Cell and Matrix Biology
Johannes Gutenberg University of Mainz

Abstract. In vertebrate sensory cells of the eye and the inner ear a group of non-classical cadherins, namely cadherin 23 (CDH23), protocadherin 15 (PCDH15) and protocadherin 21 (PCDH21) are expressed, and are essential for sensory cell development and/or sensory function. Defects in these cadherins can cause nonsyndromic blindness or deafness or leads to deaf-blindness known as Usher syndrome (USH). As all cadherin superfamily members, the "sensory" "S"-cadherins possess the common EC domain signature in their extracellular part, but the number of repetitive ECs is much more variable and the molecular interactions of the extracellular parts and the cytoplasmic protein arrangements associated with these cadherins are less uniform. CDH23 is a member of the FAT cadherins subfamily containing up to 27 EC domains. In contrast, PCDH15 and PCDH21 are typical protocadherins containing 11 or 6 EC domains, respectively.

The USH cadherins, CDH23 (USH1D) and PCDH15 (USH1F) are integrated into the protein interactome related to the USH disease by binding with their cytoplasmic part to other USH proteins. In mechanosensitive hair cells, both cadherins are part of fibrous links connecting the membranes of neighbouring stereovilli, the mechano-sensory organelles during hair bundle differentiation. In mature hair cells both USH cadherins persist as tip links. In the vetebrate photoreceptor cells the two USH cadherins are thought to contribute to membrane-membrane adhesion between the inner and outer segment, but predominatly at the ribbon synapses. PCDH21 is mainly found in photoreceptor cells of vertebrate retinae and seems not to be expressed in hair cells. In rod and cone cells, PCDH21 is localized in the rim of the newly synthesized disk membranes at the base of the outer segment. For its essential

Correspondence/Reprint request: Dr. Uwe Wolfrum, Johannes Gutenberg University, Institute of Zoology, Cell and Matrix Biology, Müllerweg 6, D-55099 Mainz, Germany. E-mail: wolfrum@uni-mainz.de

role in disk neogensis and stacking of newly formed disks PCDH21 is part of an actin associated adhesion complex containing prominin 1. For maturation of the outer segment disks it is necessary that the extracellular part of PCDH21 is proteolytically cleaved at the proximal EC6.

The present article provides an overview of current knowledge on the function of "S"-cadherins in sensory cells and thereby their role associated with sensorineuronal degenerations underlying human diseases.

Introduction

The cadherin superfamily consists of more than 100 members responsible for a variety of roles in differentiation, maintenance and function of tissues and cells. This superfamily involves: i) classical cadherins that are the major component of cell-cell adhesive junctions; ii) desmosomal cadherins (desmocolins and desmogleins); iii) protocadherins; iv) cadherin-related molecules like the *fat* protein of *Drosophila*; v) cadherins with tyrosine-kinase domains (pointing towards a role of cadherins in signal transduction pathways), and vi) cadherins with seven-transmembrane domains sharing additional sequence homology with G-protein coupled receptors, e.g. the *flamingo* protein originally identified in *Drosophila* where it is involved in planar cell polarity (1). The common, defining feature of the diverse cadherins is the cadherin or extracellular domain (EC) of their extracellular N-terminal part. ECs are compact domains of approximately 110 amino acid residues containing evolutionary highly conserved, negatively charged motifs. Classical cadherin molecules (CCDH) (C-cadherin, e.g. E-cadherins or N-cadherins) contain five ECs (EC1-EC5) joined by flexible hinge regions (Fig. 1a). Binding of Ca^{2+}-ions in the neighborhood of each hinge stiffens the extracellular part and thereby triggers homophilic interaction between the N-terminal EC1 domains of cadherin molecules which are located at the membranes of neighbouring cells (2). A short transmembrane domain links the extracellular part with the intracellular cytoplasmic domain which anchors the cell-cell adhesion complex through linker protein complexes (e.g. β/α-catenin) to the cytoskeleton (e.g. actin filaments). The cytoplasmic domain of cadherins also connects cell-cell adhesion complexes to intracellular signaling pathways (3). Although classical C-cadherins are expressed in sensory organs of vertebrates, recent studies revealed that non-classical cadherins - namely cadherin 23 (CDH23), protocadherin 15 (PCDH15), and protocadherin 21 (PCDH21) - are essential for the differentiation, the maintenance and the sensory function of sensory cells in the inner ear and the eye. As other cadherins, these "sensory" S-cadherins possess the common EC domain signature, but the number of repetitive ECs is much more variable and the molecular interactions of the extracellular parts and the cytoplasmic protein arrangements associated with these cadherins are less uniform (Fig. 1). In human patients, mutations in S-cadherins can cause non-syndromic deafness and blindness, but also combined deaf-blindness. The present article aims to present an overview of current knowledge on the function of S-cadherins in sensory cells and thereby their role associated with sensorineuronal degenerations underlying human diseases.

In the vertebrate eye, two types of photoreceptor cells, cones and rods, adapted to photopic vision allowing color perception and scotopic vision at low-light conditions, respectively, are arranged in the innermost layer of the neuronal retina. Both types are highly polarized sensory neurons consisting of morphological and functional distinct cellular compartments. From their cell body an axon projects to the synaptic terminus, where ribbon synapses connect the photoreceptor cells with the 2nd retinal neurons (4). At the other pole, a short dendrite named inner segment, terminates in a light sensitive outer
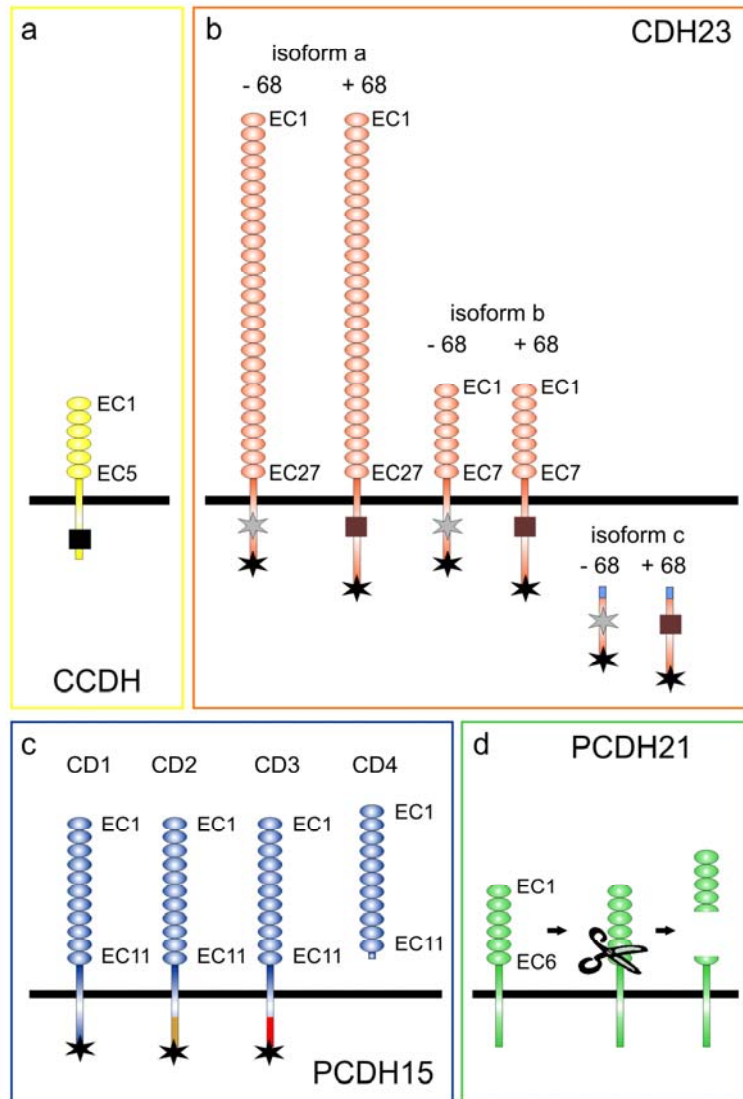
Figure 1. Domain structure of certain cadherins. **(a)** Structure of classical cadherin (CCDH) composed of 5 EC domains, a single transmembrane domain and the cytoplasmic domain containing a motif (black rectangle) mediating the association with the cytoskeleton through ß-catenin. **(b)** Cadherin 23 (CDH23) encompass three groups, a, b and c which differ in the number of EC domains. Isoform c contains an N-terminal unique seven amino acid sequence (light blue rectangles) but lacks any EC or transmembrane domain. All isoforms can alternatively spliced leading to the inclusion or exclusion of exon 68 (brown rectangle) generating an internal PDZ binding domains (grey asterisk). C-terminal class 1 PDZ binding motifs (PBM) indicated by black asterisks. **(c)** Proteocadherin 15 (PCDH15) has four known isoforms CD1-CD4. All contain 11 EC domains. CD1, CD2 and CD3 contain PBMs (black astersiks) but differ in their cytoplasmic domain (indicated by different colors). CD4 lacks the transmembrane and cytoplasmic domain. **(d)** PCDH21 contains six EC domains, a single transmembrane domain and a cytoplasmic domain. Scissors indicates the internal proteolytic cleavage site in EC6.

segment (5;6) (Fig. 2a). This outer segment is similar to other sensory cilia (7), additionally characterized by specialized flattened disk-like membranes, where all components of the visual transduction cascade are arranged (8). The visual signal transduction cascade in vertebrates is one of the best studied examples of a G-protein transduction cascade. Photoexcitation leads to photoisomerisation of the visual pigment rhodopsin (Rh*) which catalyses GDP/GTP exchange at the visual heterotrimeric G-protein transducin, which in turn activates a phosphodiesterase (PDE), catalyzing cGMP hydrolysis in the cytoplasm which leads to the closure of cGMP-gated channels in the plasma membrane, finally resulting in photoreceptor cell hyperpolarization. The phototransductive membranes of the outer segment are continually renewed throughout lifetime. Newly synthesized membranes are added at the base of the outer segment, whereas aged disks at the outer segment apex are phagocytosed by cells of the retinal pigment epithelium (9). Outer segment molecules are continually synthesized in the inner segment and transported through the slender connecting cilium to their destinations in the outer segments (6).
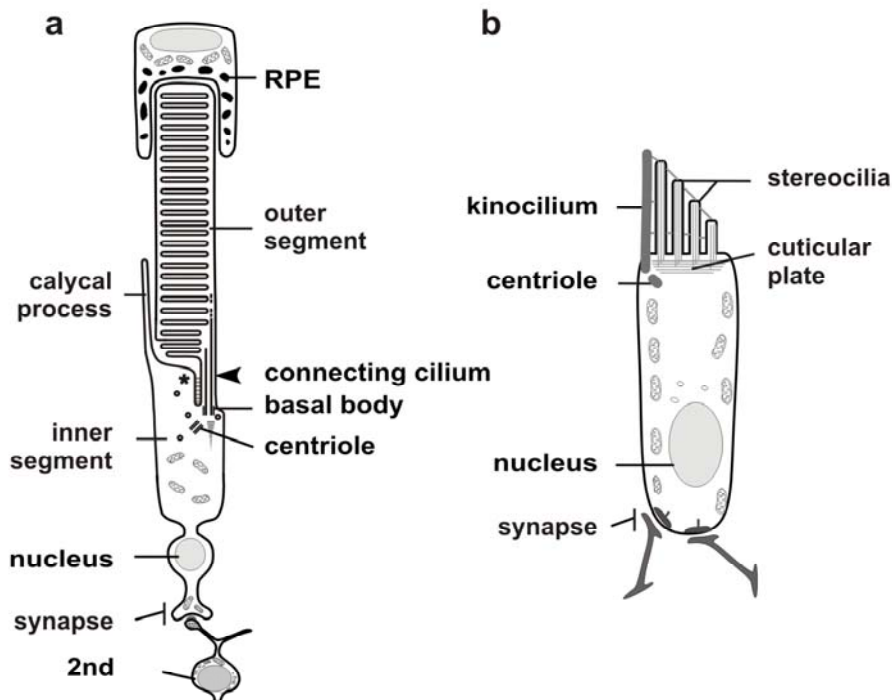
Figure 2. Schematic representation of the sensory cells in the retina and the inner ear. **(a)** Vertebrate rod photoreceptor cells are composed of distinct morphological and functional compartments. Photosensitive outer segment is connected with the biosynthetic active inner segment via the connecting cilium. At the ciliary base a basal body and the adjacent centriole are present. The proximal outer segment and the connecting cilium are enclosed by the periciliary specialization of the apical inner segment (asterisk). Calycal processes extend from the apical inner segment and project parallel to the outer segment. Ribbon synapses link photoreceptor cells and bipolar and horizontal cells. RPE: retinal pigment epithelium. **(b)** The mechanotransduction in hair cells takes place at the stereovilli (= stereocilia), at the apical part of the hair cell. Stereovilli are rigid microvilli-like structures that are organized in a staircase like manner of decreasing height.

In the inner ear, mechanosensitive sensory hair cells are found in the utricle and the saccule of the vestibular system that provides the dominant input about movement and equilibrioception and are part of the auditory system in the Organ of Corti of the cochlea. Furthermore, sensory hair cells are elemental sensory units in the lateral line of fishes and amphibians. Hair cells are specialized mechanosensitive neurons that carry out the conversion from incoming mechanical stimuli into the intrinsic electrical signals. The schematic representation in figure 2b shows the structure of a mechanosensitve hair cell. The mechanosensitive structures of hair cells are the eponymous hair-like apical extensions, the so-called stereocilia. These stereocilia are actually modified microvilli and a term change from stereocilia to stereovilli is ongoing in the literature. The stereovilli contain a cytoskeletal core of densely packed actin filaments which are anchored in the actin filament meshwork of the cuticular plate by extensions of a few central actin filaments. On the apical surface of the hair cell, rows of stereovilli form a staircase of increasing height with the tallest row of stereovilli abutting the single kinocilium, an authentic cilium containing a microtubule-based cytoskeleton. The kinocilium is not required for mechanotransduction and can be absent in maturated hair cells, but it is probably important for hair bundle development and polarity. Deflection of the hair bundle in the direction of the longest stereocilia increases the open probability of mechanotransduction channels localized towards the stereocilia tips (10).

The plasma membranes of adjacent stereovilli and the membranes of the longest stereovilli and of the kinocilium are connected by extracellular linker filaments with distinct morphological and molecular features (Figs. 2b, 4) (11). During development mouse cochlear hair cells exhibit transient lateral links, ankle links, and kinociliary links which are thought to abet the shape of differenciating hair bundles. In contrast, mature hair cells possess horizontal top connectors and tip links. The tip links are assumed to be physically connected to the mechanotransduction cation channels directly participating in the gating mechanism of the mechanosensitive channel (10). However, in the absence of molecular data the function of the linkages in the hair bundles remained speculative mostly inferred by indirect means. Only recent molecular and cellular analyses of deafness causing molecules, e.g. S-cadherins, enlightened molecular compositions of the extracellular links and thereby provide important founded insights into their function. The molecular decipherment of the link components also revealed molecular parallels between mechanosenitive hair cells and photoreceptor cells; the temporary ankle links between stereovilli and the fibres between the adjacent membranes of the periciliary inner segment and the connecting cilium of photoreceptor cells are composed of the extracellular domains of GPR98 (VLGR1), vezatin, and USH2A isoform B (Figs. 4, 5) (12-15). Further parallels are the ribbon synapses present in hair cells and photoreceptor cells. In the present review we will provide a current view of the putative function of non-classical cadherins, cadherin 23 (CDH23), protocadherin 15 (PCDH15), and protocadherin 21 (PCDH21) found in the sensory hair cells and the photoreceptor cells.

1. Cadherin 23 and protocadherin 15 are related to non-syndromic deafness or the human Usher syndrome

In human, mutations in the genes for the cadherins cadherin 23 (*CDH23*) and protocadherin 15 (*PCDH15*) lead to non-syndromic deafness (DFNB) or Usher syndrome (USH), the most common form of hereditary deaf-blindness. Genotype-phenotype correlations for *CDH23* and *PCDH15* indicated that missense or inframe alterations result in nonsyndromic deafness DFNB12 and DFNB23, whereas truncating mutations
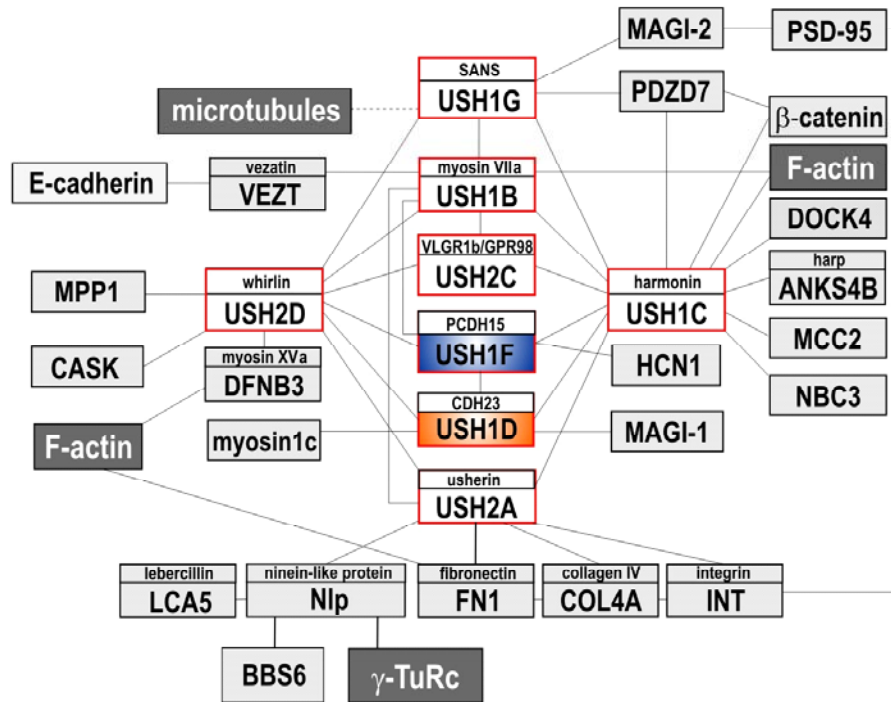
Figure 3. Scheme of the protein interactome related to the human Usher syndrome (USH). USH proteins are indicated by red boxes, CDH23 (USH1D) and PCDH15 (USH1F) are further highlighted in orange and blue, respectively; cytoskeleton components are shown in grey; other interaction partners in light grey. Confirmed interaction partners (by two or more independent methods) are indicated by solid lines; putative associations by dotted lines. Details of the interactome are reviewed in Kremer et al. (2006) and Reiners et al. (2006), currently updated in Nagel-Wolfrum et al., in prep.

are causing USH1D and USH1F, respectively (16). USH is a complex disease divided in three clinical types (USH1-3). USH1 is the most severe form characterized by congenital deafness, vestibular dysfunction and progressive retinal degeneration, *retinitis pigmentosa* (RP). All three types additionally show genetic heterogeneity and from the identified 13 genes, so far five genes have been linked to USH1, three to USH2 and one to USH3 (16). Although mutations in these genes lead to a similar phenotype, they encode for proteins of different protein families exhibiting diverse cellular functions (17). Recent studies revealed that all USH1 and USH2 molecules are integrated mainly by PDZ-containing scaffold proteins harmonin (USH1C) and whirlin (USH2D) but also by SANS (USH1G) in protein networks - the protein interactome related to the USH disease (Fig. 3) (15;17-19).

CDH23 and PCDH15 are atypical members of the large cadherin superfamily. In the cytoplasmic tails of both cadherins, the consensus R1 and R2 binding sites for β-catenins (20) are missing (21-24). But, in contrast to classical cadherins, they harbor class I PDZ-binding motifs (PBMs) in the C-terminus of their cytoplasmic tail (Fig. 1) (21-24). Through these PBMs both USH cadherins are integrated into the protein networks of the USH protein interactome via the PDZ domains-containing USH proteins harmonin

Table 1. Cadherin 23 (CDH23), protocadherin 15 (PCDH15) and protocadherin 21 (PCDH21) interaction partners

	Interacting protein	Function	ID	Reference
CDH23	CDH23 (DNFB12/USH2D)	membrane adhesion	EC	Siemens et al., 2004 (33)
	PCDH15 (DNFB23/USH1F)	membrane adhesion	EC	Kazmierczak et al., 2007 (36)
	harmonin (DNFB18/USH1C)	scaffold protein	CD	Boeda et al., 2002 (23)
				Siemens et al., 2002 (24)
				Pan et al., 2009 (31)
	whirlin (DNFB31/USH2D)	scaffold protein	CD	Kremer et al. 2006 (19)
	myosin 1c	molecular motor	CD	Siemens et al., 2004 (33)
	MAGI-1	scaffold protein	CD	Xu et al., 2008 (57)
PCDH15	PCDH15 (DNFB23/USH1F)	membrane adhesion	EC	Kazmierczak et al., 2007 (36)
	CDH23 (DNFB12/USH2D)	membrane adhesion	EC	Kazmierczak et al., 2007 (36)
	harmonin (DNFB18/USH1C)	scaffold protein	CD	Adato et al., 2005 (25)
				Reiners et al., 2005 (18)
	whirlin (DNFB31/USH2D)	scaffold protein	CD	Reiners et al., 2005 (40)
	myosin VIIa (USH1B)	molecular motor	CD	Senften et al., 2006 (26)
	HCN1	channel protein	CD	Ramakrishnan et al., 2009 (58)
PCDH21	prominin 1	transmembrane protein	CD	Yang et al., 2008 (52)
	cytoskeletal proteins?		CD	Rattner et al., 2004 (50)

ID: interaction domain; EC: extracellular cadherin domain; CD: cytoplasmic domain MAGI-1: membrane associated guanylate kinase; HCN1: Hyperpolarization activated cyclic nucleotide-gated potassium channel 1

(USH1C) (17;18;23;25) and whirlin (USH2D) (19). Furthermore, PCDH15 binds directly to the USH1B protein mysoinVIIa through its C-terminal domain (26) (Tab.1; Fig.3). Nevertheless, since similarities in sequence and in domain structure in the two USH cadherins are very low, with the exception of the class I PBM in the extreme C-terminus, it does not surprise that they belong to different branches or subfamilies of the cadherin superfamily.

1.1. Cadherin 23 (USH1D, DFNB12) - the "fat" USH cadherin

Cadherin 23 (CDH23) previously known as Otocadherin is related to the *Drosophila fat* protein, the so-called FAT cadherins which contain many more EC domains than the typically five of classical cadherins. The full length CDH23 (isoform a) contains 27 EC domains (22). In contrast, the CDH23 isoform b contains only 7 EC and the isoform c lacks all ectodomains and contains no transmembrane domain, but possesses an unique seven amino acid sequence at its N-terminus (Fig. 1b) (22;24;27;28). Since cell-cell adhesion function can be excluded for CDH23 isoform c, this isoform is thought to compete for cytoplasmic binding partners with the other CDH23 isoforms which may play a role in the regulation in signaling pathways in the cytoplasm (29). All three different isoforms have in common that additional alternative splicing leads to the inclusion or exclusion of exon 68 named CDH23 (+68) or CDH23 (-68), respectively (24). Whereas CDH23 (+68) splice variants are expressed preferentially in the inner ear sensory epithelium (24;30), CDH23 (-68) splice variants are more ubiquitously expressed and are found in the neuronal retina (24). CDH23´s exon 68 encodes for an insert in the

cytoplasmic domain which destroys an internal PDZ-binding motif (PBM) homolog to the internal PBM of the adaptor protein Ril present in CDH23 (-68) (24). Both PBMs of CDH23 (-68) participate in interactions with the PDZ-containing scaffold protein harmonin (USH1C) and whirlin (USH2D). The C-terminal PBM of CDH23 binds to the PDZ2 of harmonin while the internal PBM of the CDH23 (-68) isoform interacts with the PDZ1 of harmonin (23;24). Recent data indicated that in addition to the PDZ1 domain an internal N-terminal sequence of harmonin may be necessary for the interaction with the internal cytoplasmic domain of CDH23 (31).

In the inner ear, CDH23 expression was found in the sensory hair cells and in the Reissner´s membrane (1;23;32). Analyses of the waltzer (v) mice deficient in CDH23 revealed that CDH23 is required for the normal development of the stereocilia of hair cells (30). During the differentiation of hair cells, CDH23 is localized at transient lateral links between the membranes of neighboring stereocilia, which are absent in mature cochlear hair cells (Fig. 4) (23;28;29). In mature cochlear hair cells, CDH23 is localized at the centrosome, most probably in the form of CDH23 isoform c, in the cuticular plate, in the apical, vesicle-rich periculicular region and at the stereovilli (23;28;29). In addition, the longer isoforms of CDH23 were proposed to be a component of the tip links (33), structures linking the apical tips of the hair bundles in mature hair cells (Fig. 4) which are proposed to serve in gating the mechanosensory channels (34). This remarkable hypothesis was confirmed by the absence of tip links in the hair cells of the lateral line of zebrafish *cdh23* mutants *sputnik* (35). Robust immunolabelling of CDH23 and PCDH15 in mature hair cells of different vertebrate species further support this finding and co-localization of both proteins at the stereovilli tips suggested the interaction of CDH23 and PCDH15 as components of the tip link (36). Further analyses indicated the heteromeric adhesion of CDH23 and PCDH15 homodimers through their N-termini
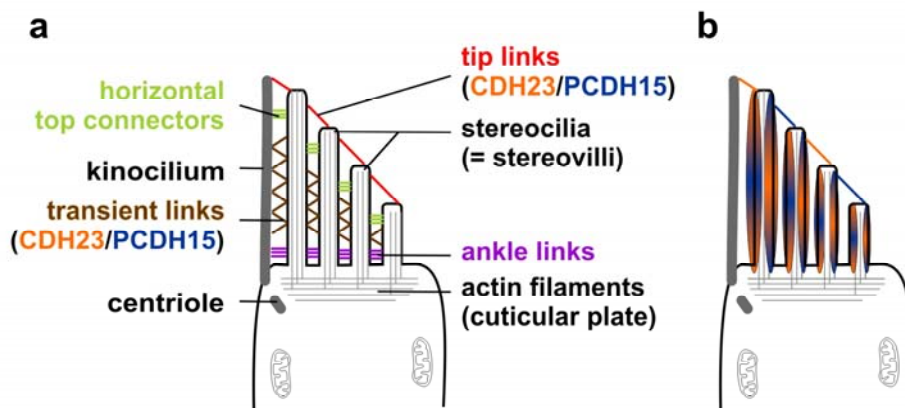
Figure 4. Localization of CDH23 and PCDH15 in inner ear hair cells. **(a)** Scheme of the apical region of an inner ear hair cell where the mechanotransduction takes place. Numerous links, interconnecting the growing stereovilli: transient links (brown), ankle links (purple) and tip links (red). During maturation transient lateral, ankle links and the kinocilium degenerate in the mammalian cochlear hair cells; horizontal top connectors (light green) and tip links (red) remain. **(b)** Localization of CDH23 and PCDH15 in the stereovilli of hair cells. During hair cell development CDH23 (orange) and PCDH15 (blue) are localized in the transient links. Isoforms of both cadherins are detected along the length of the stereovilli illustrated by the colored ovals and are components of the tip links. Similar distribution of CDH23 and PCDH15 is illustrated by means of the color gradient from orange to blue and *vice versa*.

forming fibres of an approximate length of 180 nm, which is consistent with the length of tip links. The asymmetric composition of the fibres where CDH23 and PCDH15 are localized to opposite ends of tip links indicates that other components of the mechanotransduction machinery, such as the transduction channel itself, may also be localized asymmetrically.

In contrast to the function of CDH23 in inner ear hair cells less molecular details are know about the role of CDH23 in vertebrate photoreceptor cells. In the retina, CDH23 is localized in the inner segment, the ciliary apparatus, and the ribbon synapses of rod and cone photoreceptor cells (Fig. 5) (37;38) (Lagziel et al., submitted). At the basal body complex of the photoreceptor cilium which is the structure homolog to the centrosome of non-ciliated cells the short cytoplasmic CDH23 isoform c is most likely expressed (Lagziel et al., submitted) and may contribute to ciliary functions (Fig. 5). The EC-domains of the transmembrane forms of CDH23 have been suggested to mediate membrane-membrane adhesions between the inner segment membranes of neighboring photoreceptor cells, and between the pre- and post synaptic membranes of photoreceptor cells and 2nd order retinal neurons. At synapses, it is assumed that cadherins keep the synaptic cleft in close proximity, contribute to the organization of the pre- and postsynaptic cytomatrices of a synaptic junction, and play an important role in synaptogenesis (39). Since, CDH23 and PCDH15 (see below) are co-expressed in the synaptic region they may also form asymmetric "tip link"-like fibers projecting through synaptic clefts between photoreceptor cells and retinal 2nd neurons.
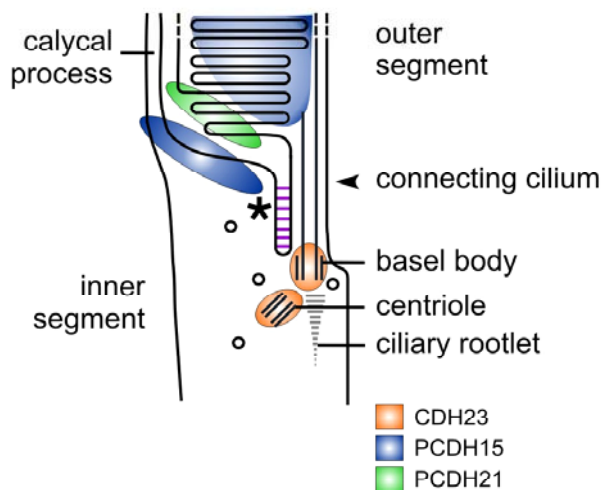
Figure 5. Localization of CDH23, PCDH15 and PCDH21 in the photoreceptor ciliary region. Schematic representation of the ciliary region of a rod photoreceptor cell: the photosensitive outer segment is linked by the connecting cilium to the biosynthetic active inner segment. A centriole is adjacent to the basal body. The membrane of the apical periciliary extension of the inner segment (asterisk) is linked by fibers (purple) to the connecting cilium membrane. Calycal processes extend from the apical inner segment and project parallel to the outer segment. In the ciliary region of vertebrate photoreceptor cells CDH23 isofroms (orange) are localized to the basal body and the centrioles. Isofroms of PCDH15 (blue) localize to the outer segment membranes and to the apical periciliary extension of the inner segment, opposing the base of the outer segment. PCDH21 (green) localization is restricted to the base of the outer segment where the nascent disks are formed.

1.2. Protocadherin 15 (USH1F, DFNB23) – the outer segment cadherin

Protocadherin 15 (PCDH15) belongs to the protocadherin family. In mammals, alternative splicing of PCDH15 results in numerous isoforms which can be divided in four groups, CD1-CD4 (Fig. 1c). The isoform CD4 does not contain any transmembrane domain and is predicted to be secreted. The isoforms CD1, CD2 and CD3 contain 11 EC domains, a single transmembrane domain and differ in their cytoplasmic domain. The cytoplasmic domain of PCDH15 CD1 consists of two prolin rich regions and a class I C-terminal PBM in the cytoplasmic domain. Via the latter PBM, PCDH15 binds to PDZ domains of harmonin (USH1C) (PDZ2) (25;40) and whirlin (19) (van Wijk, unpublished data) and is thereby integrated in the USH protein interactome (Fig. 3).

In zebrafish *Danio rerio*, two closely related *pcdh15* genes, *pcdh15a* and *pcdh15b* originated by fish-specific whole genome duplication (41), frequently found in Danio species, were detected. Interestingly, the gene duplication also resulted in the division of functional profiles indicated by distinct phenotypes caused by defects in the two *pcdh15* genes (41). Mutations in the *pcdh15a* gene in the *orbiter* mutants (42) do not affect vision, but splaying of inner-ear hair bundles causes deafness and vestibular dysfunction. In contrast, morpholino knock downs of *pcdh15b* result in a visual defect and improperly arranged morphant photoreceptor outer segments (41). In the evolutionary more distant fruit fly *Drosophila melanogaster*, *Cad99C* has been identified and characterized as an orthologue of human *PCDH15* (43). Interestingly, in the fruit fly, the Cad99C protein also participates in the morphogenesis of microvilli, present in the fly photoreceptor cells and structurally related to stereovilli of vertebrate hair cells.

In adult mammals, PCDH15 is expressed in a wide range of tissues including the liver, spleen, brain, inner ear, and retina (44;45). In the fetal cochlea, PCDH15 was detected in supporting cells, outer sacculus cells and the spiral ganglion (46) while in the mature inner ear, PCDH15 is additionally present in the stereovilli of sensory hair cells of both the cochlea and the vestibular organ (26;36;45;47) (Wolfrum, unpublished data). Studies in Ames waltzer (*av*) mice bearing mutations in the murine *pcdh15* gene indicate an essential role of PCDH15 in morphogenesis of the hair cell stereovilli and that PCDH15 is important for the correct localization of its interaction partner myosin VIIa (26;44;45;48). However, the molecular motor myosinVIIa is also necessary for correct distribution of PCDH15 in the stereovilli (26). As described in chapter 1.2, homodimers of PCDH15 and CDH23 interact thereby forming asymmetric heteromeric fibers as a backbone of the tip link (36). A specific localization of PCDH15 isoform CD3 at the tips of stereovilli indicates that the tip links contains CD3. In contrast, the PCDH15 isoform CD1 is found along the length of the stereovilli, concentrated at the base and less prominent at the tip. The CD2 isoform localization shows a broad distribution in the entire hair bundle (26;47). This expression pattern suggests that the different PCDH15 isoforms may also participate in the formation of the transient lateral links and kinociliary links during hair cell differentiation which would explain the disorganization of the hair bundles and the displacement of the kinocilium in hair cells of PCDH15 deficient Ames waltzer mice (34). In conclusion, PCDH15 is essential for the differentiation of stereovilli of hair cells and their mechanosensitve function. Furthermore, PCDH15 localization at the ribbon synapses indicates a role in synaptogenesis and/or function of synapses (17;18).

In the mammalian eye, PCDH15 expression has been described in the photoreceptor layer, the outer plexiform layer, and the ganglion cell layer of the neuronal retina, but not in the RPE layer (18;45). In rod and cone photoreceptor cells, PCDH15 was found to be present at the synaptic region, in the cell-cell adhesions of the outer limiting membrane,

in the apical region of the inner segment and in the outer segment (Fig.5) (18;45). The parallel localization of PCDH15 and scaffold protein harmonin at the outer segment membranes of the photoreceptor cell (18;37) makes their cellular interaction obvious and suggests that harmonin coordinates the outer segment function of PCDH15. Moreover, both interacting partners are also present at the photoreceptor synapses where they are integral components of the USH protein network.

PCDH15 seems obviously associated with the membranes of the entire outer segment (18), but recent results of pre-embedding labeling immunoelectron microscopy revealed that PCDH15 is most prominent in the apical membrane of the inner segment exactly in the region which faces the rim of the newly formed membrane disks at the base of the outer segment (Fig. 6). Interestingly, in this open disk region of the outer segment PCDH21, a photoreceptor specific cadherin, is distinctively found (see chapter 2. below) (49;50). Therefore, there is evidence for an intriguing hypothesis that PCDH15 and PCDH21 may also interact through their extracellular domains forming heterogenic asymmetric fiber complexes (40) as evident in the tip link arrangement of PCDH15 and CDH23 (see above, summarized in (51)). In such an adhesion complex between the membranes of the inner and outer segment, PCDH21 is thought to be positioned in rims of the "open" disks by its interaction with prominin 1 (52), whereas PCDH15 is probably anchored in the cytoplasm of the inner segment by its binding to the scaffold protein whirlin which is specifically localized there (15). Anyway, such an adhesion complex including both protocadherins would perfectly fit to stabilize the fragile newly formed disk membranes. Furthermore, more recent data on amphibian and primate photoreceptor cells have indicated that PCDH15 molecules are localized in the calycal processes
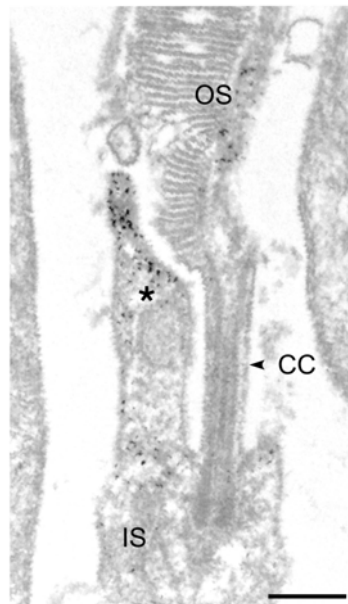
Figure 6. Subcellular localization of PCDH15 in a mouse rod photoreceptor cell by pre-embedding immunoelectron microscopy. Electron micrograph of anti-PCDH15 labeling in a longitudinal section through the ciliary region of a mouse photoreceptor cell reveals PCDH15 localization in the apical part of periciliary extension (asterisk) of the inner segment (IS) and in the outer segment (OS). CC: connecting cilium. Scale bar: 500 nm

(Nagel-Wolfrum et al., unpublished). Calycal processes are apical microvilli-like extensions of the inner segment which are thought to mechanically stabilize the outer segment, and PCDH15 may contribute to the adhesion of the membrane of calycal processes and the plasma membrane of the photoreceptor outer segment.

2. Protocadherin 21 (PCDH21) - the photoreceptor specific protocadherin

Protocadherin 21 (PCDH21), also known as MT-PCDH, KIAA1775, and prCAD, is a member of the protocadherin subfamily of cadherins (49;50;53). PCDH21 is a single pass transmembrane protein containing 6 extracellular cadherin (EC) domains and a short cytoplasmic domain (Fig. 1d) (49). PCDH21 orthologues have so far only been identified in vertebrates, but not in invertebrates. However, due to their significant similarity between PCDH21 of vertebrate species to CAD74A of *Drosophila*, CAD74A has been recently suggested as a putative invertebrate orthologue (53). In contrast to the broad tissue expression of most cadherins, PCDH21 expression is mainly found in rod and cone photoreceptor cells of vertebrate retinas. Although, the *PCDH 21* gene has been suggested as a candidate gene for a USH locus by mapping to chromosome 10q32 in the vicinity of the USH1D and USH1F loci (53), PCDH21 seems not to be expressed in hair cells. As mentioned above, PCDH21 is localized in the rim of the newly synthesized disk membranes at the base of the outer segment (49). This distinctive localization together with the obvious phenotype of disorganized outer segments in *Pcdh*^{-/-} knockout mice strongly suggests that PCDH21 is essential for correct *de novo* assembly of disks at the base of rod and cone outer segments (49;50). Absence of PCDH21 from photoreceptor cells leads to retinal degeneration in *Pcdh*^{-/-} knockout mice.

For its function PCDH21 may be integrated in the adhesion complex described above (chapter 1.2), interacting with prominin 1 (PROM1) (52). PROM1 is a 5-transmembrane protein (54) specifically associated with membrane protrusions and - like PCDH21 - it is localized to the nascent disks of rod and cone photoreceptor cells and essential for their formation (52). PROM1 may anchor the proposed adhesion complex to the actin cytoskeleton.

During maturation of the outer segment disks the extracellular domain of PCDH21 is proteolytically cleaved (50). This proteolytic cleavage in EC6 of PCDH21 drives the release of a soluble N-terminal fragment while the transmembrane C-terminal fragment remains associated with the outer segment. The shedding of PCDH21´s ectodomain should ultimately degrade the adhesion function of PCDH21 at the base of the outer segment and the rim complex proteins may take over the stabilization of disk membranes (55;56). Interestingly, in the absence of the rim complex proteins the cleavage of the PCDH21 is partially inhibited (50).

Although the role of PCDH21 in disk morphogenesis is not fully understood it certainly contributes to adhesive processes essential for photoreceptor cell disk neogenesis and stacking of outer segment disks and thereby for photoreceptor cell differentiation and maintenance.

Acknowledgments

References

1. Bolz, H., Reiners, J., Wolfrum, U., and Gal, A. (2002) *Adv Exp Med Biol* **514,** 399-410
2. Halbleib, J. M. and Nelson, W. J. (2006) *Genes Dev.* **20,** 3199-3214
3. Goodwin, M. and Yap, A. S. (2004) *J.Mol.Histol.* **35,** 839-844
4. Tom, D. S. and Brandstatter, J. H. (2006) *Cell Tissue Res.* **326,** 339-346
5. Besharse, J. C. and Horst, C. J. (1990) The photoreceptor connecting cilium - a model for the transition zone. In Bloodgood, R. A., editor. *Ciliary and flagellar membranes*, Plenum, New York
6. Roepman, R. and Wolfrum, U. (2007) *Subcell.Biochem.* **43,** 209-235
7. Insinna, C. and Besharse, J. C. (2008) *Dev.Dyn.* **237,** 1982-1992
8. Burns, M. E. and Arshavsky, V. Y. (2005) *Neuron* **48,** 387-401
9. Young, R. W. (1976) *Invest Ophthalmol.Vis.Sci.* **15,** 700-725
10. Vollrath, M. A., Kwan, K. Y., and Corey, D. P. (2007) *Annu.Rev.Neurosci.* **30,** 339-365
11. Muller, U. and Littlewood-Evans, A. (2001) *Trends Cell Biol.* **11,** 334-342
12. Adato, A., Lefevre, G., Delprat, B., Michel, V., Michalski, N., Chardenoux, S., Weil, D., El Amraoui, A., and Petit, C. (2005) *Hum.Mol.Genet.* **14,** 3921-3932
13. McGee, J., Goodyear, R. J., McMillan, D. R., Stauffer, E. A., Holt, J. R., Locke, K. G., Birch, D. G., Legan, P. K., White, P. C., Walsh, E. J., and Richardson, G. P. (2006) *J.Neurosci.* **26,** 6543-6553
14. Michalski, N., Michel, V., Bahloul, A., Lefevre, G., Barral, J., Yagi, H., Chardenoux, S., Weil, D., Martin, P., Hardelin, J. P., Sato, M., and Petit, C. (2007) *J.Neurosci.* **27,** 6478-6488
15. Maerker, T., van Wijk, E., Overlack, N., Kersten, F. F., McGee, J., Goldmann, T., Sehn, E., Roepman, R., Walsh, E. J., Kremer, H., and Wolfrum, U. (2008) *Hum.Mol.Genet.* **17,** 71-86
16. Saihan, Z., Webster, A. R., Luxon, L., and Bitner-Glindzicz, M. (2009) *Curr.Opin.Neurol.* **22,** 19-27
17. Reiners, J., Nagel-Wolfrum, K., Jürgens, K., Märker, T., and Wolfrum, U. (2006) *EXP.EYE RES.* **83,** 97-119
18. Reiners, J., Marker, T., Jurgens, K., Reidel, B., and Wolfrum, U. (2005) *Mol.Vis.* **11,** 347-355
19. Kremer, H., van Wijk, E., Marker, T., Wolfrum, U., and Roepman, R. (2006) *Hum.Mol.Genet.* **15 Spec No 2,** R262-R270
20. Imamura, Y., Itoh, M., Maeno, Y., Tsukita, S., and Nagafuchi, A. (1999) *J.Cell Biol.* **144,** 1311-1322
21. Ahmed, Z. M., Riazuddin, S., Bernstein, S. L., Ahmed, Z., Khan, S., Griffith, A. J., Morell, R. J., Friedman, T. B., Riazuddin, S., and Wilcox, E. R. (2001) *Am.J.Hum.Genet.* **69,** 25-34
22. Bork, J. M., Peters, L. M., Riazuddin, S., Bernstein, S. L., Ahmed, Z. M., Ness, S. L., Polomeno, R., Ramesh, A., Schloss, M., Srikumari, C. R. S., Wayne, S., Bellman, S., Desmukh, D., Ahmed, Z., Khan, S. N., Der Kaloustian, V. M., Li, X. C., Lalwani, A., Riazuddin, S., Bitner-Glindzicz, M., Nance, W. E., Liu, X.-Z., Wistow, G., Smith, R. J. H., Griffith, A. J., Wilcox, E. R., Friedman, T. B., and Morell, R. J. (2001) *Am.J Hum.Genet* **68,** 26-37
23. Boeda, B., El Amraoui, A., Bahloul, A., Goodyear, R., Daviet, L., Blanchard, S., Perfettini, I., Fath, K. R., Shorte, S., Reiners, J., Houdusse, A., Legrain, P., Wolfrum, U., Richardson, G., and Petit, C. (2002) *EMBO J.* **21,** 6689-6699
24. Siemens, J., Kazmierczak, P., Reynolds, A., Sticker, M., Littlewood Evans, A., and Müller, U. (2002) *Proc.Natl.Acad.Sci.USA* **99,** 14946-14951
25. Adato, A., Michel, V., Kikkawa, Y., Reiners, J., Alagramam, K. N., Weil, D., Yonekawa, H., Wolfrum, U., El Amraoui, A., and Petit, C. (2005) *Hum.Mol.Genet.* **14,** 347-356
26. Senften, M., Schwander, M., Kazmierczak, P., Lillo, C., Shin, J. B., Hasson, T., Geleoc, G. S., Gillespie, P. G., Williams, D., Holt, J. R., and Muller, U. (2006) *J.Neurosci.* **26,** 2060-2071
27. Di Palma, F., Pellegrino, R., and Noben-Trauth, K. (2001) *Gene* **281,** 31-41
28. Michel, V., Goodyear, R. J., Weil, D., Marcotti, W., Perfettini, I., Wolfrum, U., Kros, C. J., Richardson, G. P., and Petit, C. (2005) *Dev.Biol.* **280,** 281-294

29. Lagziel, A., Ahmed, Z. M., Schultz, J. M., Morell, R. J., Belyantseva, I. A., and Friedman, T. B. (2005) *Dev.Biol.* **280,** 295-306

30. Di Palma, F., Holme, R. H., Bryda, E. C., Belyantseva, I. A., Pellegrino, R., Kachar, B., Steel, K. P., and Noben-Trauth, K. (2001) *Nat.Genet.* **27,** 103-107

31. Pan, L., Yan, J., Wu, L., and Zhang, M. (2009) *Proc.Natl.Acad.Sci.U.S.A* **106,** 5575-5580

32. Wilson, S. M., Householder, D. B., Coppola, V., Tessarollo, L., Fritzsch, B., Lee, E. C., Goss, D., Carlson, G. A., Copeland, N. G., and Jenkins, N. A. (2001) *Genomics* **74,** 228-233

33. Siemens, J., Lillo, C., Dumont, R. A., Reynolds, A., Williams, D. S., Gillespie, P. G., and Muller, U. (2004) *Nature* **428,** 950-955

34. Muller, U. (2008) *Curr.Opin.Cell Biol.* **20,** 557-566

35. Sollner, C., Rauch, G. J., Siemens, J., Geisler, R., Schuster, S. C., Muller, U., and Nicolson, T. (2004) *Nature* **428,** 955-959

36. Kazmierczak, P., Sakaguchi, H., Tokita, J., Wilson-Kubalek, E. M., Milligan, R. A., Muller, U., and Kachar, B. (2007) *Nature* **449,** 87-91

37. Reiners, J., Reidel, B., El-Amraoui, A., Boeda, B., Huber, I., Petit, C., and Wolfrum, U. (2003) *Invest.Ophthalmol.Visual Sci.* **44,** 5006-5015

38. Lillo, C., Siemens, J., Kazmierczak, P., Mueller, U., and Williams, D. S. (2005) *Invest.Ophthalmol.Vis.Sci.* **46,** 5176-nn

39. Bruses, J. L. (2000) *Curr.Opin.Cell Biol.* **12,** 593-597

40. Reiners, J., van Wijk, E., Marker, T., Zimmermann, U., Jurgens, K., te, B. H., Overlack, N., Roepman, R., Knipper, M., Kremer, H., and Wolfrum, U. (2005) *Hum.Mol.Genet.* **14,** 3933-3943

41. Seiler, C., Finger-Baier, K. C., Rinner, O., Makhankov, Y. V., Schwarz, H., Neuhauss, S. C., and Nicolson, T. (2005) *Development* **132,** 615-623

42. Nicolson, T., Rusch, A., Friedrich, R. W., Granato, M., Ruppersberg, J. P., and Nusslein-Volhard, C. (1998) *Neuron* **20,** 271-283

43. D'Alterio, C., Tran, D. D., Yeung, M. W., Hwang, M. S., Li, M. A., Arana, C. J., Mulligan, V. K., Kubesh, M., Sharma, P., Chase, M., Tepass, U., and Godt, D. (2005) *J.Cell Biol.* **171,** 549-558

44. Alagramam, K. N., Murcia, C. L., Kwon, H. Y., Pawlowski, K. S., Wright, C. G., and Woychik, R. P. (2001) *Nat.Genet.* **27,** 99-102

45. Ahmed, Z. M., Morell, R. J., Riazuddin, S., Gropman, A., Shaukat, S., Ahmad, M. M., Mohiddin, S. A., Fananapazir, L., Caruso, R. C., Husnain, T., Khan, S. N., Riazuddin, S., Griffith, A. J., Friedman, T. B., and Wilcox, E. R. (2003) *Am.J.Hum.Genet.* **72,** 1315-1322

46. Alagramam, K. N., Yuan, H., Kuehn, M. H., Murcia, C. L., Wayne, S., Srisailpathy, C. R., Lowry, R. B., Knaus, R., Van Laer, L., Bernier, F. P., Schwartz, S., Lee, C., Morton, C. C., Mullins, R. F., Ramesh, A., Van Camp, G., Hageman, G. S., Woychik, R. P., and Smith, R. J. (2001) *Hum.Mol.Genet.* **10,** 1709-1718

47. Ahmed, Z. M., Goodyear, R., Riazuddin, S., Lagziel, A., Legan, P. K., Behra, M., Burgess, S. M., Lilley, K. S., Wilcox, E. R., Riazuddin, S., Griffith, A. J., Frolenkov, G. I., Belyantseva, I. A., Richardson, G. P., and Friedman, T. B. (2006) *J.Neurosci.* **26,** 7022-7034

48. El Amraoui, A. and Petit, C. (2005) *J.Cell Sci.* **118,** 4593-4603

49. Rattner, A., Smallwood, P. M., Williams, J., Cooke, C., Savchenko, A., Lyubarsky, A., Pugh, E. N., and Nathans, J. (2001) *Neuron* **32,** 775-786

50. Rattner, A., Chen, J., and Nathans, J. (2004) *J.Biol.Chem.* **279,** 42202-42210

51. Muller, U. and Gillespie, P. (2008) *Neuron* **58,** 299-301

52. Yang, Z., Chen, Y., Lillo, C., Chien, J., Yu, Z., Michaelides, M., Klein, M., Howes, K. A., Li, Y., Kaminoh, Y., Chen, H., Zhao, C., Chen, Y., Al-Sheikh, Y. T., Karan, G., Corbeil, D., Escher, P., Kamaya, S., Li, C., Johnson, S., Frederick, J. M., Zhao, Y., Wang, C., Cameron, D. J., Huttner, W. B., Schorderet, D. F., Munier, F. L., Moore, A. T., Birch, D. G., Baehr, W., Hunt, D. M., Williams, D. S., and Zhang, K. (2008) *J.Clin.Invest* **118,** 2908-2916

53. Bolz, H., Ebermann, I., and Gal, A. (2005) *Mol.Vis.* **11,** 929-933

54. Corbeil, D., Roper, K., Fargeas, C. A., Joester, A., and Huttner, W. B. (2001) *Traffic.* **2,** 82-91

55. Molday, R. S., Hicks, D., and Molday, L. (1987) *Invest Ophthalmol.Vis.Sci.* **28,** 50-61

56. Connell, G. J. and Molday, R. S. (1990) *Biochemistry* **29,** 4691-4698
57. Xu, Z., Peng, A. W., Oshima, K., and Heller, S. (2008) *J.Neurosci.* **28,** 11269-11276
58. Ramakrishnan, N. A., Drescher, M. J., Barretto, R. L., Beisel, K. W., Hatfield, J. S., and Drescher, D. G. (2009) *J.Biol.Chem.* **284,** 3227-3238

Publikation III

2.3 Overlack N, Kilic D, Bauß K, Märker T, Kremer H, van Wijk E, Wolfrum U (2011)
    Direct interaction of the Usher syndrome 1G protein SANS and myomegalin in the retina.
    Biochim. Biophys. Acta 1813, 1883-1892.
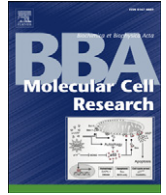
Direct interaction of the Usher syndrome 1G protein SANS and myomegalin in the retina

Nora Overlack [a], Dilek Kilic [a,1], Katharina Bauß [a], Tina Märker [a,2], Hannie Kremer [b,c,d], Erwin van Wijk [b,c,d], Uwe Wolfrum [a,*]

[a] *Institute of Zoology, Cell and Matrix Biology, Johannes Gutenberg University of Mainz, 55099 Mainz, Germany*
[b] *Department of Otorhinolaryngology, The Netherlands*
[c] *Nijmegen Centre for Molecular Life Sciences, The Netherlands*
[d] *Donders Institute for Brain, Cognition and Behaviour, Radboud University Nijmegen Medical Centre, 6500 HB Nijmegen, The Netherlands*

ARTICLE INFO

ABSTRACT

The human Usher syndrome (USH) is the most frequent cause of combined hereditary deaf-blindness. USH is genetically heterogeneous with at least 11 chromosomal loci assigned to 3 clinical types, USH1-3. We have previously demonstrated that all USH1 and 2 proteins in the eye and the inner ear are organized into protein networks by scaffold proteins. This has contributed essentially to our current understanding of the function of USH proteins and explains why defects in proteins of different families cause very similar phenotypes. We have previously shown that the USH1G protein SANS (scaffold protein containing ankyrin repeats and SAM domain) contributes to the periciliary protein network in retinal photoreceptor cells. This study aimed to further elucidate the role of SANS by identifying novel interaction partners. In yeast two-hybrid screens of retinal cDNA libraries we identified 30 novel putative interacting proteins binding to the central domain of SANS (CENT). We confirmed the direct binding of the phosphodiesterase 4D interacting protein (PDE4DIP), a Golgi associated protein synonymously named myomegalin, to the CENT domain of SANS by independent assays. Correlative immunohistochemical and electron microscopic analyses showed a co-localization of SANS and myomegalin in mammalian photoreceptor cells in close association with microtubules. Based on the present results we propose a role of the SANS-myomegalin complex in microtubule-dependent inner segment cargo transport towards the ciliary base of photoreceptor cells.

© 2011 Elsevier B.V. All rights reserved.

1. Introduction

The human Usher syndrome (USH) is the most frequent cause of combined hereditary deaf-blindness. USH is genetically heterogeneous with at least 11 chromosomal loci involved [1,2]. Depending on the degree of clinical symptoms, USH can be divided into 3 types USH1, USH2, and USH3 [3–5]. USH1 represents the most severe form, characterized by profound congenital deafness, vestibular dysfunction and prepubertal-onset of *retinitis pigmentosa* (RP) [1,6].

The gene products of the 9 so far identified USH genes are assigned to various protein classes and families [1,6,7]. The *USH1B* gene encodes the molecular motor myosin VIIa. Harmonin (*USH1C*), SANS (scaffold protein containing ankyrin repeats and SAM domain, *USH1G*) and whirlin (*DFNB31*/USH2D) belong to the group of scaffold proteins [2,8] and reviewed in [1,6]. Cadherin 23 (*CDH23*/USH1D) and protocadherin15 (*PCDH15*/USH1F) are cell–cell adhesion proteins, whereas *USH2A* and *GPR98* encode large transmembrane proteins, the USH2A isoform b and the very large G protein coupled receptor 1b/G protein-coupled receptor 98 (VLGR1b/GPR98). The four-transmembrane-domain protein clarin-1 (USH3A) encoded by *CLRN1* is so far the only identified member of USH3 (reviewed in [1,6,7]).

Previous analyses elucidated the assembly of all USH1 and USH2 proteins into USH protein networks mediated by the USH scaffold proteins harmonin, whirlin and SANS (reviewed in [1,6,7]). In inner ear hair cells the USH protein network is essential for the correct development of hair bundle stereocilia and for signal transduction [7,9–12]. Since, in the retina, all proteins of the USH network are found at the synapse of photoreceptor cells, a role of this network in maintaining the synaptic integrity was proposed [1,6,7]. More recently, we and others have demonstrated a USH protein network organized by whirlin and SANS in the ciliary–periciliary region of photoreceptor cells [13–17]. This region connects the biosynthetic

* Corresponding author at: Johannes Gutenberg University, Institute of Zoology, Cell and Matrix Biology, Müllerweg 6, D-55099 Mainz, Germany. Tel.: +49 6131 39 25148; fax: +49 6131 39 23815.

E-mail address: wolfrum@uni-mainz.de (U. Wolfrum).

[1] Current address: Sabanci University Faculty of Engineering and Natural Sciences Biological Sciences & Bioengineering Program, 34956 Istanbul, Turkey.
[2] Current address: Institute for Clinical Diabetology, German Diabetes Center, Leibniz Center for Diabetes Research at the Heinrich-Heine-University Düsseldorf, Germany.

active inner segment with the photosensitive outer segment and is crucial for transport processes between these two compartments of photoreceptor cells [18]. Our previous results indicated that the USH1G protein SANS serves as a molecular interconnector between the microtubule based transport across the inner segment to the ciliary transport in the USH protein network of photoreceptor cells [13]. We have previously shown interactions of SANS with e.g. whirlin, myosin VIIa and its homomerization [13,19]. In COS7 cells SANS is recruited to the plasma membrane by USH1 cadherins, cadherin 23 and proto-cadherin 15, indicating a physical linkage of these molecules [20]. These interactions underline the SANS scaffolding function in the USH interactome and identified SANS as one of the key organizers of the ciliary–periciliary USH protein network of vertebrate photoreceptor cells [13,19]. Furthermore, we provided first evidence for an association of SANS with microtubules linking the USH protein networks to the microtubule cytoskeleton and hence to microtu-bule-associated intracellular transport processes [13,19]. More re-cently, the association of USH protein networks including SANS with transport vesicles has been demonstrated [21] confirming the latter hypothesis.

The USH1G gene product SANS is composed of defined domains (Fig. 1A) supposed to mediate protein–protein interactions [8]. Three N-terminal ankyrin repeats are followed by a central domain (CENT), a SAM (sterile alpha motif) domain and a class I PBM (PDZ-binding motif) at the C-terminus. The identity of the ankyrin repeats, the SAM and PBM domain, as well as their roles in protein–protein interactions have been previously studied [8,13,19]. Preceding work showed a direct interaction of the SAM domain with the PDZ domains of harmonin and whirlin in vitro [13,19]. In addition, a recent study revealed a synergistic binding of the SAM domain and the C-terminal PBM to the N-domain and PDZ1 of harmonin [22].

Although sequence analyses and database search described the CENT domain of SANS as an unknown or low complexity region (www.smart.heidelberg.de), previous studies characterized it as a potent scaffold domain: preceding work demonstrated interaction of the SANS CENT domain with both MyTH4 (myosin tail homology 4) and FERM (4.1, ezrin, radixin, moesin) tandem domain repeats of myosin VIIa [19,23]. Moreover, the CENT domain is capable of mediating SANS homomerization [19]. In order to identify additional putative binding partners interacting with the CENT domain of SANS we performed
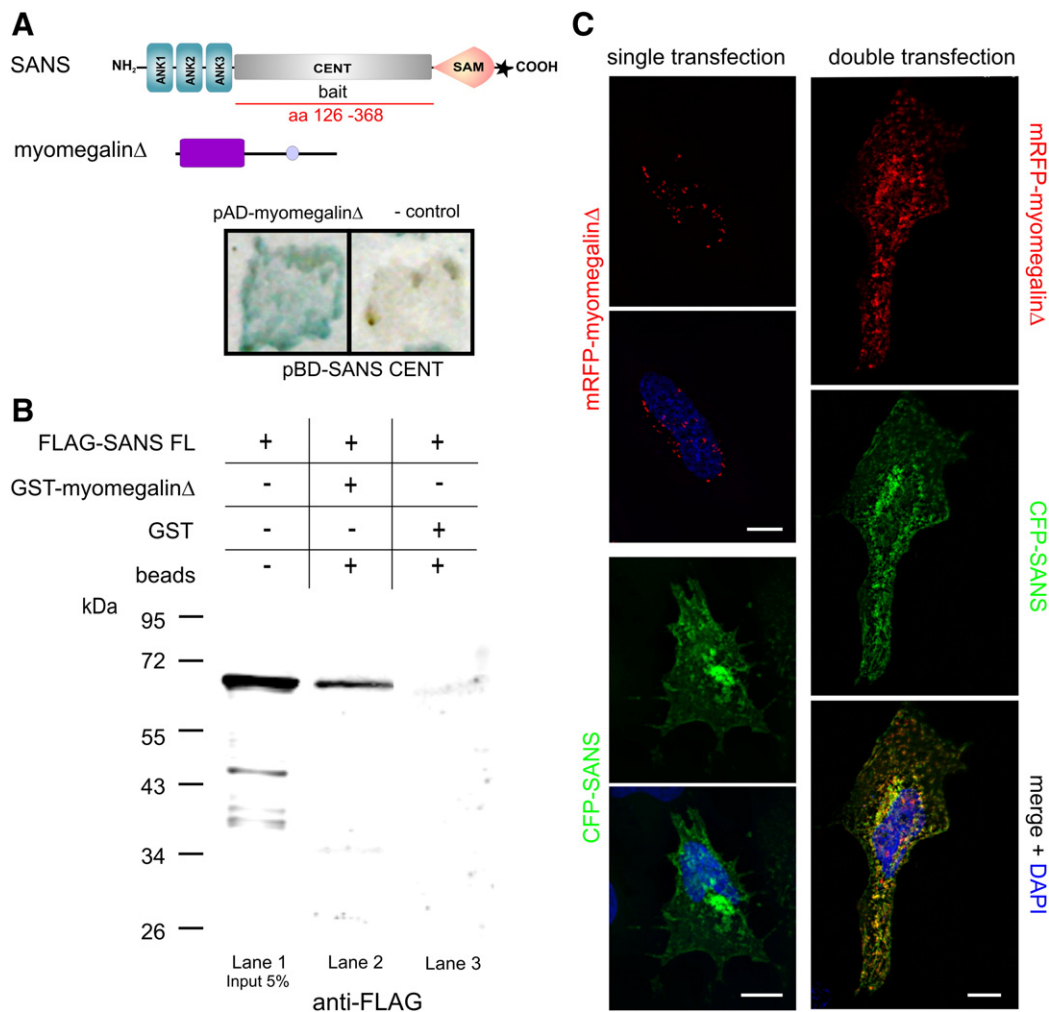
Fig. 1. Validation of the SANS-myomegalin interaction. (A) Scheme of SANS and myomegalinΔ domain structure and yeast two-hybrid assay. SANS is composed of three ankyrin repeats (ANK) at the N-terminus, a central domain (CENT) followed by a sterile alpha motif (SAM) and a PDZ-binding motif (PBM) at the C-terminus (*asterisk*). MyomegalinΔ (474 aa) contains a SCOP domain: d1gw5b (*box*) and coiled-coil domains (*circle*). Yeast two-hybrid screens were performed in a bovine retina cDNA library with SANS CENT fused to the DNA-binding domain of the GAL4 reporter. MyomegalinΔ protein was identified as one interaction candidate. (B) GST pull-down of SANS and myomegalinΔ. FLAG-tagged SANS was incubated with immobilized GST-myomegalinΔ, or GST alone. Anti-FLAG Western blot revealed pull-down of SANS by GST-myomegalinΔ (lane 2) but not GST alone (lane 3). Lane 1 shows 5% input of FLAG-SANS full length. (C) Co-localization of mRFP-myomegalinΔ and CFP-SANS in HeLa cells. Upper left panel: overexpressed mRFP-myomegalinΔ (red) is localized right around the DAPI stained nucleus in single transfected cells. Lower left panel: overexpressed CFP-SANS (green) is localized to the cytoplasm, enriched at the membrane, and as an intense spot at the periphery of the nucleus. Right panel: in mRFP-myomegalinΔ and CFP-SANS co-transfected HeLa cells, overexpressed CFP-SANS (green) recruits mRFP-myomegalinΔ (red) to the cytoplasm and an intense spot at the periphery of the nucleus. Scale bars: 10 μm.

yeast two-hybrid screens of a retinal cDNA library using the CENT domain as bait. We succeeded to identify 30 potential binding partners to SANS including myomegalin as the major SANS CENT interacting partner, most abundantly found in the screen (Fig. 1A). Myomegalin, also known as PDE4DIP (phosphodiesterase 4D interacting protein), was first identified as a novel Golgi apparatus and centrosome associated protein termed after its large size and high abundance in the muscle [24]. Data base analyses predict four isoforms for mouse myomegalin ranging in their predicted molecular weight from 15 kDa (isoform 3) to 275 kDa (isoform 1), all containing protein–protein interaction domains.

In the present study we demonstrate that myomegalin is integrated into the multifunctional protein interactome related to USH via its binding to the USH scaffold protein SANS. The SANS-myomegalin interaction was confirmed by independent assays and partial co-localization of the interacting partners was shown in mammalian retinas. Conclusively, the present data also provide further insights on the role of the SANS organized protein complex in microtubule-based inner segmental cargo transport.

2. Methods

2.1. Yeast two-hybrid screen

The yeast two-hybrid screen was performed as previously described [13]. The CENT domain of SANS (amino acids 126–368) was used as bait on a bovine oligo-dT primed retinal cDNA library. Interactions were analyzed by assessment of reporter gene activation. If yeast clones grew on selection plates and were stained in the α- and β-galactosidase activity assays, an interaction between a protein pair was indicated.

2.2. GST pull-down assays

Bovine myomegalinΔ clone, found in the yeast two-hybrid, was subcloned in the pGEX4T3 vector, expressed in *E. coli* BL21 and bound to beads as described in [25]. FLAG-tagged human SANS full length (amino acids 1–461) was produced by transfection of COS-7 cells with the appropriate vector, using Lipofectamine™ LTX and Plus Reagent as transfection reagent (Invitrogen, Karlsruhe, Germany) according to manufacturer's instructions. 24 h post-transfection cells were washed with PBS and subsequently lysed on ice in lysis buffer (50 mM Tris–HCL pH 7.5, 150 mM NaCl, and 0.5% Triton-X-100). The cell supernatant was incubated 2 h at 4 °C with equal amounts of beads pre-incubated either with GST or with GST-fusion proteins. Beads were washed with lysis buffer and precipitated protein complexes were eluted with SDS sample buffer and subjected to SDS-PAGE and Western blot.

2.3. Antibodies

Polyclonal SANS antibodies generated against a murine fragment (amino acids 1–46) and raised in rabbit were previously characterized [14]. Anti-Myomegalin polyclonal mouse antibody (H00009659-B01) and anti-FLAG-tag antibodies were acquired from Abnova (Taiwan) or Sigma-Aldrich (Sigma-Aldrich, St. Louis, MO, USA), respectively. Monoclonal antibodies against centrin 3 were previously reported [26]. Secondary antibodies were purchased from Invitrogen or Rockland.

2.4. Animals and tissue preparation

All experiments described herein conform to the statement by the Association for Research in Vision and Ophthalmology (ARVO) as to care and use of animals in research. Adult C57BL/6J mice were maintained under a 12 h light–dark cycle, with food and water *ad*

libitum. After sacrifice of the animals in CO_2 (rodents) and decapitation, subsequently entire eyeballs, and appropriate tissues were dissected, or retinas were removed through a slit in the cornea prior to further analysis. Eyes of *macaca mulatta* were obtained from the German Primate Center (DPZ, Göttingen, Germany). Human eyes were obtained from the Dept. of Ophthalmology, Mainz, Germany and guidelines to the declaration of Helsinki were followed.

2.5. Fluoresescence microscopical analysis of transfected HeLa cells

Human full-length SANS was cloned in pPalm-Myr-CFP vector resulting in an N-terminal CFP-fusion protein. Bovine myomegalinΔ was cloned in pDest-733 (Invitrogen) resulting in N-terminal fused mRFP. Both constructs were transfected individually or in combination using Lipofectamine™ LTX and Plus Reagent transfection reagent (Invitrogen) according to the manufacturer's instructions. After 24 h cells were fixed with methanol + 0.05% EGTA and air-dried. Subsequently, the samples were incubated with 0.01% Tween 20 in PBS for 20 min. After washing once with PBS, the samples were incubated in PBS with DAPI (4′,6-Diamidin-2′-phenylindoldihydrochlorid) (Sigma-Aldrich) for 1 h at room temperature in the dark. After washing with PBS sections were mounted in Mowiol 4.88 (Hoechst, Frankfurt, Germany). Samples were analyzed with a Leica DM 6000 B microscope (Leica microsystems, Bensheim, Germany) and images were processed with Adobe Photoshop CS (Adobe Systems, San Jose, CA, USA).

2.6. Western blot analyses

For Western blot analyses, the appropriate tissue samples were prepared in RIPA buffer (50 mM Tris–HCl, 150 mM NaCl, 0.1% SDS, 2 mM EDTA, 1% NP-40, 0.5% sodium-deoxycholate, 1 mM sodiumvanadate, 30 mM sodium-pyrophosphate, pH 7.4) containing a protease inhibitor cocktail (Roche Diagnostics, Risch, Suisse). For denaturing gel electrophoresis, samples were mixed with SDS-PAGE loading buffer (10% glycerine, 250 mM Tris-base, 2% SDS, 0.5 mM EDTA, 0,001% bromophenol blue, HCL pH 8.5). For myomegalin expression analyses 75 μg of each protein extract were separated on Mini-Protean® TGX™ 4–20% gels (Bio-Rad, Hercules, California, USA). For GST pull-down the samples were separated on a 12% polyacrylamide gel. Proteins were transferred to polyvinylidene difluoride membranes (Millipore, Schwalbach, Germany). After blocking the membrane with Applichem blocking reagent (Applichem, Darmstadt, Germany) for 2 h at room temperature, immunoreactivities were detected by applying primary and appropriate secondary antibodies Alexa Flour 680 (Invitrogen) or IR Dye 800 (Rockland, Gilbertsville, USA) employing the Odyssey infra red imaging system (LI-COR Biosciences, Lincoln, NE, USA).

2.7. RT-PCR analyses

Total RNA was isolated from mouse tissues by Macherey-Nagel RNA isolation kit (Macherey-Nagel, Düren, Germany). Reverse transcription was performed with 5 μg of RNA with the SuperScript III First Strand kit (Invitrogen) following manufacturer's instructions with a mixture of random hexamers and oligo-dT primers. PCR was performed in a volume of 50 μl using 2 μl of prepared cDNA according to directions and 10 nmol of each primer/reaction. Cycling conditions were 40 cycles at 94 °C for 1 min, 50 °C for 40 s, and 72 °C for 90 s followed by a 7 min 72 °C extension. The length of PCR products was determined on 1% agarose gels. As DNA marker, a 1-kb DNA ladder (GeneCraft, Lüdinghausen, Germany) was used. Primers, specific for mouse myomegalin isoforms used for RT-PCR: Isoform 1; forward (5′-TG GAGAAGTGCTGAGAGGGTTC-3′) and reverse primer (5′-CTCTGAGC-CAGTGCCTCAGAAT-3′). Isoform 2; forward (5′-AGGCAAAGATGTCTCTCGTG-3′) and reverse primer (5′-GCATCCAGAGACTCCACGGA-3′). Isoform 3; forward (5′- ATGGAGCAGACCTGGGCCAG-3′) and reverse primer (5′-

CAGGCGCGCTGGACTCACT-3′). Isoform 4; forward (5′-TG GATATCGCACTCTGTCC-CAG-3′) the reverse primer is the same as for isoform 1 reverse.

2.8. Immunofluorescence microscopy of retina cryosections

Eyes of adult wild-type mice or retinas of monkey or human were cryofixed in melting isopentane and cryosectioned as described elsewhere [27]. Cryosections were placed on poly-L-lysine-precoated coverslips and incubated with 0.01% Tween 20 in PBS for 20 min. After several PBS washing steps sections were covered with blocking solution (0.5% cold-water fish gelatin plus 0.1% ovalbumin in PBS) and incubated for a minimum of 30 min followed by an overnight incubation with primary antibodies, diluted in blocking solution at 4 °C. Washed cryosections were incubated with secondary antibodies conjugated to Alexa 488 or Alexa 568 (Invitrogen) in PBS with DAPI (Sigma-Aldrich) to stain the DNA of the cell nuclei, for 1.5 h at room temperature in the dark. After repeated washing with PBS sections were mounted in Mowiol 4.88 (Hoechst). Light microscopy analyses of immunofluorescence samples were performed with a Leica TCS SP5 or a Leica TCS STED confocal microscope (Leica microsystems) and images were processed with Adobe Photoshop CS (Adobe Systems).

2.9. Immunoelectron microscopy

For immunoelectron microscopy, the recently introduced protocol for pre-embedding labeling was applied [13,28]. Ultrathin sections were analyzed in a transmission electron microscope (Tecnai 12 BioTwin; FEI, Eindhoven, The Netherlands). Images were obtained with a charge-coupled device camera (SIS Megaview3; Surface Imaging Systems) acquired by analySIS (Soft Imaging System) and processed with Photoshop CS.

3. Results

3.1. Identification of myomegalin as a novel interaction partner of SANS CENT by yeast two-hybrid screen

Previous data have indicated that the CENT domain of SANS is an important target domain for direct protein binding to the SANS scaffold protein [19,23]. We performed yeast two-hybrid (Y2H) screens to identify novel interacting partners of SANS. For this, the CENT domain (amino acids 126–368) of human SANS (Fig. 1A) was fused to the DNA-binding domain (pBD) of the GAL4 reporter to screen a bovine retinal cDNA library. The positive clones were retested in reciprocal Y2H assays to verify the specificities of the interactions.
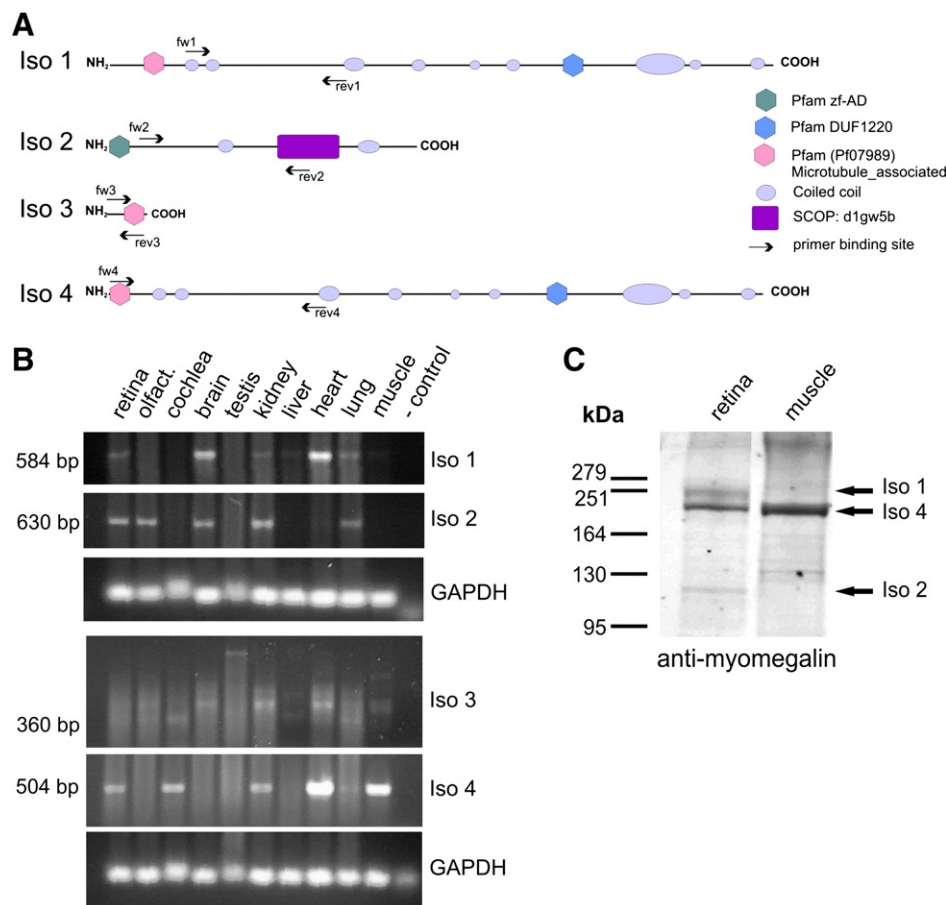
Fig. 2. Domain structure and expression profile of myomegalin isoforms in different mouse tissues. (A) Scheme of mouse myomegalin isoforms. Pfam family microtubule-associated domains (hexagon) in isoforms 1, 3 and 4, Pfam DUF1220 family domain (triangle) in isoforms 1 and 4. Pfam zf-AD domain, also known as ZAD (pentagon) and SCOP (structural classification of proteins) domain d1gw5b_ (rectangle) in isoform 2. Coiled-coil domains are present in all isoforms except for isoform 3. *Arrows* indicate primer binding sites for RT-PCR analyses. (B) RT-PCR analyses of myomegalin isoforms in murine tissues. RNA extract of different mouse tissues was used for RT-PCR. Isoform 1 can be detected in retina, brain, kidney, heart and lung. Isoform 2 is expressed in retina, olfactory epithelium (olfact.), brain, kidney and lung. Primers specific for Isoform 3 produce bands of the expected size in cochlea and lung. Amplification of isoform 4 mRNA is possible in retina, cochlea, kidney, heart and muscle. GAPDH is amplified as an internal control. (C) Western blot analyses of total protein extracts of adult murine retina and muscle with anti-myomegalin antibodies. The three larger isoforms can be detected in varying amounts in the different tissues at their estimated size (Iso1 ~275 kDa; Iso2 ~126 kDa; Iso4 ~262 kDa). In the retina all isoforms can be detected.

Sequence analyses of the 123 positive clones obtained in the Y2H assay revealed that 47 of these clones encoded for myomegalin. The identified clones contained overlapping sequences of myomegalin cDNA spanning the amino acids 577–1050 of the bovine sequence (myomegalinΔ, Fig. 1A). The interacting part of the bovine myomegalin displays 89% similarity to human and 85% similarity to mouse myomegalin. Database analysis of the myomegalinΔ interaction domain found in the Y2H screen predicted a SCOP family d1gw5b_domain (ARM repeat superfamily) and a coiled-coil domain (www.smart.heidelberg.de) (Fig. 1A).

3.2. Confirmation of direct interaction of SANS and myomegalin by GST pull-down and in cell culture

We performed GST pull-down assays and cell culture transfection assays to further validate the interaction between SANS and myomegalin *in vitro* and in cultured cells (Fig. 1B, C). Recombinant GST-myomegalinΔ fusion protein and GST alone were immobilized onto glutathione sepharose beads and incubated with FLAG-SANS full length protein. Subsequently, recovered proteins were analyzed by Western blot using anti-FLAG antibodies. GST-myomegalinΔ was able to pull-down FLAG-SANS full length (Fig. 1B), whereas GST alone was not. These data confirmed the direct interaction between SANS and myomegalin *in vitro*.

Next we analyzed whether myomegalin and SANS also interact in the cellular context. For this, we co-transfected HeLa cells with myomegalinΔ and SANS fluorescent fusion constructs. Cells expressing the mRFP-myomegalinΔ fusion proteins showed a peri-nuclear staining (Fig. 1C, upper left panel). Single transfection of HeLa cells with CFP-SANS resulted in CFP fluorescence in the cytoplasm and as a bright spot at the nucleus (Fig. 1C). Co-transfection of mRFP-myomegalinΔ and CFP-SANS induced the redistribution of mRFP-myomegalinΔ to the cytoplasm, enriched at the plasma membrane and the nuclear membrane, co-localizing with CFP-SANS (Fig. 1C). In conclusion, the *in vitro* GST pull-down and the analysis of co-transfected HeLa cells confirmed the direct binding of SANS and myomegalin.

3.3. Expression profile of myomegalin isoforms in different mouse tissues

PubMed database searches predicted four isoforms of myomegalin in the mouse (Fig. 2A). Isoform 1 represents the longest transcript and encodes a protein of an estimated molecular mass of 275 kDa. Isoforms 2 and 3 are much shorter, with estimated molecular weights of 126 kDa and 15 kDa, respectively. Isoform 4 also encodes for a relative large 262 kDa protein but in comparison to isoform 1 it contains a different 5′ untranslated segment and lacks 5′ coding sequence segments. It is of note that, isoform 4 was recently withdrawn from the PubMed database.

We analyzed the expression of myomegalin isoforms on the transcriptional level in diverse mouse tissues by RT-PCR using isoform specific primer combinations (Fig. 2B). The expression of the myomegalin isoforms varied in the different tissues tested. For example isoform 2 was detected in the retina, the olfactory epithelium, the brain, the kidney, and the lung. The long isoform 4 was expressed in the retina, the cochlea, the kidney, the heart and the muscle and thereby showed a different tissue expression profile than the similar other long isoform, isoform 1. Next we evaluated the protein expression profile of myomegalin in mouse retina and muscle. Our Western blots with antibodies against myomegalin revealed the three larger isoforms in varying amounts in the tissues analyzed. In the retina these isoforms were detected at their estimated sizes (Iso1 ~275 kDa; Iso2 ~126 kDa; Iso4 ~262 kDa) (Fig. 2C).

3.4. Spatial distribution of myomegalin expression in the mammalian retina

The eye is one of the main organs affected by the human Usher syndrome (USH). Previous studies indicated that the USH1G scaffold protein SANS contributes to USH protein networks and to transport processes in photoreceptor cells [13,14]. To elucidate the spatial distribution of myomegalin expression in the mammalian retina we subjected longitudinal cryosections of mouse, non-human primate (macaque), and human retinas to indirect immunofluorescence using antibodies against myomegalin (Fig. 3). Microscopic analyses
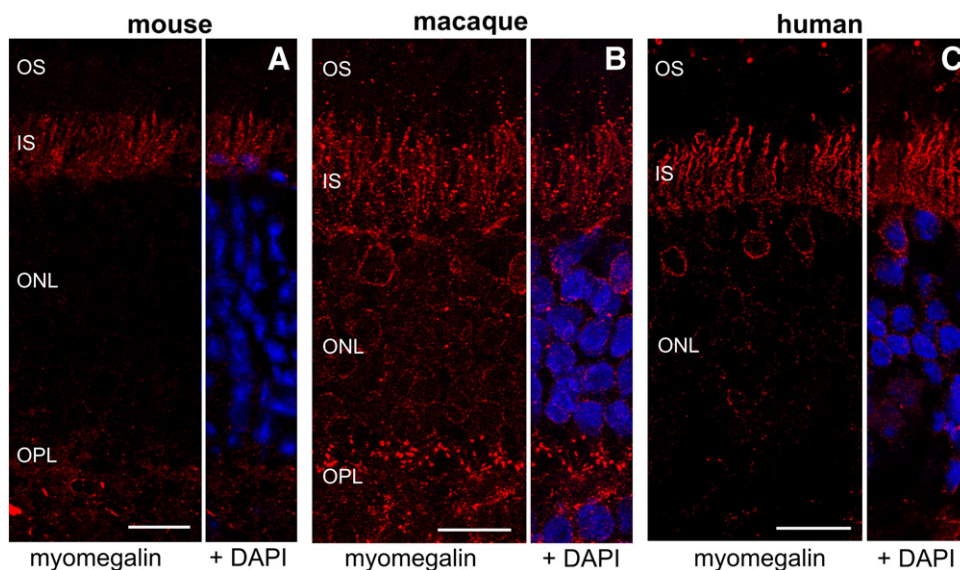
Fig. 3. Myomegalin expression in the retina of mouse, macaque and human. (A–C) Indirect immunofluorescence analyses of myomegalin (red) in longitudinal retina sections. Nuclear DAPI staining reveals the different layers of the retina. (A) In mouse retina myomegalin is localized in a fibrous pattern in the inner segment (IS) and is also found in the outer plexiform layer (OPL). (B) In macaque retina myomegalin is found in a fibrous pattern in the IS, where it is located around the nuclei in the outer nuclear layer (ONL) and in the OPL. (C) In human retina myomegalin is localized in a fibrous pattern in the IS, and is found around the nuclei in the outer nuclear layer (ONL). OS; outer segment. Scale bars: 15 μm.

revealed myomegalin staining in different layers of the mammalian retina; the outer plexiform layer, the outer nuclear layer, the outer limiting membrane, and the photoreceptor layer where it was present in the inner segment and the region of the connecting cilium (Fig. 3A, B). The myomegalin staining of the perinuclear cytoplasm was more prominent in the outer nuclear layer of macaque and human retinas (Fig. 3B, C) in comparison to the mouse retina (Fig. 3A). The unconventional localization of myomegalin in the perinuclear cytoplasm was confirmed in higher resolution immunofluorescence analysis and immunoelectron microscopy of human photoreceptor cells (Fig. 4). It is notable that the synapses in the outer plexiform layer were barely stained by anti-myomegalin in the analyzed human retina specimens (Fig. 3C). This is most probably due to post-mortem proteolytic degradation of the synaptic regions in the human donor eyes frequently observed by electron microscopic analysis (data not shown).

Since in previous studies a ciliary-periciliary USH protein network was demonstrated in photoreceptor cells [13,15–17] we next focused on a putative ciliary association of myomegalin. For this we double labeled retinal sections with antibodies against myomegalin and centrin, a validated marker for the connecting cilium, its basal body and the adjacent centriole of photoreceptor cells (Fig. 5). Myomegalin was stained in a punctuated pattern throughout the entire inner segment. Merged images revealed that the myomegalin staining overlaps with the anti-centrin immunofluorescence in the apical inner segment tips at the base of the connecting cilium, indicating the localization of myomegalin in the basal body and the adjacent centriole (Fig. 5).

3.5. Co-localization of myomegalin and SANS in retinal photoreceptor cells

A prerequisite for functional interactions of two proteins *in vivo* is that both are co-expressed in the same cell of a tissue and are co-localized in same subcellular compartment of this cell type. Previously published data [13,14] and present results on the spatial distribution of the interacting partners SANS and myomegalin indicated co-expression in retinal photoreceptor cells. To evaluate potential co-localization of the interacting partners we performed double immunofluorescence analyses on longitudinal sections
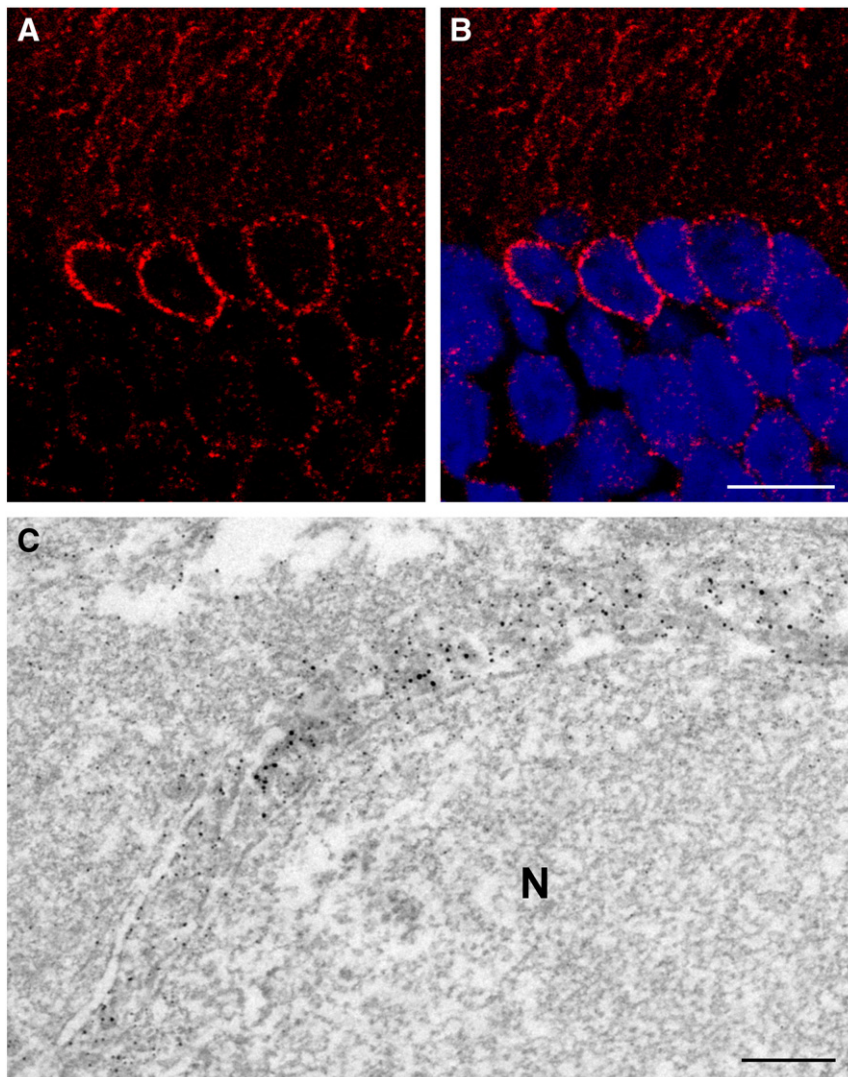
Fig. 4. Localization of myomegalin around the nucleus of photoreceptor cells by indirect immunofluorescence and immunoelectron microscopy. (A, B) Anti-myomegalin labeling (red) demonstrates localization of myomegalin around the nuclei (blue) of human photoreceptor cells. (C) Labeling of anti-myomegalin antibodies is detected around the nucleus of a human photoreceptor cell by immunoelectron microscopy. Scale bars: A, B: 7.5 μm; C: 250 nm.
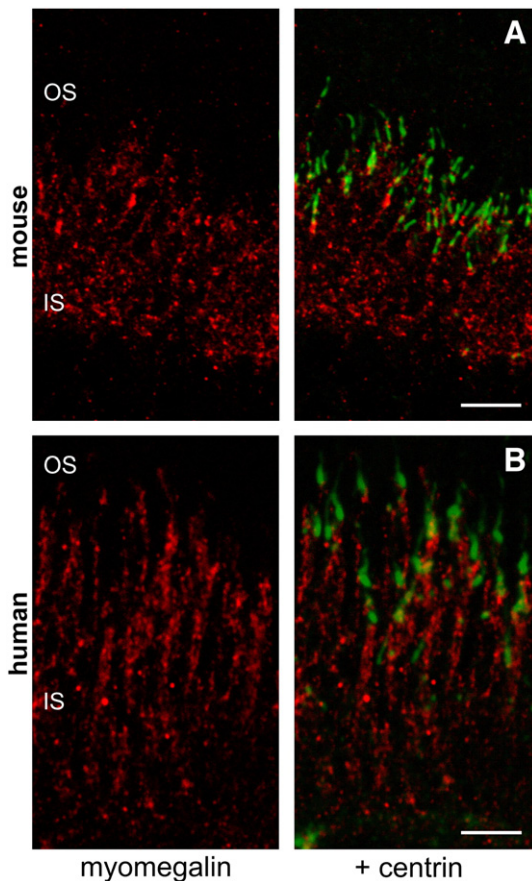
Fig. 5. Localization of myomegalin and centrin in mouse and human photoreceptor cells. (A) Indirect immunofluorescence of myomegalin and centrin as a marker for the connecting cilium and adjacent centriole on longitudinal sections through mouse retina. Confocal image shows myomegalin (red) localization as fibrous pattern in the inner segment. Overlay with centrin (green) shows partial co-localization of myomegalin with centrin in the region of the basal body and centriole. (B) Indirect immunofluorescence of myomegalin and centrin as a marker for the connecting cilium and adjacent centriole on longitudinal sections through human retina. Confocal image shows myomegalin (red) localization as fibrous pattern in the inner segment. Overlay with centrin (green) shows partial co-localization of myomegalin with centrin in the region of the basal body and centriole. Scale bars: 5 μm.

through mouse, macaque, and human retinas (Fig. 6). As already shown by single labeling of myomegalin in Fig. 3, myomegalin staining was present in the inner segment and in the peri-nuclear cytoplasm of photoreceptor cells as well as in the outer limiting membrane and at the synapses in the outer plexiform layer (Fig. 6A). Double immunofluorescence analyses revealed that myomegalin and SANS were partially co-localized in the inner segment, at the outer limiting membrane and in the periciliary region of photoreceptor cells (Fig. 6A–D). In addition, we found partial co-localization of both proteins in the outer plexiform layer of mouse retina (Fig. 6A).

Although, the analysis of higher magnifications further elucidated co-localization of SANS and myomegalin in the inner segment and at the base of the connecting cilium (Fig. 6) a more precise detection was reserved to the high resolution of electron microscopy. For the precise localization of SANS and myomegalin in photoreceptor cells we performed pre-embedding immunoelectron microscopy of human retinas (Fig. 7). The parallel analyses of ultra thin sections revealed SANS and myomegalin antibody labeling in the apical inner segment extension and in the apical part of the connecting cilium (Fig. 7A, C). On the electron micrographs SANS and myomegalin were additionally

localized along longitudinally orientated tracks spanning the inner segment (Fig. 7B, D). Post-embedding immunogold labeling of human retina ultra thin sections with anti-tubulin antibodies enabled us to identify these tracks as microtubules (Fig. 7E, F). As shown in Fig. 7E and F tubulin was also decorated in the microtubule cytoskeleton of the connecting cilium and in the apical inner segment.

4. Discussion

In this study, we demonstrate that myomegalin (phosphodiesterase 4D interacting protein, PDE4DIP) directly interacts with the USH1G protein SANS and that these proteins co-localize at distinct sites in mammalian photoreceptor cells. Three independent lines of evidence show that SANS and myomegalin can form a complex *in vivo*. First, among all 30 different clones identified in the yeast two-hybrid assay as putative binding partners to SANS, clones encoding for myomegalin were the most abundant. Second, GST pull-downs confirmed the direct interaction of myomegalin with SANS *in vitro*. Third, co-transfection of mRPF-myomegalin and CFP-SANS resulted in redistribution of mRPF-myomegalin and its co-localization with CFP-SANS. In addition, *in situ* expression analyses by indirect immunofluorescence and immunoelectron microscopy localization studies of SANS and myomegalin demonstrate the co-localization of both proteins in retinal photoreceptor cells providing evidence for the assembly of SANS-myomegalin interactions/complexes *in vivo*.

The direct binding of myomegalin to SANS is most probably mediated by the interaction of the SANS CENT domain with the myomegalin ARM domain composed of Armadillo repeats (Fig. 1A). In other proteins ARM domains are potent target sites mediating the binding to diverse interacting partners [29]. Sequence analysis of the myomegalin clone gained in our present yeast two-hybrid screen predicts a SCOP family d1gw5b ARM domain as well as a coiled-coil domain (see Fig. 1A). Latter coiled-coil motifs in proteins commonly interact with coiled-coil domains of the binding partner [30,31]. However, SANS does not possess any coiled-coil domain and the interaction of the SANS CENT domain with the tail of myosin VIIa does not occur through its coiled-coil domain but is mediated by FERM domains [19,23]. This line of evidence indicates that the interaction between SANS CENT and myomegalin also does not occur through coiled-coil domains but is based on the ARM repeat domain of myomegalin which is restricted to the isoform 2 of myomegalin.

In addition to the direct binding of myosin VIIa we have previously shown that the SANS CENT domain mediates SANS homomerization [19]. Our present yeast two-hybrid screen revealed additional 30 potential binding partners of the SANS CENT domain. Myomegalin may compete with these interaction partners in binding to the SANS CENT domain in the cell.

Previous studies have indicated that myomegalin (PDE4DIP) acts as a scaffolding protein found to be associated with centrosomes and the Golgi apparatus [24]. In muscle cells a protein complex containing myomegalin regulates intracellular signaling and trafficking [32]. As known for other proteins interaction of distinct cellular binding partners to the Armadillo repeats may specify the function of myomegalin in various cellular contexts [29]. At the Z-disk of muscle and at the Golgi myomegalin function is closely related to its interplay with PDED4 and the PKA anchoring protein AKAP450 [32–34], which recently has been shown to be required for microtubule nucleation at the Golgi [35]. Interestingly AKAP450 was also identified in our present yeast two-hybrid screen of a retinal library as a putative interacting partner of SANS (Märker et al. unpublished). Thus, SANS may also function in concert with a myomegalin-PDED4-AKAP450 complex in retinal cells.

Previous data demonstrated the association of the USH1G protein SANS with the microtubule cytoskeleton, the centrosome and transport vesicles [13,14,19,21]. Furthermore, there is evidence for a role of SANS in microtubule-based transport of post-Golgi vesicles in
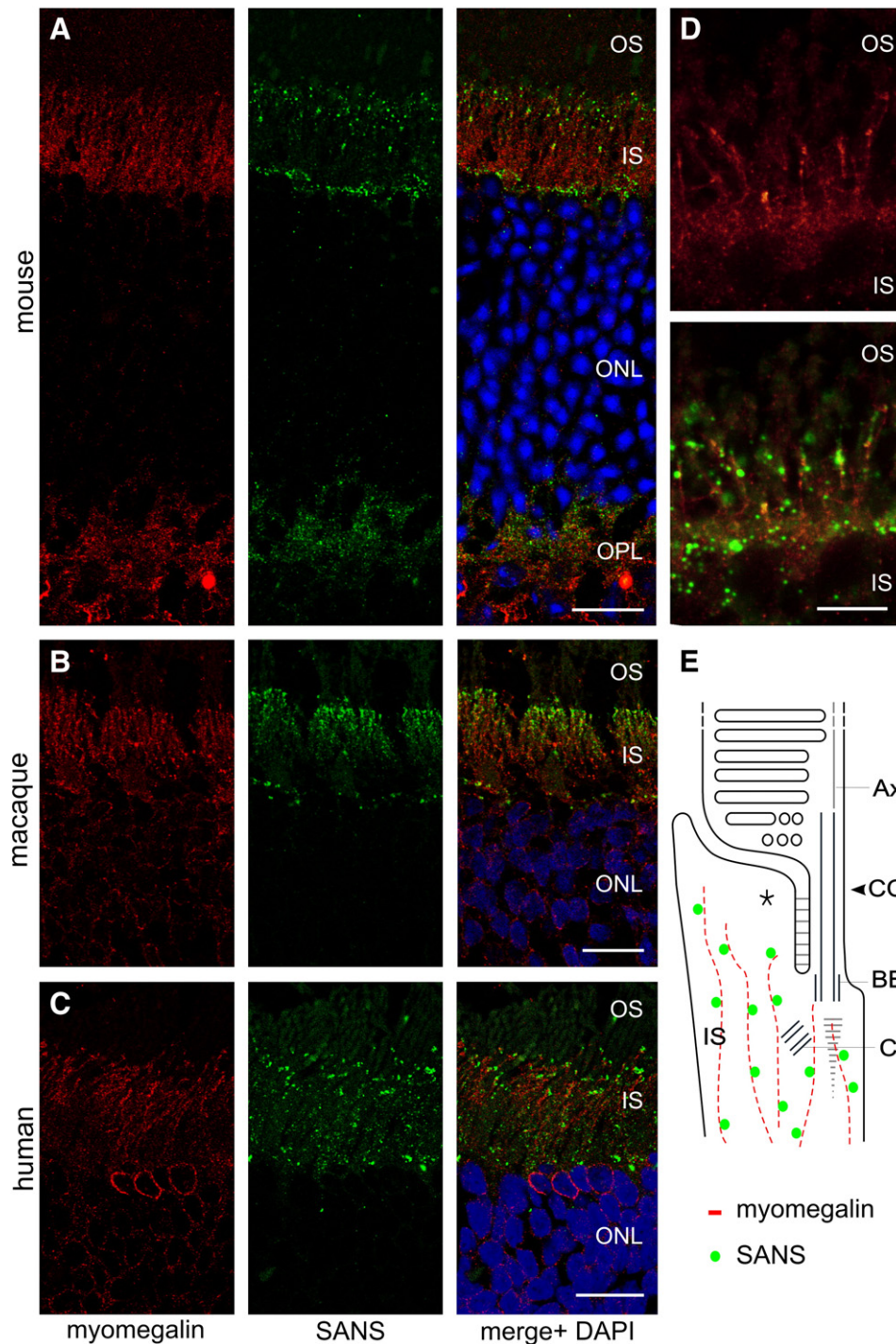
Fig. 6. Partial co-localization of myomegalin and SANS in mouse, macaque and human retina. (A–D) Indirect immunofluorescence labeling of myomegalin (red) and SANS (green) in longitudinal cryosections through mouse, macaque and human retina. Nuclear DAPI staining (blue) reveals the different layers of the retina. (A) In mouse retina myomegalin is localized in a fibrous pattern in the inner segment (IS) and detected in the outer plexiform layer (OPL). SANS is localized in the IS and at the OPL. Myomegalin and SANS are partially co-localized in the IS and OPL. (B) In macaque retina myomegalin is localized in a fibrous pattern in the IS, and detected around the nuclei in the outer nuclear layer (ONL). SANS is localized in the IS. Myomegalin and SANS are partially co-localized in the IS and OPL. (C) In human retina myomegalin is localized in a fibrous pattern in the IS, and detected around the nuclei in the outer nuclear layer (ONL). SANS is localized in the IS. Myomegalin and SANS are partially co-localized in the IS. (D) Zoom of the region of IS and outer segment (OS) by STED microscopical analysis shows myomegalin (red) localization as fibrous pattern in the inner segment. Overlay with SANS (green) shows partial co-localization of myomegalin with SANS punctuate localization. (E) Schematic of the ciliary region of a photoreceptor cell. Localization of myomegalin (red) and SANS (green) is indicated. Scale bars: A–C 15 μm, D 5 μm.

retinal photoreceptor cells [13,14,18]. Here, we show by correlative light and electron microscopy the co-localization of the interacting partners SANS and myomegalin at the microtubule tracks across the photoreceptor inner segment. The inner segmental microtubules are thought to provide the transport routes for the cytoplasmic dynein mediated vesicle transport [36]. Based on these data we propose a cooperation of the binding partners myomegalin and SANS in vesicle transport along microtubule tracks towards the base of the
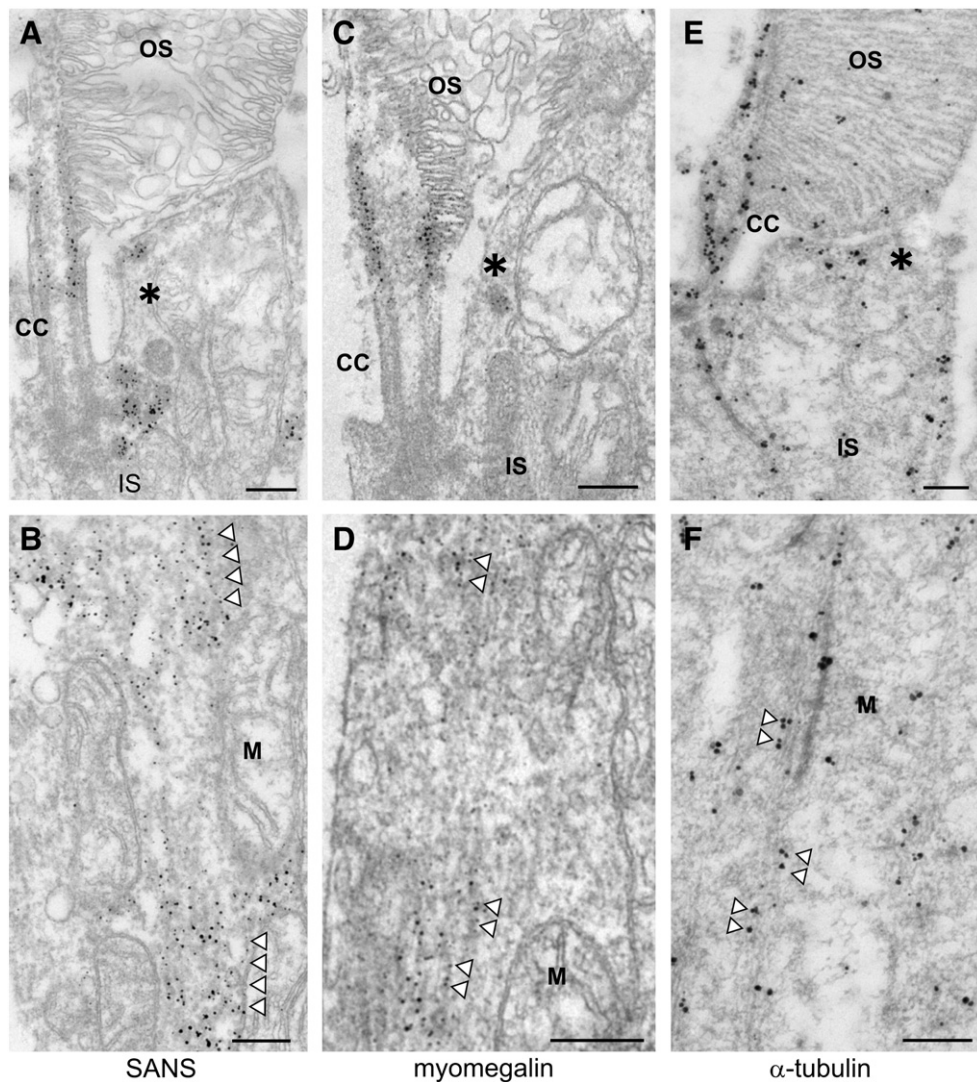
Fig. 7. Immunoelectron microscopic localization of SANS, myomegalin and tubulin in human photoreceptor cells. (A, B) Electron micrographs of anti-SANS labeling in longitudinal sections through parts of human photoreceptor cells. SANS localization is found in the apical inner segment extension (asterisk) and at the apical part of the connecting cilium (CC) and at microtubule tracks in the inner segment (IS, arrow heads). (C, D) Electron micrographs of anti-myomegalin labeling in longitudinal sections through parts of human photoreceptor cells. Myomegalin localization is found in the apical inner segment extension (asterisk) and at the apical part of the CC (C) and at microtubule tracks in IS (arrow heads in D). (E–F) Electron micrographs of anti-tubulin labeling in longitudinal sections through parts of human photoreceptor cells. Tubulin localization is found in the apical inner segment (asterisk) and in the CC (E) and along the microtubule tracks in the IS (arrow heads in F). OS; outer segment, M; mitochondrium. Scale bars: 250 nm.

photoreceptor cilium. This target compartment is characterized by the periciliary complex suitable for the cargo transfer between the inner segmental transport and the ciliary delivery to the photoreceptor outer segment [13,37] (Fig. 8). We and others have previously shown that the physical interaction of USH proteins assemble the core complex of this dynamic periciliary protein network [13,16,17]. In this USH protein network we have identified SANS as one of the major scaffolding proteins.

In conclusion, we identified myomegalin as a novel interaction partner of SANS and member of the USH protein interactome [7]. We propose that this interaction may play a role in mediating the microtubule-dependent inner segmental transport of cargo towards the connecting cilium. Here, other members of the USH interactome work together to maintain the efficient cargo transport between the inner segment and outer segment of photoreceptor cells (Fig. 8). Any defect in the interaction of proteins may lead to the disruption of the whole USH network and may result in *retinitis pigmentosa*, the clinical phenotype in the retina of USH1 patients.

Disclosure statement

All authors disclose any actual or potential conflict of interest including any financial, personal or other relationships with other people or organizations within three years of beginning the work submitted that could inappropriately influence their work.

Role of the funding source
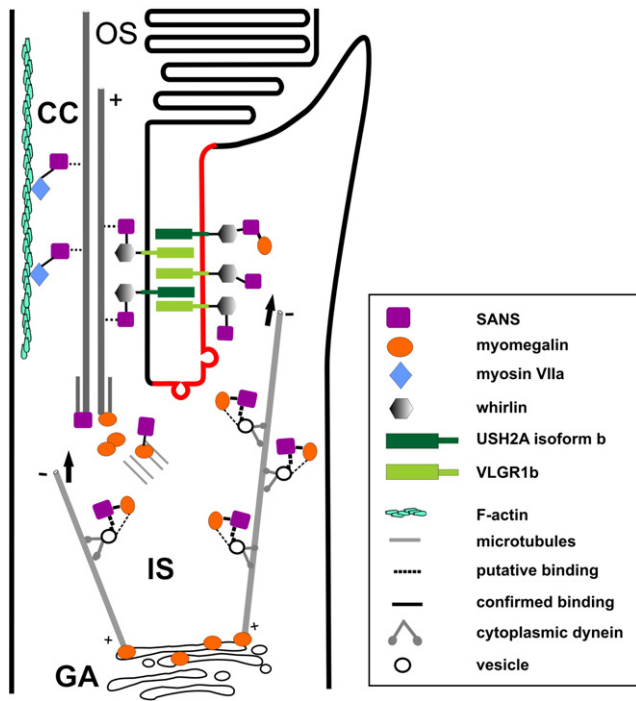
Fig. 8. Hypothesis of myomegalin participation in inner segmental transport processes in photoreceptor cells. Due to its direct interaction with SANS myomegalin can be integrated into the USH network. Therefore, putative functions of the myomegalin-SANS partnership in photoreceptor transport processes can be assumed. Vesicles from the Golgi, destined to the outer segment can either be transported by myomegalin and SANS up to the cargo reloading point at the basal body. On the other hand, SANS and myomegalin mediated transport of cargo from the Golgi network can be directed to the periciliary target membrane (red line) where vesicles dock and fuse to the apical inner segment membrane.

References

[1] J. Reiners, K. Nagel-Wolfrum, K. Jürgens, T. Märker, U. Wolfrum, Molecular basis of human Usher syndrome: deciphering the meshes of the Usher protein network provides insights into the pathomechanisms of the Usher disease, EXP. EYE RES. 83 (2006) 97–119.
[2] I. Ebermann, R. Wilke, T. Lauhoff, D. Lubben, E. Zrenner, H.J. Bolz, Two truncating USH3A mutations, including one novel, in a German family with Usher syndrome, Mol. Vis. 13 (2007) 1539–1547.
[3] S.L.H. Davenport, G.S. Omenn, The Heterogeneity of Usher Syndrome, 1977.
[4] C. Petit, Usher syndrome: from genetics to pathogenesis, Annu. Rev. Genomics Hum. Genet. 2 (2001) 271–297.
[5] Z.M. Ahmed, R.J. Morell, S. Riazuddin, A. Gropman, S. Shaukat, M.M. Ahmad, S.A. Mohiddin, L. Fananapazir, R.C. Caruso, T. Husnain, S.N. Khan, S. Riazuddin, A.J. Griffith, T.B. Friedman, E.R. Wilcox, Mutations of MYO6 are associated with recessive deafness, DFNB37, Am. J. Hum. Genet. 72 (2003) 1315–1322.
[6] H. Kremer, W.E. van, T. Marker, U. Wolfrum, R. Roepman, Usher syndrome: molecular links of pathogenesis, proteins and pathways, Hum. Mol. Genet. 15 (Spec No 2) (2006) R262–R270.
[7] U. Wolfrum, Protein networks related to the Usher syndrome gain insights in the molecular basis of the disease, in: A. Satpal (Ed.), Usher Syndrome: Pathogenesis, Diagnosis and Therapy, Nova Science Publishers, 2011, pp. 1–23.
[8] D. Weil, A. El Amraoui, S. Masmoudi, M. Mustapha, Y. Kikkawa, S. Delmaghani, A. Adato, S. Nadifi, Z.B. Zina, C. Hamel, A. Gal, H. Ayadi, H. Yonekawa, C. Petit, Usher syndrome type I G (USH1G) is caused by mutations in the gene encoding SANS, a protein that associates with the USH1C protein, harmonin, Hum. Mol. Genet. 12 (2003) 463–471.
[9] A. El Amraoui, C. Petit, Usher I syndrome: unravelling the mechanisms that underlie the cohesion of the growing hair bundle in inner ear sensory cells, J. Cell Sci. 118 (2005) 4593–4603.
[10] U. Muller, Cadherins and mechanotransduction by hair cells, Curr. Opin. Cell Biol. 20 (2008) 557–566.
[11] N. Grillet, W. Xiong, A. Reynolds, P. Kazmierczak, T. Sato, C. Lillo, R.A. Dumont, E. Hintermann, A. Sczaniecka, M. Schwander, D. Williams, B. Kachar, P.G. Gillespie, U. Muller, Harmonin mutations cause mechanotransduction defects in cochlear hair cells, Neuron 62 (2009) 375–387.
[12] M. Schwander, B. Kachar, U. Muller, Review series: the cell biology of hearing, J. Cell Biol. 190 (2010) 9–20.
[13] T. Maerker, E. van Wijk, N. Overlack, F.F. Kersten, J. McGee, T. Goldmann, E. Sehn, R. Roepman, E.J. Walsh, H. Kremer, U. Wolfrum, A novel Usher protein network at the periciliary reloading point between molecular transport machineries in vertebrate photoreceptor cells, Hum. Mol. Genet. 17 (2008) 71–86.
[14] N. Overlack, T. Maerker, M. Latz, K. Nagel-Wolfrum, U. Wolfrum, SANS (USH1G) expression in developing and mature mammalian retina, Vision Res. 48 (2008) 400–412.
[15] E. van Wijk, F.F. Kersten, A. Kartono, D.A. Mans, K. Brandwijk, S.J. Letteboer, T.A. Peters, T. Marker, X. Yan, C.W. Cremers, F.P. Cremers, U. Wolfrum, R. Roepman, H. Kremer, Usher syndrome and Leber congenital amaurosis are molecularly linked via a novel isoform of the centrosomal ninein-like protein, Hum. Mol. Genet. 18 (2009) 51–64.
[16] J. Yang, X. Liu, Y. Zhao, M. Adamian, B. Pawlyk, X. Sun, D.R. McMillan, M.C. Liberman, T. Li, Ablation of whirlin long isoform disrupts the USH2 protein complex and causes vision and hearing loss, PLoS. Genet. 6 (2010) e1000955.
[17] J. Zou, L. Luo, Z. Shen, V.A. Chiodo, B.K. Ambati, W.W. Hauswirth, J. Yang, Whirlin replacement restores the formation of the USH2 protein complex in whirlin knockout photoreceptors, Invest Ophthalmol. Vis. Sci. 52 (2011) 2343–2351.
[18] R. Roepman, U. Wolfrum, Protein networks and complexes in photoreceptor cilia, Subcell. Biochem. 43 (2007) 209–235.
[19] A. Adato, G. Lefevre, B. Delprat, V. Michel, N. Michalski, S. Chardenoux, D. Weil, A. El Amraoui, C. Petit, Usherin, the defective protein in Usher syndrome type IIA, is likely to be a component of interstereocilia ankle links in the inner ear sensory cells, Hum. Mol. Genet. 14 (2005) 3921–3932.
[20] E. Caberlotto, V. Michel, I. Foucher, A. Bahloul, R.J. Goodyear, E. Pepermans, N. Michalski, I. Perfettini, O. Alegria-Prevot, S. Chardenoux, C.M. Do, J.P. Hardelin, G.P. Richardson, P. Avan, D. Weil, C. Petit, Usher type 1G protein sans is a critical component of the tip-link complex, a structure controlling actin polymerization in stereocilia, Proc. Natl. Acad. Sci. U. S. A. 108 (2011) 5825–5830.
[21] M. Zallocchi, J.H. Sisson, D. Cosgrove, Biochemical characterization of native Usher protein complexes from a vesicular subfraction of tracheal epithelial cells, Biochemistry 49 (2010) 1236–1247.
[22] J. Yan, L. Pan, X. Chen, L. Wu, M. Zhang, The structure of the harmonin/sans complex reveals an unexpected interaction mode of the two Usher syndrome proteins, Proc. Natl. Acad. Sci. U. S. A. 107 (2010) 4040–4045.
[23] L. Wu, L. Pan, Z. Wei, M. Zhang, Structure of MyTH4-FERM domains in myosin VIIa tail bound to cargo, Science 331 (2011) 757–760.
[24] I. Verde, G. Pahlke, M. Salanova, G. Zhang, S. Wang, D. Coletti, J. Onuffer, S.L. Jin, M. Conti, Myomegalin is a novel protein of the golgi/centrosome that interacts with a cyclic nucleotide phosphodiesterase, J. Biol. Chem. 276 (2001) 11189–11198.
[25] A. Gießl, P. Trojan, A. Pulvermüller, U. Wolfrum, Centrins, potential regulators of transducin translocation in photoreceptor cells, in: D.S. Williams (Ed.), Cell Bilogy and Related Disease of the Outer Retina, World Scientific Publishing Company Pte Ltd, Singapore, 2004, pp. 195–222.
[26] P. Trojan, S. Rausch, A. Giessl, C. Klemm, E. Krause, A. Pulvermuller, U. Wolfrum, Light-dependent CK2-mediated phosphorylation of centrins regulates complex formation with visual G-protein, Biochim. Biophys. Acta 1783 (2008) 1248–1260.
[27] U. Wolfrum, Centrin- and α-actinin-like immunoreactivity in the ciliary rootlets of insect sensilla, Cell Tissue Res. 266 (1991) 231–238.
[28] T. Sedmak, E. Sehn, U. Wolfrum, Immunoelectron microscopy of vesicle transport to the primary cilium of photoreceptor cells, Methods Cell Biol. 94 (2009) 259–272.
[29] M. Hatzfeld, The armadillo family of structural proteins, Int. Rev. Cytol. 186 (1999) 179–224.
[30] P. Burkhard, J. Stetefeld, S.V. Strelkov, Coiled coils: a highly versatile protein folding motif, Trends Cell Biol. 11 (2001) 82–88.
[31] J.M. Mason, K.M. Arndt, Coiled coil domains: stability, specificity, and biological implications, ChemBioChem 5 (2004) 170–176.
[32] C. Faul, A. Dhume, A.D. Schecter, P. Mundel, Protein kinase A, Ca2+/calmodulin-dependent kinase II, and calcineurin regulate the intracellular trafficking of myopodin between the Z-disc and the nucleus of cardiac myocytes, Mol. Cell. Biol. 27 (2007) 8215–8227.
[33] M. Conti, W. Richter, C. Mehats, G. Livera, J.Y. Park, C. Jin, Cyclic AMP-specific PDE4 phosphodiesterases as critical components of cyclic AMP signaling, J. Biol. Chem. 278 (2003) 5493–5496.
[34] K.A. Tasken, P. Collas, W.A. Kemmner, O. Witczak, M. Conti, K. Tasken, Phosphodiesterase 4D and protein kinase a type II constitute a signaling unit in the centrosomal area, J. Biol. Chem. 276 (2001) 21999–22002.
[35] S. Rivero, J. Cardenas, M. Bornens, R.M. Rios, Microtubule nucleation at the cis-side of the Golgi apparatus requires AKAP450 and GM130, EMBO J. 28 (2009) 1016–1028.
[36] A.W. Tai, J.Z. Chuang, C. Bode, U. Wolfrum, C.H. Sung, Rhodopsin's carboxy-terminal cytoplasmic tail acts as a membrane receptor for cytoplasmic dynein by binding to the dynein light chain Tctex-1, Cell 97 (1999) 877–887.
[37] D.S. Papermaster, The birth and death of photoreceptors: the Friedenwald Lecture, Invest. Ophthalmol. Vis. Sci. 43 (2002) 1300–1309.
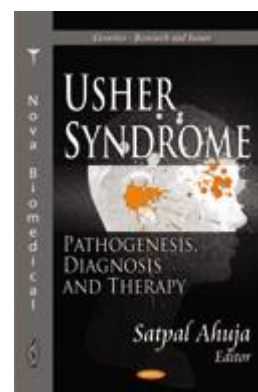
Publikation IV

2.4 Overlack N*, Goldmann T*, Wolfrum U, Nagel-Wolfrum K (2011) Current therapeutic strategies for human Usher syndrome. In: Usher Syndrome: Pathogenesis, Diagnosis and Therapy. Ed.: Satpal Ahuja, 377-395 (*both authors contributed equally to the work).

Chapter 22

CURRENT THERAPEUTIC STRATEGIES FOR HUMAN USHER SYNDROME

Nora Overlack*, Tobias Goldmann*,
Uwe Wolfrum[1], and Kerstin Nagel-Wolfrum

Johannes Gutenberg University, Institute of Zoology, Department of Cell and Matrix
Biology, D-55099 Mainz, Germany

22.1. INTRODUCTION

The human Usher syndrome (USH) is the most frequent cause of combined deaf-blindness in man. It is clinically and genetically heterogeneous and at least twelve chromosomal loci are assigned to three clinical USH types. USH1, USH2 and USH3 differ in the severity of the symptoms: hearing loss, balance problems and retinal degeneration namely *retinitis pigmentosa* (RP), as well as in the progression of the disease.

Mutations in all USH genes result in similar symptoms. Nevertheless, molecular analyses of the corresponding gene products surprisingly revealed that USH proteins belong to diverse protein classes and families: myosin VIIa (USH1B) functions as a molecular motor; harmonin (USH1C), SANS (scaffold protein containing ankyrin repeats and SAM domain, USH1G) and whirlin (USH2D) are scaffold proteins; cadherin 23 (USH1D) and protocadherin 15 (USH1F) represent cell-cell adhesion proteins; USH2A isoform b (USH2A) and the largest receptor GPR98/VLGR1b (very large G-protein coupled receptor 1b, USH2C) with seven transmembrane folds and clarin-1 (USH3A) with four transmembrane domains are transmembrane proteins (Reiners *et al.* 2006, Ebermann *et al.*, 2007). Protein interaction assays demonstrated that all USH proteins are part of protein networks present in the sensory cells of the inner ear and eye. The main organizers of the networks are the three scaffolds harmonin, SANS and whirlin. Alternative splicing further increases the complexity of the USH networks by the presence of various isoforms, mainly of the scaffold harmonin, but also

---

* Both authors contributed equally to the work.
1 Corresponding author, Univ-Professor, E-mail: wolfrum@uni-mainz.de, Tel: +49-6131-39-25148, Fax: +49-6131-39-23815.

isoforms of other USH proteins, like cadherin 23 do exist (Table 22.1) (Reiners *et al.*, 2003, 2006, Lagziel *et al.*, 2009, Overlack *et al.*, 2010).

Table 22.1. Currently evaluated USH therapy strategies

Type	Gene	Protein	Function	Size / isoforms	Cell	Virus	ZFN	Read-through
1B	*MYO7A*	Myosin VIIa	Molecular motor	3.6 - 6.6 kb / yes		Lenti X [2] AAV X [3]		
1C	*USH1C*	Harmonin	Scaffold protein	1.6 - 2.7 kb / yes		AAV ∅ [4]	∅ [6] p.R31X	∅ / X [7,8] p.R31X
1D	*CDH23*	Cdh23	Cell-cell adhesion	1.5 - 10 kb / yes				∅ [9]
1E	--	--	--					
1F	*PCDH15*	Pcdh15	Cell-cell adhesion	- 5.8 kb / yes				X [10] p.R3X; p.R245X; p.R643X; p.R929X
1G	*SANS*	SANS	Scaffold protein	1.4 kb / no				
1H	*USH1H*	--	--					
2A	*USH2A*	USH2A (usherin)	Matrix, cell adhesion	4.6 - 15.6 kb / yes	X [1]			
2B								
2C	*VLGR1b*	GPR98 (VLGR1b)	GPCR, cell adhesion	5. 9 - 19.3 kb / yes				
2D	*DFNB31*	whirlin	Scaffold protein	1.5 - 2.7 kb / yes		AAV X [5]		
3A	*CLRN-1*	Clarin-1	Cell adhesion	0.3 - 0.7 kb / yes				
3B	--	--	--					

X: published; ∅: currently in progress; [1]Lu et al., 2010; [2]Hashimoto et al., 2007; [3]Allocca et al., 2008; [4]currently evaluated in our lab; [5]Zou et al 2010; [6]currently evaluated in our lab; [7]Goldmann et al. 2010; [8]Goldmann et al. submitted; [9]Ben-Yosef, personal communication; [10]Rebibo-Sabbah et al., 2007. Cell: cell replacement; Lenti: lentivirus; AAV: recombinant adeno-associated virus; ZFN: zinc finger nuclease; read-through: translational read-through.

Additional reports indicate that USH also affects tissues and organs other than the ear and eye, which is explainable by the rather wide expression profiles of all USH proteins, for example in the nasal epithelium, brain, trachea, and sperm cells (Arden and Fox 1979, Hunter *et al.*, 1986, Petrozza *et al.*, 1991, Barrong *et al.*, 1992, Baris *et al.*, 1994, van Aarem *et al.*, 1999, Tosi *et al.*, 2003). Nonetheless, USH patients suffer mostly from the loss of the most important senses namely the ear and eye required for human social contacts and the quality of life.

The currently evaluated USH treatment strategies can be divided into two major sections: 1. Non-USH specific approaches, which include cell replacement, neuroprotective factors as well as cochlear and retina implants.

2. Contemporary gene-based therapeutic approaches, specific for each USH subtype. The identification of USH causing genes allows the development of gene specific therapies, including gene augmentation by non-viral or viral vectors, gene repair induced by homologous recombination mediated by zinc finger nucleases (ZFNs) and translational read-through therapy.

Animal models that accurately reflect the disease present in patients are imperative for the evaluation of therapeutic strategies (Smith *et al.*, 2009). Up to now, most USH animal models recapitulate the human deafness phenotype (Williams 2008), making these mice useful models for the evaluation of therapeutic protocols for the inner ear. In contrast, USH mice typically do not suffer from retinal degeneration as seen in human patients. Without representative animal models the translation of treatment strategies to clinical trials will be difficult. Of all the USH mice generated to date, only the *Ush2a*-null mouse (Liu *et al.*, 2007, Lu *et al.*, 2010), whirlin null mouse (Yang *et al.* 2010) and *Ush1c* knock-in mouse (Lentz *et al.*, 2007, Lentz *et al.*, 2010) showed a mild retinal phenotype. The *Ush1c* knock-in mouse has been created by introducing the human *Ush1c* gene containing a specific mutation, into the mouse genome. Thus, generating new mouse models with human mutations might overcome the problem of the lack of retinal phenotype in mice. However, animal models of larger mammals, particularly pigs, show probably the same or at least a more similar phenotype to human than rodent models. Such models may be a necessary option for the evaluation of therapeutic strategies.

In this chapter we want to summarize the different therapeutic approaches and possibilities for the auditory and ophthalmic phenotype of USH patients. We will explain the therapy options in more detail and provide insights into the state of the art. However, one has to keep in mind that the hearing impairment of USH is caused by developmental defects occurring during embryogenesis *in utero*. Thus with exception of cochlear implants and functional replacement strategies, all inner ear treatments discussed below, need prenatal treatment which bear high risk of miscarriage. So far cochlear implants and hearing aids are the only feasible methods for the alleviation and treatment of the auditory component of USH.

22.2. NON-USH SPECIFIC TREATMENT OPTIONS FOR THE EAR AND THE EYE

The non-USH specific treatment options for the ear and eye include the functional replacement of the damaged sensory cells with either *trans*-differentiated cells or stem cells. In the retina, the application of neurotrophic factors could prolong the vision of USH patients. Furthermore, cochlear implants and to some extent visual implants are useful for the improvement of hearing and vision in USH patients. In addition, some ophthalmologists believe in a nutritional therapy. This is based on a clinical study indicating that in some RP and USH2 patients high dose of vitamin A supplement can slow, but not halt, retinal degeneration (Berson *et al.*, 1993). Since in our opinion the data of this study are not convincing the nutritional therapy and its modifications will not be discussed in the present review.

22.2.1. Functional Replacement of the Degenerated Sensory Cells in the Inner Ear and Retina

At the time USH is typically diagnosed, a large fraction of sensory cells are either maldeveloped as is the case of inner ear hair cells or degenerated as is the case for photoreceptor cells in the retina. At this stage, functional replacement of sensory cells might be the most practical solution. Such therapies include the transplantation of stem cells or genetically modified *trans*-differentiated cells. In both cases non-sensory cells will differentiate into respective sensory cells of the cochlea or retina.

In non-mammalian vertebrates (as for example fish) injured hair cells of the cochlea and photoreceptor cells of the retina can be regenerated, leading to the near complete restoration of hearing and vision (Kesser and Lalwani 2009, Karl and Reh 2010). In humans, there seems to be no recovery of lost sensory cells in the cochlea and retina possible. To circumvent this lack of recovery in the field of regenerative medicine two strategies are currently followed namely stem cell transplantation and the *trans*-differentiation or reprogramming of existing differentiated cells.

Identification of genes that induce sensory cell differentiation is instrumental for inducing *trans*-differentiation. In the inner ear, a promising candidate is the basic helix loop helix transcription factor *Atoh1* (formally called *Math1*). Data gathered in guinea pigs showed that induction of *Atoh1* expression offers the possibility to *trans*-differentiate supporting cells into new hair cells in the organ of Corti and thereby improve auditory thresholds (Izumikawa *et al.*, 2005, Batts and Raphael 2007).

In the retina, transplantation of photoreceptor precursor cells from a stage corresponding to the onset of expression of the transcription factor *Nrl*, which is involved in photoreceptor differentiation, are being studied (MacLaren *et al.*, 2006). However, the availability of material for transplantation is a major limitation. Alternatively, cells isolated from bone marrow, the ciliary body and embryonic tissues have the potential to develop into photoreceptor cells and can be implanted (Stone 2009). Additional approaches demonstrate that four transcription factor genes from mouse (*Oct3/4, Sox2, c-Myc, Klf-4*, Takahashi and Yamanaka 2006) and human (*OCT4, SOX2, NANOG, LIN28*, Yu *et al.*, 2007) tissues can *trans*-differentiate cells of adult tissues into induced pleuripotent stem cells (iPSC) by transfection. These cells might be useful for the creation of patient specific stem cells (Stone 2009).

Cells for the applications described above with a perfect immunologic match could be achieved by deriving the cells from the USH patients themselves. These cells would still contain the genetic defect responsible for USH. Consequently, the non-mutated USH gene has to be applied in parallel of the cell generation for transplantation otherwise neither hair cells nor photoreceptor cells will acquire functions. Taking cells from healthy donors on the other hand would provide the correct gene but will require long term immune suppression to prevent host versus graft reactions.

First results on transplantation of stem cells for USH were recently published (Lu *et al.*, 2010). In their treatment approach forebrain-derived progenitor cells were transplanted into the *Ush2a*-null mouse line (Liu *et al.* 2007). Mice that received transplanted cells performed significantly better in tests assessing visual acuity and contrast sensitivity, compared to control mice. In addition, the mislocalization of red/green cone opsin, observed in untreated *Ush2a*-null mice was reversed in treated mice.

In conclusion, the current results of cell replacement strategies did not come up to high expectations of neither patients nor researchers. All strategies must be scrutinized in more detail until they are applicable in the clinic.

22.2.2. Neurotrophic Factors

USH3 and some USH2 patients have some remaining functional hair cells in the cochlea, which could be protected by neurotrophic (~ survival) factors. So far little is known about the ability of neurotrophic factors to enhance hair cell survival. Over expression of glial cell derived neurotrophic factor (GDNF) in the inner ear can protect hair cells against degeneration induced by aminoglycoside ototoxicity (Kawamoto *et al.*, 2003). Several data indicate that the application of apoptosis inhibitors (Atar and Avraham 2010) or the over expression of anti-apoptotic proteins may protect hair cells of the inner ear from degeneration (Staecker *et al.*, 2007).

In contrast to the inner ear, vision loss in USH patients is not caused by developmental defects but by degeneration of photoreceptor cells. At the time of diagnosis there are still functional photoreceptors remaining in the retina. Sustained release of neurotrophic factors could prolong the survival of sensory cells of the eye, by preventing or slowing down the degenerative processes and thereby extend the visual capacity of USH patients (Stieger *et al.*, 2007, Leveillard and Sahel 2010). The proof of concept that neurotrophic factors can slow down retinal degeneration was shown by several laboratories (Faktorovich *et al.*, 1990, La Vail *et al.*, 1992, Bok *et al.*, 2003, LaVail 2005, Stieger *et al.*, 2007, Leveillard and Sahel 2010). To date several neurotrophic factors have been analyzed for their ability to induce cell survival enhancement in the retina, for example ciliary neurotrophic factor (CNTF), rod-derived cone viability factor (RdCVF) or the fibroblast growth factor (FGF) (La Vail 2005, Sahel 2005, Leveillard and Sahel 2010). Adeno-associated virus-mediated transfer of the gene encoding the neurotrophic factor into any retinal cell type is suitable. Subsequently, the retinal cells themselves serve as factories for the production of secreted survival factors (Auricchio 2003, Sahel 2005, Leveillard and Sahel 2010). Alternatively neurotrophic factors were introduced by transgenic human cells, enclosed in semi-permeable capsules (Sieving *et al.*, 2006). A completed Phase I trial revealed that the delivery of CNTF using encapsulated cells is safe for the human retina (Sieving *et al.*, 2006). Currently, a Phase II/III study to evaluate the effectiveness of CNTF implants on vision in persons with *retinitis pigmentosa*, including patients suffering from USH2 and USH3 is being carried out (www.clinicaltrials.gov). Improvement of vision in USH patients of this study would be an important step forward for the treatment of USH.

22.2.3. Application of Implants: Cochlear Implants, Hearing Aids, Retinal Implants

In the following part we discuss the application of implants into the ear and eye as well as hearing aids. Implants for the ear or the retina electrically stimulate surviving neuronal cells in the affected organ and subsequently evoke a pseudo stimulus, which is transmitted to the respective auditory or visual processing centers in the brain (Figure 22.1A-C).
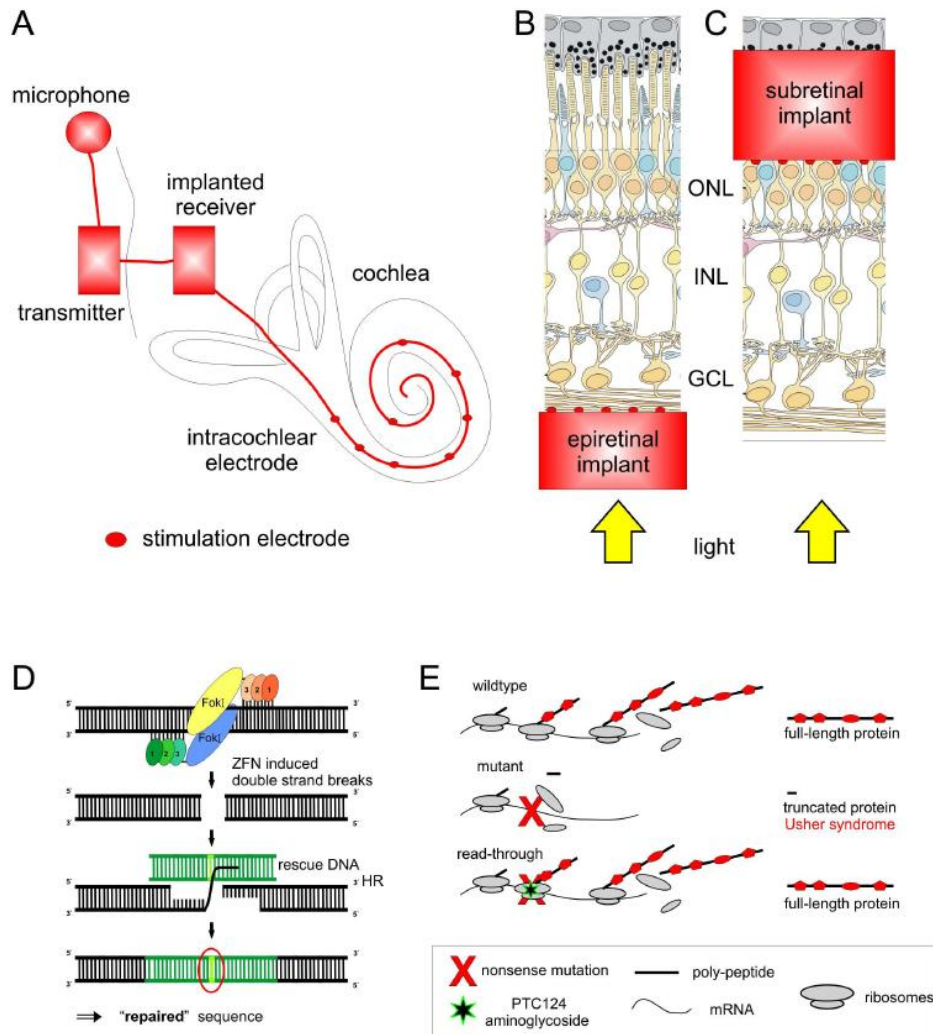
Figure 22.1. Schematic representation of different treatment approaches for USH. A. Cochlear implant. An external microphone collects sound waves and transduces them into electrical impulses. These are transmitted to the intracochlear electrode, which stimulates the corresponding auditory region within the cochlea. B. Epiretinal implant. A camera outside the eye receives light, transduces it into electrical impulses and transmits them to the epiretinal implant. The epiretinal implant is located on the cells of the ganglion cell layer (GCL), which are directly stimulated by the electrical impulse. C. Subretinal implant. The subretinal implant is packed with light sensitive microphotodiodes, which replace lost photoreceptors of the outer nuclear layer (ONL). The light is converted into an electrical stimulus, which activates the remaining secondary neurons in the inner nuclear layer (INL). D. Gene repair. A pair of zinc finger nucleases (ZFN) binds to the DNA close to the mutation, cause a double strand break and thereby activate the cell autonomous homologous recombination machinery. For DNA repair an introduced nonmutated rescue plasmid is used as template. Red circle indicates repaired mutation site. E. Translational read-through. Functional full-length protein is generated by the translation of mRNA. A premature termination codon (PTC; red cross) induces an early interruption of protein translation leading to a truncated and non functional poly-peptide. Aminoglycosides and PTC124 allow the incorporation of an amino acid at the PTC of the mutant mRNA and the generation of full-length protein.

Long-term studies indicate that cochlear implantation is beneficial in USH1 patients because they are profoundly deaf (Pennings *et al.*, 2006). In addition, these patients will develop progressive visual impairment in puberty. The decision for a cochlear implant has to be taken as early as possible, preferably within the first decade of life. The earlier the implantation occurs, the more beneficial it is for the patient. Different studies show that early employment of cochlear implants in USH1 patients results in an improved audiologic performance and better speech perception (Damen *et al.*, 2006, Pennings *et al.*, 2006). This is most likely due to a relatively high plasticity in the young auditory cortex. The cochlear implantation helps USH1 patients to remain independent during daily life and therefore greatly improve their quality of life. Hearing aids which are worn behind the patient's ear, amplify the sound stimulus. However, they can only be helpful for USH2 and USH3 patients with residual hair cell function.

The success of cochlear implants for the treatment of hearing deficiencies has inspired scientists to invent an analogous treatment for visual impairments. However, the retina is a multilayered tissue that does not only transduce visual stimuli into electrical signals but also processes them in a complex way. Thus the healthy retina gathers and transmits more than 100 times more information to the brain than the cochlea does (Stone 2009). Despite these challenges different tools have been developed and are being evaluated (Zrenner 2002, Hornig *et al.*, 2005, Yanai *et al.*, 2007, Besch *et al.*, 2008).

In general, retinal prostheses make use of surviving retinal neurons (amacrine, bipolar, horizontal cells and ganglion cells) to restore vision (Humayun *et al.* 1999). Some devices stimulate the ganglion cells at the epiretinal side by a flexible micro contact film, whereas others electrically stimulate the subretinal side of the retina (Figure 22.1B, C) (Hornig *et al.*, 2005, Besch *et al.*, 2008). In some systems special goggles project bright images into the eye stimulating subretinal photodiode arrays. Alternatively, external cameras capture the images and transmit the information to the retina (summarized in Stone 2009). The major problem for the application of retinal implants is that their technology is not yet fully developed. To date the number of electrodes is far too low to result in the perception of a real image of the object in view; and only black and white differentiation will be possible. Therefore, in the future even more sophisticated devices will be the only option for patients suffering from complete blindness. Nonetheless, this approach is certainly promising for USH patients in the late phase of disease progression, and has to be further improved and evaluated (Winter *et al.*, 2007).

22.2.4. Gene-Based Therapy

USH is a monogenetic recessive disease. Since all USH proteins are organized in USH related networks, the lack of a specific protein may result in the disruption of the entire USH protein network, causing sensorineuronal degeneration in the inner ear and retina. Consequently, restoring the natural protein expression should reverse the USH related phenotype.

Patient screening conducted over the last few years has provided detailed knowledge about mutations in the genes causing USH. This makes it possible to follow approaches specifically designed and adjusted to the affected gene or specific mutations for the treatment of USH. Such personalized gene-based therapies include gene augmentation and gene repair

by homologous recombination mediated by zinc finger nucleases (ZFN). These strategies could provide a cure of USH. In addition, specifically for nonsense mutations the application of translational read-through inducing drugs, like modified aminoglycosides or PTC124 are promising treatment options.

22.2.4.1. Gene Augmentation

USH is caused by the loss of specific USH gene expression, and consequently should be amenable to treatments by gene augmentation. Gene augmentation is based on the exogenous replacement of a mutated gene by a functional copy in the affected organ.

A well known approach to rescue functional protein expression is gene augmentation or gene replacement strategy by viral vectors, mostly by lentivirus and adeno-associated virus. Alternatively, non-viral approaches, like nanoparticles, can be applied for the delivery of non-mutated genes into the affected organs. Both the inner ear and eye affected in USH are small, compartmentalized and enclosed: This is helpful as the delivery of small quantities of vectors will have a minimal risk of systemic dissemination of the vector. Due to the blood-cochlea-barrier and the blood-retina-barrier both organs are immune privileged, providing a degree of protection from immune responses against vector antigens. A variety of non-viral and viral vectors have been tested for their ability to transduce the cells affected in USH, namely hair cells in the inner ear and photoreceptor cells and retinal pigment epithelium (RPE) cells in the retina. Therefore, different vector systems, their advantages and disadvantages for the treatment of the USH phenotype in inner ear and retina are described and discussed below.

In USH patients the hearing impairment is congenital and profound, since USH1 and USH2 proteins are necessary for the proper development and maintenance of stereocilia. Molecular strategies to treat hearing loss, namely gene augmentation to target the restoration of cochlear hair cells for USH patients are attractive (reviewed in Hildebrand *et al.*, 2008). A major problem to rescue the developmental phenotype of USH patients is that the interventions have to be applied *in utero*. Such a treatment bears high risk of miscarriage. However, the studies involving prenatal delivery of viral vectors into dogs suggest that *in utero* retinal gene delivery may be feasible (Dejneka *et al.* 2004). In USH patients the postnatal retinal development, together with the later onset of retinal degeneration makes the eye a more amenable therapeutic target for gene augmentation compared to the inner ear. In addition, the retina is a favorable system for the establishment of new therapeutic strategies because it has a highly ordered structure and it is optically and physically accessible. This facilitates the read out and evaluation of therapeutic interventions.

22.2. 4.2. Non-Viral Gene Transfer Using Nanoparticles

Utilizing nanoparticles for disease treatment has become a promising non-viral gene transfer method in recent years (Cai *et al.*, 2008). There exists a great variety of different nanoparticles, but the typical nanoparticle contains either linear or circular DNA or RNA, which is compacted with a polycationic polymer. The usual size of nanoparticles ranges from 10-100 nm in diameter (summarized in Cai *et al.* 2008). One major advantage of nanoparticles is their very large insert capacity of up to 20 kb (Fink *et al.*, 2006). Such an enormous packaging capacity would be sufficient for the largest cDNA of 19.3 kb encoding USH protein GPR98 (McMillan *et al.*, 2002). So far nanoparticles display little to no toxicity and only a modest immune response (Konstan *et al.*, 2004, Farjo *et al.*, 2006, Davis and Cooper 2007), making repetitive administration possible. Furthermore, transgene expression

can last for at least six months; it is dose dependent and not limited to the site of injection of the nanoparticles (Farjo *et al.*, 2006). Polyethylene glycol (PEG) compacted nanoparticles have been shown to efficiently transfect post-mitotic cells *in vitro* and *in vivo* (summarized in Cai *et al.* 2008). Most importantly PEG compacted nanoparticles have high transfection efficiencies in photoreceptor cells (Farjo *et al.*, 2006) and would therefore be useful for USH treatment. These encouraging results offer the opportunity to compact all USH cDNAs even the very large ones into nanoparticles for non-viral gene transfer for the studies involving USH genes.

22.2.4.3. Viral Gene Addition

For the transfer of genes into the inner ear or retina a couple of viral systems are available and most used vectors are lentivirus and recombinant adeno-associated virus (AAV).

22.2.4.3.1 Lentivirus

Lentivirus is derived from the human immunodeficiency virus (HIV) and belongs to the family of retrovirus. Lentiviral vectors are suitable to transduce RPE cells, have the advantage of a relatively large capacity to package molecules of 8 kb in size and mediate high levels of transgene expression. They integrate into the host genome, thereby providing long-term expression of the transgene. Disadvantages of the lentiviral system are high immunogenicity and ototoxicity, as well as the inability to transduce photoreceptor cells.

Hashimoto *et al.*, (2007) delivered cDNA of *MYO7A* to primary RPE cultures by lentivirus vector and via subretinal route to the *shaker1* mice, deficient in *myo7a*. Appropriate levels of myosin VIIa protein were achieved in the RPE. After restoration of the myosin VIIa phagosome expression digestion and melanosome motility were observed in cultured RPE cells. Additionally, melanosome localization and opsin clearance from the connecting cilium *in vivo* was achieved (Hashimoto *et al.* 2007). However, after lentivirus-mediated transfer restoration of myosin VIIa expression in photoreceptors was not detected. This confirmed that lentivirus mediated gene transfer might not be effective for photoreceptor cells (Smith *et al.*, 2009). Since myosin VIIa is the only USH protein expressed in RPE cells, gene transfer by currently used lentiviruses is not a treatment option for other USH subtypes.

Nevertheless, restoration of myosin VIIa expression in RPE cells can have beneficial effects on the visual capacity in USH1B patients. Thus, for USH1B lentiviral based gene-addition appears promising. With the objective of advancing to the Phase I/II clinical trials in 2011 Sanofi-Aventis and Oxford BioMedica are currently collaborating to develop a gene based therapy for USH1B patients (www.oxfordbiomedica.co.uk).

22.2.4.3.2. Adeno-Associated Viruses (AAV)

Gene augmentation using recombinant AAV is the most promising therapeutic approach for the treatment of USH. Over the past few years a number of laboratories started to evaluate the potential of this non-pathogenic virus as a vehicle for gene delivery to cells. Robust transgene expression was detectable for six months in the inner ear (Lalwani *et al.*, 1998) and several years in the retina (Acland *et al.*, 2005, Le Meur *et al.*, 2005). Thus, the risk of inflammatory and/or immune responses, which could occur following repeated treatments with virus, is reduced. Another issue that has been discussed for the AAVs is a potential random integration of the virus into the hosts' genome, thereby generating the risk of

unwanted side effects in the cells after transduction. On the contrary recent publications state an episomal localization of the AAVs (discussed in Schultz and Chamberlain 2008). Whichever the case, AAVs lead to a sustained expression of the transgene, which is an important point for USH therapy, since a life long expression of the USH genes, is necessary for maintenance of the photoreceptor cells.

The diversity of existing and designed serotypes of AAVs offers the possibility to target different cell types specifically. To restrict the transduction to a special, desired cell type, common AAV2 vector has been engineered with capsids of other serotypes. Depending on the species to be treated, different AAV serotypes show efficient application for the inner ear (as for example Luebke *et al.*, 2009). AAV2/1 was found to be the optimal vector for *in utero* cochlear gene transfer in mice (Bedrosian *et al.*, 2006). In the retina, AAV2/5 or AAV2/8 efficiently transduced photoreceptor cells, whereas AAV2/1 and AAV2/4 were more effective in transducing RPE cells (Surace and Auricchio 2008). So far AAVs are the only viral vectors, which efficiently transduce RPE, rod and cone photoreceptors (Smith *et al.*, 2009). Consequently, AAVs are the most commonly used vectors for retinal gene therapy. Recently three clinical trials of AAV-mediated gene therapy for patients with Leber congenital amaurosis (LCA) 5 showed improvement in vision of the treated LCA5 patients (Hauswirth *et al.*, 2008, Bainbridge *et al.*, 2008, Maguire *et al.*, 2008).

For the USH genes, Zou and colleagues (Zou, J. M., Luo, L., Chiodo, V. A., Ambati, B., Hauswirth, W. W., Yang, J. 2010, AAV-mediated gene replacement therapy in a mouse model of Usher syndrome type II lacking whirlin. *Invest Ophthalmol Vis Sci,* **51**: E-Abstract 3102) report successful delivery of the cDNA encoding for whirlin (USH2D) into photoreceptors of a whirlin knock-out mouse by application of AAV vectors. The transduced whirlin was correctly localized in the retina and restored the localization of the two USH proteins USH2A and GPR98, known to interact with whirlin (van Wijk *et al.* 2006).

One limitation for the application of AAV in treating USH is its lower packaging capacity of 5 kb (Grieger and Samulski 2005). However, a recent publication revealed the possibility of creating recombinant viral genomes containing at least 9 kb constructs, which were successfully cloned and transferred into cells (Allocca *et al.*, 2008). Large size packaging has already been tested with *myo7a* and successfully evaluated in cultured RPE cells. Unfortunately, most of the USH cDNAs, namely USH2A isoform b, and VLGR1/GPR98 (Kelley *et al.*, 1997, Levy *et al.*, 1997, McMillan *et al.*, 2002, Liu *et al.*, 2007), are far larger than this (Table 22.1). One conceivable possibility is to employ a *trans*-splicing strategy for cDNAs of larger proteins, meaning that fragments of cDNA should be incorporated into separate AAVs, which are then used as a mixture for the therapeutic application. The target cells namely photoreceptors produce a fusion protein encoded by all fragments of the large cDNA (Atkinson and Chalmers 2010).

An obstacle in using gene augmentation for USH gene therapy is the existence of different isoforms for most of the USH genes products (Table 22.1). For example, the *USH1C* gene consists of 28 coding exons of which eleven are differentially spliced, therefore generating a variety of alternatively spliced transcripts (Verpy *et al.*, 2000, Becker *et al.*, unpublished data). So far the isoforms necessary for the proper development or survival of inner ear hair cells and photoreceptor cells are unknown. The presence of multiple protein isoforms complicates the choice of cDNA to be used for gene augmentation. It appears that treatment of patients with several splice variants might be required. Nevertheless, due to the promising results of the clinical trials with LCA patients, who suffer like USH patients from

retinitis pigmentosa, AAVs provide a valuable tool for USH gene augmentation (Table 22.1). We hope that further clinical trials will be initiated for USH patients within the next few years.

22.2.4.4 Gene Repair by Homologous Recombination Mediated by Zinc Finger Nucleases

As mentioned above, a major problem in the application of gene augmentation therapies to USH patients is the expression of different isoforms for some USH proteins. This further complicates the choice of cDNA to be transferred. An excellent way to circumvent this problem in gene augmentation is gene repair by homologous recombination mediated by zinc finger nucleases (ZFN) (Figure 22.1D).

Homologous recombination is a cell autonomous repair mechanism activated by the introduction of double strand breaks in the DNA by e.g. x-ray irradiation. The limitation of double strand breaks for application in therapeutic strategies is that they occur at a very low frequency (10^{-6}) in somatic cells. To increase this efficiency, double strand breaks are introduced close to the mutated genomic DNA sequence by using ZFNs. ZFNs are hybrid proteins composed of an engineered DNA binding domain, designed to bind to a specific target sequence within the genome and the nonspecific cleavage domain of the FokI enzyme. Subsequent to the ZFN mediated DNA cleavage an exogenously introduced rescue plasmid, coding for the healthy gene, replaces the endogenous mutated segment of the mutated genomic DNA by homologous recombination. The repair of a gene at the site of the mutation ensures sustained and tissue specific expression of the gene product because it remains under control of its endogenous promoter.

So far the ZFN technique has been applied successfully for targeted mutagenesis in cell culture, zebra fish, *Caenorhabditis elegans* and rats (as for example Morton *et al.*, 2006, Foley *et al.*, 2009, Mashimo *et al.*, 2010) summarized in Remy *et al.*, (2009). Some laboratories have already evaluated the potential of ZFN for therapy: Urnov and colleagues (Urnov *et al.* 2005) corrected a mutated GFP and the IL2Rγ gene in cultured cells and impressively demonstrated the potential of this approach for gene based therapy. The development of specially designed ZFN for specific mutations in different genes affected in USH could be used as personalized therapy for individual USH patients. This is independent of the size of the gene, presence of splice variants or the type of mutation. In our laboratory we are currently generating and testing ZFN designed for mutations in the *USH1C* gene with promising preliminary results.

Taken together, application of ZFN offers an opportunity for the treatment of USH by adopting a repair mechanism namely homologous recombination which is endogenous to the cell. This technique to repair the defective gene in its endogenous context would be the most effective and elegant way of therapy for USH. Nevertheless, this therapy strategy is still far from being applied in patients and considerable effort has to be made to proceed in the direction of clinical trials.

22.2.4.5. Translational Read-Through

In-frame nonsense mutations synonymously called premature-termination-codon (PTC) account for approximately 11% of all USH cases (Baux *et al.*, 2008). The translation of mRNAs containing PTCs often results in truncated, mostly nonfunctional polypeptides

(Figure 22.1E). More than two decades ago, aminoglycosides were found to facilitate read-through of PTCs in eukaryotic cells and thereby stimulate the expression of full length functional proteins (Figure 22.1E). Although, the amino acid inserted at the position of the PTC is not necessarily the one present in the wild type protein, the resulting protein is still fully or at least partially functional (Zingman *et al.*, 2007, Linde and Kerem 2008). In comparison to gene augmentation the translational read-through inducing drugs have the advantage that the targeted gene remains under normal endogenous control. Therefore, tissue specific expression, timing, duration of expression and alternative splicing are not altered. These findings in basic research have raised hope for the usage of aminoglycosides as a pharmacogenetic therapy for PTCs in various genes responsible for a variety of diseases (reviewed in Linde and Kerem 2008). Indeed, encouraging results have paved the way to clinical trials on patients suffering from Duchenne muscular dystrophy and cystic fibrosis (Politano *et al.*, 2003, Wilschanski *et al.* 2003).

The most critical factor that limits the potential of aminoglycosides for "read-through therapy" is their insufficient biocompatibility namely nephrotoxicity and ototoxicity (Mingeot-Leclercq and Tulkens 1999, Forge and Schacht 2000). Two major efforts were undertaken to identify new compounds with better biocompatibility while still having a sustained read-through activity namely modification of the structure of aminoglycosides (Nudelman *et al.*, 2006, Nudelman *et al.*, 2009) and screening for novel read-through agents (Welch *et al.*, 2007).

For redesigning aminoglycosides, toxic structural motifs were exchanged and basic read-through experiments on a nonsense mutation of *PCDH15* (USH1F) were carried out (Nudelman *et al.*, 2006, Nudelman *et al.*, 2009). In these studies, newly designed compounds, NB30 and NB54, displayed a sustained read-through activity and had excellent biocompatibility. Further investigations revealed NB30 and NB54 mediated read-through of nonsense mutations causing USH1C and USH1F in transfected cells and thereby restored full length functional protein (Rebibo-Sabbah *et al.*, 2007, Goldmann *et al.* 2010). In addition NB30 induced read-through of a nonsense mutation of *USH1C* in retinal explants (Goldmann *et al.* 2010). In contrast to clinically applied aminoglycosides, the new compounds exhibited excellent biocompatibility in cultured cells, cochlear explants, retinal explants and in animals (Rebibo-Sabbah *et al.*, 2007, Nudelman *et al.*, 2009, Goldmann *et al.* 2010).

In a second attempt, a screen of 800.000 small potential molecules was performed for read-through agents with better biocompatibility. In this study, PTC124 was identified as a candidate drug (Welch *et al.*, 2007). The read-through efficiency of PTC124 was successfully demonstrated in animal models of different genetic diseases (Welch *et al.*, 2007, Du *et al.*, 2008). Recent Phase I and IIa trials demonstrated the read-through effectiveness of PTC124 treatment without serious drug related side effects (Hirawat *et al.*, 2007, Kerem *et al.*, 2008) which paved the way for clinical trials in Duchenne muscular dystrophy, hemophilia and cystic fibrosis. The potential of PTC124 as a read-through therapy for a nonsense mutation in USH was recently investigated (Goldmann *et al.* submitted). PTC124 mediated a high read-through efficiency of an USH1C causing nonsense mutation in combination with excellent biocompatibility in murine and human retinal organotypic cultures. These collective data highlight the potential of translational read-through drugs for USH and other ocular diseases to combat nonsense mutation based retinal disorders. Both, modified aminoglycosides and PTC124 are currently considered as therapeutic agents to treat USH.

22.3. CONCLUSION

Cochlear implants currently are the most practicable treatment options for hearing loss in USH. Successful applications of cochlear implants demonstrate the powerful impact of therapy on the quality of life of USH patients. In contrast, retinal electronic implants are still in the developmental stage. The technical maturation to the level of clinical application will certainly take at least a decade and more for development of sophisticated devices as an option for completely blind patients. Even today the molecular treatment opportunities are very promising to slow down the retinal degeneration or cure the retinal phenotype of USH. Recent success in gene-based approaches in other retinal dystrophies and the start of clinical test in USH1B raise hope for future efficient treatment and cure of patients suffering from USH.

22.4. SUMMARY

USH is a monogenetic autosomal recessive disorder. Mutations in twelve USH genes, identified so far, result in the dysfunction or absence of the corresponding USH protein which may lead to disruption of the USH networks causing sensorineuronal degeneration in the inner ear and the retina, the clinical symptoms of USH. Identification of USH genes and deciphering protein networks related to USH have paved the way for the accomplishment of therapeutic strategies. Nevertheless, currently only cochlear implants implemented ameliorate the hearing deficiency symptoms, but no treatment of the sensorineuronal degeneration in the eye exists so far.

In most USH types the hearing impairment of USH patients originates during the development of inner ear hair cells. Therefore, preventative gene replacement strategies would have to be implemented *in uteri*, but such therapy options are currently not practiced. Alternatively, postnatal treatments which may slow down the hearing defect are investigated: stem cell transfer or induction of trans-differentiation of supporting cells following correction of defective genes. However, application of cochlear implants in early childhood successfully benefits hearing deficiency in USH patients.

Conversely, the postnatal development of the retina and the relatively late onset of retinal degeneration make the eye a more approachable therapeutic target. For the retina, several non-gene-based therapeutic options are currently assessed: cell replacement, neuroprotective agents and retinal implants. However, the identification of USH genes allows the deployment of gene-specific treatments by gene augmentation using non-viral or viral vectors. Recent successful progress in reversion of blindness by AAV-mediated gene transfer in humans affected by Leber congenital amaurosis also raises hope for common treatment strategies for USH and other disruptive genetic conditions in the eye. Moreover, the knowledge of specific mutations causing the USH phenotype enables the development of mutation specific therapeutic strategies, namely gene repair by homologous recombination mediated by zinc finger nucleases and treatments with translational read-through drugs, namely modified aminoglycosides and PTC124. Latter compounds target in-frame nonsense mutations which account for ~11% of all USH and other retinal degeneration causing mutations. In particular,

PTC124 yielded promising results in Phase II clinical trials for the treatment of various non-ocular diseases caused by in-frame nonsense mutations.

All discussed gene based treatment strategies restore the expression of functional USH proteins. These adjustments may be sufficient to cure or at least slow down the progression of retinal degeneration which would greatly improve the quality life of USH patients.

22.5. ACKNOWLEDGMENTS

22.6. REFERENCES

Acland, G. M., Aguirre, G. D., Bennett, J. *et al.* (2005) Long-term restoration of rod and cone vision by single dose rAAV-mediated gene transfer to the retina in a canine model of childhood blindness. *Mol. Ther.* 12, 1072-1082.

Allocca, M., Doria, M., Petrillo, M. *et al.* (2008) Serotype-dependent packaging of large genes in adeno-associated viral vectors results in effective gene delivery in mice. *J. Clin. Invest* 118, 1955-1964.

Arden, G. B. and Fox, B. (1979) Increased incidence of abnormal nasal cilia in patients with retinitis pigmentosa. *Nature* 279, 534-536.

Atar, O. and Avraham, K. B. (2010) Anti-apoptotic factor z-Val-Ala-Asp-fluoromethylketone promotes the survival of cochlear hair cells in a mouse model for human deafness. *Neuroscience* 168, 851-857

Atkinson, H. and Chalmers, R. (2010) Delivering the goods: viral and non-viral gene therapy systems and the inherent limits on cargo DNA and internal sequences. *Genetica* 138, 485-498.

Auricchio, A. (2003) Pseudotyped AAV vectors for constitutive and regulated gene expression in the eye. *Vision Res.* 43, 913-918.

Bainbridge, J. W., Smith, A. J., Barker, S. S. *et al.* (2008) Effect of gene therapy on visual function in Leber's congenital amaurosis. *N. Engl. J. Med.* 358, 2231-2239.

Baris, B., Ataman, M., Sener, C., Kalyoncu, F. (1994) Bronchial asthma in a patient with Usher syndrome: case report. *J. Asthma* 31, 487-490.

Barrong, S. D., Chaitin, M. H., Fliesler, S. J., Possin, D. E., Jacobson, S. G., Milam, A. H. (1992) Ultrastructure of connecting cilia in different forms of retinitis pigmentosa. *Arch. Ophthalmol.* 110, 706-710.

Batts, S. A. and Raphael, Y. (2007) Transdifferentiation and its applicability for inner ear therapy. *Hear. Res.* 227, 41-47.

Baux, D., Faugere, V., Larrieu, L. *et al.* (2008) UMD-USHbases: a comprehensive set of databases to record and analyse pathogenic mutations and unclassified variants in seven Usher syndrome causing genes. *Hum. Mutat.* 29, E76-E87.

Bedrosian, J. C., Gratton, M. A., Brigande, J. V., Tang, W., Landau, J., Bennett, J. (2006) In vivo delivery of recombinant viruses to the fetal murine cochlea: transduction characteristics and long-term effects on auditory function. *Mol. Ther.* 14, 328-335.

Berson, E.L., Rosner, B., Sandberg, M.A., Hayes, K.C., Nicholson, B.W., Weigel-DiFranco, C, Willett, W. (1993) A Randomized trial of vitamin A and vitamin E supplementation for Retinitis pigmentosa. *Arch Ophthalmol.*, 111, 761-772.

Besch, D., Sachs, H., Szurman, P. *et al.* (2008) Extraocular surgery for implantation of an active subretinal visual prosthesis with external connections: feasibility and outcome in seven patients. *Br. J. Ophthalmol.* 92, 1361-1368.

Bok, D., Galbraith, G., Lopez, I. *et al.* (2003) Blindness and auditory impairment caused by loss of the sodium bicarbonate cotransporter NBC3. *Nat. Genet.* 34, 313-319.

Cai, X., Conley, S., Naash, M. (2008) Nanoparticle applications in ocular gene therapy. *Vision Res.* 48, 319-324.

Damen, G. W., Pennings, R. J., Snik, A. F., Mylanus, E. A. (2006) Quality of life and cochlear implantation in Usher syndrome type I. *Laryngoscope* 116, 723-728.

Davis, P. B. and Cooper, M. J. (2007) Vectors for airway gene delivery. *AAPS.J.* 9, E11-E17.

Dejneka, N. S., Surace, E. M., Aleman, T. S. *et al.* (2004) In utero gene therapy rescues vision in a murine model of congenital blindness. *Mol. Ther.* 9, 182-188.

Du, M., Liu, X., Welch, E. M., Hirawat, S., Peltz, S. W., Bedwell, D. M. (2008) PTC124 is an orally bioavailable compound that promotes suppression of the human CFTR-G542X nonsense allele in a CF mouse model. *Proc. Natl. Acad. Sci. U.S.A* 105, 2064-2069.

Ebermann, I., Wilke, R., Lauhoff, T., Lubben, D., Zrenner, E., Bolz, H. J. (2007) Two truncating USH3A mutations, including one novel, in a German family with Usher syndrome. *Mol. Vis.* 13, 1539-1547.

Faktorovich, E. G., Steinberg, R. H., Yasumura, D., Matthes, M. T., LaVail, M. M. (1990) Photoreceptor degeneration in inherited retinal dystrophy delayed by basic fibroblast growth factor. *Nature* 347, 83-86.

Farjo, R., Skaggs, J., Quiambao, A. B., Cooper, M. J., Naash, M. I. (2006) Efficient non-viral ocular gene transfer with compacted DNA nanoparticles. *PLoS.One.* 1, e38.

Fink, T. L., Klepcyk, P. J., Oette, S. M. *et al.* (2006) Plasmid size up to 20 kbp does not limit effective in vivo lung gene transfer using compacted DNA nanoparticles. *Gene Ther.* 13, 1048-1051.

Foley, J. E., Maeder, M. L., Pearlberg, J., Joung, J. K., Peterson, R. T., Yeh, J. R. (2009) Targeted mutagenesis in zebrafish using customized zinc-finger nucleases. *Nat. Protoc.* 4, 1855-1867.

Forge, A. and Schacht, J. (2000) Aminoglycoside antibiotics. *Audiol. Neurootol.* 5, 3-22.

Goldmann T., Rebibo-Sabbah A., Overlack N., *et al.* (2010) Designed aminoglycoside NB30 induces beneficial read-through of a USH1C mutation in the retina. *Invest Ophthalmol. Vis. Sci.* July 28, 2010, [Epub ahead of print]

Grieger, J. C. and Samulski, R. J. (2005) Adeno-associated virus as a gene therapy vector: vector development, production and clinical applications. *Adv. Biochem. Eng Biotechnol.* 99, 119-145.

Hashimoto, T., Gibbs, D., Lillo, C. *et al.* (2007) Lentiviral gene replacement therapy of retinas in a mouse model for Usher syndrome type 1B. *Gene Ther.* 14, 584-594.

Hauswirth, W. W., Aleman, T. S., Kaushal, S. *et al.* (2008) Treatment of leber congenital amaurosis due to RPE65 mutations by ocular subretinal injection of adeno-associated virus gene vector: short-term results of a phase I trial. *Hum. Gene Ther.* 19, 979-990.

Hildebrand, M. S., Newton, S. S., Gubbels, S. P. *et al.* (2008) Advances in molecular and cellular therapies for hearing loss. *Mol. Ther.* 16, 224-236.

Hirawat, S., Welch, E. M., Elfring, G. L. *et al.* (2007) Safety, tolerability, and pharmacokinetics of PTC124, a nonaminoglycoside nonsense mutation suppressor, following single- and multiple-dose administration to healthy male and female adult volunteers. *J. Clin. Pharmacol.* 47, 430-444.

Hornig, R., Laube, T., Walter, P. *et al.* (2005) A method and technical equipment for an acute human trial to evaluate retinal implant technology. *J. Neural Eng* 2, S129-S134.

Humayun, M. S., de Juan E Jr, Weiland, J. D. *et al.* (1999) Pattern electrical stimulation of the human retina. *Vision Res.* 39, 2569-2576.

Hunter, D. G., Fishman, G. A., Mehta, R. S., Kretzer, F. L. (1986) Abnormal sperm and photoreceptor axonemes in Usher's syndrome. *Arch. Ophthalmol.* 104, 385-389.

Izumikawa, M., Minoda, R., Kawamoto, K. *et al.* (2005) Auditory hair cell replacement and hearing improvement by Atoh1 gene therapy in deaf mammals. *Nat. Med.* 11, 271-276.

Karl, M. O. and Reh, T. A. (2010) Regenerative medicine for retinal diseases: activating endogenous repair mechanisms. *Trends Mol. Med.* 16, 193-202.

Kawamoto, K., Yagi, M., Stover, T., Kanzaki, S., Raphael, Y. (2003) Hearing and hair cells are protected by adenoviral gene therapy with TGF-beta1 and GDNF. *Mol. Ther.* 7, 484-492.

Kelley, P. M., Weston, M. D., Chen, Z. Y. *et al.* (1997) The genomic structure of the gene defective in Usher syndrome type Ib (MYO7A). *Genomics* 40, 73-79.

Kerem, E., Hirawat, S., Armoni, S. *et al.* (2008) Effectiveness of PTC124 treatment of cystic fibrosis caused by nonsense mutations: a prospective phase II trial. *Lancet* 372, 719-727.

Kesser, B. W. and Lalwani, A. K. (2009) Gene therapy and stem cell transplantation: strategies for hearing restoration. *Adv. Otorhinolaryngol.* 66, 64-86.

Konstan, M. W., Davis, P. B., Wagener, J. S. *et al.* (2004) Compacted DNA nanoparticles administered to the nasal mucosa of cystic fibrosis subjects are safe and demonstrate partial to complete cystic fibrosis transmembrane regulator reconstitution. *Hum. Gene Ther.* 15, 1255-1269.

Lagziel, A., Overlack, N., Bernstein, S. L., Morell, R. J., Wolfrum, U., Friedman, T. B. (2009) Expression of cadherin 23 isoforms is not conserved: implications for a mouse model of Usher syndrome type 1D. *Mol. Vis.* 15, 1843-1857.

Lalwani, A., Walsh, B., Reilly, P. *et al.* (1998) Long-term in vivo cochlear transgene expression mediated by recombinant adeno-associated virus. *Gene Ther.* 5, 277-281.

La Vail, M. M. (2005) Survival factors for treatment of retinal degenerative disorders: preclinical gains and issues for translation into clinical studies. *Retina* 25, S25-S26.

La Vail, M. M., Unoki, K., Yasumura, D., Matthes, M. T., Yancopoulos, G. D., Steinberg, R. H. (1992) Multiple growth factors, cytokines, and neurotrophins rescue photoreceptors from the damaging effects of constant light. *Proc. Natl. Acad. Sci. U.S.A* 89, 11249-11253.

Le Meur, G., Weber, M., Pereon, Y. *et al.* (2005) Postsurgical assessment and long-term safety of recombinant adeno-associated virus-mediated gene transfer into the retinas of dogs and primates. *Arch. Ophthalmol.* 123, 500-506.

Lentz, J., Pan, F., Ng, S. S., Deininger, P., Keats, B. (2007) Ush1c216A knock-in mouse survives Katrina. *Mutat. Res.* 616, 139-144.

Lentz, J. J., Gordon, W. C., Farris, H. E. *et al.* (2010) Deafness and retinal degeneration in a novel USH1C knock-in mouse model. *Dev. Neurobiol.* 70, 253-267.

Leveillard, T. and Sahel, J. A. (2010) Rod-derived cone viability factor for treating blinding diseases: from clinic to redox signaling. *Sci. Transl. Med.* 2, 26ps16.

Levy, G., Levi-Acobas, F., Blanchard, S. *et al.* (1997) Myosin VIIA gene: heterogeneity of the mutations responsible for Usher syndrome type IB. *Hum. Mol. Genet.* 6, 111-116.

Linde, L. and Kerem, B. (2008) Introducing sense into nonsense in treatments of human genetic diseases. *Trends Genet.* 24, 552-563.

Liu, X., Bulgakov, O. V., Darrow, K. N. *et al.* (2007) Usherin is required for maintenance of retinal photoreceptors and normal development of cochlear hair cells. *Proc. Natl. Acad. Sci. U.S.A* 104, 4413-4418.

Lu, B., Wang, S., Francis, P. J. *et al.* (2010) Cell transplantation to arrest early changes in an ush2a animal model. *Invest Ophthalmol. Vis. Sci.* 51, 2269-2276.

Luebke, A. E., Rova, C., Von Doersten, P. G., Poulsen, D. J. (2009) Adenoviral and AAV-mediated gene transfer to the inner ear: role of serotype, promoter, and viral load on in vivo and in vitro infection efficiencies. *Adv. Otorhinolaryngol.* 66, 87-98.

MacLaren, R. E., Pearson, R. A., MacNeil, A. *et al.* (2006) Retinal repair by transplantation of photoreceptor precursors. *Nature* 444, 203-207.

Maguire, A. M., Simonelli, F., Pierce, E. A. *et al.* (2008) Safety and efficacy of gene transfer for Leber's congenital amaurosis. *N. Engl. J. Med.* 358, 2240-2248.

Mashimo, T., Takizawa, A., Voigt, B. *et al.* (2010) Generation of knockout rats with X-linked severe combined immunodeficiency (X-SCID) using zinc-finger nucleases. *PLoS. One.* 5, e8870.

McMillan, D. R., Kayes-Wandover, K. M., Richardson, J. A., White, P. C. (2002) Very large G protein-coupled receptor-1, the largest known cell surface protein, is highly expressed in the developing central nervous system. *J. Biol. Chem.* 277, 785-792.

Mingeot-Leclercq, M. P. and Tulkens, P. M. (1999) Aminoglycosides: nephrotoxicity. *Antimicrob.Agents Chemother.* 43, 1003-1012.

Morton, J., Davis, M. W., Jorgensen, E. M., Carroll, D. (2006) Induction and repair of zinc-finger nuclease-targeted double-strand breaks in Caenorhabditis elegans somatic cells. *Proc. Natl. Acad. Sci. U.S.A* 103, 16370-16375.

Nudelman, I., Rebibo-Sabbah, A., Cherniavsky, M. *et al.* (2009) Development of novel aminoglycoside (NB54) with reduced toxicity and enhanced suppression of disease-causing premature stop mutations. *J. Med. Chem.* 52, 2836-2845.

Nudelman, I., Rebibo-Sabbah, A., Shallom-Shezifi, D. *et al.* (2006) Redesign of aminoglycosides for treatment of human genetic diseases caused by premature stop mutations. *Bioorg. Med. Chem. Lett.* 16, 6310-6315.

Overlack, N., Nagel-Wolfrum, K., Wolfrum, U. (2010) 17. The role of cadherins in sensory cell function.In: Yoshida, K. (eds.) *Molecular and Functional Diversities of Cadherin and Protocadherin*. Research Signpost, Kerala, India, pp.1-15.

Pennings, R. J., Damen, G. W., Snik, A. F., Hoefsloot, L., Cremers, C. W., Mylanus, E. A. (2006) Audiologic performance and benefit of cochlear implantation in Usher syndrome type I. *Laryngoscope* 116, 717-722.

Petrozza, V., Vingolo, E. M., Pacini Costa, J. L., de, R. G., Carpino, F., Melis, M. (1991) Scanning electron microscopy observations of nasal mucosa in patients affected by retinitis pigmentosa. *Histol. Histopathol.* 6, 247-250.

Politano, L., Nigro, G., Nigro, V. *et al.* (2003) Gentamicin administration in Duchenne patients with premature stop codon. Preliminary results. *Acta Myol.* 22, 15-21.

Rebibo-Sabbah, A., Nudelman, I., Ahmed, Z. M., Baasov, T., Ben Yosef, T. (2007) In vitro and ex vivo suppression by aminoglycosides of PCDH15 nonsense mutations underlying type 1 Usher syndrome. *Hum. Genet.* 122, 373-381.

Reiners, J., Nagel-Wolfrum, K., Jürgens, K., Märker, T., Wolfrum, U. (2006) Molecular basis of human Usher syndrome: deciphering the meshes of the Usher protein network provides insights into the pathomechanisms of the Usher disease. *Exp. Eye Res.* 83, 97-119.

Reiners, J., Reidel, B., El-Amraoui, A. *et al.* (2003) Differential distribution of harmonin isoforms and their possible role in Usher-1 protein complexes in mammalian photoreceptor cells. *Invest. Ophthalmol. Visual Sci.* 44, 5006-5015.

Remy, S., Tesson, L., Menoret, S., Usal, C., Scharenberg, A. M., Anegon, I. (2009) Zinc-finger nucleases: a powerful tool for genetic engineering of animals. *Transgenic Res.*

Sahel, J. A. (2005) Saving cone cells in hereditary rod diseases: a possible role for rod-derived cone viability factor (RdCVF) therapy. *Retina* 25, S38-S39.

Schultz, B. R. and Chamberlain, J. S. (2008) Recombinant adeno-associated virus transduction and integration. *Mol. Ther.* 16, 1189-1199.

Sieving, P. A., Caruso, R. C., Tao, W. *et al.* (2006) Ciliary neurotrophic factor (CNTF) for human retinal degeneration: phase I trial of CNTF delivered by encapsulated cell intraocular implants. *Proc. Natl. Acad. Sci. U.S.A* 103, 3896-3901.

Smith, A. J., Bainbridge, J. W., Ali, R. R. (2009) Prospects for retinal gene replacement therapy. *Trends Genet.* 25, 156-165.

Staecker, H., Liu, W., Malgrange, B., Lefebvre, P. P., Van De Water, T. R. (2007) Vector-mediated delivery of bcl-2 prevents degeneration of auditory hair cells and neurons after injury. *ORL J. Otorhinolaryngol. Relat Spec.* 69, 43-50.

Stieger, K., Mendes-Madeira, A., Meur, G. L. *et al.* (2007) Oral administration of doxycycline allows tight control of transgene expression: a key step towards gene therapy of retinal diseases. *Gene Ther.* 14, 1668-1673.

Stone, E. M. (2009) Progress toward effective treatments for human photoreceptor degenerations. *Curr. Opin. Genet. Dev.* 19, 283-289.

Surace, E. M. and Auricchio, A. (2008) Versatility of AAV vectors for retinal gene transfer. *Vision Res.* 48, 353-359.

Takahashi, K. and Yamanaka, S. (2006) Induction of pluripotent stem cells from mouse embryonic and adult fibroblast cultures by defined factors. *Cell* 126, 663-676.

Tosi, G. M., de Santi, M. M., Pradal, U., Braggion, C., Luzi, P. (2003) Clinicopathologic reports, case reports, and small case series: usher syndrome type 1 associated with primary ciliary aplasia. *Arch. Ophthalmol.* 121, 407-408.

Urnov, F. D., Miller, J. C., Lee, Y. L. *et al.* (2005) Highly efficient endogenous human gene correction using designed zinc-finger nucleases. *Nature* 435, 646-651.

van Aarem, A., Wagenaar, M., Tonnaer, E. *et al.* (1999) Semen analysis in the Usher syndrome type 2A. *ORL J .Otorhinolaryngol. Relat Spec.* 61, 126-130.

van Wijk, E., van der Zwaag, B., Peters, T. *et al.* (2006) The DFNB31 gene product whirlin connects to the Usher protein network in the cochlea and retina by direct association with USH2A and VLGR1. *Hum. Mol. Genet.* 15, 751-765.

Verpy, E., Leibovici, M., Zwaenepoel, I. *et al.* (2000) A defect in harmonin, a PDZ domain-containing protein expressed in the inner ear sensory hair cells, underlies Usher syndrome type 1C. *Nat. Genet.* 26, 51-55.

Welch, E. M., Barton, E. R., Zhuo, J. *et al.* (2007) PTC124 targets genetic disorders caused by nonsense mutations. *Nature* 447, 87-91.

Williams, D. S. (2008) Usher syndrome: animal models, retinal function of Usher proteins, and prospects for gene therapy. *Vision Res.* 48, 433-441.

Wilschanski, M., Yahav, Y., Yaacov, Y. *et al.* (2003) Gentamicin-induced correction of CFTR function in patients with cystic fibrosis and CFTR stop mutations. *N. Engl. J. Med.* 349, 1433-1441.

Winter, J. O., Cogan, S. F., Rizzo, J. F., III (2007) Retinal prostheses: current challenges and future outlook. *J. Biomater. Sci. Polym. Ed* 18, 1031-1055.

Yanai, D., Weiland, J. D., Mahadevappa, M., Greenberg, R. J., Fine, I., Humayun, M. S. (2007) Visual performance using a retinal prosthesis in three subjects with retinitis pigmentosa. *Am. J. Ophthalmol.* 143, 820-827.

Yang J., Liu X., Zhao Y.et al. (2010) Ablation of whirlin long isoform disrupts the USH2 protein complex and causes vision and hearing loss. *PloS Genet* 6, e1000955.

Yu, J., Vodyanik, M. A., Smuga-Otto, K. *et al.* (2007) Induced pluripotent stem cell lines derived from human somatic cells. *Science* 318, 1917-1920.

Zingman, L. V., Park, S., Olson, T. M., Alekseev, A. E., Terzic, A. (2007) Aminoglycoside-induced translational read-through in disease: overcoming nonsense mutations by pharmacogenetic therapy. *Clin. Pharmacol. Ther.* 81, 99-103.

Zrenner, E. (2002) Will retinal implants restore vision? *Science* 295, 1022-1025.

18

Publikation V

2.5 Overlack N, Goldmann T, Wolfrum U, Nagel-Wolfrum K. Gene Repair of an Usher Syndrome Causing Mutation.- eingreicht

Gene Repair of an Usher Syndrome Causing Mutation

Nora Overlack, Tobias Goldmann, Uwe Wolfrum, and Kerstin Nagel-Wolfrum

The most precise and elegant way to treat genetic disorders would be to directly repair the mutated DNA. This may be achieved by introducing focal double strand breaks, which activates the cell endogenous pathway of homologous recombination. Zinc-finger nucleases (ZFNs) introduce double stranded DNA breaks at predetermined sites and thereby stimulate homologous recombination. Concurrent application of rescue DNA provides the template for gene correction during the repair process. Here, we investigated ZFN induced homologous recombination as a retinal treatment option for gene repair of the Ush1c-p.R31X nonsense mutation. This mutation causes the human Usher syndrome (USH), the most frequent cause of inherited combined deaf-blindness. To date, no effective treatment for the ophthalmic component of USH exists. In the present work, we designed and generated ZFNs specific for the p.R31X mutation in Ush1c. We confirmed the ability of designed ZFNs to cleave their target sequence and did not observe ZFN related toxicity in a p.R31X cell line. Furthermore, our results demonstrate ZFN-mediated gene repair, as well as a recovery in protein expression. These data highlight the ability of ZFNs to induce targeted homologous recombination and thereby mediate gene repair in inherited genetic disorders like the human Usher syndrome.

zinc-finger nucleases | retinitis pigmentosa | gene targeting | homologous recombination | gene correction

Introduction

The most elegant way to treat a genetic disorder is to repair the disease causing mutation in its endogenous locus (1). In contrast to other gene based therapy approaches the expression and splicing of the corrected gene remains under endogenous control, the size of the gene is no issue and the type of the disease causing mutation does not have to be taken into account. Gene repair, also called genome editing or gene correction, can be achieved by homologous recombination (HR) within the cell. Unfortunately, HR occurs under normal conditions at a very low frequency of 10-6 and therefore cannot be used for therapeutic means (2, 3). However, the frequency of HR can be increased several 1000 fold by the introduction of double strand breaks (DSBs) in the DNA (4). Zinc-finger nucleases (ZFNs) are engineered genetic tools to specifically create DSBs at a preselected genomic target sequence and thereby activate HR (5, 6). ZFN modules are chimeric proteins composed of a DNA binding domain (ZF domain) fused to the non-specific nuclease domain of FokI (Fig. 1) (1). The ZF domains can be specifically designed to bind to almost any preselected DNA sequence in the genome (6). To introduce a DSB, two ZFN modules have to form a dimer in order to activate the FokI nuclease activity (Fig. 1) (1). This requires two ZFN modules, binding opposing targets across a spacer where the FokI domains come together to create the break (Fig. 1) (1, 3). In a ZFN module each zinc-finger subunit (Fig. 1, grey ovals, ZF) recognizes and binds to three base pairs. Cloning of three ZF in line, results in the binding to nine consecutive base pairs. Dimerization of two ZFN modules therefore recognize 18 base pairs, making binding of the ZFN to DNA strands a likely unique event (1, 5). To repair the DSB during HR an exogenously introduced rescue plasmid, containing the desired sequence, can be used as a template (7-9).

In the present study we applied the ZFN technology to repair an Usher syndrome type 1 causing mutation. The human Usher syndrome (USH) is the most frequent cause of combined hereditary deaf-blindness. Based on its heterogenic clinical symptoms USH is divided into three clinical subtypes (USH1-3) (10). The most severe form of the disease is USH1, characterized by profound prelingual hearing loss, vestibular areflexia, and prepubertal onset of retinitis pigmentosa (RP) (10, 11). The auditory deficit of USH can be successfully treated with cochlear implants (12). However, to date no effective treatment for the retinal phenotype of USH exists.

We evaluated the ZFN induced gene repair strategy specifically for the p.R31X mutation in USH1C. The USH1C gene encodes the scaffold protein harmonin (13), previously identified as one of the key organizers in the USH protein interactome (10, 11). The gene encodes numerous splice variants (13, 14), yet, it remained elusive which isoform is essential for maintenance and or restoration of retinal function (10). Ambiguity concerning the activities of different harmonin isoforms, taken together with the numerous transcripts makes USH1C a difficult target for conventional gene addition approaches by viral strategies.

Here we designed customized ZFNs specific for the p.R31X mutation of murine Ush1c. We show the activity of ZFN by cleavage of the DNA target sequence. In addition, we demonstrate gene correction of the p.R31X mutation on the genomic level and expression of the repaired gene product, harmonin. These results highlight the capacity of ZFNs to treat individuals with mutations in USH1C and other inherited ocular and non-ocular diseases as well.

Results

Design of specific zinc-finger nucleases for a nonsense mutation in Ush1c. In order to design specific zinc-finger nucleases (ZFNs) for target sites in the relevant mutation in USH1C we used the ZiFiT software (15). We screened the sequence coding for the murine Ush1c orthologe which contains a USH1 disease causing p.R31X nonsense mutation. In this mutation the wild type CGA arginine codon (R) at position 91 is altered to a premature stop codon TGA (X). For the ZFN design using ZiFiT we applied software settings for ZF modules which recognize a nine-base pair (bp) sequence at the putative cleavage site separated by a spacer of five base pairs (Fig. 1A). Based on these prerequisites we identified bp 74-96 and bp 87-109 as targets in the mutated Ush1c coding sequence for the design of promising specific ZFNs (Fig. 1A, B). We designed the ZF domains in order that one ZF directly binds to mutated base pairs. We generated a total of seven predicted ZF domains by modular assembly which were fused with the FokI nuclease domain to form customized ZFN modules (15, 16). This strategy resulted in six matching ZFNs (A/C, A/D, B/C, B/D, E/F, and

E/G) and one not matching control (E/C) (Fig. 1). We transfected the ZFN modules into HEK293 cells and analyzed their cellular distribution. Immunofluorescence analysis revealed localization of ZFN modules as expected mainly within the nucleus (Fig. 2A).

Next we established a cellular reporter system to monitor ZFN mediated genome editing of the mutated Ush1c in the genomic context. For this, cDNA coding for the N-terminal part of the murine Ush1c gene product harmonin including the p.R31X mutation, the first two PDZ domains, and a C-terminal Myc-tag was stably integrated at a single location in the genome of Flp in-HEK293 cells (data not shown). In parallel Ush1c cells carrying the non-mutated construct were established.

Customized ZFNs have no cytotoxicity. Since application of ZFNs is often associated with significant cytotoxicity, presumably due to DNA cleavage at off-target sites (17) we examined potential side effects of ZFNs in the p.R31X reporter system by measuring the cell viability in a XTT-based assay. For this p.R31X cells were transfected with combinations of ZFN modules suitable to assemble active ZFN heterodimers and 48 h post-transfection the relative number of viable cells was determined (Fig. 2B). Transfection of p.R31X cells with ZFN did not lead to a significant alteration in the number of viable cells compared to mock or empty vector transfected cells indicating no cytotoxic side effects of the applied ZFNs.

DNA cleavage capability of customized ZFN. To evaluate the cleavage capability of generated active ZFNs the p.R31X cell line was either transfected with matching ZFNs or the control ZFN. Cells were harvested, genomic DNA was purified and semi-quantitative PCR with a primer pair flanking the putative ZFN cleavage site was performed (Fig. 2B). Efficient ZFN mediated cleavage resulted in the lack of a PCR product after transfection of ZFN module combinations A/C, B/D, and E/F (Fig. 2B). In contrast, the transfection of combinations A/D, B/C, E/G and the control ZFN resulted in a PCR amplicon, indicating that these ZFNs do not cleave the target sequence. Based on these results we focused on ZFNs A/C and E/F in the following experiments as these seemed to be the most efficient ZFNs.

Gene repair mediated by ZFN induced homologous recombination. Next we evaluated whether we can stimulate gene repair of the p.R31X mutation mediated by ZFN induced homologous recombination (HR). For this purpose we co-transfected p.R31X cells with ZFN and a rescue plasmid which contains the non-mutated Ush1c sequence without any promotor. Cells were harvested, genomic DNA was purified and a PCR with a primer pair flanking the mutation was performed. To omit amplification of the rescue plasmid we designed a forward primer binding within the CMV promotor located at the 5end of the integrated p.R31X construct in the Flp in-HEK293 cells and a reverse primer specific for the Ush1c sequence (Fig. 3A). The PCR products were digested with TseI which only cleaves the Ush1c (GCT/GC) but not the mutated p.R31X sequence (GCT/GT). The digestion resulted in a single band (500 bp) in the un-transfected p.R31X cells and a double band (200 bp and 300 bp) in Ush1c cells (Fig. 3B). TseI digest after transfection of matching ZFN modules A/C and E/F resulted in clear double bands (200 and 300 bp) showing an efficient gene repair of the p.R31X mutation mediated by ZFN (Fig. 3B). Transfection of the control ZFN resulted in three bands (200, 300 and 500 bp) indicating only weak repair efficiency of the mutated sequence. To further verify these results for repair by HR we sequenced the undigested 500 bp PCR product generated with the CMV and Ush1c primer pair. Sequencing confirmed that the generated PCR product after transfection of matching ZFN was a mix of Ush1c and p.R31X sequences, with a higher peak for Ush1c confirming HR at this locus, shown for ZFN E/F (Fig. 3C).

ZFN induced gene correction by homologous recombination recovers harmonin protein expression. To demonstrate recovered expression of the wild type Ush1c gene product harmonin on protein level we co-transfected p.R31X cells with matching ZFNs and the rescue plasmid. Gene repair was analyzed by indirect immunofluorescence using anti-Myc antibody against the C-terminal tag of the recovered protein and Western blot analyses with antibodies against harmonin (Fig. 4). No Myc positive cells were detected in un-transfected cells (Fig. 4A, upper

panel). In contrast, co-transfection of matching ZFNs (A/C and E/F) with rescue plasmid resulted in Myc positive cells (Fig. 4A). This clearly indicated gene repair of the mutated Ush1c sequence resulting in recovered expression of the harmonin construct.

In Western blots of un-transfected p.R31X cells or p.R31X cells transfected with the control ZFN no anti-harmonin positive band was detected, indicating that harmonin was not expressed (Fig. 4B). As expected anti-harmonin Western blot analyses from lysates of Ush1c cells revealed a band of about 43 kDa, corresponding to the calculated molecular weight of the harmonin construct (Fig. 4B). A band of the same molecular weight was detected in lysates of p.R31X cells co-transfected with matching ZFNs and rescue plasmid, demonstrating ZFN induced restoration of harmonin (Fig. 4B).

Discussion

Continual efforts have brought the zinc-finger nuclease (ZFN) technology into the focus of faster and more efficient genome editing at selected predetermined sites in diverse eukaryotic species (1, 5, 6, 18-20). So far most successful applications of the ZFN technology were reported for the introduction of targeted modifications in the genome to create transgenic species (21-26). More recently a series of key publications emphasized the significant therapeutic potential of ZFNs placing this technology into the spot light in the field of gene based therapy (27-29). In our present study we introduced the ZFN technology using customized ZFNs to induce homologues recombination (HR) for gene repair of a specific disease causing mutation responsible for a severe senso-neuronal degeneration, namely the human Usher syndrome. Our data indicate that the designed ZFNs are suitable for gene targeting to induce HR to correct the p.R31X mutation in the USH1C gene.

To ensure the ZFN mediated introduction of double stand breaks (DBS) at the site of the mutation to be repaired we have designed ZFNs containing one ZF binding directly to the p.R31X mutated site. Based on this strategy we selected ZFs which did not always target to GNN triplets, which were thought to be required for efficient binding of the ZF domain to the target DNA (30, 31). Nevertheless, the efficient cleavage and the high biocompatibility of the generated ZFNs indicate that the ZF domain composition out of ZF exclusively recognizing GNN triplets is not crucial which is in line with previously reported data (22). The observed differences in the binding and cleavage efficiency of the tested ZFNs are probably due to varying synergistic effects between adjacent ZF as previously discussed (32).

In the present study we provide proof-of-concept results that designed ZFNs mediate gene correction of a mutated Usher syndrome gene efficiently through the introduction of site-specific double strand breaks (DSBs) at the mutation. Cells have developed two in principle different mechanisms to repair DSBs, non-homologues end joining (NHEJ) and homology-directed repair (33). Since in NHEJ DNA ends are re-ligated without any use of homology NHEJ is an error-prone mechanism often introducing mutagenic changes (34). In contrast HR is a copy and paste mechanism using a DNA template for the correct repair of DSBs preferred for therapeutic gene correction (35). In our study we activate HR providing the rescue DNA as the correct template for repair of ZFN induced DSB. Our results provide several lines of evidence for the site specific gene correction of the USH disease causing p.R31X mutation by HR and exclude NHEJ. The present cleavage assay revealed introduction of the wild type sequence into the mutant p.R31X cell line after application of matching ZFNs in concert with the rescue DNA. Sequence analysis revealed the rescue-specific genotype indicating that rescue DNA was used as template to fill up the gap introduced by ZFN induced DSB. Finally, we demonstrated the recovery of harmonin protein expression by immunocytochemistry and Western blot analysis.

One significant drawback for the therapeutic application of the ZFN technology are the frequently reported toxic side effects of ZFNs introduced by off target DNA cleavage (36-38). Nevertheless, based on the results of cell viability tests we can exclude cytotoxicity of the

customized p.R31X ZFNs. Our findings are in line with previous publication (8, 25).

We customized our ZFNs to target the Ush1c gene with the future goal of correcting mutations causing human Usher syndrome affecting the sensory neurons in the inner ear and the retina. Although the mechanism HR has been well-established for cycling cells (39), only recently HR was identified as a DSB repair pathway in terminally differentiated neurons (40) further qualifying our ZFN based strategy for correcting Usher syndrome genes in the eye and ear.

Gene addition by viral vectors is traded as a promising strategy for the treatment of the Usher syndrome and is in preclinical trials for USH1B (41) (www.oxfordbiomedica.co.uk). Since Usher syndrome genes frequently are very large and/or have various splice variants gene addition approaches are very challenging. More recently, we succeeded to introduce translational read-through inducing drugs as therapeutic intervention for Usher syndrome type 1 nonsense mutations (42, 43). However, this drug treatment is only suitable for ~ 12% Usher syndrome mutations (44) and lifelong drug medication is needed. The presented strategy of ZFN technology has apparent advantages over established gene based therapy approaches (45), as i) the repaired gene stays under control of its endogenous promotor, so expression level, splicing and spatio-temporal expression remains unaffected, ii) no lifelong medication is necessary, iii) the size of the gene effected, iv) was well as the type of the disease causing mutation are no issues.

Taken together, the good biocompatibility of our ZFNs and repair of the p.R31X mutation in our cell culture system provides evidence that ZFN induced HR is suitable for the treatment of inherited genetic disorders as the Usher syndrome or related ciliopathies to cure the affected terminally differentiated sensory neurons. Conclusively, the ZFN technology holds an extensive potential for the treatment of known mutations in the direction of personalized therapy strategies.

Methods

Design and generation of ZFN for Ush1c-p.R31X mutation. The mutated Ush1c sequence was screened for putative ZF binding sites with the Zinc Finger consortium based software ZiFiT (http://bindr.gdcb.iastate.edu/ZiFiT) (15). Cloning of ZFN by modular assembly was performed as previously described (16). ZFN consisted of three individual ZF DNA binding sites fused to the FokI domain (Addgene plasmid 13426) Resulting ZFN modules were each cloned into an eukaryotic expression vector (Addgene plasmid pST1374) with a nuclear localization signal (NLS) and a Flag-tag to allow detection of the ZFN module.

p.R31X, Ush1c stable cell line and rescue plasmid. The p.R31X mutation was introduced into mouse Ush1c cDNA by PCR site-directed mutagenesis applying the QuickChange Lightning Site-Directed Mutagenesis Kit (Stratgene, LaJolla, CA). The Ush1c and mutated cDNA (bp 1-999) was sub-cloned in a pDEST expression vector with a C-terminal Myc-tag. Stable cell lines were generated by transfecting plasmids containing either p.R31X-Ush1c or Ush1c cDNA regulated by a CMV promoter into Flp in-HEK293 cells and selection by hygromycin B according to manufacturer's protocol (Invitrogen, Karlsruhe, Germany). The rescue plasmid contained the wild type Ush1c cDNA (bp 1-999). The sequence was cloned into pGL3-Basic vector (Promega, Fitchburg, WI, USA) which has no promotor.

Cell culture. Cells were grown in Dulbecco's Modified Eagle Medium with GlutaMaxTM supplemented with 10% fetal calf serum (Invitrogen), 1% penicillin/streptomycin (Invitrogen) at 37C and 5% CO2. Transfections were performed, with Lipofectamine LTX and PLUS reagent (Invitrogen) according to manufacturer's protocol. After 6 h medium was changed to fresh medium and cells were grown for 48-72 h.

Assessment of ZFN related cytotoxicity. Stable p.R31X cells were transfected with ZFNs. 48 h post-transfection ZFN toxicity was assessed by XTT cell viability assay (Roche, Dren, Germany) according to manufacturer's instructions. Assays were performed as triplets. Presented data are an average of five to nine independent experiments. G418 (1 mg/ml) was used as positive control for the assay.

Semi-quantitative PCR. 48 h post-transfection of stable p.R31X cells with ZFN genomic DNA was isolated by the High Pure PCR Template Preparation Kit (Roche). As positive control for the cleavage genomic DNA of stable p.R31X cells was digested with EcoRI. Duplex PCRs were performed in a volume of 50 l using 12 ng genomic DNA and 10 nmol of each primer/reaction. Cycling conditions were 25 cycles at 94C for 40 s, 60C for 40 s, and 72C for 1 min followed by a 7 min 72C extension. Harmonin specific primers flanking the potential cleavage site forward (5-ATGGACCGGAAGGTGGCCCGA-3) and reverse primer (5 CCTTCTGGGTGCAGACGGTCCAAG-3) were used. Primer set for GAPDH (forward 5-TGCACCACCAACTGCTTAGC-3 and reverse 5-GGCATGGACTGTGGTCATGAG-3) was used as internal control for the PCR reaction. PCR products were analyzed on 1% agarose gels.

TseI digest. 72 h post-transfection genomic DNA was isolated from cells transfected with ZFNs and rescue plasmid by the High Pure PCR Template Preparation Kit (Roche). PCRs were performed in a volume of 50 l using 300 ng of prepared genomic DNA and 10 nmol of each primer perreaction. Cycling conditions were 35 cycles at 94C for 40 s, 60C for 40 s, and 72C for 1 min followed by a 7 min 72C extension. Forward primer binding in the CMV-promotor of stable transfected p.R31X construct (5-GTACGGTGGGAGGTCTATAT-3) and a harmonin specific reverse primer (5 CCTTCTGGGTGCAGACGGTCCAAG-3) were used. 10 l PCR product were digested with 0.5 l TseI (New England Biolabs, Ipswich, MA, USA) for 2 h at 65C and digestion analyzed on 2% agarose gels.

Antibodies and dyes. Monoclonal mouse antibodies to a-tubulin (clone DM1A), Flag (M2), and Myc (clone 9B11) were obtained from Sigma-Aldrich (St. Louis, MO, USA) and cell signaling (Danvers, MA, USA), respectively. Polyclonal rabbit antibodies against harmonin (H3) were used as previously described (14). Secondary antibodies conjugated to Alexa 488 or 568 were purchased from Molecular Probes (Leiden, NL) and DAPI from Sigma-Aldrich. For Western blot secondary antibodies were purchased from Invitrogen or Rockland (Gilbertsville, PA).

Immunofluorescence microscopy. Immunofluorescence analyses were carried out on stable transfected p.R31X cells seeded on coverslips, followed by fixation with methanol and proceeded as previously described (46). Specimens were analyzed in a Leica DM 6000 B microscope (Leica microsystems, Bensheim, Germany) and processed with Adobe Photoshop CS (Adobe Systems, San Jose, CA, USA).

Western blot analyses. Harvesting of cells and Western blot analyses were performed as previously described (47, 48).

Abbreviations. DAPI, 4,6-Diamidino-2-phenylindol; DSB, double strand break; HR, homologous recombination; NHEJ, non-homologous end joining; PDZ, PSD-95, DLG, ZO-1; USH, Usher syndrome; ZF, zinc-finger; ZFN, zinc-finger nuclease.

Urnov FD, Rebar EJ, Holmes MC, Zhang HS, & Gregory PD (2010) Genome editing with engineered zinc finger nucleases. Nat.Rev.Genet. 11(9):636-646.

Orr-Weaver TL, Szostak JW, & Rothstein RJ (1981) Yeast transformation: a model system for the study of recombination. Proc.Natl.Acad.Sci.U.S.A 78(10):6354-6358.
Porteus MH & Baltimore D (2003) Chimeric nucleases stimulate gene targeting in human cells. Science 300(5620):763.

Rouet P, Smih F, & Jasin M (1994) Introduction of double-strand breaks into the genome of mouse cells by expression of a rare-cutting endonuclease. Mol.Cell Biol. 14(12):8096-8106.

Bibikova M et al. (2001) Stimulation of homologous recombination through targeted cleavage by chimeric nucleases. Mol.Cell Biol. 21(1):289-297.

Carroll D (2008) Progress and prospects: zinc-finger nucleases as gene therapy agents. Gene Ther. 15(22):1463-1468.

Lombardo A et al. (2007) Gene editing in human stem cells using zinc finger nucleases and integrase-defective lentiviral vector delivery. Nat.Biotechnol. 25(11):1298-1306.

Greenwald DL, Cashman SM, & Kumar-Singh R (2010) Engineered zinc finger nuclease-mediated homologous recombination of the human rhodopsin gene. Invest Ophthalmol.Vis.Sci. 51(12):6374-6380.

Rahman SH, Maeder ML, Joung JK, & Cathomen T (2011) Zinc-finger nucleases for somatic gene therapy: the next frontier. Hum.Gene Ther. 22(8):925-933.

Reiners J, Nagel-Wolfrum K, Jrgens K, Mrker T, & Wolfrum U (2006) Molecular basis of human Usher syndrome: deciphering the meshes of the Usher protein network provides insights into the pathomechanisms of the Usher disease. EXP.EYE RES. 83:97-119.

Wolfrum U (2011) Protein networks related to the Usher syndrome gain insights in the molecular basis of the disease. Usher Syndrome: Pathogenesis, Diagnosis and Therapy., (Nova Science Publishers,) pp 51-73.

Damen GW, Beynon AJ, Krabbe PF, Mulder JJ, & Mylanus EA (2007) Cochlear implantation and quality of life in postlingually deaf adults: long-term follow-up. Otolaryngol.Head Neck Surg. 136(4):597-604.

Verpy E et al. (2000) A defect in harmonin, a PDZ domain-containing protein expressed in the inner ear sensory hair cells, underlies Usher syndrome type 1C. Nat.Genet. 26(1):51-55.

Reiners J et al. (2003) Differential distribution of harmonin isoforms and their possible role in Usher-1 protein complexes in mammalian photoreceptor cells. Invest.Ophthalmol.Visual Sci. 44:5006-5015.

Sander JD, Zaback P, Joung JK, Voytas DF, & Dobbs D (2007) Zinc Finger Targeter (ZiFiT): an engineered zinc finger/target site design tool. Nucleic Acids Res. 35(Web Server issue):W599-W605.

Wright DA et al. (2006) Standardized reagents and protocols for engineering zinc finger nucleases by modular assembly. Nat.Protoc. 1(3):1637-1652.

Szczepek M et al. (2007) Structure-based redesign of the dimerization interface reduces the toxicity of zinc-finger nucleases. Nat.Biotechnol. 25(7):786-793.

Morton J, Davis MW, Jorgensen EM, & Carroll D (2006) Induction and repair of zinc-finger nuclease-targeted double-strand breaks in Caenorhabditis elegans somatic cells. Proc.Natl.Acad.Sci.U.S.A 103(44):16370-16375.

Cathomen T & Joung JK (2008) Zinc-finger nucleases: the next generation emerges. Mol.Ther. 16(7):1200-1207.

Doyon Y et al. (2008) Heritable targeted gene disruption in zebrafish using designed zinc-finger nucleases. Nat.Biotechnol. 26(6):702-708.

Geurts AM et al. (2009) Knockout rats via embryo microinjection of zinc-finger nucleases. Science 325(5939):433.

Takasu Y et al. (2010) Targeted mutagenesis in the silkworm Bombyx mori using zinc finger nuclease mRNA injection. Insect Biochem.Mol.Biol. 40(10):759-765.

Baylis HA & Vazquez-Manrique RP (2011) Reverse Genetic Strategies in Caenorhabditis elegans: Towards Controlled Manipulation of the Genome. ScientificWorldJournal. 11:1394-1410.

Even-Faitelson L, Samach A, Melamed-Bessudo C, Avivi-Ragolsky N, & Levy AA (2011) Localized egg-cell expression of effector proteins for targeted modification of the Arabidopsis genome. Plant J.

Hauschild J et al. (2011) Efficient generation of a biallelic knockout in pigs using zinc-finger nucleases. Proc.Natl.Acad.Sci.U.S.A 108(29):12013-12017.

McCammon JM, Doyon Y, & Amacher SL (2011) Inducing High Rates of Targeted Mutagenesis in Zebrafish Using Zinc Finger Nucleases (ZFNs). Methods Mol.Biol. 770:505-527.

Li H et al. (2011) In vivo genome editing restores haemostasis in a mouse model of haemophilia. Nature 475(7355):217-221.

Soldner F et al. (2011) Generation of isogenic pluripotent stem cells differing exclusively at two early onset Parkinson point mutations. Cell 146(2):318-331.

Zou J et al. (2011) Whirlin replacement restores the formation of the USH2 protein complex in whirlin knockout photoreceptors. Invest Ophthalmol.Vis.Sci. 52(5):2343-2351.

Beumer K, Bhattacharyya G, Bibikova M, Trautman JK, & Carroll D (2006) Efficient gene targeting in Drosophila with zinc-finger nucleases. Genetics 172(4):2391-2403.

Ramirez CL et al. (2008) Unexpected failure rates for modular assembly of engineered zinc fingers. Nat.Methods 5(5):374-375.

Isalan M, Choo Y, & Klug A (1997) Synergy between adjacent zinc fingers in sequence-specific DNA recognition. Proc.Natl.Acad.Sci.U.S.A 94(11):5617-5621.

Pardo B, Gomez-Gonzalez B, & Aguilera A (2009) DNA repair in mammalian cells: DNA double-strand break repair: how to fix a broken relationship. Cell Mol.Life Sci. 66(6):1039-1056.

Jensen NM et al. (2011) An update on targeted gene repair in mammalian cells: methods and mechanisms. J.Biomed.Sci. 18:10.

Kramer O, Klausing S, & Noll T (2010) Methods in mammalian cell line engineering: from random mutagenesis to sequence-specific approaches. Appl.Microbiol.Biotechnol. 88(2):425-436.

Pruett-Miller SM, Reading DW, Porter SN, & Porteus MH (2009) Attenuation of zinc finger nuclease toxicity by small-molecule regulation of protein levels. PLoS.Genet. 5(2):e1000376.

Cornu TI & Cathomen T (2010) Quantification of zinc finger nuclease-associated toxicity. Methods Mol.Biol. 649:237-245.

Gupta A, Meng X, Zhu LJ, Lawson ND, & Wolfe SA (2011) Zinc finger protein-dependent and -independent contributions to the in vivo off-target activity of zinc finger nucleases. Nucleic Acids Res. 39(1):381-392.

Kass EM & Jasin M (2010) Collaboration and competition between DNA double-strand break repair pathways. FEBS Lett. 584(17):3703-3708.

Chan F, Hauswirth WW, Wensel TG, & Wilson JH (2011) Efficient mutagenesis of the rhodopsin gene in rod photoreceptor neurons in mice. Nucleic Acids Res.

Hashimoto T et al. (2007) Lentiviral gene replacement therapy of retinas in a mouse model for Usher syndrome type 1B. Gene Ther. 14(7):584-594.

Goldmann T et al. (2010) Beneficial read-through of a USH1C nonsense mutation by designed aminoglycoside NB30 in the retina. Invest Ophthalmol.Vis.Sci. 51(12):6671-6680.

Goldmann T, Overlack N, Wolfrum U, & Nagel-Wolfrum K (2011) PTC124-mediated translational readthrough of a nonsense mutation causing Usher syndrome type 1C. Hum.Gene Ther. 22(5):537-547.

Kellermayer R (2006) Translational readthrough induction of pathogenic nonsense mutations. Eur.J.Med.Genet. 49:445-450.

Overlack N, Goldmann T, Wolfrum U, & Nagel-Wolfrum K (2011) Current Therapeutic Strategies for Human Usher syndrome. Usher Syndrome: Pathogenesis, Diagnosis and Therapy. (Nova Science Publishers, Inc. USA,) pp 377-395.

Overlack N, Maerker T, Latz M, Nagel-Wolfrum K, & Wolfrum U (2008) SANS (USH1G) expression in developing and mature mammalian retina. Vision Res. 48(3):400-412.

Nagel-Wolfrum K et al. (2004) The interaction of specific peptide aptamers with the DNA binding domain and the dimerization domain of the transcription factor Stat3 inhibits transactivation and induces apoptosis in tumor cells. Mol.Cancer Res. 2(3):170-182.

Maerker T et al. (2008) A novel Usher protein network at the periciliary reloading point between molecular transport machineries in vertebrate photoreceptor cells. Hum.Mol.Genet. 17(1):71-86.

Figure 1. Zinc-finger nucleases for the Ush1c p.R31X mutation. (A) Zinc-finger nucleases are chimeric proteins consisting of DNA binding zinc-fingers (ZF) fused to the non-specific cleaving endonuclease FokI (ZFN module). We designed ZFN modules with three DNA binding ZFs (1-3 grey ovals, ZF domain). The FokI is only functional when dimerized, making a pair of ZFN modules necessary to from an active ZFN heterodimer and introduce a DNA double strand break. Segments from bp 74-96 and bp 87-109 were chosen because one ZF is binding directly to a mutated base pair (asterisks). (B) In silico screens resulted in seven different potential ZFN modules for p.R31X (A-G).

Figure 2. ZFN expression and evaluation in cell culture. (A) ZFNs are mainly localized in the nucleus of HEK293 cells, detected by anti-Flag antibody, exemplarily shown for ZFN module D. DAPI, nuclear DNA staining. Scale bar: 25 µm (B) ZFN related cytotoxicity was analyzed by measurement of cell viability in XTT assay. Cells transfected with matching or control ZFNs do not show an elevated rate of cell death compared to mock transfected cells or p.R31X cells transfected with the empty vector. Addition of G418 was used as positive control for the assay. (C) In vitro cleavage of ZFN. Semi-quantitative duplex PCR with genomic DNA of p.R31X cells transfected with ZFN or un-transfected was performed with a primer pair (arrows) flanking the putative ZFN cleavage site (X). The lack of an amplicon after transfection with matching ZFN A/C, B/D, and E/F indicated highly efficient ZFN mediated cleavage of the DNA. The weak band after transfection of B/C suggested a less efficient binding or cleavage of this ZFN combination compared to the others. ZFNs A/D

and E/G and the not matching E/C do not bind or cleave their target properly. The EcoRI digestion served as a positive control for the cleavage and GAPDH amplification as internal PCR control.

Figure 3. Gene repair mediated by ZFN induced homologous recombination on the genomic level. (A) Stable transfected p.R31X cells were triple transfected with ZFN modules and rescue plasmid. PCR was performed on genomic DNA with a primer pair (arrows) flanking the mutation (X). (B) TseI digestion of PCR products. TseI cleaved only the Ush1c, not the mutated p.R31X sequence. Fragment sizes: wild type 200/300 bp; mutated p.R31X sequence 500 bp. Transfection of with matching ZFN A/C and E/F resulted in gene repair of p.R31X to the Ush1c sequence. (C) Sequencing confirmed an exchange of the mutated codon TGA to the wild type CGG, generated from the rescue plasmid, exemplarily shown for ZFN E/F. Asterisks indicate exchanged nucleotides due to ZFN mediated HR.

Figure 4. Gene repair mediated by ZFN induced homologous recombination on protein level. (A) Indirect immunofluorescence analysis of p.R31X cells revealed Myc positive cells after transfection of ZFN A/C and E/F together with the rescue plasmid. No Myc labeling was detected in un-transfected cells. DAPI, nuclear DNA staining. Scale bars: 25 µm (B) Western blot analysis of p.R31X cells either un-transfected or transfected with ZFN and rescue plasmid. Cell lysates were subjected to Western blot with anti-harmonin and anti-tubulin antibodies (loading control). Harmonin-PDZ2-Myc expression (~ 43 kDa) was detected by anti-H3 in Ush1c wild type cells and in pR31X cells transfected with ZFN A/C and E/F.

Reserved for publication footnotes

A

ZFN

bp 74-96

5´ TATCTTTATGATGTGCTGTGAATGTAT 3´
3´ ATAGAAATACTACACGACACTTACATA 5´

ZF   nuclease domain
ZF domain
ZFN module

bp 87-109

5´ GTGCTGTGAATGTATCACCAGACCATG 3´
3´ CACGACACTTACATAGTGGTCTGGTAC 5´

B

			1	2	3
bp 74-96	bp 87-96 5´- 3´	A	TSGNLVR	QRANLRA	TSGNLTE
		B	ISSNLQR	—II—	—II—
	bp 74-82 3´- 5´	C	RRDELNV	RNDALTE	RSDALRE
		D	—II—	QAGHLAS	—II—
bp 87-109	bp 101-109 5´- 3´	E	ERSHLRE	SKKALTE	HKNALQN
	bp 87-95 3´- 5´	F	TSHSLTE	QLAHLRA	DKKDLTR
		G	—II—	QSSHLLT	—II—

Figure1

Figure 2

A p.R31X

pCMV —X— p.R31X cells

+ ZFN, rescue plasmid

B

p.R31X GTGCTGTGAATGTAT

Ush1c wild type GTGCTGCGGATGTAT

TseI

bp	A/C	E/F	control	p.R31X	*Ush1c*
1000					
500					← p.R31X
					← *Ush1c*
250					← *Ush1c*

C

G T G C T G C/T G G/A A T G T A T

* *

Figure 3

A p.R31X cell line

un-transfected

A/C

E/F

anti-MYC   anti-MYC + DAPI

B

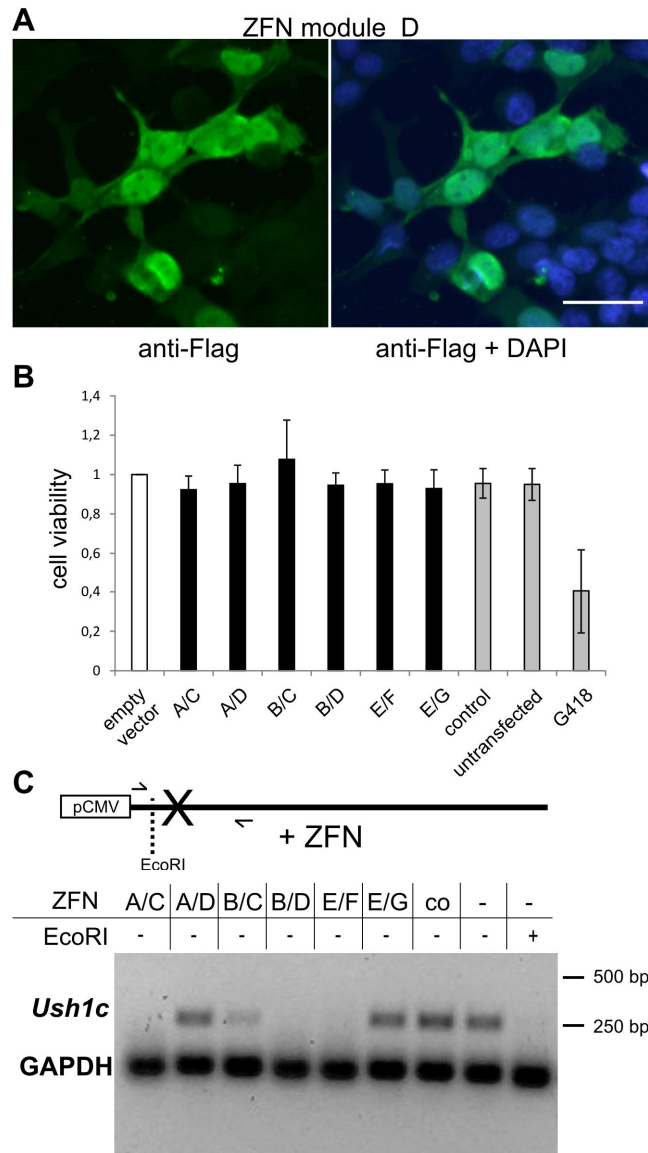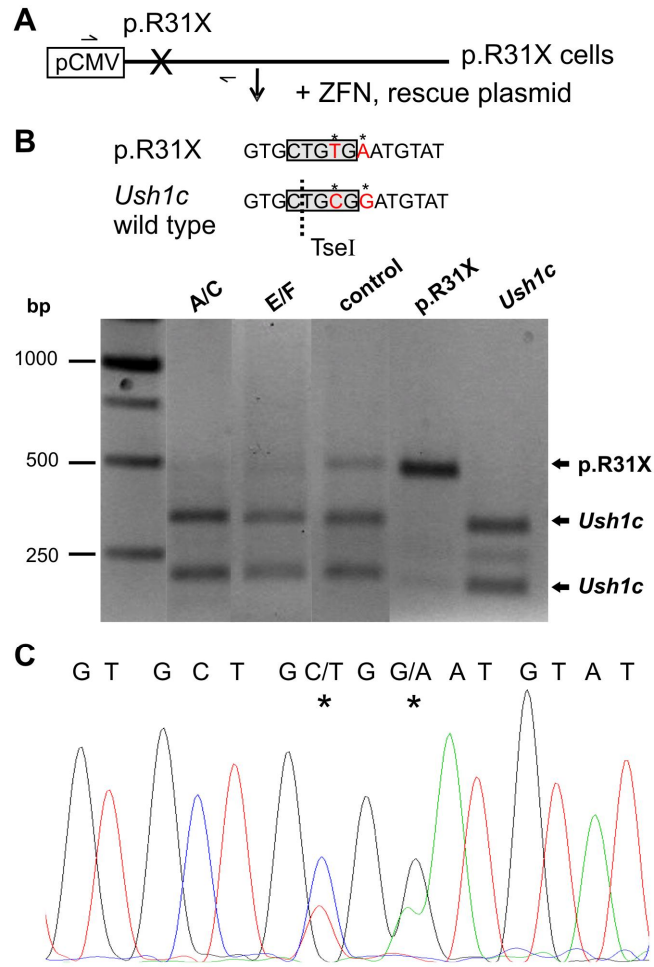|	un-trans.	control	A/C	E/F	
43 —					harm
55 —					tub

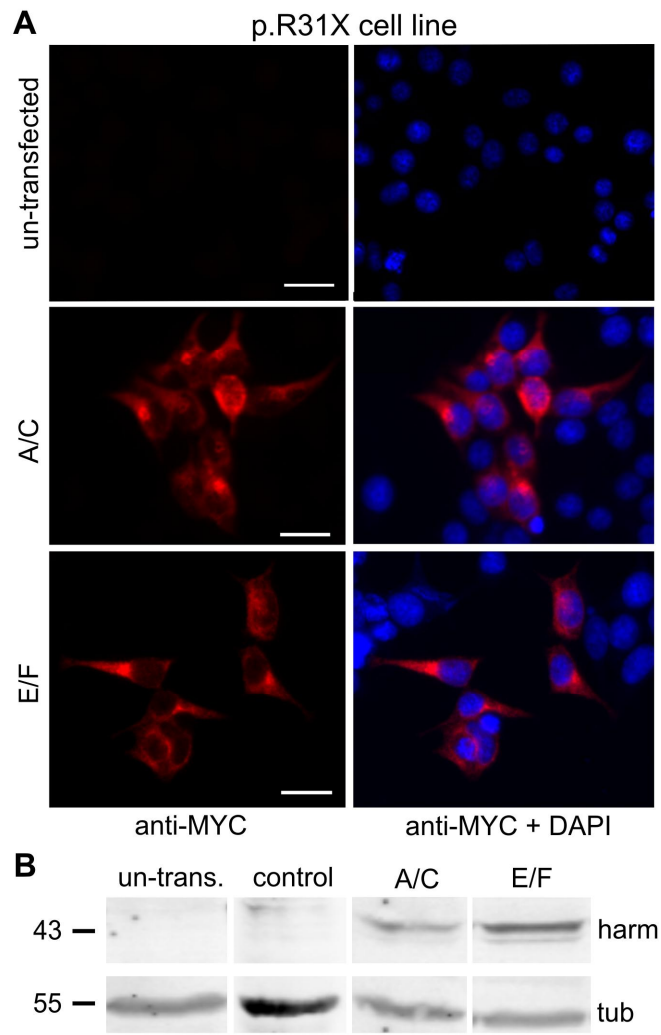Figure 4

3. Zusammenfassung der Ergebnisse und Diskussion

3.1 Expression und Lokalisation von USH-Molekülen in der Retina

Die Kenntnis des Expressionsprofils eines Proteins und dessen transkriptionellen und postranskriptionellen Modifikationen ist eine wichtige Voraussetzung für die Evaluation der zellulären Funktion sowie von Therapiemöglichkeiten. In Publikation I der vorliegenden Arbeit wurde die Expression und Lokalisation von USH-Proteinen, speziell des USH1D-Proteins Cadherin23 (CDH23), analysiert.

CDH23 wird differentiell gespleißt (Bolz et al., 2001; Bork et al., 2001). Die Isoformen werden in drei Gruppen, a, b und c unterteilt, die sich in der Anzahl bzw. Vorhandensein der extrazellulären EC-Domänen und einer Transmembrandomäne unterscheiden (Bolz et al., 2001; Bork et al., 2001) (Publikation I und II). Expressionsanalysen mittels RT-PCR und Western Blot ergaben eine entwicklungsabhängige Expression der Isoform a im Innenohr der Maus. Des Weiteren wird die a Isoform in der Retina von Primaten exprimiert (Publikation I, Abb. 1, 8, 9). In der Mausretina und dem Innenohr CDH23-defizenter *waltzer*-Mäuse konnte zu keinem der analysierten Zeitpunkte eine Expression der a Isoform nachgewiesen werden (Publikation I, Abb. 1, 8). Dies weist auf eine unterschiedliche Expression der CDH23-Isoformen in Mäusen und Primaten hin (Publikation I).

In der Mausretina sind CDH23-Isoformen im Bereich des Verbindungsciliums, der Kerne und an den Synapsen lokalisiert (Publikation I, Abb. 3-5). Die hochauflösenden Analysen bestätigten CDH23 als Komponente des ciliären Apparates von Photorezeptorzellen (Reiners et al., 2003) (Publikation I, Abb. 4, 5). Spezifische Antikörper zeigten die kleine c Isoform exklusiv an den Synapsen der Photorezeptorzellen sowie der auditorischen und vestibulären Zellen im Innenohr (Publikation I, Abb. 3, 6).

Die in Publikation I beobachteten Unterschiede der CDH23-Expression wurden durch korrelative Lokalisationsstudien weiter bestätigt (Abb. 5). Die Analysen ergaben eine Lokalisation von CDH23 im Bereich des Verbindungsciliums, der Zellkerne und der Synapsen in der Retina von Maus und Mensch (Abb. 5 A, B). Hochauflösende mikroskopische Aufnahmen von CDH23 zeigten eine Lokalisation am Basalkörper und Centriol in beiden Spezies (Abb. 5 C, D). Beim Menschen projizierte CDH23 zusätzlich am Verbindungscilium entlang des Axonems in den basalen Bereich des Außensegments (Abb. 5 E, F).

Insgesamt zeigten die Analysen eine unterschiedliche Expression von CDH23-Isoformen in der Cochlea und Retina der Maus, ebenso wie Unterscheide in der CDH23-Expression

zwischen den Retinae von Mäusen und Primaten (Abb. 5 und Publikation I). Der Expressionsunterschied könnte erklären, weshalb die CDH23-defizienten *waltzer*-Mäuse keine retinale Degeneration zeigen und deshalb nicht als USH-Tiermodell für die Retina geeignet sind (Publikation I).
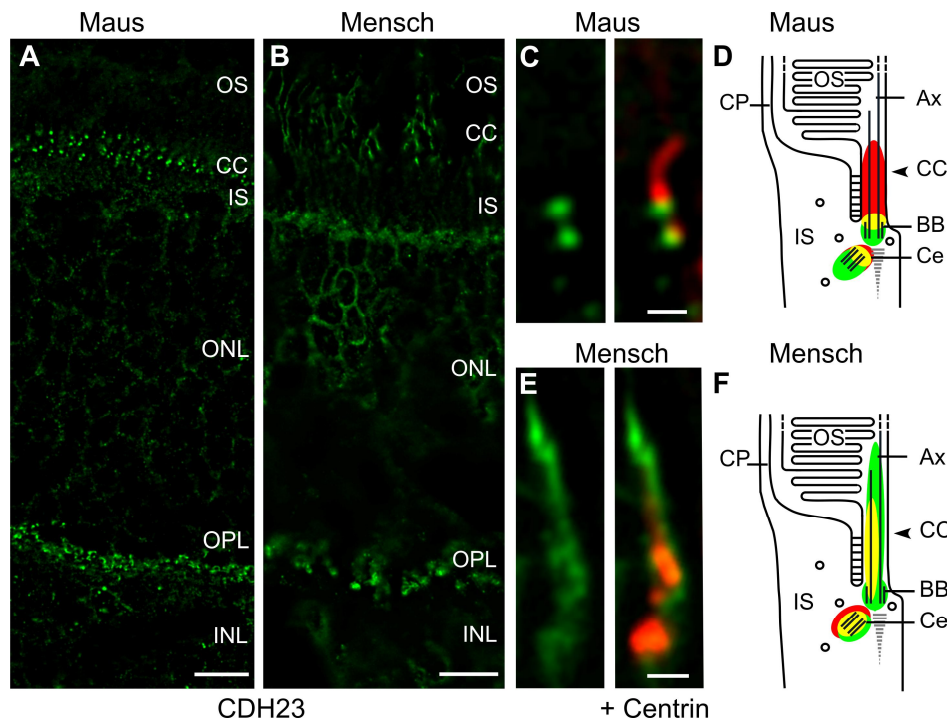
Abbildung 5: CDH23 Lokalisation in der Retina von Maus und Mensch. (A, B) CDH23 ist im Bereich des Verbindungsciliums (CC), der äußeren Körnerschicht (ONL) und der äußeren plexiformen Schicht (OPL) lokalisiert. **(C, E)** Doppelmarkierung von CDH23 (grün) mit Centrin (Cilienmarker, rot). CDH23 ist am Basalkörper (BB) und dem Centriol lokalisiert (C, E). Beim Mensch projiziert CDH23 zusätzlich entlang des Axonems (Ax) ins Außensegment (OS) (E). **(D, F)** Schema des ciliären Bereichs einer Photorezeptorzelle. Die Lokalisation von CDH23 (grün) und die partielle Kolokalisation (gelb) mit Centrin (rot) in Maus (D) und Mensch (F) sind dargestellt. IS: Innensegment, INL: innere Körnerschicht, CP: calycal process. Größenbalken: A, B: 10 µm, C, E: 1 µm.

Aufgrund vorangegangener Arbeiten unserer Arbeitsgruppe zu CDH23, Protocadherin15 (PCDH15) und der Analyse zur Expression und Lokalisation von CDH23-Isoformen (Reiners et al., 2003; Reiners et al., 2005a; Reiners et al., 2006; Lagziel et al., 2009), wurden wir eingeladen, die Rolle der USH-Cadherine in sensorischen Systemen in Form eines Buchkapitels zu beschreiben (Publikation II). Der Übersichtsartikel fasst die Erkenntnisse über Expression, Lokalisation und Funktion der sensorischen USH-Cadherine, CDH23 und PCDH15 in den Haarzellen der Cochlea und den Photorezeptorzellen zusammen (Publikation II). Des Weiteren wird auf Protocadherin21 (PCDH21) eingegangen, das an der Diskneogenese an der Basis des Außensegments der Photorezeptorzellen beteiligt ist (Rattner et al., 2001).

3.2 Molekulare Integration von USH-Proteinen in Netzwerken

Ein weiterer Teil der vorliegenden Doktorarbeit widmete sich der „zweiten" Ebene der hier verfolgten USH-Forschung, in der unser zuvor gewonnenes Wissen über Expression und Lokalisation der USH-Proteine erweitert werden sollte. Die Suche nach Interaktionspartnern ist notwendig, um die zelluläre Funktion von Proteinen zu verstehen. Vorexperimente unserer Arbeitsgruppe wiesen auf eine mögliche Interaktion des USH1G-Proteins SANS mit Myomegalin hin (Märker, 2007; Publikation III). Im Rahmen der vorliegenden Dissertation sollte diese Interaktion zwischen SANS und Myomegalin validiert und die zelluläre Funktion der Interaktion näher beleuchtet werden (Publikation III).

Myomegalin, dessen Name aufgrund der Größe und der Expression des Proteins in Muskelzellen gewählt wurde, ist ein Interaktionspartner der Phosphodiesterse 4 D, weshalb es alternativ in der Literatur als PDE4DIP (phosphodiesterase 4 D interacting protein) bezeichnet wird (Verde et al., 2001). Im Rahmen komplementärer biochemischer und zellbiologischer Analysen konnte die direkte Interaktion zwischen den Gerüstproteinen SANS und Myomegalin bestätigt und das USH-Interaktom um Myomegalin erweitert werden (Abb. 1) (Publikation III, Abb. 1).

In Datenbankanalysen fanden wir vier mögliche Myomegalin-Isoformen unter-schiedlicher Größe in der Maus (Publikation III, Abb. 2). Die anschließenden Analysen auf Transkriptions- und Proteinebene verschiedener Mausgewebe ergaben eine differentielle Expression der Myomegalin-Isoformen, wobei in der Retina drei Isoformen exprimiert werden (Publikation III, Abb. 2).

Mikroskopische Analysen in der Retina von Mäusen, nicht-humaner Primaten und des Menschen zeigten die Expression von Myomegalin in Photorezeptorzellen im Innensegment, im Bereich der Zellkerne und an den Synapsen (Publikation III, Abb. 3-7). Doppelmarkierungen von Myomegalin und SANS zeigten eine partielle Kolokalisation beider Proteine in den Photorezeptorzellen von Mäusen und Primaten (Publikation III, Abb. 6, 7). Die korrelativen Analysen der vorliegenden Arbeit zur Lokalisation von SANS und Myomegalin, die eine Assoziation beider Proteine mit den Mikrotubuli zeigen, deuten auf eine Rolle beider Proteine in zellulären Transportprozessen hin (Publikation III, Abb. 7, 8). Eine Assoziation von SANS mit dem Mikrotubili-Cytoskelett, dem Centrosom und Transportvesikeln wurde bereits in früheren Arbeiten diskutiert (Adato et al., 2005; Märker et al., 2008*; Overlack et al., 2008*; Zallocchi et al., 2010). (Eine Hypothese der Transportbeteiligung der USH-Proteine in Photorezeptorzellen ist in Publikation III, im Schema der Abb. 8 dargestellt.) Weitere, im Hefe-2-Hybrid nachgewiesene,

Interaktionspartner liefern zusätzliche Hinweise auf eine Beteiligung von SANS an gerichteten Transportprozessen (Märker, 2007). Außerdem deuten die mehr als 30 weiteren potentiellen Interaktionspartner von SANS auf eine mögliche Konkurrenz zwischen Myomegalin und den anderen Interaktoren um die Bindung zu SANS hin. Die vielseitigen Interaktionsmöglichkeiten des USH1G-Proteins verdeutlichen die Rolle und Funktion von SANS als Gerüst im Komplex der USH-Proteinnetzwerke (Publikation III).

Wie zuvor erwähnt handelt es sich bei Interaktionspartnern von USH-Proteinen um potentielle USH-Gene, bzw. um mögliche „Modifier" von USH-Genen (Bolz et al., 2005; Schneider et al., 2009; Ebermann et al., 2010). Durch die direkte Interaktion mit dem USH1G-Protein SANS kommt Myomegalin als Kandidat für ein potentielles neues USH-Gen in Frage. Aufgrund der Lokalisation des Myomegalin Gens (1q12) im Genom ist es allerdings unwahrscheinlich, dass es sich um ein USH-Gen handelt, da es zu keinem der bislang bekannten USH-Genloki passt (Tab. 1). Eine modifizierende Rolle von Myomegalin auf *SANS* oder andere USH-Gene, wie bereits für einige USH-Gene beschrieben (Ebermann et al., 2010), könnte jedoch möglich sein.

Insgesamt unterstützen die vorgelegten Daten unsere Hypothese der Beteiligung von SANS vermittelten USH-Proteinnetzwerken an intrazellulären Transportvorgängen (Märker et al., 2008*; Wolfrum, 2011). Die Interaktion der Proteine in den USH-Netzwerken dient gerichteten intrazellulären Transportprozessen, der Stabilisierung von Strukturen und damit der Aufrechterhaltung der Funktion der Photorezeptorzellen (Reiners et al., 2005a; Reiners et al., 2005b*; Märker et al., 2008*; Overlack et al., 2008*; Wolfrum, 2011). Der Verlust eines der Proteine des USH-Interaktoms kann zum Funktionsverlust des ganzen Komplexes führen und damit zur klinischen Ausprägung von USH. Dies macht die Notwendigkeit deutlich, die molekularen Grundlagen von USH und die Degeneration der Retina weiter zu erforschen, um fundierte Therapiemaßnahmen entwickeln zu können.

3.3 Therapiemöglichkeiten für das Usher-Syndrom des Menschen

Im dritten Teil meiner Arbeit wurden auf Grundlage der fundierten Expressions-, Lokalisation- und Funktionsanalyse zu USH-Proteinen (Publikation I, II und III) Therapiemöglichkeiten für USH in der Retina evaluiert (Publikationen IV und V). Hierbei konzentrierte ich mich auf den retinalen Phänotyp, da Cochleaimplantate eine praktikable Möglichkeit für die Behandlung des Phänotyps im Innenohr darstellen (Publikation IV).

In Publikation IV werden die potentiellen Therapiemöglichkeiten für USH ausführlich dargelegt und diskutiert. Die vielversprechendsten Therapieformen bieten genbasierte Ansätze. Wie oben beschrieben werden ungefähr 80% der USH-Fälle durch Mutationen in

einem der neun bekannten Gene verursacht (Bolz, 2009). Daher ist ein gezieltes Screening der Patienten auf die individuelle Mutation theoretisch möglich (Bolz, 2009). Durch die Identifizierung der spezifischen Mutationen können genbasierte Therapien eingesetzt werden. Dies führte in den letzten Jahren zur Entwicklung verschiedener gentherapeutischer Ansätze, die für die Behandlung von USH-Patienten genutzt werden können (zusammengefasst in Publikation IV).

Im Rahmen meiner Doktorarbeit war ich an der Evaluation verschiedener genbasierter Ansätze für eine mögliche Behandlung von USH beteiligt. Dies umfasste die Genaddition mittels adeno-assoziierter Viren (AAV), das Überlesen von Nonsense-Mutationen und die Genreparatur durch Zinkfinger-Nukleasen-vermittelte Homologe Rekombination. Eine Übersicht, welche Therapiestrategie potentiell für welche genetischen Defekte besonders geeignet ist, wird in Tabelle 1, Publikation IV gegeben. Analysiert wurden die Ansätze am für Harmonin kodierenden *USH1C*-Gen, bei dem erkrankungsbedingende Mutationen zum schwerwiegendsten klinischen USH-Typ1 führen können (Zwaenepoel et al., 2001; Saihan et al., 2009). Für die Analyse der Genreparatur und der Überlese-Strategie lag der Fokus auf der 91C>T/p.R31X-Mutation im *USH1C*-Gen.

Die etablierteste Methode zur Behandlung von vererbten retinalen Erkrankungen ist zurzeit die Genaddition, die viral, in der Regel mittels AAV oder nicht-viral, z.B. mittels Nanopartikeln erfolgen kann (Stone, 2009). Dabei wird die funktionale kodierende Sequenz eines Gens exogen mit Hilfe der Transfersysteme in die betroffenen Zellen eingebracht und zum vorhandenen Genom addiert. In den letzten Jahren wurden mit AAV als Transfersystem bereits große Erfolge für retinale Erkrankungen sowohl in Tiermodellen als auch im Menschen, erzielt (Acland et al., 2005; Bainbridge et al., 2008; Hauswirth et al., 2008; Maguire et al., 2008).

In unserer Arbeitsgruppe war ich am Gentransfer von AAV mittels subretinaler Injektion beteiligt. Dadurch wurde erfolgreich eine Expression von Harmonin-Konstrukten in der Retina von Mäusen induziert (Abb. 6). Die ersten Ergebnisse, die wir mittels AAV-Transfer in die Retina erreichen konnten, zeigen die grundsätzliche Möglichkeit dieses Ansatzes als Therapiekonzept. Limitiert wird die virale Genaddition allerdings durch die in fast allen USH-Typen vorkommenden Spleißvarianten und die Größe der zu transferierenden cDNA (Publikation IV). Auch die neuste Generation von AAVs kann maximal 8,9 kb aufnehmen (Allocca et al., 2008), was für viele USH-Gene nicht ausreichend ist (Publikation IV).
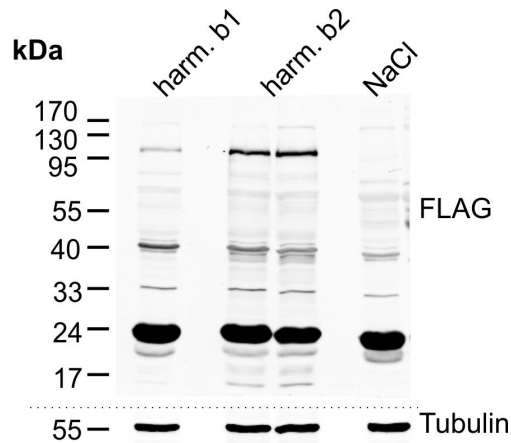
Abbildung 6: Harmonin b1 und b2 Transgenexpression in der Mausretina nach AAV-vermittelter Genaddition. Nach subretinaler Injektion von AAV5-harmonin Viren (harm.b1, harm.b2) bzw. physiologischer Kochsalzlösung (NaCl; Kontrolle) konnte die Transgenexpression mit anti-FLAG Antikörpern in AAV-injizierten Augen detektiert werden. Tubulin diente als Ladekontrolle.

Aufgrund dieser Einschränkungen werden in unserer Arbeitsgruppe im USH-Therapieteam weitere Ansätze zur Behandlung von genetischen Erkrankungen verfolgt: die Anwendung von „translational read-through inducing drugs" (TRIDs), die zu einem Überlesen von Nonsense-Mutationen führen (Keeling und Bedwell, 2011) und die durch Zinkfinger-Nukleasen vermittelte Genreparatur (Publikation IV und V). Aktuelle Arbeiten unserer Arbeitsgruppe, zu denen ich beitragen konnte, zeigen, dass durch den Einsatz von TRIDs die 91C>T/p.R31X Nonsense-Mutation überlesen und dabei funktionales Protein generiert wird (Goldmann et al., 2010*; Goldmann et al., 2011*). Die größte Schwierigkeit der „Überlese"-Methode liegt allerdings in der notwendigen Langzeitapplikation der TRIDs in therapierelevanten Konzentrationen ins Auge (Publikation IV). Zudem können nur Nonsense-Mutationen so behandelt werden, und - obwohl ca. 11% der USH-Fälle durch Nonsense-Mutationen verursacht werden (Baux et al., 2008) - bleibt die Frage nach einer Behandlungsmöglichkeit von nicht Nonsense-Mutationen.

Die Reparatur eines Gens im endogenen Lokus durch „genomische Chirurgie" stellt die wahrscheinlich eleganteste Methode zur Behandlung genetischer Erkrankungen dar (Publikation IV und V). In der vorliegenden Doktorarbeit lag ein Hauptfokus auf der Analyse der Genreparatur durch Homologe Rekombination als Therapiekonzept für USH (Publikation V). Der zelleigene Reparaturmechanismus der Homologen Rekombination kann über Zinkfinger-Nukleasen (ZFN) künstlich induziert werden (Kim et al., 1996; Bibikova et al., 2001) (Publikation IV und V).

Im Rahmen der vorliegenden Arbeit wurden für die 91C>T/p.R31X-Mutation im *USH1C*-Gen verschiedene ZFN für die Erkennung und das Schneiden der mutierten Maussequenz identifiziert und kloniert (Publikation V, Abb. 1). *In vitro* Experimente in

Kombination mit semi-quantitativer PCR zeigten ein effizientes Schneiden der DNA-Zielsequenz durch unterschiedliche ZFN-Kombinationen (Publikation V, Abb. 2). Die analysierten ZFN wiesen keine toxischen Nebeneffekte auf, wie sie in anderen Arbeiten beobachtete wurden (Pruett-Miller et al., 2009; Cornu und Cathomen, 2010; Gupta et al., 2011) (Publikation V, Abb. 2). PCR-Ansätze in Verbindung mit Restriktionsverdau zeigten die Reparatur der 91C>T/p.R31X-Mutation auf genomischer Ebene, validiert durch Sequenzierungen (Publikation V, Abb. 3). Die Resultate der Sequenzierungen nach Behandlung der Zellen schließen auch einen Verschluss des Strangbruchs durch den fehleranfälligen, unspezifischen Reparaturmechanismus des nonhomologous end-joining (NHEJ) aus. Der Einbau der korrekten Basensequenz bestätigt die Reparatur mittels Homologer Rekombination (Publikation V, Abb. 3).

Für die Therapie einer genetischen Erkrankung ist nicht nur die Behandlung auf der genetischen Ebene der DNA notwendig. Die korrekte Expression und Funktionalität des betroffenen Proteins sind mitentscheidend. In der vorliegenden Arbeit wurde die Expression des reparierten *Ush1c*-Proteins Harmonin biochemisch nachgewiesen (Publikation V, Abb. 4). Durch die Expressionsanalysen des reparierten Harmonin-Proteins wird die Homologe Rekombination unabhängig von den Sequenzierungen als Reparaturmechanismus bestätigt (Publikation V). Zusammenfassend zeigen unsere Ergebnisse eine Reparatur der 91C>T/p.R31X-Mutation durch Homologe Rekombination, sowohl auf genomischer Ebene, als auch auf Proteinniveau (Publikation V).

Nach einem Doppelstrangbruch kann durch Homologe Rekombination eine Region von bis zu 8000 bp effizient und exakt von der rescue-DNA auf den genomischen Bereich transferiert werden (Moehle et al., 2007). Dies zeigt, dass ZFN generiert werden könnten, die nicht nur spezifisch für Patienten mit einer Mutation maßgeschneidert sind, sondern die für mehrere Patienten „passen", die eine Mutation im selben genomischen Bereich haben. Dadurch könnten Aufwand und Kosten für die Herstellung und Tests der ZFN dramatisch gesenkt werden und so den Einsatz einer semi-personalisierten Therapie ermöglichen.

Die bislang geringe Effizienz der Genreparatur ist kritisch zu betrachten und muss weiter erhöht werden, um größtmöglichen therapeutischen Nutzen zu erzielen. Wie einleitend eingeführt hat die ZFN-induzierte Homologe Rekombination gegenüber anderen genbasierten Strategien jedoch grundlegende Vorteile, 1. das reparierte Gen verbleibt unter Kontrolle des endogenen Promotors, die Expressionsmenge, sowie das gewebespezifische Spleißen werden dadurch kontrolliert, 2. es ist keine Langzeittherapie notwendig und 3. die Art der krankheitsauslösenden Mutation spielt keine Rolle. Eine aktuelle Arbeit zeigte jetzt

erstmals den therapeutischen Effekt einer ZFN-basierten Genkorrektur *in vivo* in der Leber von Mäusen (Li et al., 2011b) und bestätigt damit die Wirksamkeit der ZFN-induzierten Homologen Rekombination als Therapiestrategie für genetische Erkrankungen.

Insgesamt demonstriert die vorliegende Arbeit die Reparatur der 91C>T/p.R31X-Mutation in unserem Zellkultursystem sowie die gute Biokompatibilität der generierten ZFN. Dies zeigt, dass die ZFN ein enormes Potential für die Behandlung von bekannten Mutationen, wie z.B. USH, auf dem Weg zu personalisierten Therapiestrategien besitzen.

4. Ausblick

4.1 USH-Grundlagenforschung

Die Kenntnis der molekularen Grundlagen von USH ist eine notwendige Voraussetzung für die Etablierung von fundierten Therapiestrategien. Für die Weiterentwicklung der Behandlungsmöglichkeiten und die Aufklärung der zellulären Funktionen der USH-Proteine sind weitere Analysen der zellulären Zusammensetzung des USH-Interaktoms, bzw. der USH-Proteinnetzwerke notwendig.

Die detaillierte Analyse der Expression von USH-Proteinen, deren Isoformen und Interaktionspartnern liefert wichtige Grundlagen für das Verständnis des Aufbaus der USH-Proteinnetzwerke. Eine Möglichkeit zur weiteren Erforschung der Komposition des USH-Interaktoms bieten TAP-Tag Analysen. Diese ermöglichen eine schonende Aufreinigung von nativen Proteinkomplexen (Rigaut et al., 1999; Gloeckner et al., 2009). Diese Methode wird in Kulturzellen bereits angewendet (den Hollander et al., 2007). Allerdings wäre eine Analyse im Kontext des Gewebes von Interesse weit gewinnbringender. Zu diesem Zweck habe ich im Rahmen der vorliegenden Dissertation begonnen, transgene Mäuse zu generieren. Es wurden Konstrukte für die Expression eines Strep-FLAG-Tags fusioniert mit Harmonin a1, SANS oder Harmonin-p.R31X kloniert, um verschiedene Mauslinien herzustellen. Die Harmonin a1- und SANS-Mauslinien sollen für TAP-Tag Analysen verwendet werden, um weitere Komplexpartner von Harmonin, bzw. SANS *in vivo* zu identifizieren. Unabhängige Analysen der Interaktionen sind notwendig, um die gefundenen Zusammenhänge zu verifizieren. Die bislang bekannten Interaktionen der USH-Proteine in Netzwerken könnten mit Hilfe bioinformatisch gestützter Analysen in einen größeren systembiologischen Zusammenhang gebracht werden. Auf diese Weise könnten mögliche Verbindungen unterschiedlicher Proteininteraktome festgestellt werden. Des Weiteren könnten mögliche Beteiligungen der Proteine oder Netzwerke an zellulären „pathways" aufgedeckt werden, die in Erkrankungen wie USH oder anderen Ciliopathien resultieren. Insgesamt könnte durch die ganzheitliche Betrachtung der Proteininteraktionen auch die Grundlage für gemeinsame, interferierende Therapiestrategien zur Behandlung von Erkrankungen in demselben pathway gelegt werden.

Ein Aspekt, der in der USH-Forschung bislang nur wenig Beachtung fand, ist die Analyse einer möglichen Regulation einzelner Proteine oder ganzer Proteinnetzwerke, beispielsweise durch posttranskriptionale Modifikationen. So existieren aus TAP-Tag Experimenten erste Hinweise auf eine mögliche Regulation von SANS über den Phosporylierungsstatus (Jores *et al.,* in prep). Auch die Analyse der Bindungsaffinitäten der einzelnen Interaktionspartner an ein Protein könnte zur weiteren Aufklärung der Funktionen von USH-Proteinnetzwerken

beitragen. Die Interaktionspartner von SANS beispielsweise scheinen um die Bindung an die zentrale Domäne zu konkurrieren (Publikation III). Die Stärke der Bindungen könnte zum Beispiel mit Hilfe von Plasmonresonanzexperimenten überprüft werden. Dies könnte Aufschluss darüber geben, wie wahrscheinlich eine Interaktion im zellulären Umfeld mit konkurrierenden Interaktionspartnern ist. All diese Informationen würden helfen, das Wissen über die Grundlagen von USH, die zellulären Funktionen der Proteine und die Pathophysiologie von USH zu erweitern.

4.2 Weiterführung der Therapieansätze für USH

Die in Publikation IV und V vorgestellten Therapiestrategien für USH und deren Evaluation liefern die Grundlage, die Behandlungsmöglichkeiten weiter voranzutreiben. Die Funktionalität und Biokompatibilität der ZFN in den 91C>T/p.R31X-Zellen ermöglichen die Analyse der ZFN-basierten Therapiestrategie in weiterführenden Experimenten mit dem Ziel der *in vivo* Genreparatur im (Maus)Auge. Zu diesem Zweck wurde im Rahmen der vorliegenden Arbeit die transgene Harmonin-p.R31X-Mauslinie generiert. Mit Hilfe dieses Modells können zukünftig die verschiedenen vorgestellten Therapiekonzepte *in vivo* im Auge der Maus evaluiert werden. Die Tiere enthalten die mutierte 91C>T/p.R31X-*Ush1c*-Maussequenz als zusätzliche Kopie im Genom. Die Mäuse eigenen sich sowohl zur Überprüfung der ZFN induzierten Homologen Rekombination, als auch für die Evaluation der parallel in der Arbeitsgruppe verfolgten Überlesestrategie von Nonsense-Mutationen mit Hilfe von TRIDs.

4.2.1 Transfermethoden der ZFN-Komponenten in die Retina

Für eine effiziente Wirkungsweise der Genreparatur in Zellen und Geweben ist eine effektive Transfermethode für die einzelnen Komponenten in die Photorezeptorzellen der Retina essentiell. Für Analyse der optimalen Transfermethode kann auf das etablierte *ex vivo* System der organotypischen Retinakultur zurückgegriffen werden (Reidel et al., 2006). Für eine erfolgreiche Reparatur müssen zwei ZFN-Module und die rescue-DNA in die Zellen eingebracht werden. Für diesen Transfer stehen potentiell verschiedene alternative Systeme zur Verfügung: AAV, Nanopartikel, Proteintransduktion, mRNA oder Oligonukleotide.

Eine Methode zum Einbringen der ZFN und rescue-DNA, ist der Transfer mittels AAVs. Die Effektivität bestimmter AAV-Serotypen für die Transduktion speziell von Photorezeptorzellen konnte eindrucksvoll gezeigt werden (Allocca et al., 2007). Bislang traten keine toxischen Nebeneffekte bei der Verwendung von AAVs auf und sie werden erfolgreich in klinischen Studien eingesetzt (Bainbridge et al., 2008; Hauswirth et al., 2008; Maguire et

al., 2008). Allerdings ist eine langanhaltende Expression der transferierten DNA über Jahre, wie sie für AAVs gezeigt wurde (Acland et al., 2005), für die ZFN eher negativ. Die ZFN würden wahrscheinlich auch die reparierte Sequenz aufgrund ihrer hohen Ähnlichkeit zur mutierten Sequenz immer wieder schneiden. Die Problematik, die mit einer anhaltenden Expression der ZFN einhergeht, könnte durch den Einbau einer Schnittstelle für die ZFN in das Virusrückrat umgangen werden. In den transduzierten Zellen würden die exprimierten ZFN durch ein Schneiden des Virusrückrats selbst dafür sorgen, dass es nicht zu einer langanhaltenden Expression kommen kann.

Eine andere Möglichkeit für den Transfer der Reparatureinzelteile bieten Nanopartikel. Bei Nanopartikeln handelt es sich um neutral geladene Komplexe, in die DNA-Moleküle verpackt werden können (Farjo et al., 2006). Die Komplexe werden von Zellen aufgenommen und die DNA exprimiert (Cai et al., 2008). Die verpackte DNA wird von den Zellen bis zu 200-mal effektiver aufgenommen als unverpackte, „nackte" DNA (Ziady et al., 2003; Cai et al., 2008). Vorteile der Nanopartikel bestehen darin, dass sie nahezu keine Toxizität aufweisen, effizient von Photorezeptorzellen aufgenommen werden (Farjo et al., 2006; Cai et al., 2010) und für Genadditionsansätze bereits erfolgreich in klinischen Studien getestet wurden (Konstan et al., 2004). Ein Nachteil ist - wie bei dem Transfer mittels AAV - die Langzeitexpression, die nach Nanopartikeltransfer nachgewiesen wurde (Farjo et al., 2006). Die Nanopartikel würden sich also nur für den Transfer der rescue-DNA eignen, nicht jedoch für den Transfer der ZFN.

Eine weitere vielversprechende Transfermethode ist der Einsatz von ZFN-kodierender mRNA. Diese würde eine schnelle und lediglich transiente Expression der ZFN ermöglichen (Doyon et al., 2008; Foley et al., 2009; Geurts et al., 2009; Flisikowska et al., 2011).

Die Proteintransduktion bietet einen weiteren Weg des Transfers der ZFN. Eine Form der Proteintransduktion basiert auf einer sogenannten TAT-Sequenz (*trans*-aktivator) (Frankel und Pabo, 1988; Green und Loewenstein, 1988; Wadia und Dowdy, 2002). Durch das Anhängen einer TAT-Sequenz wird eine effektive Aufnahme der Proteine in die Zelle induziert (Frankel und Pabo, 1988; Green und Loewenstein, 1988; Wadia und Dowdy, 2002). Bei dieser Transfermethode könnte die rescue-DNA in Form von Oligonukleotiden in die Zellen transferiert werden, um dort als Matrize für die Reparatur zu dienen.

Denkbar wäre auch eine Kombination der unterschiedlichen Transfermethoden, um die Komponenten effizient in die Photorezeptorzellen einzubringen. So könnten die ZFN mittels Proteintransduktion oder AAVs und die rescue-DNA über Nanopartikel oder Oligonukleotide eingebracht werden. Nach Abwägung der bisher bekannten Informationen zur

Transfereffektivität wäre Proteintransduktion oder mRNA für den Transfer der ZFN in Kombination mit rescue-DNA in Form von Nanopartikeln oder Oligonukleotiden meiner Meinung nach am besten geeignet.

Außer der Analyse der Effektivität der Transfersysteme in die Retina muss des Weiteren das Verhältnis, in dem ZFN und rescue-DNA für eine effiziente Genreparatur eingesetzt werden müssen, titriert werden. Die eventuelle Toxizität der Genreparaturkomponenten für die Zellen der Retina kann z.B. mittels TUNEL-Assay analysiert werden. Nachdem die idealen Bedingungen für die Genreparatur in organotypischen Retinakulturen evaluiert wurden, kann die Genreparatur der 91C>T/p.R31X-Mutation *in vivo* in den transgenen p.R31X-Mäusen analysiert werden.

4.2.2 Grundsätzliche Anwendbarkeit der Genreparatur

Die hier an der 91C>T/p.R31X-Mutation im *USH1C*-Gen vorgestellte Strategie der Genkorrektur ist nicht gen- oder mutationsspezifisch, sondern kann auch auf andere USH-Mutationen oder retinale Dystrophien ausgeweitet werden. Die grundsätzliche Voraussetzung für eine gentherapeutische Behandlung ist die Kenntnis der verursachenden Mutation (Stone, 2009). In den meisten USH-Genen lassen sich ZFN-Bindestellen identifizieren (https://grenada.lumc.nl/LOVD2/Usher_montpellier/USHbases.html), mit denen nicht nur eine Mutation, sondern mehrere Mutationen im gleichen genomischen Bereich behandelt werden könnten. Beispielsweise könnte für die Behandlung der 216G>A-Mutation und auch der 238-239insC-Mutation, die beide häufig vorkommen (Zwaenepoel et al., 2001; Ouyang et al., 2003; Ebermann et al., 2007), das gleiche ZFN-Paar eingesetzt werden. Im Rahmen der vorliegenden Doktorarbeit konnten hierfür bereits ZFN identifiziert werden.

Es existiert eine Vielzahl von USH-Tiermodellen, von denen allerdings die meisten den retinalen USH-Phänotyp des Menschen nicht überzeugend wiederspiegeln (Williams, 2008). Lediglich ein *Ush2a-* sowie ein *Ush2d*-Mausmodell zeigen eine spät einsetzende Degeneration der Retina (Liu et al., 2007; Yang et al., 2010). Dies erschwert die breitgefächerte Anwendung der unterschiedlichen Therapiekonzepte auf die Mutationen der einzelnen USH-Gene, da es keine Möglichkeit gibt, die Reparatur anhand der wiederhergestellten Funktion in der Retina zu überprüfen. Ein Weg, die Effektivität der generierten ZFN zu testen, solange keine adäquaten Tiermodelle zur Verfügung stehen, bieten primäre Zelllinien von Patienten. Es müsste sich um einfach zugängliche Zellen handeln, die den Patienten ohne großen Aufwand oder Schmerzen entnommen und kultiviert werden könnten, wie Zellen der Haut, des Blutes, oder der Schleimhäute. Geeignet wären beispielsweise die Epithelzellen der Nasenschleimhaut, da hier alle USH1- und USH2-Gene

exprimiert werden (Vache et al., 2010). In den Zelllinien könnte die Spezifität der ZFN für die Induktion von Doppelstrangbrüchen sowie die Effizienz der Genreparatur unter den gleichen genetischen Voraussetzungen, unter denen auch die Therapie stattfinden muss, evaluiert werden. In primären Zelllinien von Patienten würden die Intron- und Exonstrukturen im genomischen Kontext mit berücksichtigt. Eine effizientere Vorauswahl und Analyse der ZFN für spezifische Mutationen wären dadurch möglich.

4.2.3 Weiterentwicklung der ZFN und Alternativen

Seit Beginn meiner Doktorarbeit und der Herstellung der in Publikation V verwendeten ZFN gab es viele Vorschläge zur Verbesserung der ZFN, besonders in Bezug auf die Erhöhung der Spezifität und des Designs, aber auch zur Herstellung anderer Chimäre als molekulare Schere. Die nächste Generation von ZFN soll spezifischer und weniger toxisch sein (Ramalingam et al., 2011). Die neuen Plattformen für das Design berücksichtigen nicht nur die Bindungsspezifität der ZFN an die Ziel-DNA, sondern beziehen auch die Wechselwirkungen zwischen den einzelnen Zinkfingern mit ein (Szczepek et al., 2007; Carroll, 2008; Cathomen und Joung, 2008; Pruett-Miller et al., 2009; Ramalingam et al., 2011).

Zinkfinger (ZF) sind nicht die einzigen DNA-Bindeproteine, die modifiziert wurden, um als molekulare Scheren zu wirken. Neue Ansätze verwenden andere DNA-Bindeproteine, gekoppelt an eine Nuklease als Alternative für spezifisches Gentargeting. Dazu zählen die sogenannten TALE-Nukleasen (Transcription Activator-Like Effector) des Pflanzenpathogens *Xanthomonas* (Boch et al., 2009; Cermak et al., 2011; Li et al., 2011a). TALE-Nukleasen wurden erfolgreich für Gentargeting und genetische Modifikationen in verschiedenen Organismen wie Hefen, Pflanzen und in humanen Kulturzellen eingesetzt (Cermak et al., 2011; Li et al., 2011a). Es bleibt abzuwarten, welches System zum gezielten Gentargeting, die ZF- oder TALE-Nukleasen, sich als das effektivere für Therapieansätze erweist. Wobei eine aktuelle Publikation in einem Vergleich der beiden Nukleasen eine ähnliche Effektivität in der Induktion von spezifischen Doppelstrangbrüchen feststellte (Mussolino et al., 2011).

4.2.4 Kombination von Therapien

Eine Möglichkeit zur Therapie von genetischen Erkrankungen könnte auch in der Kombination von verschiedenen therapeutischen Ansätzen bestehen. So wird beispielsweise in einer aktuellen Arbeit die ZFN-Technologie zur Reparatur einer Mutation mit patienten-spezifischen induzierten pluripotenten Stammzellen (iPS) kombiniert (Soldner et al., 2011). Bislang dienen diese Zellen als Modellsystem zur Analyse der molekularen Krankheitsmechanismen oder zum Test von Therapiestrategien. Die Zellen könnten aber auch

dem Patienten wieder zugeführt werden. Dass sich eine Transplantationen von Zellen in einer Art Zellersatztherapie positiv auf ein USH-Modell auswirkt, konnte bereits in der Retina der *Ush2a*-null Mauslinie gezeigt werden (Liu et al., 2007). In einer zukünftigen Kombinationstherapie könnten die Zellen *ex vivo* mit Hilfe von ZFN repariert werden und als iPS-Zellen in das betroffene Gewebe des Patienten transplantiert werden.

Insgesamt eignet sich eine einmalige effiziente Reparatur des Gens am endogenen Lokus nicht nur für USH, sondern potentiell für alle genetisch vererbten Erkrankungen, deren Mutationen bekannt sind. Der Einsatz von ZFN oder anderer molekularer Scheren für die Induktion des DNA-Strangbruchs zur Aktivierung der Homologen Rekombination ist nicht abhängig von der Größe des Gens, von Spleißvarianten oder der Art der zu reparierenden Mutation. Dies macht die Genreparatur zum Therapiekonzept der Zukunft für die personalisierte Behandlung von genetischen Erkrankungen.

5. Zusammenfassung

Das humane Usher Syndrom (USH) ist die häufigste Form vererbter Taub-Blindheit. In der vorliegenden Dissertation wurde diese komplexe Erkrankung auf verschiedenen Ebenen analysiert: in Arbeiten zur Expression und Lokalisation von USH-Proteinen, der Analyse der USH-Proteinnetzwerke und deren Funktionen sowie darauf aufbauend die Entwicklung von Therapiestrategien für USH.

Im Rahmen der Arbeit wurde die Expression und (sub)-zelluläre Lokalisation des USH1D-Genproduktes CDH23 in der Retina und Cochlea analysiert. CDH23-Isoformen werden in der Maus zeitlich und räumlich differentiell exprimiert. In den Retinae von Mäusen, nicht humanen Primaten und Menschen zeigten Analysen eine unterschiedliche Expression und Lokalisation des Zell-Zelladhäsionsmoleküls CDH23, was auf Funktionsunterschiede der einzelnen Isoformen in den analysierten Spezies hindeutet.

Analysen zur Aufklärung der USH-Proteinnetzwerke ergaben eine potentielle Interaktion des USH1G-Gerüstproteins SANS mit dem Golgi- und Centrosom-assoziierten Protein Myomegalin. Die direkte Interaktion der Proteine konnte durch unabhängige Experimente verifiziert werden. Beide Interaktionspartner sind in den Retinae verschiedener Spezies partiell kolokalisiert und partizipieren im periciliären USH-Proteinnetzwerk. Die Assoziation von SANS und Myomegalin mit dem Mikrotubuli-Cytoskelett weist auf eine Funktion des Proteinkomplexes in gerichteten Transportprozessen innerhalb der Photorezeptoren hin und bekräftigt die Hypothese einer Rolle von SANS und assoziierten Netzwerken mit Transportprozessen.

Das hier gewonnene erweiterte Verständnis der molekularen Grundlagen sowie die Aufklärung der zellulären Funktion der Proteinnetzwerke ermöglichen die Entwicklung therapeutischer Strategien für USH. Ein Fokus der vorliegenden Arbeit lag auf der Entwicklung genbasierter Therapiestrategien und deren Evaluation, wobei der Schwerpunkt auf der Therapiestrategie der Genreparatur lag. Die mit Hilfe von Zinkfinger-Nukleasen (ZFN) induzierte Homologe Rekombination für die Genkorrektur wurde exemplarisch an der 91C>T/p.R31X-Mutation im *USH1C*-Gen gezeigt. Effiziente ZFN wurden identifiziert, generiert und erfolgreich im Zellkulturmodellsystem eingesetzt. Die Analysen demonstrierten eine Reparatur der Mutation durch Homologe Rekombination auf genomischer Ebene und die Expression des wiederhergestellten Proteins. Durch die Genkorrektur im endogenen Lokus sind Größe des Gens, Isoformen oder die Art der Mutation keine limitierenden Faktoren für die Therapie. Die in der vorliegenden Arbeit durchgeführten Experimente unterstreichen das enorme Potential ZFN-basierter Therapiestrategien hin zu personalisierten Therapieformen nicht nur für USH sondern auch für andere erbliche Erkrankungen, deren genetische Grundlagen bekannt sind.

6. Referenzen

Acland,G.M., Aguirre,G.D., Bennett,J., Aleman,T.S., Cideciyan,A.V., Bennicelli,J., Dejneka,N.S., Pearce-Kelling,S.E., Maguire,A.M., Palczewski,K., Hauswirth,W.W., and Jacobson,S.G. (2005). Long-term restoration of rod and cone vision by single dose rAAV-mediated gene transfer to the retina in a canine model of childhood blindness. Mol. Ther. *12*, 1072-1082.

Adato,A., Lefevre,G., Delprat,B., Michel,V., Michalski,N., Chardenoux,S., Weil,D., El Amraoui,A., and Petit,C. (2005). Usherin, the defective protein in Usher syndrome type IIA, is likely to be a component of interstereocilia ankle links in the inner ear sensory cells. Hum. Mol. Genet. *14*, 3921-3932.

Alagramam,K.N., Goodyear,R.J., Geng,R., Furness,D.N., van Aken,A.F., Marcotti,W., Kros,C.J., and Richardson,G.P. (2011). Mutations in protocadherin 15 and cadherin 23 affect tip links and mechanotransduction in mammalian sensory hair cells. PLoS. One. *6*, e19183.

Allocca,M., Di Vicino,U., Petrillo,M., Carlomagno,F., Domenici,L., and Auricchio,A. (2007). Constitutive and AP20187-induced Ret activation in photoreceptors does not protect from light-induced damage. Invest. Ophthalmol. Vis. Sci. *48*, 5199-5206.

Allocca,M., Doria,M., Petrillo,M., Colella,P., Garcia-Hoyos,M., Gibbs,D., Kim,S.R., Maguire,A., Rex,T.S., Di,V.U., Cutillo,L., Sparrow,J.R., Williams,D.S., Bennett,J., and Auricchio,A. (2008). Serotype-dependent packaging of large genes in adeno-associated viral vectors results in effective gene delivery in mice. J. Clin. Invest. *118*, 1955-1964.

Bahloul,A., Michel,V., Hardelin,J.P., Nouaille,S., Hoos,S., Houdusse,A., England,P., and Petit,C. (2010). Cadherin-23, myosin VIIa and harmonin, encoded by Usher syndrome type I genes, form a ternary complex and interact with membrane phospholipids. Hum. Mol. Genet. *19*, 3557-3565.

Bainbridge,J.W., Smith,A.J., Barker,S.S., Robbie,S., Henderson,R., Balaggan,K., Viswanathan,A., Holder,G.E., Stockman,A., Tyler,N., Petersen-Jones,S., Bhattacharya,S.S., Thrasher,A.J., Fitzke,F.W., Carter,B.J., Rubin,G.S., Moore,A.T., and Ali,R.R. (2008). Effect of gene therapy on visual function in Leber's congenital amaurosis. N. Engl. J. Med. *358*, 2231-2239.

Baux,D., Faugere,V., Larrieu,L., Le Guedard-Mereuze,S., Hamroun,D., Beroud,C., Malcolm,S., Claustres,M., and Roux,A.F. (2008). UMD-USHbases: a comprehensive set of databases to record and analyse pathogenic mutations and unclassified variants in seven Usher syndrome causing genes. Hum. Mutat. *29*, E76-E87.

Bedrosian,J.C., Gratton,M.A., Brigande,J.V., Tang,W., Landau,J., and Bennett,J. (2006). In vivo delivery of recombinant viruses to the fetal murine cochlea: transduction characteristics and long-term effects on auditory function. Mol. Ther. *14*, 328-335.

Bibikova,M., Carroll,D., Segal,D.J., Trautman,J.K., Smith,J., Kim,Y.G., and Chandrasegaran,S. (2001). Stimulation of homologous recombination through targeted cleavage by chimeric nucleases. Mol. Cell Biol. *21*, 289-297.

Boch,J., Scholze,H., Schornack,S., Landgraf,A., Hahn,S., Kay,S., Lahaye,T., Nickstadt,A., and Bonas,U. (2009). Breaking the code of DNA binding specificity of TAL-type III effectors. Science *326*, 1509-1512.

Boëda,B., El Amraoui,A., Bahloul,A., Goodyear,R., Daviet,L., Blanchard,S., Perfettini,I., Fath,K.R., Shorte,S., Reiners,J., Houdusse,A., Legrain,P., Wolfrum,U., Richardson,G., and Petit,C. (2002). Myosin VIIa, harmonin and cadherin 23, three Usher I gene products that cooperate to shape the sensory hair cell bundle. EMBO J. *21*, 6689-6699.

Bolz,H., Ebermann,I., and Gal,A. (2005). Protocadherin-21 (PCDH21), a candidate gene for human retinal dystrophies. Mol. Vis. *11*, 929-933.

Bolz,H., von Brederlow,B., Ramirez,A., Bryda,E.C., Kutsche,K., Nothwang,H.G., Seeliger,M., Salcedo Cabrera,M.d., Caballero Vila,M., Pelaez Molina,O., Gal,A., and Kubisch,C. (2001). Mutation of *CDH23*, encoding a new member of the cadherin gene family, causes Usher syndrome type 1D. Nat. Genet. *27*, 108-112.

Bolz,H.J. (2009). [Genetics of Usher syndrome]. Ophthalmologe *106*, 496-504.

Bork,J.M., Peters,L.M., Riazuddin,S., Bernstein,S.L., Ahmed,Z.M., Ness,S.L., Polomeno,R., Ramesh,A., Schloss,M., Srikumari,C.R.S., Wayne,S., Bellman,S., Desmukh,D., Ahmed,Z., Khan,S.N., Der Kaloustian,V.M., Li,X.C., Lalwani,A., Riazuddin,S., Bitner-Glindzicz,M., Nance,W.E., Liu,X.-Z., Wistow,G., Smith,R.J.H., Griffith,A.J., Wilcox,E.R., Friedman,T.B., and Morell,R.J. (2001). Usher syndrome 1D and nonsyndromic autosomal recessive deafness DFNB12 are caused by allelic mutations of the novel cadherin-like gene *CDH23*. Am. J Hum. Genet. *68*, 26-37.

Caberlotto,E., Michel,V., Foucher,I., Bahloul,A., Goodyear,R.J., Pepermans,E., Michalski,N., Perfettini,I., Alegria-Prevot,O., Chardenoux,S., Do,C.M., Hardelin,J.P., Richardson,G.P., Avan,P., Weil,D., and Petit,C. (2011). Usher type 1G protein sans is a critical component of the tip-link complex, a structure controlling actin polymerization in stereocilia. Proc. Natl. Acad. Sci. U. S. A. *108*, 5825-5830.

Cai,X., Conley,S., and Naash,M. (2008). Nanoparticle applications in ocular gene therapy. Vision Res. *48*, 319-324.

Cai,X., Conley,S.M., Nash,Z., Fliesler,S.J., Cooper,M.J., and Naash,M.I. (2010). Gene delivery to mitotic and postmitotic photoreceptors via compacted DNA nanoparticles results in improved phenotype in a mouse model of retinitis pigmentosa. FASEB J. *24*, 1178-1191.

Carroll,D. (2008). Progress and prospects: zinc-finger nucleases as gene therapy agents. Gene Ther. *15*, 1463-1468.

Cathomen,T. and Joung,J.K. (2008). Zinc-finger nucleases: the next generation emerges. Mol. Ther. *16*, 1200-1207.

Cermak,T., Doyle,E.L., Christian,M., Wang,L., Zhang,Y., Schmidt,C., Baller,J.A., Somia,N.V., Bogdanove,A.J., and Voytas,D.F. (2011). Efficient design and assembly of custom TALEN and other TAL effector-based constructs for DNA targeting. Nucleic Acids Res. *39*, e82.

Choulika,A., Perrin,A., Dujon,B., and Nicolas,J.F. (1995). Induction of homologous recombination in mammalian chromosomes by using the I-SceI system of Saccharomyces cerevisiae. Mol. Cell Biol. *15*, 1968-1973.

Cornu,T.I. and Cathomen,T. (2010). Quantification of zinc finger nuclease-associated toxicity. Methods Mol. Biol. *649*, 237-245.

Dejneka,N.S., Surace,E.M., Aleman,T.S., Cideciyan,A.V., Lyubarsky,A., Savchenko,A., Redmond,T.M., Tang,W., Wei,Z., Rex,T.S., Glover,E., Maguire,A.M., Pugh,E.N., Jr., Jacobson,S.G., and Bennett,J. (2004). In utero gene therapy rescues vision in a murine model of congenital blindness. Mol. Ther. *9*, 182-188.

den Hollander,A.I., Black,A., Bennett,J., and Cremers,F.P. (2010). Lighting a candle in the dark: advances in genetics and gene therapy of recessive retinal dystrophies. J. Clin. Invest *120*, 3042-3053.

den Hollander,A.I., Koenekoop,R.K., Mohamed,M.D., Arts,H.H., Boldt,K., Towns,K.V., Sedmak,T., Beer,M., Nagel-Wolfrum,K., McKibbin,M., Dharmaraj,S., Lopez,I., Ivings,L., Williams,G.A., Springell,K., Woods,C.G., Jafri,H., Rashid,Y., Strom,T.M., van der

Zwaag,B., Gosens,I., Kersten,F.F., van Wijk,E., Veltman,J.A., Zonneveld,M.N., van Beersum,S.E., Maumenee,I.H., Wolfrum,U., Cheetham,M.E., Ueffing,M., Cremers,F.P., Inglehearn,C.F., and Roepman,R. (2007). Mutations in LCA5, encoding the ciliary protein lebercilin, cause Leber congenital amaurosis. Nat. Genet. *39*, 889-895.

Di Palma,F., Holme,R.H., Bryda,E.C., Belyantseva,I.A., Pellegrino,R., Kachar,B., Steel,K.P., and Noben-Trauth,K. (2001a). Mutations in *Cdh23*, encoding a new type of cadherin, cause stereocilia disorganization in waltzer, the mouse model for Usher syndrome type 1D. Nat. Genet. *27*, 103-107.

Di Palma,F., Pellegrino,R., and Noben-Trauth,K. (2001b). Genomic structure, alternative splice forms and normal and mutant alleles of cadherin (Cdh23). Gene *281*, 31-41.

Doyon,Y., McCammon,J.M., Miller,J.C., Faraji,F., Ngo,C., Katibah,G.E., Amora,R., Hocking,T.D., Zhang,L., Rebar,E.J., Gregory,P.D., Urnov,F.D., and Amacher,S.L. (2008). Heritable targeted gene disruption in zebrafish using designed zinc-finger nucleases. Nat. Biotechnol. *26*, 702-708.

Ebermann,I., Phillips,J.B., Liebau,M.C., Koenekoop,R.K., Schermer,B., Lopez,I., Schafer,E., Roux,A.F., Dafinger,C., Bernd,A., Zrenner,E., Claustres,M., Blanco,B., Nurnberg,G., Nurnberg,P., Ruland,R., Westerfield,M., Benzing,T., and Bolz,H.J. (2010). PDZD7 is a modifier of retinal disease and a contributor to digenic Usher syndrome. J. Clin. Invest. *120*, 1812-1823.

Ebermann,I., Wilke,R., Lauhoff,T., Lubben,D., Zrenner,E., and Bolz,H.J. (2007). Two truncating USH3A mutations, including one novel, in a German family with Usher syndrome. Mol. Vis. *13*, 1539-1547.

El Amraoui,A. and Petit,C. (2005). Usher I syndrome: unravelling the mechanisms that underlie the cohesion of the growing hair bundle in inner ear sensory cells. J. Cell Sci. *118*, 4593-4603.

Eudy,J.D., Yao,S., Weston,M.D., Ma-Edmonds,M., Talmadge,C.B., Cheng,J.J., Kimberling,W.J., and Sumegi,J. (1998). Isolation of a gene encoding a novel member of the nuclear receptor superfamily from the critical region of Usher syndrome type IIa at 1q41. Genomics *50*, 382-384.

Farjo,R., Skaggs,J., Quiambao,A.B., Cooper,M.J., and Naash,M.I. (2006). Efficient non-viral ocular gene transfer with compacted DNA nanoparticles. PLoS. One. *1*, e38.

Flisikowska,T., Thorey,I.S., Offner,S., Ros,F., Lifke,V., Zeitler,B., Rottmann,O., Vincent,A., Zhang,L., Jenkins,S., Niersbach,H., Kind,A.J., Gregory,P.D., Schnieke,A.E., and Platzer,J. (2011). Efficient immunoglobulin gene disruption and targeted replacement in rabbit using zinc finger nucleases. PLoS. One. *6*, e21045.

Foley,J.E., Maeder,M.L., Pearlberg,J., Joung,J.K., Peterson,R.T., and Yeh,J.R. (2009). Targeted mutagenesis in zebrafish using customized zinc-finger nucleases. Nat. Protoc. *4*, 1855-1867.

Frankel,A.D. and Pabo,C.O. (1988). Cellular uptake of the tat protein from human immunodeficiency virus. Cell *55*, 1189-1193.

Geurts,A.M., Cost,G.J., Freyvert,Y., Zeitler,B., Miller,J.C., Choi,V.M., Jenkins,S.S., Wood,A., Cui,X., Meng,X., Vincent,A., Lam,S., Michalkiewicz,M., Schilling,R., Foeckler,J., Kalloway,S., Weiler,H., Menoret,S., Anegon,I., Davis,G.D., Zhang,L., Rebar,E.J., Gregory,P.D., Urnov,F.D., Jacob,H.J., and Buelow,R. (2009). Knockout rats via embryo microinjection of zinc-finger nucleases. Science *325*, 433.

Gloeckner,C.J., Boldt,K., and Ueffing,M. (2009). Strep/FLAG tandem affinity purification (SF-TAP) to study protein interactions. Curr. Protoc. Protein Sci. *Chapter 19*, Unit19.

Goldmann,T., Overlack,N., Wolfrum,U., and Nagel-Wolfrum,K. (2011). PTC124-mediated translational readthrough of a nonsense mutation causing Usher syndrome type 1C. Hum. Gene Ther. *22*, 537-547.

Goldmann,T., Rebibo-Sabbah,A., Overlack,N., Nudelman,I., Belakhov,V., Baasov,T., Ben Yosef,T., Wolfrum,U., and Nagel-Wolfrum,K. (2010). Beneficial read-through of a USH1C nonsense mutation by designed aminoglycoside NB30 in the retina. Invest. Ophthalmol. Vis. Sci. *51*, 6671-6680.

Grati,M. and Kachar,B. (2011). Myosin VIIa and sans localization at stereocilia upper tip-link density implicates these Usher syndrome proteins in mechanotransduction. Proc. Natl. Acad. Sci. U. S. A. *108*, 11476-11481.

Green,M. and Loewenstein,P.M. (1988). Autonomous functional domains of chemically synthesized human immunodeficiency virus tat trans-activator protein. Cell *55*, 1179-1188.

Gregory,F.D., Bryan,K.E., Pangrsic,T., Calin-Jageman,I.E., Moser,T., and Lee,A. (2011). Harmonin inhibits presynaptic Ca(v)1.3 Ca(2+) channels in mouse inner hair cells. Nat. Neurosci. [Epub ahead of print].

Gupta,A., Meng,X., Zhu,L.J., Lawson,N.D., and Wolfe,S.A. (2011). Zinc finger protein-dependent and -independent contributions to the in vivo off-target activity of zinc finger nucleases. Nucleic Acids Res. *39*, 381-392.

Hauswirth,W.W., Aleman,T.S., Kaushal,S., Cideciyan,A.V., Schwartz,S.B., Wang,L., Conlon,T.J., Boye,S.L., Flotte,T.R., Byrne,B.J., and Jacobson,S.G. (2008). Treatment of leber congenital amaurosis due to RPE65 mutations by ocular subretinal injection of adeno-associated virus gene vector: short-term results of a phase I trial. Hum. Gene Ther. *19*, 979-990.

Inoue,A. and Ikebe,M. (2003). Characterization of the motor activity of mammalian myosin VIIA. J. Biol. Chem. *278*, 5478-5487.

Kazmierczak,P., Sakaguchi,H., Tokita,J., Wilson-Kubalek,E.M., Milligan,R.A., Muller,U., and Kachar,B. (2007). Cadherin 23 and protocadherin 15 interact to form tip-link filaments in sensory hair cells. Nature *449*, 87-91.

Keeling,K.M. and Bedwell,D.M. (2011). Suppression of nonsense mutations as a therapeutic approach to treat genetic diseases. Wiley Interdisciplinary Reviews: RNA 1-16. [Epub ahead of print].

Kim,Y.G., Cha,J., and Chandrasegaran,S. (1996). Hybrid restriction enzymes: zinc finger fusions to Fok I cleavage domain. Proc. Natl. Acad. Sci. U. S. A. *93*, 1156-1160.

Konstan,M.W., Davis,P.B., Wagener,J.S., Hilliard,K.A., Stern,R.C., Milgram,L.J., Kowalczyk,T.H., Hyatt,S.L., Fink,T.L., Gedeon,C.R., Oette,S.M., Payne,J.M., Muhammad,O., Ziady,A.G., Moen,R.C., and Cooper,M.J. (2004). Compacted DNA nanoparticles administered to the nasal mucosa of cystic fibrosis subjects are safe and demonstrate partial to complete cystic fibrosis transmembrane regulator reconstitution. Hum. Gene Ther. *15*, 1255-1269.

Kremer,H., van,W.E., Marker,T., Wolfrum,U., and Roepman,R. (2006). Usher syndrome: molecular links of pathogenesis, proteins and pathways. Hum. Mol. Genet. *15 Spec No 2*, R262-R270.

Lagziel,A., Ahmed,Z.M., Schultz,J.M., Morell,R.J., Belyantseva,I.A., and Friedman,T.B. (2005). Spatiotemporal pattern and isoforms of cadherin 23 in wild type and waltzer mice during inner ear hair cell development. Dev. Biol. *280*, 295-306.

Lagziel,A., Overlack,N., Bernstein,S.L., Morell,R.J., Wolfrum,U., and Friedman,T.B. (2009). Expression of cadherin 23 isoforms is not conserved: implications for a mouse model of Usher syndrome type 1D. Mol. Vis. *15*, 1843-1857.

Li,T., Huang,S., Zhao,X., Wright,D.A., Carpenter,S., Spalding,M.H., Weeks,D.P., and Yang,B. (2011a). Modularly assembled designer TAL effector nucleases for targeted gene knockout and gene replacement in eukaryotes. Nucleic Acids Res. *39*, 6315-6325.

Li,H., Haurigot,V., Doyon,Y., Li,T., Wong,S.Y., Bhagwat,A.S., Malani,N., Anguela,X.M., Sharma,R., Ivanciu,L., Murphy,S.L., Finn,J.D., Khazi,F.R., Zhou,S., Paschon,D.E., Rebar,E.J., Bushman,F.D., Gregory,P.D., Holmes,M.C., and High,K.A. (2011b). In vivo genome editing restores haemostasis in a mouse model of haemophilia. Nature 475, 217-221.

Liu,X., Bulgakov,O.V., Darrow,K.N., Pawlyk,B., Adamian,M., Liberman,M.C., and Li,T. (2007). Usherin is required for maintenance of retinal photoreceptors and normal development of cochlear hair cells. Proc. Natl. Acad. Sci. U. S. A. *104*, 4413-4418.

Märker, T (2007) SANS (USH1G) in USH-Proteinnetzwerken von Photorezeptorzellen der Vertebratenretina. Promotionsarbeit, Johannes Gutenberg-Universität Mainz.

Märker,T., van Wijk,E., Overlack,N., Kersten,F.F., McGee,J., Goldmann,T., Sehn,E., Roepman,R., Walsh,E.J., Kremer,H., and Wolfrum,U. (2008). A novel Usher protein network at the periciliary reloading point between molecular transport machineries in vertebrate photoreceptor cells. Hum. Mol. Genet. *17*, 71-86.

Maguire,A.M., Simonelli,F., Pierce,E.A., Pugh,E.N., Jr., Mingozzi,F., Bennicelli,J., Banfi,S., Marshall,K.A., Testa,F., Surace,E.M., Rossi,S., Lyubarsky,A., Arruda,V.R., Konkle,B., Stone,E., Sun,J., Jacobs,J., Dell'osso,L., Hertle,R., Ma,J.X., Redmond,T.M., Zhu,X., Hauck,B., Zelenaia,O., Shindler,K.S., Maguire,M.G., Wright,J.F., Volpe,N.J., McDonnell,J.W., Auricchio,A., High,K.A., and Bennett,J. (2008). Safety and efficacy of gene transfer for Leber's congenital amaurosis. N. Engl. J. Med. *358*, 2240-2248.

Mani,M., Smith,J., Kandavelou,K., Berg,J.M., and Chandrasegaran,S. (2005). Binding of two zinc finger nuclease monomers to two specific sites is required for effective double-strand DNA cleavage. Biochem. Biophys. Res. Commun. *334*, 1191-1197.

Moehle,E.A., Rock,J.M., Lee,Y.L., Jouvenot,Y., DeKelver,R.C., Gregory,P.D., Urnov,F.D., and Holmes,M.C. (2007). Targeted gene addition into a specified location in the human genome using designed zinc finger nucleases. Proc. Natl. Acad. Sci. U. S. A. *104*, 3055-3060.

Mussolino,C., Morbitzer,R., Lutge,F., Dannemann,N., Lahaye,T., and Cathomen,T. (2011). A novel TALE nuclease scaffold enables high genome editing activity in combination with low toxicity. Nucleic Acids Res. [Epub ahead of print].

Orr-Weaver,T.L., Szostak,J.W., and Rothstein,R.J. (1981). Yeast transformation: a model system for the study of recombination. Proc. Natl. Acad. Sci. U. S. A. *78*, 6354-6358.

Ouyang,X.M., Hejtmancik,J.F., Jacobson,S.G., Xia,X.J., Li,A., Du,L.L., Newton,V., Kaiser,M., Balkany,T., Nance,W.E., and Liu,X.Z. (2003). USH1C: a rare cause of USH1 in a non-Acadian population and a founder effect of the Acadian allele. Clin. Genet. *63*, 150-153.

Overlack,N., Märker,T., Latz,M., Nagel-Wolfrum,K., and Wolfrum,U. (2008). SANS (USH1G) expression in developing and mature mammalian retina. Vision Res. *48*, 400-412.

Pan,L., Yan,J., Wu,L., and Zhang,M. (2009). Assembling stable hair cell tip link complex via multidentate interactions between harmonin and cadherin 23. Proc. Natl. Acad. Sci. U. S. A. *106*, 5575-5580.

Papermaster,D.S. (2002). The birth and death of photoreceptors: the Friedenwald Lecture. Invest Ophthalmol. Vis. Sci. *43*, 1300-1309.

Pavletich,N.P. and Pabo,C.O. (1991). Zinc finger-DNA recognition: crystal structure of a Zif268-DNA complex at 2.1 A. Science *252*, 809-817.

Pennings,R.J., Damen,G.W., Snik,A.F., Hoefsloot,L., Cremers,C.W., and Mylanus,E.A. (2006). Audiologic performance and benefit of cochlear implantation in Usher syndrome type I. Laryngoscope *116*, 717-722.

Porteus,M.H. and Baltimore,D. (2003). Chimeric nucleases stimulate gene targeting in human cells. Science *300*, 763.

Pruett-Miller,S.M., Reading,D.W., Porter,S.N., and Porteus,M.H. (2009). Attenuation of zinc finger nuclease toxicity by small-molecule regulation of protein levels. PLoS. Genet. *5*, e1000376.

Ramalingam,S., Kandavelou,K., Rajenderan,R., and Chandrasegaran,S. (2011). Creating designed zinc-finger nucleases with minimal cytotoxicity. J. Mol. Biol. *405*, 630-641.

Rattner,A., Smallwood,P.M., Williams,J., Cooke,C., Savchenko,A., Lyubarsky,A., Pugh,E.N., and Nathans,J. (2001). A photoreceptor-specific cadherin is essential for the structural integrity of the outer segment and for photoreceptor survival. Neuron *32*, 775-786.

Reidel,B., Orisme,W., Goldmann,T., Smith,W.C., and Wolfrum,U. (2006). Photoreceptor vitality in organotypic cultures of mature vertebrate retinas validated by light-dependent molecular movements. Vision Res. *46*, 4464-4471.

Reiners,J., Marker,T., Jurgens,K., Reidel,B., and Wolfrum,U. (2005a). Photoreceptor expression of the Usher syndrome type 1 protein protocadherin 15 (USH1F) and its interaction with the scaffold protein harmonin (USH1C). Mol. Vis. *11*, 347-355.

Reiners,J., Nagel-Wolfrum,K., Jürgens,K., Märker,T., and Wolfrum,U. (2006). Molecular basis of human Usher syndrome: deciphering the meshes of the Usher protein network provides insights into the pathomechanisms of the Usher disease. Exp. Eye Res. *83*, 97-119.

Reiners,J., Reidel,B., El-Amraoui,A., Boeda,B., Huber,I., Petit,C., and Wolfrum,U. (2003). Differential distribution of harmonin isoforms and their possible role in Usher-1 protein complexes in mammalian photoreceptor cells. Invest. Ophthalmol. Visual Sci. *44*, 5006-5015.

Reiners,J., van Wijk,E., Marker,T., Zimmermann,U., Jurgens,K., te Brinke,H., Overlack,N., Roepman,R., Knipper,M., Kremer,H., and Wolfrum,U. (2005b). Scaffold protein harmonin (USH1C) provides molecular links between Usher syndrome type 1 and type 2. Hum. Mol. Genet. *14*, 3933-3943.

Rigaut,G., Shevchenko,A., Rutz,B., Wilm,M., Mann,M., and Seraphin,B. (1999). A generic protein purification method for protein complex characterization and proteome exploration. Nat. Biotechnol. *17*, 1030-1032.

Roepman,R. and Wolfrum,U. (2007). Protein networks and complexes in photoreceptor cilia. Subcell. Biochem. *43*, 209-235.

Rouet,P., Smih,F., and Jasin,M. (1994). Introduction of double-strand breaks into the genome of mouse cells by expression of a rare-cutting endonuclease. Mol. Cell Biol. *14*, 8096-8106.

Saihan,Z., Webster,A.R., Luxon,L., and Bitner-Glindzicz,M. (2009). Update on Usher syndrome. Curr. Opin. Neurol. *22*, 19-27.

Schneider,E., Marker,T., Daser,A., Frey-Mahn,G., Beyer,V., Farcas,R., Schneider-Ratzke,B., Kohlschmidt,N., Grossmann,B., Bauss,K., Napiontek,U., Keilmann,A., Bartsch,O., Zechner,U., Wolfrum,U., and Haaf,T. (2009). Homozygous disruption of PDZD7 by reciprocal translocation in a consanguineous family: a new member of the Usher syndrome

protein interactome causing congenital hearing impairment. Hum. Mol. Genet. *18*, 655-666.

Siemens,J., Kazmierczak,P., Reynolds,A., Sticker,M., Littlewood Evans,A., and Müller,U. (2002). The Usher syndrome proteins cadherin 23 and harmonin form a complex by means of PDZ-domain interactions. Proc. Natl. Acad. Sci. U. S. A. *99*, 14946-14951.

Siemens,J., Lillo,C., Dumont,R.A., Reynolds,A., Williams,D.S., Gillespie,P.G., and Muller,U. (2004). Cadherin 23 is a component of the tip link in hair-cell stereocilia. Nature *428*, 950-955.

Smith,J., Bibikova,M., Whitby,F.G., Reddy,A.R., Chandrasegaran,S., and Carroll,D. (2000). Requirements for double-strand cleavage by chimeric restriction enzymes with zinc finger DNA-recognition domains. Nucleic Acids Res. *28*, 3361-3369.

Soldner,F., Laganiere,J., Cheng,A.W., Hockemeyer,D., Gao,Q., Alagappan,R., Khurana,V., Golbe,L.I., Myers,R.H., Lindquist,S., Zhang,L., Guschin,D., Fong,L.K., Vu,B.J., Meng,X., Urnov,F.D., Rebar,E.J., Gregory,P.D., Zhang,H.S., and Jaenisch,R. (2011). Generation of isogenic pluripotent stem cells differing exclusively at two early onset Parkinson point mutations. Cell *146*, 318-331.

Stone,E.M. (2009). Progress toward effective treatments for human photoreceptor degenerations. Curr. Opin. Genet. Dev. *19*, 283-289.

Su,Z., Ning,B., Fang,H., Hong,H., Perkins,R., Tong,W., and Shi,L. (2011). Next-generation sequencing and its applications in molecular diagnostics. Expert. Rev. Mol. Diagn. *11*, 333-343.

Szczepek,M., Brondani,V., Buchel,J., Serrano,L., Segal,D.J., and Cathomen,T. (2007). Structure-based redesign of the dimerization interface reduces the toxicity of zinc-finger nucleases. Nat. Biotechnol. *25*, 786-793.

Udovichenko,I.P., Gibbs,D., and Williams,D.S. (2002). Actin-based motor properties of native myosin VIIa. J. Cell Sci. *115*, 445-450.

Urnov,F.D., Miller,J.C., Lee,Y.L., Beausejour,C.M., Rock,J.M., Augustus,S., Jamieson,A.C., Porteus,M.H., Gregory,P.D., and Holmes,M.C. (2005). Highly efficient endogenous human gene correction using designed zinc-finger nucleases. Nature *435*, 646-651.

Urnov,F.D., Rebar,E.J., Holmes,M.C., Zhang,H.S., and Gregory,P.D. (2010). Genome editing with engineered zinc finger nucleases. Nat. Rev. Genet. *11*, 636-646.

Vache,C., Besnard,T., Blanchet,C., Baux,D., Larrieu,L., Faugere,V., Mondain,M., Hamel,C., Malcolm,S., Claustres,M., and Roux,A.F. (2010). Nasal epithelial cells are a reliable source to study splicing variants in Usher syndrome. Hum. Mutat. *31*, 734-741.

van Wijk,E., Pennings,R.J., te Brinke,H., Claassen,A., Yntema,H.G., Hoefsloot,L.H., Cremers,F.P., Cremers,C.W., and Kremer,H. (2004). Identification of 51 Novel Exons of the Usher Syndrome Type 2A (USH2A) Gene That Encode Multiple Conserved Functional Domains and That Are Mutated in Patients with Usher Syndrome Type II. Am. J. Hum. Genet. *74*, 738-744.

van Wijk,E., van der Zwaag,B., Peters,T., Zimmermann,U., te Brinke,H., Kersten,F.F., Marker,T., Aller,E., Hoefsloot,L.H., Cremers,C.W., Cremers,F.P., Wolfrum,U., Knipper,M., Roepman,R., and Kremer,H. (2006). The DFNB31 gene product whirlin connects to the Usher protein network in the cochlea and retina by direct association with USH2A and VLGR1. Hum. Mol. Genet. *15*, 751-765.

Verde,I., Pahlke,G., Salanova,M., Zhang,G., Wang,S., Coletti,D., Onuffer,J., Jin,S.L., and Conti,M. (2001). Myomegalin is a novel protein of the golgi/centrosome that interacts with a cyclic nucleotide phosphodiesterase. J. Biol. Chem. *276*, 11189-11198.

Verpy,E., Leibovici,M., Zwaenepoel,I., Liu,X.Z., Gal,A., Salem,N., Mansour,A., Blanchard,S., Kobayashi,I., Keats,B.J., Slim,R., and Petit,C. (2000). A defect in harmonin, a PDZ domain-containing protein expressed in the inner ear sensory hair cells, underlies Usher syndrome type 1C. Nat. Genet. *26*, 51-55.

Wadia,J.S. and Dowdy,S.F. (2002). Protein transduction technology. Curr. Opin. Biotechnol. *13*, 52-56.

Weil,D., Blanchard,S., Kaplan,J., Guilford,P., Gibson,F., Walsh,J., Mburu,P., Varela,A., Levilliers,J., Weston,M.D., and . (1995). Defective myosin VIIA gene responsible for Usher syndrome type 1B. Nature *374*, 60-61.

Weston,M.D., Luijendijk,M.W., Humphrey,K.D., Moller,C., and Kimberling,W.J. (2004). Mutations in the VLGR1 gene implicate G-protein signaling in the pathogenesis of Usher syndrome type II. Am. J. Hum. Genet. *74*, 357-366.

Williams,D.S. (2008). Usher syndrome: animal models, retinal function of Usher proteins, and prospects for gene therapy. Vision Res. *48*, 433-441.

Wolfrum,U. (2011). Protein networks related to the Usher syndrome gain insights in the molecular basis of the disease. In Usher Syndrome: Pathogenesis, Diagnosis and Therapy., Satpal A, ed. Nova Science Publishers, 51-73.

Xu,Z., Peng,A.W., Oshima,K., and Heller,S. (2008). MAGI-1, a candidate stereociliary scaffolding protein, associates with the tip-link component cadherin 23. J. Neurosci. *28*, 11269-11276.

Yan,D. and Liu,X.Z. (2010). Genetics and pathological mechanisms of Usher syndrome. J. Hum. Genet. *55*, 327-335.

Yan,J., Pan,L., Chen,X., Wu,L., and Zhang,M. (2010). The structure of the harmonin/sans complex reveals an unexpected interaction mode of the two Usher syndrome proteins. Proc. Natl. Acad. Sci. U. S. A. *107*, 4040-4045.

Yang,J., Liu,X., Zhao,Y., Adamian,M., Pawlyk,B., Sun,X., McMillan,D.R., Liberman,M.C., and Li,T. (2010). Ablation of whirlin long isoform disrupts the USH2 protein complex and causes vision and hearing loss. PLoS. Genet. *6*, e1000955.

Zallocchi,M., Sisson,J.H., and Cosgrove,D. (2010). Biochemical characterization of native Usher protein complexes from a vesicular subfraction of tracheal epithelial cells. Biochemistry *49*, 1236-1247.

Zheng,L., Zheng,J., Whitlon,D.S., Garcia-Anoveros,J., and Bartles,J.R. (2010). Targeting of the hair cell proteins cadherin 23, harmonin, myosin XVa, espin, and prestin in an epithelial cell model. J. Neurosci. *30*, 7187-7201.

Ziady,A.G., Gedeon,C.R., Muhammad,O., Stillwell,V., Oette,S.M., Fink,T.L., Quan,W., Kowalczyk,T.H., Hyatt,S.L., Payne,J., Peischl,A., Seng,J.E., Moen,R.C., Cooper,M.J., and Davis,P.B. (2003). Minimal toxicity of stabilized compacted DNA nanoparticles in the murine lung. Mol. Ther. *8*, 948-956.

Zou,J., Luo,L., Shen,Z., Chiodo,V.A., Ambati,B.K., Hauswirth,W.W., and Yang,J. (2011). Whirlin replacement restores the formation of the USH2 protein complex in whirlin knockout photoreceptors. Invest. Ophthalmol. Vis. Sci. *52*, 2343-2351.

Zwaenepoel,I., Verpy,E., Blanchard,S., Meins,M., Apfelstedt-Sylla,E., Gal,A., and Petit,C. (2001). Identification of three novel mutations in the USH1C gene and detection of thirty-one polymorphisms used for haplotype analysis. Hum. Mutat. *17*, 34-41.

7. Anhang

7.1 Zuordnung der geleisteten Beiträge zu den einzelnen Publikationen der vorliegenden kumulativen Dissertation

An dieser Stelle möchte ich ausführen, welche Beiträge ich zu den einzelnen Publikationen, in denen ich als Autor auftrete, geleistet habe. Zunächst werde ich daher auf die fünf Hauptpublikationen Lagziel et al., 2009 (I), Overlack et al., 2010 (II), Overlack et al., 2011a epub (III), Overlack et al., 2011 (IV) und Overlack et al., eingereicht (V) eingehen. Anschließend werde ich meine Beiträge zu weiteren Publikationen des Gentherapiefeldes der Arbeitsgruppe von Prof. Dr. Uwe Wolfrum darstellen.

In der Arbeit von Lagziel et al., (Publikation I) war ich verantwortlich für die Analyse der Expression und Lokalisation von Cadherin23-Isoformen in der Mausretina, mit Hilfe spezifischer Antikörper. Die Auswertung erfolgte mittels indirekter Immunfluoreszenz-mikroskopie (Abb. 3 und 4) sowie Immunelektronenmikroskopie (Abb. 5). Die Arbeiten im Innenohr sowie die Expressionsanalysen mittels RT-PCR und Western Blot wurden von unseren Kooperationspartnern um Prof. T. Friedman durchgeführt. Die Zusammenstellung und das Schreiben der Arbeit wurden in enger Kooperation zwischen den Arbeitsgruppen erreicht.

Die zweite Publikation, Overlack et al., 2010 (II), stellt einen Übersichtsartikel zu Cadherin23, Protocadherin15 und Protocadherin21 in den Photorezeptorzellen der Retina und den Haarzellen im Innenohr dar, bei dem ich als Erstautor auftrete. Der konzeptionelle Entwurf dieser Arbeit wurde in erster Linie von mir und Prof. Dr. Uwe Wolfrum durchgeführt. Alle Teile und Abbildungen wurden zunächst von mir vorbereitet und anschließend mit Prof. Dr. Uwe Wolfrum überarbeitet.

Für die dritte Publikation Overlack et al., 2011a in press (III) wurde der Hefe-2-Hybrid Screen mit unseren Kooperationspartnern in den Niederlanden durchgeführt. Die Datenbankanalysen der potentiellen Myomegalin-Isoformen (Abb. 1, 2), ebenso wie die Validierung der Interaktion von SANS und Myomegalin in Kulturzellen (Abb. 1) wurden von mir durchgeführt. Die unabhängige Bestätigung der Interaktion mittels GST-Pull down wurde von D. Kilic ausgeführt (Abb. 1). Die Expressionsanalysen auf DNA-Ebene wurden von mir durchgeführt (Abb. 2). Die Proteinexpression in unterschiedlichen Mausgeweben wurde von mir mit Unterstützung von Ulrike Maas analysiert (Abb. 2). Die erarbeitete und visualisierte (sub-) zelluläre Lokalisation von Myomegalin und SANS in der Retina von Maus, Affe und Mensch auf elektronenmikroskopischem Niveau wurde von mir, mit technischer Unterstützung von Elisabeth Sehn und Gabriele Stern-Schneider, erreicht (Abb. 3-7).

Bei der vierten Publikation Overlack et al., 2011 (IV) handelt es sich um einen Übersichtsartikel zum Thema Therapiemöglichkeiten für das humane Usher-Syndrom. In diesem Artikel treten Tobias Goldmann und ich als gleichberechtigte Erstautoren auf. Alle Teile und Abbildungen wurden zunächst von Tobias Goldmann und mir vorbereitet und anschließend mit Prof. Dr. Uwe Wolfrum und Dr. Kerstin Nagel-Wolfrum überarbeitet.

In der fünften Publikation, Overlack et al., eingereicht (V), wurden die Experimente von mir durchgeführt sowie alle Abbildungen erstellt. Von Tobias Goldmann wurden Begleitexperimente durchgeführt. Der erste konzeptionelle Entwurf der Publikation wurde von mir und Prof. Dr. Uwe Wolfrum ausgearbeitet. Eine Überarbeitung erfolgte anschließend durch mich, Prof. Dr. Uwe Wolfrum und Dr. Kerstin Nagel-Wolfrum.

Neben den genannten Hauptpublikationen konnten weitere Beiträge zu Veröffentlichungen unserer Arbeitsgruppe sowie gemeinsamer Publikationen mit unseren Kooperationspartnern geleistet werden. So konnte ich einen Beitrag zu den Publikationen Goldmann et al., 2010 sowie Goldmann et al., 2011 und Goldmann et al., in Vorbereitung leisten. Hierbei war ich am Anlegen der organotypischen Retinakulturen für die *ex vivo* Analyse der eingesetzten Wirkstoffe beteiligt. Des Weiteren wurden die subretinalen Injektionen für die Analyse der Wirkung von PTC124 und NB54 *in vivo* in Mausaugen von mir durchgeführt.

7.2 Abkürzungen

Im Folgenden sind die im Text häufig verwendeten Abkürzungen nochmals in alphabetischer Reihenfolge zusammengefasst.

AAV	adeno-assoziierter Virus
AL	„ankle links"
BB	Basalkörper
CC	Verbindungscilium
cDNA	komplementäre DNA
Ce	Centriol
CP	Calycal Process
DAPI	4,6-Diamidino-2-Phenylindol
DNA	Desoxyribonukleinsäure
HTC	„horizontal top connectors"
IS	Innensegment
K	Kinocilium
Kb	Kilobasenpaare
N	Nukleus
NHEJ	„nonhomologous end joining"
ONL	äußere Körnerschicht
OPL	äußere plexiforme Schicht
OS	Außensegment der Photorezeptorzellen
PBM	PDZ-Bindemotif
PDZ	PSD-95, DLG, ZO-1
PST	Prolin-Serin-Threonin reiche Domäne
RPE	retinales Pigmentepithel
S	Synapse
SC	Stereocilium
TAP	Tandem-affinity-purification
TAT	trans-activator Domäne
TipL	„tip Link"
TL	„transient links"
TRID	„Translational read through inducing drug"
USH	humanes Usher Syndrom
ZF	Zinkfinger
ZFN	Zinkfinger Nuklease

7.3 Curriculum Vitae

Eidesstattliche Erklärung

Hiermit erkläre ich an Eides statt, dass ich meine Dissertation selbstständig und nur unter
Verwendung der angegebenen Hilfsmittel angefertigt habe.
Ich habe keinen anderen Promotionsversuch unternommen.

Mainz, ... 2011

....

Nora-Lena Overlack